Dissertation

submitted to the Combined Faculty of Mathematics, Engineering and Natural Sciences of Heidelberg University, Germany

> for the degree of Doctor of Natural Sciences

 $\begin{array}{c} {\rm Put\ forward\ by} \\ {\bf Tristan\ Raphael\ Daus,\ M.Sc.} \end{array}$

born in: Offenbach am Main

Oral examination: 24.07.2025

From Koopman-von Neumann to Cosmic Structure Formation – Path Integral Approach to Classical Many-Body Systems

Referees:

Prof. Dr. Matthias Bartelmann Prof. Dr. Thomas Gasenzer

Abstract

We develop a functional integral formalism for classical many-body systems based on the Klimontovich equation, which governs the exact evolution of the N-particle phase-space density without loss of microscopic information. Since no assumptions are made on the exact form of the initial state, this formalism is well suited to describe out-of-equilibrium systems. The formalism is discussed in detail and compared to alternative approaches. Analytical solutions to the tree-level equations for homogeneous systems are presented. Importantly, a first application to cosmic large scale structure formation is given, and numerical results are discussed. We present one-loop results for the density fluctuation power spectrum which agree well with results from numerical simulations and conventional approaches.

Zusammenfassung

Wir entwickeln einen Funktionalintegral-Formalismus für klassische Vielteilchensysteme, der auf der Klimontovich-Gleichung basiert. Diese beschreibt die exakte zeitliche Entwicklung der N-Teilchen-Phasenraumdichte, ohne mikroskopische Informationen zu verlieren. Da keine Annahmen über die genaue Form des Anfangszustands gemacht werden, eignet sich der Formalismus besonders gut zur Beschreibung von Nichtgleichgewichtssystemen. Wir präsentieren den Formalismus im Detail und vergleichen ihn mit alternativen Ansätzen. Analytische Lösungen der Tree-level-Näherung für homogene Systeme werden präsentiert. Eine erste Anwendung auf die Entstehung großräumiger kosmischer Strukturen wird vorgestellt und numerische Ergebnisse werden diskutiert. Insbesondere zeigen wir Ein-Schleifen-Ergebnisse für das Leistungsspektrum der Dichtefluktuationen, die gut mit numerischen Simulationen und etablierten Methoden übereinstimmen.

Contents

1.	Int	roduction	11
1.		th Integrals for Classical $N ext{-Particle}$ Systems - Particle	
	Pic	cture	15
2.	Ge	neral Concepts of Classical Statistical Mechanics	17
	2.1.	Hamiltonian Mechanics of N Particles	17
		2.1.1. The N -particle Hamiltonian Function	20
		2.1.2. The <i>N</i> -Particle Phase-Space Density	23
	2.2.	Observables and Expectation Values	25
		2.2.1. The Klimontovich Phase-Space Density	26
		2.2.2. Correlations	28
	2.3.	The Klimontovich Equation and the BBGKY Hierarchy	32
	2.4.	Important Truncations of the BBGKY Hierarchy	35
		2.4.1. Free Streaming	35
		2.4.2. The Vlasov Equation	36
		2.4.3. Including Collisions	38
	2.5.	Unequal Time Correlation Functions	39
	2.6.	N-particle Initial Conditions from a Correlated Density Field	40
3.	Fui	nctional Integrals for Deterministic Systems	43
		The Koopman-von Neumann Formulation of Classical Mechanics	43
		3.1.1. Axiomatic Derivation of Liouville's Equation - The Koopman	
		Operator	44
		3.1.2. Recovering Liouville's Equation	46
		3.1.3. Path Integral Representation and the Koopman-von Neumann	
		Propagator	48
	3.2.	Path Integrals for General Stochastic Theories	52
		3.2.1. The MSR/JD-Path Integral Construction	52
		3.2.2. Stochastic Initial Conditions	55
4.	For	rmal Solution to Liouville's Equation	57
-		Dyson-Series Expansion of the Liouville Propagator	57
		4.1.1. Free Theory	59
		4.1.2. Interacting Theory	59
	4.2.		63

8 Contents

5.	Re	summed Field Theory for Microscopic Particles	67
		Construction of the Field Theory	67
		5.1.1. Construction via a Modified Hubbard-Stratonovich Transfor-	
		mation	68
	5.2.	Resummed Field Theory	70
		5.2.1. Free Cumulants	72
		5.2.2. Propagators and Feynman Diagrams	73
		5.2.3. One Loop Corrections	75
2.		th Integrals for Classical $N ext{-Particle Systems}$ - Field neory Picture	79
6.		atistical Field Theory Approach to the Klimontovich Equation	81
-	6.1.		
	6.2.		
	6.3.	•	
	6.4.		
	6.5.	Bare Theory	
		6.5.1. Free Propagators and Resummation of the External Potential	91
		6.5.2. Bare Feynman Diagrams	93
	6.6.	The Background Field Approximation	95
		6.6.1. Tree-Level Theory	
		6.6.2. Feynman Diagrams for the Tree-Level Theory	
		6.6.3. Loop Expansion and Perturbation Theory	101
	6.7.	Comparison to the Microscopic Picture	103
	6.8.	(Un)avoidable non-Gaussianity of Initial Conditions – Vlasov Limit .	103
7.		rmal Development - Full Statistical Equations of Motion	107
	7.1.	Generating Functionals for the Full Theory	
		7.1.1. Correlation Functions and Cumulants	
	7.0	7.1.2. The One-Particle Irreducible Effective Action	
	7.2.	One-Loop Effective Action	
	7.3. 7.4.	The Master Dyson-Schwinger Equation	
8.	Sta	atistically Homogeneous and Isotropic Systems	123
	8.1.	v 1	
		8.1.1. Statistically Homogeneous and Isotropic Initial Conditions $$	123
		8.1.2. Homogeneous and Isotropic Potentials	125
		8.1.3. A Note on Long-Range Interaction Potentials	
		8.1.4. Free Particle Green Function	126
		8.1.5. Fourier-Space Treatment of Correlation Functions	127
	8.2.	Field Theory	128
		8.2.1. Tree-Level Propagators	
		8.2.2. Analytical Toy Model	132

Contents 9

Αp	-	ix B. Discretized Stochastic Evolution Equations Itô vs. Stratonovich in the Linear Case	187 187
Αp		ix A. Summary of Field Theory Notation Condensed Notation	185 185
4.	Аp	pendices	183
12	. Co	nclusion	177
		11.3.1. Results for the Power Spectrum at One-Loop Order	
		Cosmic Structure Formation in Klimontovich Field Theory	
	11.2.	Loop Corrections to the Power Spectrum at Tree Level	
		11.1.2. Numerical Results for the Power Spectrum at Tree Level 11.1.3. Numerical Results for the Bispectrum at Tree Level	
		11.1.1. Analytical Solution for an Einstein-de Sitter Cosmology in the Large-Scale Limit	
		Tree-Level Results for Cosmic n -Point Statistics	
11	. Res	ults for Cosmic Large-Scale Structure Formation	165
		Initial Conditions for Cosmic Structure Formation	
		Particle Trajectories on an Expanding Background	
10	. Ne [,] Tin	vtonian Dynamics of Correlated Particles on an Expanding Space-	157
		9.3.4. State of the Art in Cosmic Structure Formation	156
		9.3.3. Lagrangian Perturbation Theory	155
		9.3.2. Path-Integral Formulation of SPT	
	9.3.	Cosmic Structure Formation	
	0.0	9.2.1. Inflation and the Seeds for Initial Structures	
	9.2.	From Inflation to Today's Large-Scale Structures	147
		9.1.4. The ΛCDM Paradigm	
		9.1.2. Space-Time Dynamics of the Universe	
		9.1.1. Lovelock's Theorem and Einstein's Field Equations	
		Cosmological Standard Model	
9.	Cos	mology	141
3.	Аp	plication to Cosmic Large Scale Structure Formation	139
		8.3.3. Beyond Hartree-Fock - 2PI Loop Expansion	136
		8.3.2. Self Consistent Hartree-Fock Approximation	
	8.5.	8.3.1. 1PI Resummation and One-Loop Effective Action	
	8 3	Truncated Dyson-Schwinger Equations	125

10 Con	itents
--------	--------

B.2. The Discretized MSR/JD-Path Integral	189
Acknowledgements	191
Publications	193
Bibliography	195

1 Introduction

The central object of this thesis is the development and application of methods for the study of in- and out-of-equilibrium classical many-body systems. The range of applicability for such methods ranges from laboratory systems such as plasmas to cosmic structure formation. To study such systems, numerical N-body simulations have become the standard method. These are, however, computationally expensive, especially for systems with long-ranged interactions, and heavily tailored to each particular application. Although they can successfully reproduce results for those systems they were designed to simulate, they are not suitable as a general framework to gain a fundamental understanding of many-body physics.

The general idea is, therefore, to establish an analytical approach for the study of classical N-particle systems based on the path integral formulation of classical mechanics. This functional integral formulation provides a general framework which allows us to describe systems in- and out-of-equilibrium and makes the application of non-perturbative methods from quantum field theory to classical systems possible. Our main interest is then to study the structure formation and evolution in terms of n-point correlation functions of the Klimontovich phase-space densities in the context of cosmology.

The universe today is incredibly rich in structure: From galaxies that accumulate to clusters and filaments up to the celebrated $cosmic\ web$. However, high redshift observations of the Cosmic Microwave Background (CMB) reveal that the structures once emerged from a nearly perfectly homogeneous matter distribution, with only tiny fluctuations present. The study of cosmic large scale structure formation is thus the study of how these initial fluctuations have evolved into the structures we observe today. So far, numerical N-body simulations provide the most accurate results for cosmic structure formation. They are built on the simple idea of propagating particles according to Newtonian dynamics. Although they reproduce the observable structures in accordance with available observational data, they come expectedly with high computational cost and offer only limited insight into the underlying physical processes governing cosmic structure formation. Thus, to develop a deeper theoretical understanding, numerical simulations have to be complemented by analytical approaches.

The prospect of newly available data from current and next generation surveys

1. Introduction

such as Euclid, LSST and SDSS [1, 2, 3] has sparked a renewed interest in progressing existing analytical methods for the description of structure formation, which are needed in order to analyze the available data. The most prominent approaches, such as SPT, EFT or EFTofLSS [4, 5, 6, 7, 8, 9, 10, 11], are based on the set of hydrodynamical equations obtained from the Vlasov equation by taking its moments with respect to the momentum. As this procedure results in an infinite hierarchy of coupled differential equations, since each moment depends on the next-higher one, a truncation must be introduced to close this hierarchy. A typical truncation procedure is to use the single-stream approximation (SSA) which neglects the shear tensor appearing in the second moment of the Vlasov equation, i.e., the energy-momentum tensor. This truncation is well-justified, if a quasi-equilibrium is assumed, where the system can be fully described by its collisional invariants and transport effects are absent. However, as recent works suggest, this assumption may not hold for cosmic structure formation so that higher moments of the Vlasov equation have to be taken into account [12, 13, 14, 15]. Doing so, however, requires the introduction of initial conditions for higher moments of the Vlasov equation which cannot be assumed to be Gaussian and which cannot be inferred as easily from measurements of the Cosmic Microwave Background as is the case for the density and velocity field. In addition, there is no longer a valid justification to truncate the hierarchy of moments at a specific order since the assumption of a quasi-equilibrium clearly no longer holds. It is, therefore, desirable to work with the full phase-space information of the system and to avoid introducing a truncation based on the moments of the distribution. In this thesis we present two approaches based on the path-integral formulation of classical mechanics which allow us to do that.

In the early 1930s, Bernard Koopman [16] and John von Neumann [17] constructed an operatorial formulation of classical mechanics, in close analogy to the then newly established formalism of quantum mechanics. A few decades later, this idea was generalized by Martin, Siggia, and Rose [18]—now known as the MSR formalism—to more general deterministic and stochastic systems. Functional integral methods were subsequently introduced by Janssen and DeDominicis [19, 20, 21], who were able to reproduce and further generalize the results of MSR to systems with arbitrary deterministic and stochastic forces, therefore referred to as the MSR/JD formalism. Building on these developments, Gozzi et al. [22, 23] extensively studied and pioneered a systematic path-integral formulation of classical Hamiltonian mechanics, directly grounded in the Koopman-von Neumann framework. The underlying idea behind all these developments was to apply the wealth of existing functional methods—most prominently the Dyson-Schwinger equations of motion—to classical systems [24] with the goal of formulating classical statistical mechanics in the same language, and with the same generality and rigor, as quantum field theory [18]. After providing a basic introduction to classical statistical mechanics in 2, we briefly summarize the path-integral formalisms of KvN and MSR/JD in 3.

We use the KvN path-integral formulation in chapter 4 to derive a formal solution to the Liouville equation [25] and set up a perturbation theory which allows us to compute unequal-time correlation functions of the Klimontovich phase-space density.

The idea behind this perturbative approach is the propagation of individual particles along their respective trajectories and the inclusion of particle interactions order by order in the interaction potential. This is, of course, not a novel idea and bears a resemblance to the resolvent theory developed by [26], the theory developed by [27, 28] and corresponds to the idea of the Kinetic Field Theory approach developed and extensively studied by [29, 30, 31]. It is clear that such a perturbative approach can be insufficient to deal with realistic systems as the convergence of such a perturbation theory is too slow. We, therefore, take this perturbative approach as a starting point for the derivation of a field theory which allows us to resum certain effects.

The path integral formulation of chapter 4 makes it convenient to develop a resummed field theory for microscopic particles by applying a Hubbard-Stratonovich transformation (HST) [32, 33] to the generating functional in chapter 5. The HST leads to an effective field theoretic description which contains the full statistics of the microscopic system in its vertices. Such an approach was first explored in [34, 35], but was derived differently. While this approach allows us to resum certain microscopic effects and yields viable results for cosmic large-scale formation, its vertex structure poses a major difficulty.

The main result of this thesis is developed and presented in chapters 6 and 7. Building on the methods described in [21, 36, 37] a new approach based on the path-integral of classical mechanics and the Klimontovich equation is developed. Instead of microscopic particle trajectories, this field theory is directly built on the dynamics of the fields themselves. In chapter 6 we first provide an intuitive derivation for the new field theory and make the connection to the resummed field theory of chapter 5. Next, in chapter 7 we then present a technical and complete derivation of the theory and derive the associated Dyson-Schwinger equations. The specification of the formalism to statistically homogeneous and isotropic systems is presented in chapter 8, where analytical solutions are discussed.

After providing a basic introduction to cosmology in chapter 9 and specifying the dynamics and initial conditions for the ensemble of cosmic particles in the Universe in 10, we finally present the results for the density-fluctuation power spectrum up to first-loop order and the tree-level result for the bispectrum 11 obtained in the frameworks developed in this work.

1

Path Integrals for Classical N-Particle Systems - Particle Picture

2 General Concepts of Classical Statistical Mechanics

In this first chapter we briefly recap the most important concepts of classical statistical dynamics that we are going to use throughout this work. We first introduce the statistical ensemble as a whole, discuss the interparticle interactions and free motion, before turning to the probabilistic description, including the concept of correlations and the dynamical evolution equations. Throughout the whole chapter we follow [26, 38, 37], and we reference further literature when appropriate.

2.1. Hamiltonian Mechanics of N Particles

We consider a classical dynamical system composed of N identical point-like particles confined to a volume $\mathcal{V} \subset \mathbb{R}^3$. The instantaneous spatial state of the system is specified by the positions $\vec{q}_j \in \mathcal{V}$, $j = 1 \dots, N$ of all particles at a given time t. The space of all such possible position configurations defines the *configuration space* of the system,

$$Q = \left\{ (\vec{q}_1, \vec{q}_2, \dots, \vec{q}_N) | \vec{q}_j \in \mathcal{V} \subset \mathbb{R}^3, \right\} \subset \mathbb{R}^{3N}.$$
 (2.1)

In order to describe the exact microscopic state, one has to additionally include the particles' conjugate momenta $\vec{p}_j \in \mathbb{R}^3$, such that each particle is characterized by its six-dimensional phase-space coordinate¹ $x_j = (\vec{q}_j, \vec{p}_j), j = 1, ..., N$. The coordinates (\vec{q}_j, \vec{p}_j) are often referred to as the canonical variables. At any given time t, the exact microstate of the system is therefore entirely specified by the set $\{x_j\}_{j=1}^N$ of particle phase-space coordinates which together constitute a point in a 6N-dimensional combined phase-space, which we will refer to as Γ -space,

$$\Gamma = \left\{ (\mathsf{x}_1, \mathsf{x}_2, \dots, \mathsf{x}_N) | \ \mathsf{x}_j = (\vec{\mathsf{q}}_j, \vec{\mathsf{p}}_j), \ \vec{\mathsf{q}}_j \in \mathcal{V} \subset \mathbb{R}^3, \ \vec{\mathsf{p}}_j \in \mathbb{R}^3 \right\} \subset \mathbb{R}^{6N}. \tag{2.2}$$

Therefore, any point $\{x_j\} \in \Gamma$ represents a specific microscopic configuration of the system.

Due to the indistinguishable nature of the particles, most quantities of interest,

¹In general, \vec{q}_j and \vec{p}_j are the generalized positions and momenta of the Hamiltonian system. They can additionally represent internal degrees of freedom, if the particles under consideration are not strictly point-like.

such as the Hamilton function, depend on the entire particle ensemble. Therefore, to simplify notation and avoid excessive indexing, following [29] we collect all quantities with a particle index into multi-particle tensors, i. e.,

$$\mathbf{A}(t) = \sum_{j=1}^{N} \mathbf{A}_{j}(t) \otimes e_{j}, \qquad (2.3)$$

where e_j is the N-dimensional canonical unit vector in \mathbb{R}^N . This allows us to collect the coordinates of Γ -space into a single object, $\mathbf{x} = (\mathsf{x}_1, \mathsf{x}_2, \dots, \mathsf{x}_N)$, representing the state of the system. Furthermore, the scalar product between two tensor-valued objects \mathbf{A} and \mathbf{B} decomposes as

$$\mathbf{A} \cdot \mathbf{B} = \sum_{j,i=1}^{N} (\mathsf{A}_i \otimes e_i) \cdot (\mathsf{B}_j \otimes e_j) = \sum_{j,i=1}^{N} \mathsf{A}_i \mathsf{B}_j \underbrace{e_i \cdot e_j}_{=\delta_{i,i}} = \sum_{i=1}^{N} \mathsf{A}_i \mathsf{B}_i. \tag{2.4}$$

Functions depending on all particle positions can be compactly written as $F(\mathbf{x}, t)$ and the integration measure on Γ -space is given by

$$d^{6N}\mathbf{x} = d^{3N}\mathbf{q} d^{3N}\mathbf{p} \equiv d\mathbf{q} d\mathbf{p} = d\mathbf{x}. \tag{2.5}$$

The time evolution of the system is then given by a trajectory $\mathbf{x}(t)$ in Γ -space. Thus, in order to understand the time evolution of the system as a whole we need to understand the dynamical laws governing the motion of the individual particles. In the Hamiltonian description of classical mechanics these dynamics are fully determined by the (possibly time-dependent) Hamiltonian function $H(\mathbf{x},t)$, which, in many physical systems, corresponds to the total energy. More precisely, the individual trajectories are subject to the Hamiltonian equations of motion

$$\frac{\mathrm{d}}{\mathrm{d}t}\vec{q}_{j}\left(t\right) = \nabla_{\vec{p}_{j}}H(\{\mathsf{x}_{j}\},t), \qquad \frac{\mathrm{d}}{\mathrm{d}t}\vec{p}_{j}\left(t\right) = -\nabla_{\vec{q}_{j}}H(\{\mathsf{x}_{j}\},t), \quad j = 1,\ldots,N. \quad (2.6)$$

Introducing the canonical symplectic structure

$$\omega = \begin{pmatrix} 0 & \mathbb{1}_{3\times 3} \\ -\mathbb{1}_{3\times 3} & 0 \end{pmatrix} \in \mathbb{R}^{6\times 6}, \qquad (2.7)$$

the above equations can be brought into a compact form,

$$\dot{x}_j(t) = \omega \cdot \nabla_{x_j} H(\{\mathsf{x}_j\}, t), \quad j = 1, \dots, N,$$
(2.8)

where $\nabla_{x_j} = (\nabla_{\vec{q}_j}, \nabla_{\vec{p}_j})^{\top}$ denotes the gradient on the single-particle phase space. Bundled together in the tensorial notation, we find

$$\dot{\mathbf{x}}(t) = \boldsymbol{\omega} \cdot \boldsymbol{\nabla}_{\mathbf{x}} H(\mathbf{x}, t) \,, \tag{2.9}$$

where ω is the N-particle generalization of the symplectic structure,

$$\boldsymbol{\omega} = \omega \otimes \mathbb{1}_{N \times N} \,. \tag{2.10}$$

Supplemented by a suitable initial configuration $\mathbf{x}^{(i)} = \mathbf{x}(t = t^{(i)})$ at initial time $t^{(i)}$, the solution to the equations of motion (2.9) exists and is unique². The initial configuration $\mathbf{x}^{(i)} \in \Gamma$ is then mapped to $\mathbf{x}_{cl}(t) \in \Gamma$ at a later time $t > t^{(i)}$ under the Hamiltonian flow,

$$\Phi_{\text{cl}}^t: \Gamma \to \Gamma, \quad \mathbf{x}^{(i)} \mapsto \mathbf{x}_{\text{cl}}(t) = \Phi_{\text{cl}}^t(\mathbf{x}^{(i)}, t^{(i)}), \quad \text{with} \quad \Phi_{\text{cl}}^{t^{(i)}} = \text{id}.$$
 (2.11)

We call $\mathbf{x}_{cl}(t)$ the classical trajectory in Γ -space. Importantly, the flow is symplectic,

$$\left[\nabla_{\mathbf{x}^{(i)}} \Phi_{\text{cl}}^t(\mathbf{x}^{(i)}, t^{(i)}) \right]^{\top} \cdot \boldsymbol{\omega} \cdot \left[\nabla_{\mathbf{x}^{(i)}} \Phi_{\text{cl}}^t(\mathbf{x}^{(i)}, t^{(i)}) \right] = \boldsymbol{\omega}, \qquad (2.12)$$

which in turn implies that the flow is also volume preserving,

$$\det\left(\mathbf{\nabla}_{\mathbf{x}^{(i)}}\Phi_{\mathrm{cl}}^{t}(\mathbf{x}^{(i)}, t^{(i)})\right) = 1. \tag{2.13}$$

This statement is famously known as the *Liouville theorem*, which is a cornerstone of classical statistical mechanics.

The total time derivative of a sufficiently smooth function $f(\mathbf{x}, t) : \Gamma \times \mathbb{R} \to \mathbb{R}$, depending on the canonical variables of all N particles, is given by

$$\frac{\mathrm{d}}{\mathrm{d}t} f(\mathbf{x}(t), t) = \mathbf{\nabla}_{\mathbf{x}}^{\top} f(\mathbf{x}, t) \cdot \dot{\mathbf{x}}(t) + \frac{\partial}{\partial t} f(\mathbf{x}, t)$$

$$= \mathbf{\nabla}_{\mathbf{x}}^{\top} f(\mathbf{x}, t) \cdot \boldsymbol{\omega} \cdot \mathbf{\nabla}_{\mathbf{x}} H(\mathbf{x}, t) + \frac{\partial}{\partial t} f(\mathbf{x}, t) , \tag{2.14}$$

where we applied the chain rule and inserted the Hamiltonian equations of motion $(2.9)^3$.

$$\{f(\mathbf{x},t),g(\mathbf{x},t)\} := \sum_{j=1}^{N} \left(\nabla_{\vec{\mathbf{q}}_{j}}^{\top} f(\mathbf{x},t) \cdot \nabla_{\vec{\mathbf{p}}_{j}} g(\mathbf{x},t) - \nabla_{\vec{\mathbf{q}}_{j}}^{\top} g(\mathbf{x},t) \cdot \nabla_{\vec{\mathbf{p}}_{j}} f(\mathbf{x},t) \right), \qquad (2.15)$$

such that the total time derivative becomes:

$$\frac{\mathrm{d}}{\mathrm{d}t}f(\mathbf{x},t) = \{f(\mathbf{x},t), H(\mathbf{x},t)\} + \frac{\partial}{\partial t}f(\mathbf{x},t),. \tag{2.16}$$

Throughout this thesis, we use the symplectic structure ω rather than the Poisson bracket for notational convenience. Both are, of course, equivalent and related via

$$\{f(\mathbf{x},t),g(\mathbf{x},t)\} = \nabla_{\mathbf{x}}^{\top} f(\mathbf{x},t) \cdot \boldsymbol{\omega} \cdot \nabla_{\mathbf{x}} g(\mathbf{x},t). \tag{2.17}$$

²Here and in the following we assume that all functions are sufficiently smooth, such that no problems arise from a purely mathematical point of view.

³At this point, standard textbooks usually introduce the N-particle Poisson bracket between two functions $f(\mathbf{x},t)$ and $g(\mathbf{x},t)$ as

We conclude this short summary of classical mechanics by emphasizing again that the Hamiltonian equations of motion (2.9) are fully deterministic: once the Hamiltonian function $H(\mathbf{x},t)$ is specified and supplemented by an initial particle configuration $\mathbf{x}^{(i)}$, the evolution of the system is uniquely determined. Accordingly, there is one and only one trajectory through each individual point in Γ -space. In the next two sections we, therefore, discuss the specific form of the Hamiltonian function and the subtleties concerning the initial configuration in more detail.

2.1.1. The *N*-particle Hamiltonian Function

In most physically relevant systems, the Hamiltonian $H(\mathbf{x},t)$ is too complex to allow for a closed-form solution of the equations of motion. Therefore, one usually decomposes $H(\mathbf{x},t)$ into an exactly solvable part $H_0(\mathbf{x},t)$ and a residual part $H_{\text{int}}(\mathbf{x},t)$ which accounts for *interactions*,

$$H(\mathbf{x},t) = H_0(\mathbf{x},t) + H_{\text{int}}(\mathbf{x},t). \tag{2.18}$$

Typically, this latter part arises from an external potential or, in the case of multiparticle systems, from inter-particle interactions. This decomposition allows to incorporate the interactions in a given approximation procedure around the exact solution which hence serves as a reference trajectory in the formulation. Let us first discuss the dynamics given by $H_0(\mathbf{x},t)$, before considering the more complex case involving interactions.

Free Hamiltonian To enable an analytic treatment, we assume that $H_0(\mathbf{x}, t)$ is quadratic in the phase-space coordinates. This structure ensures that the corresponding Hamiltonian equations of motion are linear and can, in principle, be solved using the method of Green's functions. More specifically, we demand that

$$H_0(\mathbf{x}, t) := \frac{1}{2} \mathbf{x}^\top \cdot \mathbf{A}(t) \cdot \mathbf{x},$$
 (2.19)

where the symmetric, possibly time dependent matrix A(t) contains information about the free motion, and may also receive harmonic contributions that may be included in the exactly solvable dynamics. Since the particles are indistinguishable, the contributions to A(t) have to be the same for all particles, i. e.,

$$\mathbf{A}(t) = A(t) \otimes \mathbb{1}_{N \times N}. \tag{2.20}$$

Throughout this work we will refer to $H_0(\mathbf{x},t)$ as the *free* Hamiltonian, meaning the exactly solvable part of the dynamics, regardless of whether it describes purely non-interacting or including harmonic motion. The corresponding free Hamiltonian equations of motion are then given by

$$\dot{\mathbf{x}}^{(0)}(t) = \boldsymbol{\omega} \cdot \boldsymbol{A}(t) \cdot \mathbf{x}^{(0)}(t), \qquad (2.21)$$

which, due to their linearity, admit a solution in terms of a retarded Green function for a free particle $\mathbf{G}(t, t^{(i)})$. It maps the initial phase-space coordinate $\mathbf{x}^{(i)}$ to the

later coordinate $\mathbf{x}_{\mathrm{cl}}^{(0)}(t)$ at time t according to

$$\mathbf{x}_{cl}^{(0)}(t) = \mathbf{G}(t, t^{(i)}) \cdot \mathbf{x}^{(i)}. \tag{2.22}$$

Clearly, the free-particle Green function is identical for every particle,

$$G(t, t') = G(t, t') \otimes \mathbb{1}_{N \times N}, \text{ with } G(t, t') \propto \Theta(t - t'),$$
 (2.23)

where the Heaviside function ensures the causal propagation of particles. The single-particle Green function can generally be decomposed into four 3×3 blocks,

$$G(t,t') = \begin{pmatrix} g_{qq}(t,t')\mathbb{1}_{3\times 3} & g_{qp}(t,t')\mathbb{1}_{3\times 3} \\ g_{pq}(t,t')\mathbb{1}_{3\times 3} & g_{pp}(t,t')\mathbb{1}_{3\times 3} \end{pmatrix} \Theta(t-t'), \qquad (2.24)$$

where the g's describe the mapping of the phase-space positions and momenta at earlier times to the ones at later times. We find for the components of the respective trajectory,

$$\vec{q}_{j}(t) = g_{qq}(t, t^{(i)}) \vec{q}_{j}^{(i)} + g_{qp}(t, t^{(i)}) \vec{p}_{j}^{(i)}, \qquad j = 1, \dots, N.$$

$$\vec{p}_{j}(t) = g_{pq}(t, t^{(i)}) \vec{q}_{j}^{(i)} + g_{pp}(t, t^{(i)}) \vec{p}_{j}^{(i)}, \qquad j = 1, \dots, N.$$
(2.25)

Therefore, solving the equations of motion directly for the components $g_{ab}(t, t')$ is equivalent to solving for the full Green's function G(t, t'). In order to establish a connection between the particle Green function G(t, t') and the matrix A(t), one finds, by substituting the formal solution (2.22) into the equations of motion (2.21), that the *retarded* Green's function satisfies the inhomogeneous symplectic flow equation

$$\left[\frac{\partial}{\partial t} - \boldsymbol{\omega} \cdot \boldsymbol{A}(t)\right] \boldsymbol{G}(t, t') = \delta_{\mathrm{D}}(t - t') \, \mathbb{1}_{6N \times 6N}, \quad \boldsymbol{G}(t, t') = 0 \quad (t < t'). \quad (2.26)$$

The general solution to the above equation is given by the time-ordered exponential,

$$\boldsymbol{G}(t,t') = \hat{\mathcal{T}} \exp\left[\int_{t'}^{t} d\bar{t} \,\boldsymbol{\omega} \cdot \boldsymbol{A}(\bar{t})\right] \Theta(t-t'). \qquad (2.27)$$

Since this form is usually quite complicated to handle due to the generally non-commutative structure of the generator $\boldsymbol{\omega} \cdot \boldsymbol{A}(t)$, we can employ a *Magnus expansion* [39] which replaces the above time-ordered exponential by a true matrix exponential,

$$G(t, t') = \exp \left[\Omega(t, t')\right] \Theta(t - t'), \qquad (2.28)$$

where the matrix operator $\Omega(t,t')$ is given by a series expansion of nested commutators of $\boldsymbol{\omega} \cdot \boldsymbol{A}(t)$, i. e., $\Omega(t,t') = \sum_{n=0}^{\infty} \Omega_n(t,t')$. The first terms read

$$\Omega_1(t,t') = \int_{t'}^t dt_1 \boldsymbol{\omega} \cdot \boldsymbol{A}(t_1)$$
 (2.29)

$$\Omega_2(t, t') = \frac{1}{2} \int_{t'}^t dt_1 \int_{t'}^{t_1} dt_2 \left[\boldsymbol{\omega} \cdot \boldsymbol{A}(t_1), \boldsymbol{\omega} \cdot \boldsymbol{A}(t_2) \right]$$
(2.30)

$$\mathbf{\Omega}_{3}(t,t') = \frac{1}{6} \int_{t'}^{t} \mathrm{d}t_{1} \int_{t'}^{t_{1}} \mathrm{d}t_{2} \int_{t'}^{t_{2}} \mathrm{d}t_{3} \left(\left[\boldsymbol{\omega} \cdot \boldsymbol{A}(t_{1}), \left[\boldsymbol{\omega} \cdot \boldsymbol{A}(t_{2}), \boldsymbol{\omega} \cdot \boldsymbol{A}(t_{3}) \right] \right]$$
(2.31)

+
$$[\boldsymbol{\omega} \cdot \boldsymbol{A}(t_3), [\boldsymbol{\omega} \cdot \boldsymbol{A}(t_2), \boldsymbol{\omega} \cdot \boldsymbol{A}(t_1)]]$$
 (2.32)

:

with the matrix commutator $[\mathbf{A}, \mathbf{B}] = \mathbf{A} \cdot \mathbf{B} - \mathbf{B} \cdot \mathbf{A}$. In particular, if $\boldsymbol{\omega} \cdot \mathbf{A}(t)$ commutes with itself at different times, the solution is given by

$$\boldsymbol{G}(t,t') = \exp\left[\int_{t'}^{t} d\bar{t} \,\boldsymbol{\omega} \cdot \boldsymbol{A}(\bar{t})\right] \Theta(t-t'). \qquad (2.33)$$

The Green's function, being derived from a Hamiltonian flow (2.26), possesses several important properties that are analogous to the general properties of the Hamiltonian flow (2.12) and (2.13). First, it is symplectic, i.e.,

$$\mathbf{G}^{\mathsf{T}}(t,t') \cdot \boldsymbol{\omega} \cdot \mathbf{G}(t,t') = \boldsymbol{\omega}, \quad \forall t > t',$$
 (2.34)

which reflects the preservation of phase-space volume and the canonical structure underlying the free Hamiltonian evolution. An immediate consequence of symplecticity is that the determinant of G is unity,

$$\det\left(\boldsymbol{G}(t,t')\right) = 1, \quad \forall t > t'. \tag{2.35}$$

Moreover, the Green function satisfies the additivity property,

$$G(t, t'') = G(t, t') \cdot G(t', t''), \quad \forall t > t' > t''.$$
 (2.36)

This property follows directly from the uniqueness of solutions to the linear equations of motion and reflects the fact that evolving the system in two steps is equivalent to evolving it in one. This concludes our discussion of the free motion.

Interacting Hamiltonian Moving on to the interacting part, we recall that it will generally be a function of all N particles,

$$H_{\rm int}(\mathbf{x},t) \equiv H_{\rm int}(x_1,\dots,x_N,t). \tag{2.37}$$

Since the particles are identical and therefore indistinguishable, $H_{\text{int}}(x_1, \ldots, x_N, t)$ is necessarily symmetrical under any permutation of the particles, i.e., $\forall i, j = 1 \ldots N$,

we have

$$H_{\text{int}}(x_1, \dots, x_i, \dots, x_j, \dots, x_N, t) = H_{\text{int}}(x_1, \dots, x_j, \dots, x_i, \dots, x_N, t),$$
 (2.38)

and may thus be uniquely decomposed as

$$H_{\text{int}}(\mathbf{x},t) = \sum_{i_1=1}^{N} v_1(\mathbf{x}_{i_1},t) + \frac{1}{2!} \sum_{i_1 \neq i_2=1}^{N} v_2(\mathbf{x}_{i_1},\mathbf{x}_{i_2},t) + \dots + v_N(x_1,\dots,x_N,t) . \quad (2.39)$$

The functions v_k are non-additive symmetric functions of k variables and are referred to as k-particle potentials⁴. The indistinguishability of the particles implies that v_1 must be identical for each particle, and likewise for v_2 and all higher-order interaction potentials. The combinatorial prefactor $\frac{1}{k!}$ compensates the overcounting of particle pairs in the summation. In almost all cases of interest⁵ $v_k = 0$ for k > 2, which is what we are going to assume throughout this work. Thus, we find

$$H_{\text{int}}(\mathbf{x},t) = \sum_{i=1}^{N} v_1(\mathbf{x}_i,t) + \frac{1}{2!} \sum_{i\neq j=1}^{N} v_2(\mathbf{x}_i,\mathbf{x}_j,t).$$
 (2.40)

The single-particle potential $v_1(x_i, t)$ describes the influence of a time-dependent external potential on the motion of particles, for instance due to an external electric or magnetic field. In general, it can depend on the particle position and momentum. The possibly time-dependent two-particle potential $v_2(x_i, x_j, t)$, on the other hand, governs the pairwise interactions between particles. Typical examples would be the Newtonian gravitational interaction potential or the Lennard-Jones potential.

With the dynamical evolution governed by the Hamiltonian function now established, we next turn to the discussion of initial conditions, which are required to uniquely determine the system's trajectory through phase space.

2.1.2. The N-Particle Phase-Space Density

Given the exact positions and momenta of all particles at some initial time $t^{(i)}$, the deterministic nature of the Hamiltonian equations of motion ensures that their values at any late time are uniquely determined. However, for systems with a very large number of particles, $N \gg 1$, this microscopic information is neither practically accessible, nor is it necessary. In most cases one is not interested in the precise state of every individual particle, but rather in collective phenomena, such as density correlations or phase-transitions, that are properties of the particle ensemble as a whole. This gives rise to the idea of a probabilistic description of the system. Instead of specifying the exact microstate of the system, one investigates the *probability* of

⁴In the above decomposition we have neglected the zero-particle potential v_0 which has to be a constant and thus does not appear in the equations of motion.

⁵In practice, one rarely encounters an explicit three-particle interaction as a fundamental term in the classical Hamiltonian. Those effects usually emerge as effective contributions from underlying two-body potentials. Nonetheless, extending our phase-space formalism to include such higher-order k-particle potentials is straightforward.

finding the system in a given microscopic configuration. One therefore introduces the N-particle Liouville phase-space density distribution (from here on called Liouville phase-space density) $\varrho_N(\mathbf{x},t)$ at time t on Γ -space. It is always non-negative and normalized to unity,

$$\varrho_N(\mathbf{x}, t) \ge 0 \quad \forall \; \mathbf{x}, t, \quad \text{and} \quad \int_{\Gamma} d^{6N} \mathbf{x} \, \varrho_N(\mathbf{x}, t) = 1,$$
(2.41)

where the integration runs over the whole Γ -space. Thus, $\varrho_N(\mathbf{x},t)\mathrm{d}\mathbf{x}$ describes the probability of finding the system in the infinitesimal volume $\mathrm{d}\mathbf{x}$ around the specific microstate \mathbf{x} . We may therefore see the position \mathbf{x} in the 6N-dimensional phase-space as a random variable with probability distribution $\varrho_N(\mathbf{x},t)$. The fact that particles can neither be destroyed nor created in the full Γ -space, combined with the volume preserving property of the Hamiltonian flow (2.13), implies that the phase-space density must remain constant along the trajectories of the system. In other words, the total time derivative of $\varrho_N(\mathbf{x},t)$ must vanish. From the general expression (2.14) for the time evolution of functions in phase-space, we deduce the N-particle Liouville equation,

$$0 = \frac{\partial}{\partial t} \varrho_N(\mathbf{x}, t) + \mathbf{\nabla}_{\mathbf{x}}^{\top} \varrho_N(\mathbf{x}, t) \cdot \boldsymbol{\omega} \cdot \mathbf{\nabla}_{\mathbf{x}} H(\mathbf{x}, t), \qquad (2.42)$$

which may be written as

$$\frac{\partial}{\partial t}\varrho_N(\mathbf{x},t) = \hat{\mathcal{L}}(t)\,\varrho_N(\mathbf{x},t)\,,\tag{2.43}$$

with the Liouvillian

$$\hat{\mathcal{L}}(t) := \mathbf{\nabla}_{\mathbf{x}}^{\top} H(\mathbf{x}, t) \cdot \boldsymbol{\omega} \cdot \mathbf{\nabla}_{\mathbf{x}}. \tag{2.44}$$

Inserting the decomposition of the Hamiltonian function (2.18) into free and interacting dynamics, we find the analogous decomposition of the Liouvillian,

$$\hat{\mathcal{L}}(t) = \hat{\mathcal{L}}_0(t) + \hat{\mathcal{L}}_{int}(t). \tag{2.45}$$

The Liouville equation can be interpreted as a 6N-dimensional continuity equation describing the conservation of the total probability density in Γ -space. The knowledge of the Liouville phase-space density at a given time t, thus, provides us with the complete information about the system's macroscopic state. In the next section we will therefore define how actual macroscopic quantities can be computed from it.

Before concluding, we note that the Liouville equation, due to its linearity, admits the formal solution,

$$\varrho_N(\mathbf{x}, t) = \hat{U}(t, t^{(i)}) \, \varrho_N^{(i)}(\mathbf{x}), \quad \text{with} \quad \varrho_N^{(i)}(\mathbf{x}) \equiv \varrho_N(\mathbf{x}, t = t^{(i)}).$$
(2.46)

The operator $\hat{U}(t, t^{(i)})$ is called the *time-evolution operator* of the Liouville equation and is given by

$$\hat{U}(t, t^{(i)}) = \hat{\mathcal{T}} \exp\left[\int_{t^{(i)}}^{t} dt_1 \,\hat{\mathcal{L}}(t_1)\right], \qquad (2.47)$$

where $\hat{\mathcal{T}}$ is the time-ordering operator necessary if the Liouvillian is explicitly time-

dependent. The Liouville propagator describes the deterministic time evolution of the entire phase-space distribution. Thus, once an initial phase-space density is specified the statistical state of the system is, in principle, exactly known at all later times. However, the exact form of the Liouville propagator (2.47) is too abstract to be practically useful. Hence, we need to find a different approach to solving the Liouville equation. The standard approach summarized in the forthcoming sections is based on the idea of reducing the number of relevant degrees of freedom and deriving differential equations similar to the Liouville equation (2.42) that approximate the exact evolution.

2.2. Observables and Expectation Values

The previous discussion makes it clear that one has to distinguish between the *microscopic description* of the system and the *macroscopic description*. While the former contains the detailed particle-level dynamics and is therefore generally inaccessible to our measurements, the latter provides a coarse-grained view of the system that does not rely on the exact microscopic state.

In order to connect both levels of description we first introduce the concept of (microscopic) dynamical functions that represent a specific physical property associated with the microscopic degrees of freedom. On a mathematical level, a dynamical function is defined as a function $b(\mathbf{x}) \equiv b(x_1, \ldots, x_N)$ on the full 6N-dimensional phase space which, thus, depends on the exact microscopic configuration⁶. The same reasoning as for the interacting Hamiltonian (2.39) leads to the general decomposition

$$b(x_1, \dots, x_N) = b_0 + \sum_{i_1=1}^N b_1(x_{i_1}) + \frac{1}{2!} \sum_{i_1 \neq i_2=1}^N b_2(x_{i_1}, x_{i_2}) + \dots + b_N(x_1, \dots, x_N), \quad (2.48)$$

where b_s is symmetric, non-additive function of s phase-space coordinates. Therefore, we refer to b_s as the irreducible s-particle contribution to the dynamical function b as it involves information of s distinct particles. In general, we will be interested in dynamical functions with only a small number of irreducible s-particle contributions. The dynamical functions generally exhibit strong fluctuations that are due to the discrete nature of the particle description.

We can now define the $macroscopic\ observable$ associated to the dynamical function $b(\mathbf{x})$ by taking the $ensemble\ average$ over the Liouville phase-space density at time t,

$$B(t) := \langle b(\mathbf{x}) \rangle = \int d\mathbf{x} \, b(\mathbf{x}) \varrho_N(\mathbf{x}, t) \,. \tag{2.49}$$

We, thus, sum over multiple realizations of the microscopic quantity $b(\mathbf{x})$, weighted by the respective probability at time t. Importantly, in the above picture, the time

⁶Here, we assume for simplicity that the dynamical functions are not explicitly time-dependent, i.e., their time-dependence solely arise via the particle trajectories.

dependence of the observable B(t) is contained in the Liouville phase-space density, such that we can refer to the above description as the *Schrödinger picture* in close analogy to quantum mechanics. We may just as well consider the case where the phase-space density $\varrho_N^{(i)}(\mathbf{x}^{(i)})$ is specified at initial time $t^{(i)}$ once and for all, and let the particles evolve along their respective Hamiltonian trajectories, which explicitly enter the dynamical function itself. In that picture, the time evolution is given by

$$B(t) = \int d\mathbf{x} \, b(\mathbf{x}_{cl}(t; \mathbf{x}^{(i)}, t^{(i)})) \varrho_N^{(i)}(\mathbf{x}^{(i)}), \qquad (2.50)$$

where we made the parametric dependence of the classical trajectory on the initial conditions explicit, (cf. (2.11)). In the latter picture, the time evolution is contained in the microscopic degrees of freedom and thus in the dynamical functions, while the probability density remains constant in time. Ensemble averaging then corresponds to drawing multiple realizations of the initial particle coordinates and evolving each along its respective trajectory. Thus, randomness enters only in the initial uncertainty of the particle positions. We will refer to this picture as the *Heisenberg picture* of statistical mechanics. Both pictures are, of course, equivalent⁷. Throughout this work, we will generally adopt the intuition of the Heisenberg picture, specifying an initial Liouville density and describing the evolution of the system via the resulting approximate particle trajectories.

2.2.1. The Klimontovich Phase-Space Density

Our main macroscopic observables of interest are the *local densities*, which associate a physical quantity, such as mass, momentum, or energy, to a specific region in physical space. These local densities are typically continuous⁸ functions. In contrast, the corresponding microscopic dynamical functions are highly discontinuous, as they depend on the exact positions and momenta of individual particles which are discretely distributed in physical space. To bridge the microscopic and macroscopic descriptions, we introduce the μ -space, as opposed to the 6N-dimensional Γ -space, as the six-dimensional phase space of a single particle, spanned by coordinates⁹

$$\frac{\mathrm{d}}{\mathrm{d}t}b(\mathbf{x}(t)) = -\hat{\mathcal{L}}(t)b(\mathbf{x}(t)).$$

We note the important sign difference compared to the Liouville equation (2.43). The equivalence between the two pictures can be made explicit by a partial integration over phase space, assuming that the N-particle Liouville density vanishes sufficiently rapidly at infinity. This yields

$$\int_{\Gamma} b(\mathbf{x}(t))\hat{\mathcal{L}}(t)\varrho_{N}(\mathbf{x},t) = \int_{\Gamma} \left(-\hat{\mathcal{L}}(t)b(\mathbf{x}(t))\right)\varrho_{N}(\mathbf{x},t),,$$
(2.51)

showing that the time evolution can equivalently be assigned either to the phase-space density or to the dynamical observables [26].

⁷Indeed, from the general time-evolution of a function in phase-space, described by (2.14), we find for the dynamical function and equation similar to Liouville's equation,

⁸When considering boundaries in physical space, the local densities are given by piece-wise continuous functions.

⁹In order to make the distinction between the coordinates in μ - and Γ-space clear, we denote coordinates in Γ-space by sans serif letters, e. g., $\mathbf{x} = (\vec{\mathbf{q}}, \vec{\mathbf{p}})$. This will avoid confusion when the

 $x=(\vec{q},\vec{p})$. A microstate of the system can now equivalently be represented by N points in μ -space, corresponding to the N particles. The microscopic number density of particles at a given μ -space coordinate x is given by the $Klimontovich\ phase-space\ density\ \Phi_f(x,t)$, defined as

$$\Phi_f(x,t) := \sum_{i=1}^N \delta_{\mathcal{D}} \left(x - \mathsf{x}_i(t) \right) \,, \tag{2.52}$$

where every particle contributes a term $\delta_{\rm D}\left(x-{\sf x}_i(t)\right)$, meaning that either particle i is not located at x and does not contribute, or it is located at x and contributes an infinite amount due to the point-like nature of the particles. It is clear that Φ_f is a highly discontinuous object, with a sharp peak at every particle position, that contains the full phase-space information. It maps the 6N-dimensional Γ -space to the six-dimensional μ -space. The corresponding macroscopic density is obtained by averaging Φ_f over the whole particle ensemble. We define the one-particle reduced phase-space density at time t and position x as,

$$f_1(x,t) = \langle \Phi_f(x,t) \rangle = \int d\mathbf{x} \sum_{i=1}^N \delta_{\mathrm{D}} \left(x - \mathsf{x}_i(t) \right) \, \varrho_N(\mathbf{x},t) \,, \tag{2.53}$$

which describes the expected number of particles in an infinitesimal volume around the point x in μ -space at time t. The function f_1 is smooth by construction and forms the starting point for a coarse-grained macroscopic description. Note, that by its definition, $f_1(x,t)$ is normalized as

$$\int d^6x \, f_1(x,t) = N \,. \tag{2.54}$$

Many local densities can now be derived from Φ_f or f_1 , respectively. At each point \vec{q} and time t of physical space, the local physical densities can generally be defined as the momentum average of a function $F_{\mathcal{O}}(\vec{q}, \vec{p})$ w.r.t. the one-particle phase-space density $f_1(x,t)$,

$$\mathcal{O}(\vec{q}, t) = \int d^3 p \, F_{\mathcal{O}}(\vec{q}, \vec{p}) \, f_1(\vec{q}, \vec{p}, t) \,.$$
 (2.55)

Here, the function $F_{\mathcal{O}}(\vec{q}, \vec{p})$ encodes the physical quantity that one wishes to measure at \vec{q} . An important class of local densities are those for which the function $F_{\mathcal{O}}$ only depends on the momentum \vec{p} , $F_{\mathcal{O}}(\vec{q}, \vec{p}) = F_{\mathcal{O}}(\vec{p})$. These represent the important moments of the momentum distribution. For instance, we define the *physical particle number density* $\rho(\vec{q}, t)$, the momentum density $\vec{\Pi}(\vec{q}, t)$ and the stress-energy density

 $[\]mu$ -space coordinates will get external labels.

tensor $\hat{T}(\vec{q},t)$ as

$$\rho(\vec{q},t) = \int d^3p \, f_1(x,t) \tag{2.56}$$

$$\vec{\Pi}(\vec{q},t) = \int d^3p \, \vec{p} \, f_1(x,t)$$
 (2.57)

$$\hat{T}(\vec{q},t) = \int d^3p \, \vec{p} \otimes \vec{p} \, f_1(x,t) \,. \tag{2.58}$$

The respective microscopic dynamical functions are then defined as

$$\Phi_{\mathcal{O}}(\vec{q},t) = \sum_{i=1}^{N} F_{\mathcal{O}}(\vec{\mathsf{p}}_i(t)) \,\delta_{\mathrm{D}}\left(\vec{q} - \vec{\mathsf{q}}_i(t)\right) \,, \tag{2.59}$$

such that

$$\mathcal{O}(\vec{q},t) = \langle \Phi_{\mathcal{O}}(\vec{q},t) \rangle = \int d^3 p \, F_{\mathcal{O}}(\vec{p}) \, \langle \Phi_f(x,t) \rangle . \qquad (2.60)$$

Thus, both, Φ_f and f_1 , will play a fundamental role during the course of this work. We will generally not only be interested in the local average of a given observable at \vec{q} , but more generally how different observables measured at different positions are related to each other. This brings us to the next section.

2.2.2. Correlations

One of the most important concepts of statistical mechanics is that of correlations. Let us therefore note that the one-particle reduced phase-space density f_1 describes the probability of finding a *single* particle at the phase-space coordinate x independent of the other particles. It is a one particle effect, which can clearly be seen from its dynamical function Φ_f , where there is only one particle index which is summed over. In order to understand how two densities at different positions are related, we have to average over the product of two Φ_f 's. We define the two-point phase-space density correlation function¹⁰ (or simply two-point correlation function) as

$$\bar{C}_{ff}(x_1, x_2, t) = \langle \Phi_f(x_1, t) \Phi_f(x_2, t) \rangle
= \int d\mathbf{x} \sum_{i,j=1}^N \delta_D(x_1 - \mathbf{x}_i(t)) \, \delta_D(x_2 - \mathbf{x}_j(t)) \, \varrho_N(\mathbf{x}, t)$$

$$= \delta_D(x_1 - x_2) \, f_1(x_1, t) + f_2(x_1, x_2, t) \, .$$
(2.61)

The first term is the single-particle contribution to the two-point correlation function and arises from the i = j part of the double sum. It describes the effect of picking the same particle twice and is thus proportional to the one-particle reduced phase space density f_1 . For the second term, we have defined the two-particle reduced

 $^{^{10}}$ We added a "bar" on C here to distinguish these equal-time correlation functions from the unequal-time correlation functions introduced later.

phase-space density f_2 as

$$f_2(x_1, x_2, t) := \left\langle \sum_{i \neq j=1}^N \delta_{\mathcal{D}} \left(x_1 - \mathsf{x}_i(t) \right) \delta_{\mathcal{D}} \left(x_2 - \mathsf{x}_j(t) \right) \right\rangle. \tag{2.62}$$

It describes the joint probability of finding two distinct particles at the specified phase-space coordinates. Clearly, if the particles are completely independent, the resulting probability distributions are too, and we find that the joint probability f_2 factorizes,

$$f_2(x_1, x_2, t) = f_1(x_1, t) f_1(x_2, t), (2.63)$$

which describes an uncorrelated distribution of particles. In general, however, we expect that interactions among particles induce deviations of f_2 from the above product: Every particle influences the behavior of its neighboring particles, hence creating *correlations*. In order to measure correlations we define the *true two-particle correlation*

$$g_2(x_1, x_2, t) := f_2(x_1, x_2, t) - f_1(x_1, t) f_1(x_2, t),$$
 (2.64)

measuring the correlation between particles at x_1 and x_2 . With the help of g_2 we can define the connected part of the two-point correlation function (2.61) as

$$\bar{G}_{ff}(x_1, x_2, t) := \langle \Phi_f(x_1, t) \Phi_f(x_2, t) \rangle_c$$

$$= \langle \Phi_f(x_1, t) \Phi_f(x_2, t) \rangle - \langle \Phi_f(x_1, t) \rangle \langle \Phi_f(x_2, t) \rangle$$

$$= \delta_D(x_1 - x_2) f_1(x_1, t) + g_2(x_1, x_2, t),$$
(2.65)

where the subscript "c" denotes the connected part of the correlation function.

With the above motivation we can now introduce the general form of our main statistical quantities of interest. First, we define the s-particle reduced phase-space $density^{11}$ as

$$f_s(x_1, \dots, x_s, t) := \left\langle \sum_{i_1 \neq \dots \neq i_s = 1}^N \prod_{n=1}^s \delta_D \left(x_n - \mathsf{x}_{i_n}(t) \right) \right\rangle, \tag{2.66}$$

describing the joint probability of finding s distinct particles located at x_1, \ldots, x_s . Clearly, the normalization of the Liouville density implies the following normalization

$$f_s(\mathsf{x}_1,\ldots,\mathsf{x}_s,t) = \frac{N!}{(N-s)!} \int \mathrm{d}\mathsf{x}_{s+1}\ldots\mathrm{d}\mathsf{x}_N \,\varrho_N(\mathsf{x},t) \,.$$

This expression describes f_s as the marginalized probability distribution for finding any s particles at phase-space positions x_1, \ldots, x_s . The alternative definition used in the main text is mathematically equivalent but formulated to more directly support an interpretation in terms of correlation functions.

 $^{^{11}}$ We adopt a definition that differs from the conventional one often found in the literature, where the reduced s-particle distribution function is defined as

for the s-particle reduced densities,

$$\int d^6 x_1 \dots d^6 x_s f_s(x_1, \dots, x_s, t) = \frac{N!}{(N-s)!}.$$
 (2.67)

For an uncorrelated state, f_s decomposes into a product

$$f_s(x_1, \dots, x_s, t) = \prod_{n=1}^s f_1(x_n, t), \quad \forall s.$$
 (2.68)

In order to distinguish a correlated from an uncorrelated state, we decompose f_s into irreducible s-particle reduced correlation functions g_s . This can be achieved by subdividing the set $\{1, \ldots s\}$ into all possible non-empty disjoint subsets. Interpreting each subset as representing a group of mutually correlated particles, statistically independent of the other subsets, we obtain the required decomposition¹². For instance, for s = 2 and s = 3, we find¹³

$$f_{2}(x_{1}, x_{2}, t) = f_{1}(x_{1}, t)f_{1}(x_{2}, t) + g_{2}(x_{1}, x_{2}, t)$$

$$f_{3}(x_{1}, x_{2}, x_{3}, t) = f_{1}(x_{1}, t)f_{1}(x_{2}, t)f_{1}(x_{3}, t) + f_{1}(x_{1}, t)g_{2}(x_{2}, x_{3}, t)$$

$$+ f_{1}(x_{2}, t)g_{2}(x_{1}, x_{3}, t) + f_{1}(x_{3}, t)g_{2}(x_{1}, x_{2}, t)$$

$$+ g_{3}(x_{1}, x_{2}, x_{3}, t).$$

$$(2.69)$$

Analogously, we can describe the system by analyzing the k-point correlation function¹⁴

$$\bar{C}_{f\dots f}(x_1,\dots,x_k,t) := \langle \Phi_f(x_1,t)\dots\Phi_f(x_k,t)\rangle
= \int d\mathbf{x} \prod_{n=1}^k \sum_{i_n=1}^N \delta_{\mathcal{D}}(x_n - \mathsf{x}_{i_n}(t)) \,\varrho_N(\mathbf{x},t),$$
(2.70)

which decomposes into s-particle reduced densities as

$$\bar{C}_{f...f}(x_1, \dots, x_k, t) = \dots + f_k(x_1, \dots, x_k, t),$$
 (2.71)

where the ellipses stand for all s-particle contributions with s < k. They reflect the possibility of randomly picking the same particle multiple times. For instance, for

¹²We refer to [26] for a comprehensive and complete discussion of the decomposition of f_s into correlation patterns.

¹³Clearly, for s=1 the decomposition is trivial and a g_1 is not introduced.

¹⁴Note that in contrast to the s-particle reduced densities (2.66), the k-point correlation function does not exclude summation over same indices.

k = 3 we find

$$\bar{C}_{fff}(x_1, x_2, x_3, t) = \delta_{\rm D}(x_1 - x_2) \,\delta_{\rm D}(x_1 - x_3) \,f_1(x_1, t) + \delta_{\rm D}(x_1 - x_2) \,f_2(x_1, x_3, t)
+ \delta_{\rm D}(x_1 - x_3) \,f_2(x_1, x_2, t) + \delta_{\rm D}(x_2 - x_3) \,f_2(x_1, x_2, t)
+ f_3(x_1, x_2, x_3, t).$$
(2.72)

We will generally refer to these s-particle contributions with s < k as shot-noise effects, as they arise due to the discrete nature of the particles. This discreteness is reflected by the sharp Dirac-delta peak that accompanies them. They will play an important role in the description of particle collisions. The connected part of the correlators $\bar{C}_{f...f}$ has a similar representation in terms of s-particle correlation functions g_s ,

$$\bar{G}_{f\dots f}(x_1,\dots,x_k,t) = \langle \Phi_f(x_1,t)\dots\Phi_f(x_k,t)\rangle_c
= \dots + g_k(x_1,\dots,x_k,t),$$
(2.73)

where the ellipses again represent the corresponding connected shot-noise contributions. Although the distinction between the density correlation functions $\bar{C}_{f...f}$ and $\bar{G}_{f...f}$, and the s-particle reduced densities f_s and g_s may appear redundant at first, this distinction becomes crucial in later chapters. In particular, even for an uncorrelated state where $g_s = 0$ for all s > 1, the connected correlation functions still include a lowest-order shot-noise term that arises from the self-correlation of individual particles.

In some cases it will be useful to define the connected correlators for specific local densities at hand. For instance if one requires the correlation between the particle density at x_1 and the momentum density at x_2 . We therefore define

$$\bar{G}_{\mathcal{O}_1\dots\mathcal{O}_k}(\vec{q}_1,\dots,\vec{q}_k,t) = \langle \Phi_{\mathcal{O}_1}(\vec{q}_1,t)\dots\Phi_{\mathcal{O}_k}(\vec{q}_k,t)\rangle_c$$

$$= \int d^3p_1\dots d^3p_k F_{\mathcal{O}_1}(\vec{p}_1)\dots F_{\mathcal{O}_k}(\vec{p}_k)\bar{G}_{f\dots f}(x_1,\dots,x_k,t) ,$$
(2.74)

where the last equality shows how these are related to the connected Klimontovich phase-space density correlators. This makes the deep role played by the Klimontovich phase-space density manifest.

In summary, the full set of s-point correlation functions $\bar{C}_{f...f}$ or equivalently the s-particle reduced densities f_s , contains all the information encoded in the full N-particle phase-space density $\varrho_N(\mathbf{x},t)$. We have, thus, simply restructured the complexity contained in $\varrho_N(\mathbf{x},t)$. The advantage, however, lies in the fact that by studying the time evolution of the reduced densities f_s , we can now systematically introduce approximations in order to reduce the complexity of the full N-particle system.

2.3. The Klimontovich Equation and the BBGKY Hierarchy

Since the Klimontovich phase-space density plays a similar role in μ -space as the Liouville equation in Γ -space, we can derive an evolution equation for Φ_f , analogous to the Liouville equation, formulated purely in terms of μ -space coordinates [40]. To that end, we first note that the time dependence of $\Phi_f(x,t)$ enters only implicitly through the trajectories of individual particles. We, therefore, find from (2.14) for the time derivative of $\Phi_f(x,t)$ given in (2.52),

$$\frac{\partial}{\partial t_1} \Phi_f(x_1, t_1) = \sum_{i=1}^N \nabla_{\mathsf{x}_i}^\top \delta_{\mathsf{D}} \left(x_1 - \mathsf{x}_i(t_1) \right) \cdot \omega \cdot \nabla_{\mathsf{x}_i} H(\mathbf{x}, t) \,, \tag{2.75}$$

where the N-particle Hamiltonian function reads (c.f. (2.19) and (2.39))

$$H(\mathbf{x},t) = \sum_{i=1}^{N} \frac{1}{2} \mathbf{x}_{i}^{\top} \cdot A(t) \cdot \mathbf{x}_{i} + \sum_{i=1}^{N} v_{1}(\mathbf{x}_{i},t) + \frac{1}{2!} \sum_{i \neq j=1}^{N} v_{2}(\mathbf{x}_{i},\mathbf{x}_{j},t).$$
 (2.76)

Inserted into (2.75), we find

$$\frac{\partial}{\partial t_1} \Phi_f(x_1, t_1) = -\nabla_{x_1}^{\top} \Phi_f(x_1, t_1) \cdot \omega \cdot A(t_1) \cdot x_1 - \nabla_{x_1}^{\top} \Phi_f(x_1, t_1) \cdot \omega \cdot \nabla_{x_1} v_1(x_1, t_1)
- \int d^6 x_2 \nabla_{x_1}^{\top} \Phi_f(x_1, t_1) \cdot \omega \cdot \nabla_{x_1} v_2(x_1, x_2, t) \Phi_f(x_2, t_1), \qquad (2.77)$$

where we have replaced the particle coordinates x by the μ -space coordinates x using the Dirac-delta distributions of Φ_f^{15} . The resulting equation can be compactly written as

$$\left[\frac{\partial}{\partial t_{1}} - \hat{\mathcal{L}}_{1}^{(0)}(t_{1}) - \hat{\mathcal{L}}_{1}^{(1)}(t_{1})\right] \Phi_{f}(x_{1}, t_{1}) = \int d^{6}x_{2} \,\hat{\mathcal{L}}_{12}^{(2)}(t_{1}) \,\Phi_{f}(x_{1}, t_{1}) \,\Phi_{f}(x_{2}, t_{1}),$$

$$\hat{\mathcal{L}}_{1}^{(0)}(t_{1}) \coloneqq x_{1}^{\top} \cdot A(t_{1}) \cdot \omega \cdot \nabla_{x_{1}},$$

$$\hat{\mathcal{L}}_{1}^{(1)}(t_{1}) \coloneqq \nabla_{x_{1}}^{\top} v_{1}(x_{1}, t_{1}) \cdot \omega \cdot \nabla_{x_{1}},$$

$$\hat{\mathcal{L}}_{12}^{(2)}(t_{1}) \coloneqq \nabla_{x_{1}}^{\top} v_{2}(x_{1}, x_{2}, t) \cdot \omega \cdot \nabla_{x_{1}}.$$
(2.78)

Equation (2.78), thus, describes the time evolution of the Klimontovich phase-space density Φ_f in terms of a set of linear and nonlinear operators. The left-hand side contains the free evolution operator $\hat{\mathcal{L}}^{(0)}$, which generates the Hamiltonian flow associated with the free Hamiltonian (cf. (2.19)), and the one-particle interaction operator $\hat{\mathcal{L}}^{(1)}$, which accounts for the influence of external fields acting independently on each particle. Both of these terms are linear in Φ_f and hence do not induce correlations, as they do not couple the phase-space densities at different positions.

¹⁵Note that the differential operators now act on the μ -space coordinates x.

The right-hand side, in contrast, contains a nonlinear term involving the two-particle interaction operator $\hat{\mathcal{L}}^{(2)}$, which governs the effects of pairwise interactions. This term introduces a coupling between the fields $\Phi_f(x_1, t_1)$ and $\Phi_f(x_2, t_1)$, such that the density at position x_2 acts as a source for the interaction potential $v_2(x_1, x_2, t_1)$, affecting the evolution of the density at x_1 . As a result, this term is responsible for the generation of correlations between particles through their mutual interactions. Equation (2.78) is known as the **Klimontovich equation**¹⁶. It is an exact representation of the microscopic dynamics in μ -space and contains the same information as the N-particle Liouville equation (2.42). In this sense, it can be interpreted as the μ -space counterpart of the Liouville equation, describing the evolution of the microscopic density field rather than the full probability distribution in Γ -space. The Klimontovich equation will play a central role in the developments presented in chapters 6 and 7.

In order to systematically analyze and structure the macroscopic information contained in (2.78) we take the ensemble average on both sides and find, with the definitions (2.53) and (2.62),

$$\left[\frac{\partial}{\partial t_1} - \hat{\mathcal{L}}_1^{(0)}(t_1) - \hat{\mathcal{L}}_1^{(1)}(t_1) \right] f_1(x_1, t_1) = \int d^6 x_2 \, \hat{\mathcal{L}}_{12}^{(2)}(t_1) f_2(x_1, x_2, t_1) \,. \tag{2.79}$$

This equation governs the evolution of the continuous one-particle probability density $f_1(x_1, t_1)$, which describes the probability of finding a particle at phase-space coordinate x_1 at time t_1 . In contrast to the Klimontovich equation (2.78), however, it is not closed, as the two-particle reduced phase-space distribution $f_2(x_1, x_2, t_1)$ enters on the right-hand side. This matches the intuition that in the presence of two-particle interactions, the evolution of the one-particle distribution $f_1(x_1, t_1)$ depends on the probability of simultaneously finding another particle at x_2 . Since this information is encoded in the two-particle distribution function $f_2(x_1, x_2, t_1)$, the evolution of f_1 cannot be closed at the level of f_1 alone. Thus, we have to complement (2.79) by an evolution equation for $f_2(x_1, x_2, t_1)$. To derive this next equation, we apply a partial time derivative to expression (2.62) and use the product rule, following analogous steps to those used above, to arrive at

$$\left[\frac{\partial}{\partial t_1} - \sum_{i=1}^2 \left\{ \hat{\mathcal{L}}_i^{(0)}(t_1) + \hat{\mathcal{L}}_i^{(1)}(t_1) \right\} \right] f_2(x_1, x_2, t_1) =$$

$$\int d^6 x_3 \sum_{i=1}^2 \left\{ \hat{\mathcal{L}}_{i3}^{(2)}(t_1) \right\} f_3(x_1, x_2, x_3, t_1) .$$
(2.80)

Again, the left-hand side represents the free streaming of particles and interactions with an external potential. The operators $\mathcal{L}^{(0)}$ and $\mathcal{L}^{(1)}$ are now applied to both particles at x_1 and x_2 . The right-hand side introduces the three-particle reduced distribution $f_3(x_1, x_2, x_3, t_1)$ through the two-particle interaction operators $\hat{\mathcal{L}}^{(2)}$,

¹⁶Named after Yuri Lvovich Klimontovich, who extensively studied this equation in the context of non-equilibrium plasma dynamics [41].

reflecting interactions between each of the two particles at x_1 , x_2 and a third, external¹⁷ particle at x_3 . As with the first equation for f_1 , this equation is not closed, and its evolution depends on the next distribution in the hierarchy, f_3 . Clearly, this recursive structure gives rise to a hierarchy of coupled equations for the reduced phase-space distributions, known as the **BBGKY hierarchy**¹⁸ (c.f. [42, 43, 44]). The s-th member of this hierarchy can be computed similarly to the above and reads

$$\left[\frac{\partial}{\partial t_{1}} - \sum_{i=1}^{s} \left\{\hat{\mathcal{L}}_{i}^{(0)}(t_{1}) + \hat{\mathcal{L}}_{i}^{(1)}(t_{1})\right\}\right] f_{s}(x_{1}, \dots, x_{s}, t_{1}) =$$

$$\int d^{6}x_{s+1} \sum_{i=1}^{s} \left\{\hat{\mathcal{L}}_{i(s+1)}^{(2)}(t_{1})\right\} f_{s+1}(x_{1}, \dots, x_{s}, x_{s+1}, t_{1}).$$
(2.81)

Each equation in the hierarchy thus describes the time evolution of the s-particle reduced distribution $f_s(x_1, \ldots, x_s, t_1)$ and involves the (s+1)-particle distribution f_{s+1} on the right-hand side. The left-hand side describes the free streaming of particles including the influence of an external potential. The integral on the right-hand side of (2.79), (2.80) and (2.81) respectively, is usually referred to as the collision integral, describing the interaction between any of these s particles and an external particle from the group of the other, not measured, particles.

In literature, one often also encounters the BBGKY hierarchy in terms of the irreducible correlation functions g_s as they contain the full non-redundant information of the correlation structure of the system. These can be found by inserting the decomposition of the s-particle reduced densities f_s into s-particle correlations g_s (c.f. (2.69)) into the above BBGKY equations. For instance, for f_1 one finds

$$\left[\frac{\partial}{\partial t_1} - \hat{\mathcal{L}}_1^{(0)}(t_1) - \hat{\mathcal{L}}_1^{(1)}(t_1)\right] f_1(x_1, t_1) = \int d^6 x_2 \, \hat{\mathcal{L}}_{12}^{(2)}(t_1) f_1(x_1, t_1) f_1(x_2, t_1)
+ \int d^6 x_2 \, \hat{\mathcal{L}}_{12}^{(2)}(t_1) g_2(x_1, x_2, t_1)$$
(2.82)

Clearly, the BBGKY hierarchy, as it stands, is exact and does not introduce any approximation nor simplifications of the system. It retains the full complexity of the Liouville equation and only closes after the N-th iteration of the above procedure, where the full phase-space density¹⁹ f_N reappears. One main focus of kinetic theory therefore is to find systematic truncation procedures that break the full hierarchy down to a closed set of only the lowest few members of the hierarchy. In the next section we briefly review the most common of these approaches.

¹⁷Here, external means that the particle at x_3 is not included in the two-particle density f_2 , but enters as an interaction partner in the evolution equation.

¹⁸Named after the authors who first derived it, Bogolioubov, Born, Green, Kirkwood, and Yvon, in alphabetically, but *not* chronological order, [26].

¹⁹In fact, f_N only differs from the Liouville phase-space density ϱ_N by a combinatorial prefactor N! taking care of particle permutations.

2.4. Important Truncations of the BBGKY Hierarchy

In practice, it is necessary to truncate the BBGKY hierarchy by introducing a closure relation, i. e., a prescription that expresses a higher-order reduced density by a lower-order one, such that the hierarchy terminates after few iterations. These closure relations often rely, among other conditions, on the assumption that the irreducible correlation functions g_s obey an intrinsic ordering in terms of an appropriately chosen parameter λ [38],

$$g_s \sim \mathcal{O}(\lambda^s)$$
. (2.83)

The choice of an adequate parameter is highly non-trivial and represents a central task in kinetic theory. In order to not get out of scope of this thesis, we focus exclusively on the most "natural" choice of a *weakly coupled* system since it will be important for the long-range interactions covered later in this work.

Let us, therefore, assume that the two-particle potential multiplies a small dimensionless coupling parameter,

$$v_2(x_1, x_2, t) \to \lambda \, v_2(x_1, x_2, t)$$
 (2.84)

and assume $\lambda \ll 1$. In order to find the corresponding ordering of the correlation functions, we note that in order to satisfy the normalization (2.67) (even if λ =0), to leading order the one-particle reduced density must be independent of λ ,

$$f_1(x_1, t_1) \sim \mathcal{O}(\lambda^0). \tag{2.85}$$

On the other hand, in order to create correlations between two particles²⁰ at least one interaction is needed. Similarly, the irreducible correlation between three particles requires at least two interactions, thus

$$g_2(x_1, x_2, t) \sim \mathcal{O}(\lambda^1)$$
, and generally $g_s(x_1, \dots, x_s, t) \sim \mathcal{O}(\lambda^{s-1})$, (2.86)

to leading order. This is the ordering of the correlations that we were looking for. Let us now study the lowest orders in more detail.

2.4.1. Free Streaming

In the simplest case, $\lambda=0$ or order λ^0 , there are no inter-particle interactions. We refer to this case as the *free streaming* of the particles, and we also neglect the external potential, such that the equations are analytically solvable. Clearly, each equation of the BBGKY hierarchy closes individually and thus, no correlations are created or destroyed. In particular, we find for f_1 the following linear initial value

²⁰Here, we must assume that the state was uncorrelated initially, or respects the above ordering with respect to λ , which is necessary for the ordering considerations to work.

problem

$$\left[\frac{\partial}{\partial t_1} - \hat{\mathcal{L}}_1^{(0)}(t_1)\right] f_1(x_1, t_1) = 0$$

$$f_1(x_1, t_1 = t^{(i)}) = f_1^{(i)}(x_1).$$
(2.87)

It can easily be verified that the retarded Green function to the above linear differential operator $[\partial_t - \hat{\mathcal{L}}^{(0)}]$ is given by

$$D_{0,R}(x_1, t_1, x_2, t_2) = \delta_D (x_1 - G(t_1, t_2) \cdot x_2) \Theta(t_1 - t_2), \qquad (2.88)$$

since

$$\left[\frac{\partial}{\partial t_1} - \hat{\mathcal{L}}_1^{(0)}(t_1)\right] D_{0,R}(x_1, t_1, x_2, t_2) = \delta_{\mathcal{D}}(x_1 - x_2) \,\delta_{\mathcal{D}}(t_1 - t_2) \ . \tag{2.89}$$

In the above Green function, G is the retarded particle propagator (2.24) that describes the free propagation of a particle in μ -space located at x_2 at time t_2 to the phase-space coordinate x_1 at a *later* time t_1 . Causality is ensured by the Heaviside function. Thus, the solution to (2.87) is found to be

$$f_1(x_1, t_1) = \int d^6 x_2 D_{0,R}(x_1, t_1, x_2, t^{(i)}) f_1^{(i)}(x_1)$$

$$= f_1^{(i)} (G^{-1}(t_1, t^{(i)}) \cdot x_1) \Theta(t_1 - t^{(i)}),$$
(2.90)

where in the second line we used that det(G) = 1, since the free particle propagator is symplectic (2.34). We have thus solved the complete free system: The phase-space density at time t_1 at the coordinate x_1 corresponds to the phase-space density at initial time $t^{(i)}$ at the position where the particle was initially located. This position is given by tracing the trajectory backwards in time. The free case is constructed such that this trajectory is exactly known and given by (2.22). We will refer back to this free theory multiple times, as it serves as the reference case around which the subsequent discussions are built.

2.4.2. The Vlasov Equation

To next order in the coupling, we collect all terms in the evolution operator for f_1 that are at most linear in λ . Since the two-particle interaction operator satisfies $\hat{\mathcal{L}}^{(2)} \sim \lambda$, the two terms on the right-hand side of equation (2.82) scale as

$$\hat{\mathcal{L}}^{(2)} f_1 f_1 \sim \lambda$$
, and $\hat{\mathcal{L}}^{(2)} g_2 \sim \lambda^2$. (2.91)

Neglecting the subleading correlation term g_2 , we obtain the *Vlasov equation* (c.f. [45]), which reads

$$\left[\frac{\partial}{\partial t_1} - \hat{\mathcal{L}}_1^{(0)}(t_1) - \hat{\mathcal{L}}_1^{(1)}(t_1) \right] f_1(x_1, t_1) = \int d^6 x_2 \, \hat{\mathcal{L}}_{12}^{(2)}(t_1) \, f_1(x_1, t_1) \, f_1(x_2, t_1) \,. \tag{2.92}$$

This equation plays a central role in the study of weakly coupled systems and, as we will argue in chapter 8, governs the $N \to \infty$ limit of long-range interacting systems

such as Coulomb and gravitational systems—the latter being the primary focus of our application in chapter 11. It will therefore be essential to understand the physics underlying (2.92). First, the most obvious property of the Vlasov equation is the absence of the two-particle correlation g_2 . It is therefore a closed equation for the one-particle reduced density f_1 . The role of the two-particle interaction potential can be seen by expanding the last term of (2.92) to find

$$\int d^6 x_2 \,\hat{\mathcal{L}}_{12}^{(2)}(t_1) f_1(x_1, t_1) f_1(x_2, t_1) = \nabla_{x_1}^{\top} \overline{v}_2(x_1, t_1) \cdot \omega \cdot \nabla_{x_1} f_1(x_1, t_1) , \qquad (2.93)$$

where we defined the mean two-particle potential

$$\overline{v}_2(x_1, t_1) = \int d^6 x_2 f_1(x_2, t_1) v_2(x_1, x_2, t_1).$$
(2.94)

It represents the value of a potential at phase-space position x_1 sourced by a particle at x_2 and averaged over all possible positions x_2 weighted by the respective density $f_1(x_2, t_1)$. The Vlasov equation (2.92) may therefore be written as

$$\left[\frac{\partial}{\partial t_1} - \hat{\mathcal{L}}_1^{(0)}(t_1) - \nabla_{x_1}^{\top} \left(v_1(x_1, t_1) + \overline{v}_2(x_1, t_1)\right) \cdot \omega \cdot \nabla_{x_1}\right] f_1(x_1, t_1) = 0.$$
 (2.95)

In this form, the effect of the mean interaction potential appears as an additional effective external field, determined self-consistently by f_1 through equation (2.94). The Vlasov equation is therefore often referred to as the mean field equation. Any change in the distribution function instantaneously modifies the mean field, which in turn feeds back into the dynamics. As a result, the Vlasov equation is a nonlinear partial differential equation, and finding its solutions requires dealing with this self-consistent feedback loop. Throughout this work we will develop methods to deal with such situations.

Historically, the Vlasov equation is obtained by introducing a closure relation via the famous Stosszahlansatz $f_2(x_1, x_2, t_1) \approx f_1(x_1, t_1)f_1(x_2, t_1)$ in order to close the BBGKY hierarchy. In this work, we choose to present a different derivation based on a perturbative expansion, as it allows one to derive evolution equations which go beyond the assumption of molecular chaos systematically as we shall see in Section 2.4.3.

Another remarkable feature of (2.92) is its clear resemblance to the Klimontovich equation (2.78). The former can be obtained from the latter by taking the ensemble average of the Klimontovich equation as shown in (2.82) and neglecting the collision integral²¹ containing two-particle correlations g_2 on the right-hand side of the equation, thus, "replacing" the exact microscopic density Φ_f by the averaged mean phase-space density f_1 .

²¹In the context of the Boltzmann equation, often, both terms on the right-hand side of (2.82) are referred to as the collision integral C[f] since it is assumed that there are no long-range interactions and particles interact only via collisions. Throughout this thesis, however, we only consider the second term on the right-hand side of (2.82) as the collision integral.

Closure	Term A	Term B	Term C	Term D
Landau	X	-	-	-
Lennard-Balescu	X	-	X	-
Boltzmann	X	X	_	_

Table 2.1.: Terms kept (x) and neglected (-) in (2.96) for the Landau, Lennard-Balescu and Boltzmann closure condition. All terms are of order λ^2 . The last term is always neglected due to $g_3 = 0$. Table taken from [37].

2.4.3. Including Collisions

Before concluding, let us note that neglecting correlations, as we did in the derivation of the Vlasov equation, is not always justified. When interactions become stronger, the linear approximation in the coupling strength λ may no longer be valid. If the interactions between individual particles remain weak enough, one possibility is to go to next-to-leading order in the perturbative expansion. At order λ^2 , this requires incorporating the two-particle correlation function g_2 , which accounts for binary collisions between particles. The evolution equation for g_2 is given by

$$\left[\frac{\partial}{\partial t_{1}} - \sum_{i=1}^{2} \left\{\hat{\mathcal{L}}_{i}^{(0)}(t_{1}) + \hat{\mathcal{L}}_{i}^{(1)}(t_{1})\right\}\right] g_{2}(x_{1}, x_{2}, t_{1}) = \underbrace{\hat{\mathcal{L}}_{12}^{(2)}(t_{1}) f_{1}(x_{1}, t_{1}) f_{1}(x_{2}, t_{1})}_{A} + \underbrace{\hat{\mathcal{L}}_{12}^{(2)}(t_{1}) g_{2}(x_{1}, x_{2}, t_{1})}_{B} + \int d^{6}x_{3} \sum_{i=1}^{2} \left\{\hat{\mathcal{L}}_{i3}^{(2)}(t_{1})\right\} \left(f_{1}(x_{1}, t_{1}) g_{2}(x_{2}, x_{3}, t_{1}) + f_{1}(x_{2}, t_{1}) g_{2}(x_{1}, x_{2}, t_{1})\right) - \underbrace{\int d^{6}x_{3} \sum_{i=1}^{2} \left\{\hat{\mathcal{L}}_{i3}^{(2)}(t_{1})\right\} g_{3}(x_{1}, x_{2}, x_{3}, t_{1})}_{D \sim \mathcal{O}(\lambda^{3})} . \tag{2.96}$$

Keeping only the first term on the right-hand side of (2.96), leads to the well-known Landau equation, which describes the collisional evolution of weakly coupled plasmas with long-range Coulomb interactions where λ is the strength of the potential.

One can derive other kinetic equations by solving the second equation of the BBGKY hierarchy g_2 (2.96), in a self-consistent manner. Truncating the hierarchy at this level by neglecting the three-particle correlation g_3 , and using appropriate assumptions about the structure of g_2 , one obtains different kinetic equations depending on the physical regime and interaction range: the *Boltzmann equation* emerges for dilute gases with short-range interactions, where collisions are rare but strong and

 λ is the density parameter $\lambda = \bar{\rho} \, l_C^3$ with particle density $\bar{\rho}$ and correlation length l_C . The Lennard-Balescu equation, on the other hand, arises in weakly coupled plasmas, with long-range Coulomb interactions, where collective effects and dynamical screening are essential and are not described by the Landau equation. In this context λ corresponds to the plasma parameter $\lambda = \frac{q^2}{a \, k_B \, T}$ with the mean inter-particle distance $a = \bar{\rho}^{-\frac{1}{3}}$ and temperature T. Table 2.1 provides an overview of the closure conditions for these three cases.

Our main application will deal with systems, where particle collisions are negligible. Nevertheless, we will present all derivations in full generality, so that collisional effects—whenever relevant—can be incorporated within the same framework. References to such effects will be made at appropriate points throughout the main text.

2.5. Unequal Time Correlation Functions

As we have seen, the time evolution of the system can be equivalently described through the hierarchy of reduced phase-space densities f_s , governed by the BBGKY hierarchy, or through the equal-time correlation functions of the Klimontovich phase-space density $\bar{C}_{f...f}$, which can be expanded in terms of the reduced densities, as discussed in (2.71). While for equal-time observables both descriptions are essentially equivalent and the distinction may appear unnecessary, this changes when we consider unequal-time correlation functions. In that case, it becomes more practical and physically transparent to work directly with the correlation functions of the phase-space density itself.

Let us therefore introduce the natural generalization of the equal-time correlation functions $\bar{C}_{f...f}$ and their connected components $\bar{G}_{f...f}$, and define their unequal-time counterparts as

$$C_{f...f}(x_1, t_1, \dots, x_k, t_k) = \langle \Phi_f(x_1, t_1) \dots \Phi_f(x_k, t_k) \rangle$$
, (2.97)

and

$$G_{f...f}(x_1, t_1, \dots, x_k, t_k) = \langle \Phi_f(x_1, t_1) \dots \Phi_f(x_k, t_k) \rangle_c$$
, (2.98)

respectively. Completely analogously to (2.74), we define the connected correlation functions for arbitrary local densities $\mathcal{O}_1(\vec{q}_1, t_1), \dots \mathcal{O}_k(\vec{q}_k, t_k)$, as

$$G_{\mathcal{O}_{1}...\mathcal{O}_{k}}(\vec{q}_{1}, t_{1}, ..., \vec{q}_{k}, t_{k}) = \langle \Phi_{\mathcal{O}_{1}}(\vec{q}_{1}, t_{1}) ... \Phi_{\mathcal{O}_{k}}(\vec{q}_{k}, t_{k}) \rangle_{c}$$

$$= \int d^{3}p_{1} ... d^{3}p_{k} F_{\mathcal{O}_{1}}(\vec{p}_{1}) ... F_{\mathcal{O}_{k}}(\vec{p}_{k}) G_{f...f}(x_{1}, t_{1}, ..., x_{k}, t_{k}).$$
(2.99)

From the discussion in Section 2.2 it is clear that working in the Heisenberg picture of the statistical system will be more appropriate, since the time evolution is contained in the microscopic trajectories themselves rather than in the Liouville phase-space density²². Thus, the expectation value (2.97) is computed according to

$$C_{f...f}(x_1, t_1, \dots, x_k, t_k) = \int d\mathbf{x}^{(i)} \Phi_{f,cl}(x_1, t_1) \dots \Phi_{f,cl}(x_k, t_k) \, \varrho_N^{(i)}(\mathbf{x}^{(i)}) \,, \qquad (2.100)$$

where $\Phi_{f,\text{cl}}$ denotes the Klimontovich phase-space density that contains the classical particle trajectories, and therefore parametrically depends on the initial conditions,

$$\Phi_{f,\text{cl}}(x_1, t_1) = \Phi_f(x_1; \mathbf{x}_{\text{cl}}(t_1; \mathbf{x}^{(i)}, t^{(i)})) = \sum_{i=1}^N \delta_{\text{D}}\left(x_1 - \mathbf{x}_{i,\text{cl}}(t_1; \mathbf{x}^{(i)}, t^{(i)})\right). \tag{2.101}$$

The physical intuition behind equation (2.100) is to draw particles from an initial phase-space density distribution and to evolve them up to their respective time, averaging over all possible initial configurations. We therefore have to discuss the explicit form of the initial Liouville phase-space density in more detail.

2.6. N-particle Initial Conditions from a Correlated Density Field

Let us first assume that the initial phase-space density is exactly known in terms of a continuous single-particle density distribution function $f_1^{(i)}(x) \equiv f_1(x, t^{(i)})$ on μ -space²³. From the discussion in Section 2.2 and the normalization (2.54), we infer

$$P(\mathbf{x}_{j}^{(i)} | f_{1}(\mathbf{x}_{j}^{(i)})) d^{6}\mathbf{x}_{j}^{(i)} \equiv \frac{1}{N} f_{1}(\mathbf{x}_{j}^{(i)}) d^{6}\mathbf{x}_{j}^{(i)}$$
(2.102)

as the normalized probability of finding particle j inside the infinitesimal volume $d^6x_j^{(i)}$ around the point $x_j^{(i)}$, given the phase-space density $f_1(x_j^{(i)})$ at that point. We now iterate through all N particles and distribute them in a statistically independent way according to the above probability density. This procedure is commonly referred to as $Poisson\ sampling$, since each particle is drawn independently from the same probability-density function. As a result, the number of particles found within a given region of space follows a Poisson distribution in the limit of large N^{24} . We refer to [30] for more details. Since the individual particles are picked independently of each other, the joint probability for the whole ensemble, i. e., the Liouville phase-space density is given by

$$\varrho_N^{(i)}(\mathbf{x}^{(i)}) = \prod_{j=1}^N \frac{1}{N} f_1^{(i)}(\mathbf{x}_j^{(i)}). \tag{2.103}$$

 $^{^{22}}$ We refer the reader to the elaborate discussion in [26] for an alternative treatment of unequal-time objects with generalized reduced distribution functions which is, of course, equivalently possible.

²³As we have discussed before, the physically measurable quantities are (piece-wise) continuous functions on \mathbb{R}^3 . Thus, from a practical point view, one would typically start from a set of macroscopic local densities $\mathcal{O}(\vec{q})$ such as the physical particle number density or the momentum density. In chapter 9 we will consider such a scenario. However, for our conceptual discussion here, it is sufficient to assume the full phase-space density $f_1^{(i)}(x)$ to be known.

²⁴More precisely, this corresponds to a binomial point process with fixed particle number N, which approaches a Poisson point process in the limit $N \to \infty$ with appropriately rescaled density, see [30] for more details.

This describes an uncorrelated state at initial time, which is clearly expected from a statistically independent random process.

In realistic scenarios, however, the initial phase-space density $f_1^{(i)}(x)$ is itself only known on a statistical level, i. e., as a random field with associated probability density functional $\mathcal{P}[f_1^{(i)}]$. In this case, equation (2.102) must be understood as a conditional probability, given a realization of $f_1^{(i)}(\mathsf{x}_j^{(i)})$, and the full ensemble is obtained by marginalizing over $\mathcal{P}[f_1^{(i)}]$,

$$\varrho_N^{(i)}(\mathbf{x}^{(i)}) = \int \mathcal{D}f_1^{(i)} \prod_{j=1}^N P(\mathbf{x}_j^{(i)} | f_1(\mathbf{x}_j^{(i)})) \mathcal{P}[f_1^{(i)}].$$
 (2.104)

Here, $\mathcal{D}f_1^{(i)}$ is the functional integration measure running over all possible continuous realizations of the density profile $f_1^{(i)}(x)$. Thus, the total Liouville phase-space density reads

$$\varrho_N^{(i)}(\mathbf{x}^{(i)}) = \frac{1}{N^N} \int \mathcal{D} f_1^{(i)} \prod_{j=1}^N f_1^{(i)}(\mathbf{x}_j^{(i)}) \mathcal{P} \left[f_1^{(i)} \right], \qquad (2.105)$$

where we have used (2.102). Inserting the Liouville phase-space density (2.105) into the definition (2.66), we find

$$f_s^{(i)}(x_1, \dots, x_s) = \frac{1}{N^N} \int d\mathbf{x}^{(i)} \sum_{i_1 \neq \dots \neq i_s = 1}^N \prod_{n=1}^s \delta_{\mathcal{D}} \left(x_n - \mathbf{x}_{i_n}^{(i)} \right) \int \mathcal{D} f_1^{(i)} \prod_{j=1}^N f_1^{(i)}(\mathbf{x}_j^{(i)}) \mathcal{P} \left[f_1^{(i)} \right]$$
(2.106)

$$= \frac{N!}{N^s(N-s)!} \int \mathcal{D}f_1^{(i)} f_1^{(i)}(x_1) \dots f_1^{(i)}(x_s) \mathcal{P}[f_1^{(i)}]. \tag{2.107}$$

With the moments and cumulants of the probability functional $\mathcal{P}[f_1^{(i)}]$ defined in the usual way as

$$C_{\mathcal{P}}^{(k)}(x_1, \dots, x_k) \equiv \left\langle f_1^{(i)}(x_1) \dots f_1^{(i)}(x_k) \right\rangle_{\mathcal{P}} = \int \mathcal{D}f_1 \, f_1^{(i)}(x_1) \dots f_1^{(i)}(x_k) \, \mathcal{P}\left[f_1^{(i)}\right],$$
(2.108)

and

$$G_{\mathcal{P}}^{(k)}(x_1,\dots,x_k) \equiv \left\langle f_1^{(i)}(x_1)\dots f_1^{(i)}(x_k) \right\rangle_{\mathcal{CP}},$$
 (2.109)

we immediately see that for large N the s-particle reduced distribution function f_s corresponds to the s-point correlation function $C_{\mathcal{P}}^{(s)}$,

$$f_s^{(i)}(x_1, \dots, x_s) = \frac{N!}{N^s(N-s)!} C_{\mathcal{P}}^{(s)}(x_1, \dots, x_s) \stackrel{N \gg 1}{=} C_{\mathcal{P}}^{(s)}(x_1, \dots, x_s).$$
 (2.110)

Equivalently, the s-particle reduced correlation function g_s corresponds to the s-point connected correlation function, i. e., the cumulant $G_{\mathcal{P}}^{(s)}$. Thus, subtracting the disconnected part yields

$$g_s^{(i)}(x_1, \dots, x_s) = G_{\mathcal{P}}^{(s)}(x_1, \dots, x_s).$$
 (2.111)

We, thus, find that the uncertainty in the initial field $f_1^{(i)}$ is imprinted on the reduced particle correlations, even though the particles are sampled independently. In this sense, the initial statistical fluctuations of the density field act as a seed for correlations in the particle ensemble. These initial correlations must therefore be carefully distinguished from those that arise dynamically due to the two-particle interactions.

3 Functional Integrals for Deterministic Systems

The central challenge that arises in most physically relevant systems, is that they are not exactly solvable, due to the often very complicated structure of interactions between the underlying degrees of freedom, and therefore require an approximative treatment. A natural strategy is to separate the *known*, exactly solvable dynamics, from the *unknown* contributions and to systematically include the latter into the description. In quantum mechanical systems a powerful tool to achieve this separation is famously provided by the path integral approach for which many advanced methods have been developed. At first glance, such an "integrate over all possible paths"-approach seems contradictory to classical determinism which lacks the superposition principle of quantum mechanics. However, as we will see, classical mechanics may be reformulated in a way that is both, elegant and practically useful, enabling us to apply well-established methods from quantum and statistical field theory in the upcoming chapters within a classical context.

3.1. The Koopman-von Neumann Formulation of Classical Mechanics

One of the most important properties—if not the most important property—of the Liouville equation is its linearity, which introduces a grain of simplicity into an otherwise highly complex theory. Indeed, it is the linearity that allows us to write down the formal solution in terms of a time-evolution operator (c.f. (2.43)). This is strongly reminiscent of the well-known structure of the Schrödinger equation which, therefore, hints at a formal unified description of both, classical and quantum mechanics. This was first observed by Koopman [16] in the early 1930s and later formalized by von Neumann [17] and is today known as the Koopman-von Neumann formulation of classical mechanics. It presents an axiomatic derivation of classical mechanics and in particular the Liouville equation. Based on this description we can introduce the idea of a path-integral formulation of classical mechanics [22, 23, 46, 47]. Let us therefore summarize the key thoughts underlying the Koopman-von Neumann formalism following [48].

3.1.1. Axiomatic Derivation of Liouville's Equation - The Koopman Operator

Consider an abstract Hilbert space \mathcal{H} , together with the inner product

$$\langle \cdot | \cdot \rangle : \mathcal{H} \times \mathcal{H} \to \mathbb{C}.$$
 (3.1)

The elements of the Hilbert space, $|\psi\rangle \in \mathcal{H}$ are physically interpreted as probability density amplitudes. The basic construction of the Koopman-von Neumann theory now emerges by imposing the following operator axioms:

- 1. The physical state of the system is represented by a normalized vector $|\psi\rangle \in \mathcal{H}$, with $\langle \psi | \psi \rangle = 1$.
- 2. The observables are represented by hermitian operators $\hat{\mathcal{O}}: \mathcal{H} \to \mathcal{H}$ acting on the states. The expectation value of a given observable at time t associated to the state $|\psi(t)\rangle \in \mathcal{H}$ is given by $\langle \hat{\mathcal{O}} \rangle = \langle \psi(t)|\hat{\mathcal{O}}|\psi(t)\rangle$.
- 3. The probability of measuring an observable $\hat{\mathcal{O}}$ at time t with the result \mathcal{O} is given by $P(\mathcal{O}) = |\langle \psi(t) | \mathcal{O} \rangle|^2$, where $|\mathcal{O}\rangle \in \mathcal{H}$ solves the eigenvalue problem $\hat{\mathcal{O}}|\mathcal{O}\rangle = \mathcal{O}|\mathcal{O}\rangle$.
- 4. The state space of a composite system is given by the tensor product of the Hilbert spaces of the respective subsystems.

Importantly, these axioms do not differ from the axiomatic derivation of quantum mechanics. Let us now deduce the implication of the above axioms to our classical system. First, we postulate that the time evolution is determined by a unitary operator $\hat{U}(t, t^{(i)})$, the *time-evolution operator*, such that

$$|\psi(t)\rangle = \hat{U}(t, t^{(i)}) |\psi(t^{(i)})\rangle, \text{ with } \hat{U}^{\dagger}(t, t^{(i)}) = \hat{U}^{-1}(t, t^{(i)}).$$
 (3.2)

Stone's theorem [49] implies the unique existence¹ of an operator \hat{K} , the generator of time translations, satisfying

$$\frac{\partial}{\partial t}\hat{U}(t,t^{(i)}) = -i\hat{K}\hat{U}(t,t^{(i)}), \qquad (3.3)$$

or equivalently,

$$\hat{U}(t, t^{(i)}) = e^{-i(t-t^{(i)})\hat{K}}$$
 (3.4)

We will now deduce the explicit form of \hat{K} . Introducing the operators $\hat{\vec{q}}$ and $\hat{\vec{p}}$ referring to the observable of position and momentum respectively, we impose the *Ehrenfest theorem* [50], i. e., that the Hamiltonian equations of motion hold for the

¹To be more specific, Stone's theorem requires that time evolution is governed by a *strongly* continuous one-parameter group of unitary operators, i. e., $\forall t \in \mathbb{R}$, the operator \hat{U}_t is unitary, $\forall t, s \in \mathbb{R}$ we have $\hat{U}_{s+t} = \hat{U}_s \hat{U}_t$ and $\forall t_0 \in \mathbb{R}, |\psi\rangle \in \mathcal{H}$, we have $\lim_{t \to t_0} \hat{U}_t |\psi\rangle = \hat{U}_{t_0} |\psi\rangle$.

expectation values of $\hat{\vec{q}}$ and $\hat{\vec{p}}$,

$$\frac{\mathrm{d}}{\mathrm{d}t} \left\langle \hat{\vec{q}} \right\rangle = \frac{\mathrm{d}}{\mathrm{d}t} \left\langle \psi(t) | \hat{\vec{q}} | \psi(t) \right\rangle = \left\langle \nabla_{\hat{p}} H(\hat{\vec{q}}, \hat{\vec{p}}) \right\rangle
\frac{\mathrm{d}}{\mathrm{d}t} \left\langle \hat{\vec{p}} \right\rangle = \frac{\mathrm{d}}{\mathrm{d}t} \left\langle \psi(t) | \hat{\vec{p}} | \psi(t) \right\rangle = -\left\langle \nabla_{\hat{q}} H(\hat{\vec{q}}, \hat{\vec{p}}) \right\rangle.$$
(3.5)

Equation (3.3) then implies by the chain rule

$$-i \left\langle \left[\hat{K}, \hat{\vec{q}} \right] \right\rangle = \left\langle \nabla_{\hat{p}} H(\hat{\vec{q}}, \hat{\vec{p}}) \right\rangle
-i \left\langle \left[\hat{K}, \hat{\vec{p}} \right] \right\rangle = - \left\langle \nabla_{\hat{q}} H(\hat{\vec{q}}, \hat{\vec{p}}) \right\rangle.$$
(3.6)

Since the above set of expectation values have to hold for arbitrary states $|\psi(t)\rangle$, we find the following set of commutator relations for the generator \hat{K} ,

$$-i\left[\hat{K}, \hat{\vec{q}}\right] = \nabla_{\hat{p}} H\left(\hat{\vec{q}}, \hat{\vec{p}}\right)$$

$$-i\left[\hat{K}, \hat{\vec{p}}\right] = -\nabla_{\hat{q}} H\left(\hat{\vec{q}}, \hat{\vec{p}}\right)$$
(3.7)

There is now an obvious difficulty regarding the operator \hat{K} . From a classical mechanical perspective, we demand the simultaneous measurability of position and momentum,

$$\left[\hat{\vec{q}}, \hat{\vec{p}}\right] = 0. \tag{3.8}$$

However, if the generator \hat{K} depends on position and momentum only, $\hat{K} = \hat{K}(\hat{\vec{q}}, \hat{\vec{p}})$, it is not possible to realize (3.7) in a non-trivial way, since any commutator of \hat{K} with $\hat{\vec{q}}$ and $\hat{\vec{p}}$ respectively vanishes identically. To bypass this problem, we introduce two further operators called $\hat{\chi}_q$ and $\hat{\chi}_p$ on which \hat{K} may depend. The extended commutator algebra now reads

$$\begin{bmatrix}
\hat{q}, \hat{\chi}_q \end{bmatrix} = i = \begin{bmatrix} \hat{p}, \hat{\chi}_p \end{bmatrix},
\begin{bmatrix}
\hat{q}, \hat{\chi}_p \end{bmatrix} = \begin{bmatrix} \hat{p}, \hat{\chi}_q \end{bmatrix} = \begin{bmatrix} \hat{\chi}_q, \hat{\chi}_p \end{bmatrix} = \begin{bmatrix} \hat{q}, \hat{p} \end{bmatrix} = 0.$$
(3.9)

By standard procedures of non-commutative operators [48], these commutator relations can be used to derive the following differential equation for $\hat{K} = \hat{K}(\hat{\vec{q}}, \hat{\vec{\chi}}_q, \hat{\vec{p}}, \hat{\vec{\chi}}_p)$,

$$\nabla_{\hat{\chi}_q} \hat{K}(\hat{q}, \hat{\chi}_q, \hat{p}, \hat{\chi}_p) = \nabla_{\hat{p}} H(\hat{q}, \hat{p})$$

$$\nabla_{\hat{\chi}_p} \hat{K}(\hat{q}, \hat{\chi}_q, \hat{p}, \hat{\chi}_p) = -\nabla_{\hat{q}} H(\hat{q}, \hat{p})$$
(3.10)

The solution for \hat{K} is then found to be²

$$\hat{K}(\hat{\vec{q}}, \hat{\vec{\chi}}_q, \hat{\vec{p}}, \hat{\vec{\chi}}_p) = \nabla_{\hat{p}} H(\hat{\vec{q}}, \hat{\vec{p}}) \cdot \hat{\vec{\chi}}_q - \nabla_{\hat{q}} H(\hat{\vec{q}}, \hat{\vec{p}}) \cdot \hat{\vec{\chi}}_p.$$
(3.11)

The operator \hat{K} , which generates the time evolution, is called the *Koopman operator*³. As we can see, the new operators $\hat{\chi}_q$ and $\hat{\chi}_p$ each introduce one of the equations of motion in (3.5). In this operatorial language, they are referred to as *Bopp operators* [51, 52] and act like operatorial Lagrangian multipliers.

3.1.2. Recovering Liouville's Equation

In order to make the above abstract construction more concrete and to simplify the physical interpretation, let us choose a specific representation of the above algebra over the Hilbert space

$$\mathcal{H} \equiv \mathcal{L}^2(\mathcal{P}, d^6 x) = \left\{ \psi : \mathcal{P} \to \mathbb{C} \,\middle|\, \int d^6 x \,|\psi(x)|^2 < \infty \right\}, \tag{3.12}$$

of complex-valued, square-integrable functions defined over the particle phase-space⁴ \mathcal{P} with measure d^6x , and inner product

$$\langle \psi \mid \phi \rangle = \int d^6 x \, \psi^*(x) \phi(x) \,. \tag{3.13}$$

Since $\hat{\vec{q}}$ and $\hat{\vec{p}}$ commute for the classical system, (3.8), we can simultaneously work in the combined $\hat{\vec{q}}$ and $\hat{\vec{p}}$ eigenbasis, represented by

$$\langle x | \equiv \langle \vec{q}, \vec{p} | \equiv \langle \vec{q} | \otimes \langle \vec{p} |.$$
 (3.14)

These form an orthonormal eigenbasis, and we find the usual relationships,

$$\hat{\vec{q}} | \vec{q}, \vec{p} \rangle = \vec{q} | \vec{q}, \vec{p} \rangle, \quad \hat{\vec{p}} | \vec{q}, \vec{p} \rangle = \vec{p} | \vec{q}, \vec{p} \rangle,
\mathbb{1} = \int d^3 q \, d^3 p \, | \vec{q}, \vec{p} \rangle \langle \vec{q}, \vec{p} | \quad \langle \vec{q}, \vec{p} | \vec{q}', \vec{p}' \rangle = \delta_{\rm D} \left(\vec{q} - \vec{q}' \right) \delta_{\rm D} \left(\vec{p} - \vec{p}' \right).$$
(3.15)

In this phase-space representation the state of the system is given by a classical wave function,

$$\psi(x,t) \equiv \psi(\vec{q},\vec{p},t) \equiv \langle \vec{q},\vec{p} | \psi(t) \rangle. \tag{3.16}$$

²The general solution to the above equations includes an undetermined additive function $f(\hat{\vec{q}}, \hat{\vec{p}})$ to \hat{K} . However, it does not affect the dynamics, and we set it to zero here to recover the classical dynamics [48].

³Here, we have chosen to put the $\hat{\chi}$ operators on the right of the Hamiltonian function. As one can easily verify, inserting the commutation relations and interchanging the order does not alter the Koopman operator due to the divergence free Hamiltonian flow. However, this order will play a crucial role when it comes to the discretization to obtain the path integral formulation.

⁴We assume that the particle phase space is $\mathcal{P} \subseteq \mathbb{R}^6$ with the usual flat measure on \mathbb{R}^6 .

Clearly, in the $\hat{\vec{q}}$ and $\hat{\vec{p}}$ eigenbasis the operator algebra (3.9) can be represented by

$$\hat{\vec{q}} = \vec{q}, \quad \hat{\vec{p}} = \vec{p}, \quad \hat{\vec{\chi}}_q = -i\nabla_{\vec{q}}, \quad \hat{\vec{\chi}}_{\vec{p}} = -i\nabla_p,$$
 (3.17)

where position and momentum operators become multiplicative operators, while the additional operators $\hat{\vec{\chi}}_q$ and $\hat{\vec{\chi}}_p$ become differential operators. The time evolution of the classical wave function in this representation is given by

$$\frac{\partial}{\partial t}\psi(\vec{q},\vec{p},t) = -i\hat{K}\psi(\vec{q},\vec{p},t), \qquad (3.18)$$

where the Koopman operator \hat{K} takes the form

$$\hat{K} = i \left(\nabla_{\vec{q}} H(\vec{q}, \vec{p}) \cdot \nabla_{\vec{p}} - \nabla_{\vec{p}} H(\vec{q}, \vec{p}) \cdot \nabla_{\vec{q}} \right). \tag{3.19}$$

The classical wave function evolves according to (3.2). In the phase-space representation, we therefore find

$$\psi(x^{(f)}, t^{(f)}) = \int d^6 x^{(i)} U(x^{(f)}, t^{(f)} | x^{(i)}, t^{(i)}) \psi(x^{(i)}, t^{(i)}), \qquad (3.20)$$

where the phase-space matrix element of the time-evolution operator is defined as

$$U(x^{(f)}, t^{(f)}|x^{(i)}, t^{(i)}) = \langle x^{(f)}|e^{-i(t^{(f)}-t^{(i)})\hat{K}}|x^{(i)}\rangle.$$
(3.21)

Let us now define the real-valued *probability density* in the usual way as

$$\varrho(x,t) = |\psi(x,t)|^2 = |\langle \psi(t)|x\rangle|^2. \tag{3.22}$$

Importantly, the second axiom implies for the expectation value of an operator $\hat{\mathcal{O}} = \mathcal{O}(\hat{x})$,

$$\langle \hat{O} \rangle = \langle \psi(t) | \mathcal{O}(\hat{x}) | \psi(t) \rangle$$
 (3.23)

$$= \int d^6 x \langle \psi(t) | \mathcal{O}(x) | x \rangle \langle x | \psi(t) \rangle$$
 (3.24)

$$= \int d^6x \, \mathcal{O}(x) \varrho(x,t) \,, \tag{3.25}$$

which is thus consistent with the definition of expectation values in statistical mechanics (2.49). Furthermore, the Koopman operator is only first order in the derivatives. We therefore easily find the evolution equation for the probability density $\varrho(x)$,

$$\frac{\partial}{\partial t}\varrho(x,t) = -i\hat{K}\varrho(x,t). \tag{3.26}$$

Compared to (2.42), we deduce the relationship

$$\hat{K} = i\hat{\mathcal{L}}, \qquad (3.27)$$

between the Koopman operator and the Liouville operator. We have thus deduced Liouville's equation from an axiomatic construction on a Hilbert space where classicality enters via the commutation of the position and momentum operators. The fact that the evolution equation for the classical wave function $\psi(x,t)$ and the associated probability density $\varrho(x,t)$ are identical, implies that both are evolved by the same propagator. In the phase-space representation we therefore find

$$\varrho(x^{(f)}, t^{(f)}) = \int d^6 x^{(i)} U(x^{(f)}, t^{(f)} | x^{(i)}, t^{(i)}) \,\varrho(x^{(i)}, t^{(i)}) \,, \tag{3.28}$$

where $U(x^{(f)}, t^{(f)}|x^{(i)}, t^{(i)})$ is given by (3.21). In view of (2.47) we can see that $U(x^{(f)}, t^{(f)}|x^{(i)}, t^{(i)})$ corresponds to the phase-space representation of the Liouville propagator in this time-independent case. We have thus fully recovered the main evolution equations of classical mechanics in this Hilbert space formulation.

In conclusion, the Koopman-von Neumann formulation elegantly unifies classical and quantum mechanical descriptions by recasting the deterministic Liouville equation into a unitary evolution on a Hilbert space, similar to the Schrödinger equation in quantum theory. Indeed, the above formalism can be used to derive the Schrödinger equation in exactly the same way. As we have seen, classicality enters the derivation solely via the classical commutator relation (3.8). If one instead postulates the quantum mechanical commutation relation, $\left[\hat{\vec{q}},\hat{\vec{p}}\right]=i\hbar$, one can analogously derive the Schrödinger equation from these general axioms [48]. Although the latter is intrinsically probabilistic, while classical mechanics is deterministic at the level of individual trajectories, these parallels become very useful when it comes to the description of statistical N-particle systems, which share the intrinsic probabilistic description of quantum mechanics as we have seen in chapter 2. This insight motivates the application of quantum mechanical methods in order to study the dynamics of N-particle systems. One particularly powerful tool in this context is the path integral formalism, which—based on the Koopman-von Neumann framework—can be constructed in direct analogy to its quantum mechanical counterpart. We therefore review the main steps in the next section.

3.1.3. Path Integral Representation and the Koopman-von Neumann Propagator

With the previous motivation of describing classical and quantum mechanics in a unified language, we now turn to the functional-integral formulation associated with our operatorial Koopman-von Neumann construction. In principle, we can follow the same steps as in the usual quantum mechanical description by applying the Trotter product decomposition to the phase-space matrix element (3.21). For that approach, we refer to the appendix of [53]. Instead, we follow [47] and present a related but different construction of the classical-mechanical functional integral, which is more closely related to the general discretization procedure that we will use throughout this work.

The starting point of our construction is the transition amplitude (3.21),

$$U(x^{(f)}, t^{(f)} | x^{(i)}, t^{(i)}) = \langle x^{(f)} | e^{-i(t^{(f)} - t^{(i)})\hat{K}} | x^{(i)} \rangle.$$
(3.29)

Consider the evolution of the initial state $|x^{(i)}\rangle$ by an infinitesimal time step ϵ , and apply the phase-space operator \hat{x} on that evolved state. To first order in ϵ we find, using the commutation relation (3.7) and (3.9), the relation

$$\hat{x} e^{-i\epsilon \hat{K}} | x^{(i)} \rangle = e^{-i\epsilon \hat{K}} \hat{x} | x^{(i)} \rangle + \left[\hat{x}, e^{-i\epsilon \hat{K}} \right] | x^{(i)} \rangle$$
(3.30)

$$= x^{(i)} e^{-i \epsilon \hat{K}} | x^{(i)} \rangle - i \epsilon \left[\hat{x}, \hat{K} \right] e^{-i \epsilon \hat{K}} | x^{(i)} \rangle$$
 (3.31)

$$= x^{(i)} e^{-i \epsilon \hat{K}} | x^{(i)} \rangle + \epsilon \omega \cdot \nabla_x H(x^{(i)}) e^{-i \epsilon \hat{K}} | x^{(i)} \rangle$$
 (3.32)

$$= \left(x^{(i)} + \epsilon \ \omega \cdot \nabla_x H(x^{(i)})\right) e^{-i \epsilon \hat{K}} |x^{(i)}\rangle \tag{3.33}$$

$$\simeq x_{\rm cl}(\epsilon, x^{(i)}, t^{(i)}) e^{-i\epsilon \hat{K}} | x^{(i)} \rangle, \qquad (3.34)$$

where we expressed the commutation relations (3.7) in terms of the symplectic structure (2.7) and identified the first order approximation to the classical trajectory,

$$x_{\rm cl}(\epsilon, x^{\rm (i)}, t^{\rm (i)}) \simeq x^{\rm (i)} + \epsilon \,\dot{x}(t^{\rm (i)}) = x^{\rm (i)} + \epsilon \,\omega \cdot \nabla_x H(x^{\rm (i)})$$
 (3.35)

in the last line. This equation thus implies that the state $e^{-i\epsilon \hat{K}} | x^{(i)} \rangle$ is an eigenstate of \hat{x} with corresponding eigenvalue $x_{\rm cl}(\epsilon, x^{(i)}, t^{(i)})$. Extending this result to finite time shifts, we obtain

$$e^{-i\epsilon \hat{K}} | x^{(i)} \rangle = | x_{cl}(t^{(f)}, x^{(i)}, t^{(i)}) \rangle.$$
 (3.36)

The orthogonality property of the eigenstates of \hat{x} , given by (3.15) implies

$$\langle x^{(f)} | e^{-i(t^{(f)} - t^{(i)})\hat{K}} | x^{(i)} \rangle = \langle x^{(f)} | x_{cl}(t^{(f)}, x^{(i)}, t^{(i)}) \rangle = \delta_{D} \left(x^{(f)} - x_{cl}(t^{(f)}, x^{(i)}, t^{(i)}) \right),$$
(3.37)

which confirms the intuitive expectation that the transition amplitude from the initial state $x^{(i)}$ at time $t^{(i)}$ to the final state $x^{(f)}$ at time $t^{(f)}$ is only non-vanishing if $x^{(f)}$ is located on the classical trajectory at time $t^{(f)}$. We have thus found the important relation

$$U(x^{(f)}, t^{(f)} | x^{(i)}, t^{(i)}) = \delta_{D} \left(x^{(f)} - x_{cl}(t^{(f)}, x^{(i)}, t^{(i)}) \right), \tag{3.38}$$

which is a point-wise comparison between the given microscopic position $x^{(f)}$, and the expected position $x_{cl}(t^{(f)}, x^{(i)}, t^{(i)})$. We will now use this result as a starting point for our path integral derivation. Clearly, the propagator $U(x^{(f)}, t^{(f)} | x^{(i)}, t^{(i)})$ satisfies the *Chapman-Kolmogorov equation*,

$$U(x^{(f)}, t^{(f)}|x^{(i)}, t^{(i)}) = \int d^6x \, U(x^{(f)}, t^{(f)}|x, t) \, U(x, t|x^{(i)}, t^{(i)})$$
(3.39)

which corresponds to decomposing the time evolution into two steps: first propagating

the system to an intermediate configuration x at time t, and then to the final configuration $x^{(f)}$, integrating over all such intermediate states. This procedure can be used to split the evolution into N steps, $t^{(f)} = t_{N+1} > t_N > \ldots > t_1 > t_0 = t^{(i)}$. The Dirac-deltas then ensure that at every time step the particles can be found on the respective classical trajectories. We find⁵

$$U(x^{(f)}, t^{(f)}|x^{(i)}, t^{(i)}) = \left[\prod_{j=1}^{N} \int dx_j\right] \prod_{j=0}^{N} U(x_{j+1}, t_{j+1}|x_j, t_j).$$
 (3.40)

In the continuum limit $N \to \infty$ we may then formally represent the result as

$$U(x^{(f)}, t^{(f)}|x^{(i)}, t^{(i)}) = \int_{x^{(i)}}^{x^{(f)}} \mathcal{D}x \, \delta_{\mathcal{D}} \left[x(t) - x_{\mathcal{C}l}(t; x^{(i)}, t^{(i)}) \right], \tag{3.41}$$

where the functional Dirac-delta distribution $\delta_D[x(t) - x_{\rm cl}(t; x^{(i)}, t^{(i)})]$ gives weight 0 to all trajectories but the classical one, with fixed end points at $x^{(i)}$ and $x^{(f)}$. This enforces that only the full classical trajectory as a whole contributes to the path integral. The classical trajectory is defined as the unique solution to

$$\mathcal{E}[x]\Big|_{x=x_{\text{cl}}} = 0$$
, with $\mathcal{E}[x] = \frac{\mathrm{d}}{\mathrm{d}t}x(t) - \omega \cdot \nabla_x H(x)$. (3.42)

Rather than working directly with the full classical trajectory—which is generally not known in closed form—it is more convenient to enforce the dynamics via the equations of motion. We therefore rewrite the propagator as

$$U(x^{(f)}, t^{(f)}|x^{(i)}, t^{(i)}) = \int_{x^{(i)}}^{x^{(f)}} \mathcal{D}x \, \delta_{\mathcal{D}} \left[\mathcal{E}[x] \right] , \qquad (3.43)$$

which singles out the classical trajectory as the root of $\mathcal{E}[x]$. The transition from (3.41) to (3.43) involves a change of variables that, strictly speaking, requires the inclusion of a functional Jacobian determinant. While this determinant turns out to be constant in the case of symplectic dynamics, this is not true in general. We postpone a more detailed discussion of this point to the next section, where we address the general case, and in particular to the appendices, where we explicitly compute the Jacobian and show that it is unity for symplectic systems. Replacing the Dirac-delta distribution by its functional Fourier representation finally ends up with

$$U(x^{(f)}, t^{(f)}|x^{(i)}, t^{(i)}) = \int_{x^{(i)}}^{x^{(f)}} \mathcal{D}x \, \mathcal{D}\chi \, \exp\left[i \int_{t^{(i)}}^{t^{(f)}} dt \, \chi(t)^{\top} \cdot \mathcal{E}[x]\right], \quad (3.44)$$

where we introduced the doublet $\chi = (\chi_q, \chi_p)$ as Fourier dual variables to $x = (\vec{q}, \vec{p})$. Equation (3.47) is the final result of the Koopman-von Neumann path integral representation of the classical time-evolution operator. The final density can now be

⁵This is often referred to as the compounded Chapman-Kolmogorov equation.

obtained following (3.28) as

$$\varrho_N(x^{(f)}, t^{(f)}) = \int dx^{(i)} \int_{x^{(i)}}^{x^{(f)}} \mathcal{D}x \, \mathcal{D}\chi \, e^{i\mathcal{S}[x,\chi]} \varrho_N(x^{(i)}, t^{(i)}) \,. \tag{3.45}$$

With the "classical action",

$$\mathcal{S}[x,\chi] = \int_{t^{(i)}}^{t^{(f)}} dt \ \chi(t)^{\top} \cdot \mathcal{E}[x]$$
(3.46)

It is straightforward to show [47], that the usual path-integral representation of expectation values of observables $\mathcal{O}(t) = \mathcal{O}(x(t))$, given by

$$\langle \mathcal{O}_1(t_1)\cdots\mathcal{O}_k(t_k)\rangle = \int \mathrm{d}x^{(f)} \int \mathrm{d}x^{(i)} \varrho_N(x^{(i)}, t^{(i)}) \times \\ \times \int_{x^{(i)}}^{x^{(f)}} \mathcal{D}x \mathcal{D}\chi \, \mathcal{O}_1(t_1) \cdots \mathcal{O}_k(t_k) \, \exp\left[\mathrm{i}\mathcal{S}[x, \chi]\right].$$

matches the definition of expectation values in the Heisenberg picture (2.50).

Before concluding our brief summary of the Koopman-von Neumann formalism, we state the general results for the full time-dependent N-particle system. While the derivation follows the same conceptual steps as in the single-particle case, it is mathematically more involved, requiring a generalization of Stone's theorem to time-dependent generators [54]. We therefore omit the details here and present only the final result. In the next section, we provide a more general derivation that does not rely on the underlying Hilbert space structure and is better suited for our purposes. The N-particle Liouville propagator is given by

$$U(\mathbf{x}^{(f)}, t^{(f)}|\mathbf{x}^{(i)}, t^{(i)}) = \int_{\mathbf{x}^{(i)}}^{\mathbf{x}^{(f)}} \mathcal{D}\mathbf{x} \, \mathcal{D}\mathbf{\chi} \, \exp\left[\int_{t^{(i)}}^{t^{(f)}} dt \, \mathbf{\chi}(t)^{\top} \cdot \boldsymbol{\mathcal{E}}[\mathbf{x}, t]\right], \quad (3.47)$$

where the classical trajectory is defined as the unique solution to

$$\left. \mathcal{E}[\mathbf{x}, t] \right|_{\mathbf{x} = \mathbf{x}_{cl}} = 0, \quad \text{with} \quad \left. \mathcal{E}[\mathbf{x}, t] = \frac{\mathrm{d}}{\mathrm{d}t} \mathbf{x}(t) - \boldsymbol{\omega} \cdot \boldsymbol{\nabla}_{\mathbf{x}} H(\mathbf{x}, t). \right.$$
 (3.48)

The time evolution of the full N-particle Liouville density is hence given by

$$\varrho_{N}(\mathbf{x}^{(f)}, t^{(f)}) = \int d\mathbf{x}^{(i)} \int_{\mathbf{x}^{(i)}}^{\mathbf{x}^{(f)}} \mathcal{D}\mathbf{x} \, \mathcal{D}\mathbf{\chi} \, \exp \left[i \int_{t^{(i)}}^{t^{(f)}} dt \, \mathbf{\chi}(t)^{\top} \cdot \boldsymbol{\mathcal{E}}[\mathbf{x}, t] \right] \varrho_{N}(\mathbf{x}^{(i)}, t^{(i)}) \,. \tag{3.49}$$

In chapter 4 we will use this equation as a starting point for a perturbative expansion. Last but not least, ensemble averages of observables are computed analogously to (3.50) as

$$\langle \mathcal{O}_{1}(t_{1}) \cdots \mathcal{O}_{k}(t_{k}) \rangle = \int d\mathbf{x}^{(f)} \int d\mathbf{x}^{(i)} \varrho_{N}(\mathbf{x}^{(i)}, t^{(i)}) \times$$

$$\times \int_{\mathbf{x}^{(i)}}^{\mathbf{x}^{(f)}} \mathcal{D}\mathbf{x} \mathcal{D}\mathbf{\chi} \, \mathcal{O}_{1}(\mathbf{x}(t_{1})) \cdots \mathcal{O}_{k}(\mathbf{x}(t_{k})) \, \exp \left[i \mathcal{S}[\mathbf{x}, \mathbf{\chi}] \right],$$
(3.50)

where the associated action is defined as

$$\mathcal{S}[\mathbf{x}, \boldsymbol{\chi}] = \int_{t^{(i)}}^{t^{(f)}} dt \ \boldsymbol{\chi}(t)^{\top} \cdot \boldsymbol{\mathcal{E}}[\mathbf{x}, t].$$
 (3.51)

The Koopman-von Neumann construction has shown us that it is possible to artificially enlarge the algebra of operators in order to encode the equations of motion within a Hilbert space framework, even if the underlying degrees of freedom commute. At the level of the path integral, this translates into the insertion of functional Dirac delta distributions that enforce the deterministic evolution of the underlying degrees of freedom. This naturally raises the question whether such a construction is generally possible for arbitrary dynamical systems that involve a deterministic evolution subject to stochastic elements, such as random initial conditions or external noise without relying on the abstract Hilbert space construction. The answer lies in the Martin-Siggia-Rose (MSR) formalism [18] and its generalization, the Martin-Siggia-Rose-Janssen-De Dominicis (MSR/JD) path integral [55, 19, 20], which implements these ideas and provides a functional framework that generalizes the operatorial Koopman-von Neumann construction to a broader class of classical systems.

3.2. Path Integrals for General Stochastic Theories

We first start with the general construction of the MSR/JD functional integral for a general stochastic differential equation. Hereby we follow [21]. In the second part, we specialize to the case, where stochasticity only enters via the initial probability distribution, which is the special case relevant for our application.

3.2.1. The MSR/JD-Path Integral Construction

Consider a general real, n-component, classical field

$$\psi_a : \mathbb{R}^{d+1} \to \mathbb{R}^n$$

$$X = (t, x) \mapsto \psi_a(X) = \psi_a(t, x)$$
(3.52)

representing the fundamental degree of freedom of some physical theory. We assume its evolution is governed by the Langevin-type equation,

$$\frac{\partial}{\partial t}\psi_a(X) = F_a[\psi] + \eta_a(X), \qquad (3.53)$$

where for the moment we set the initial value of ψ_a to zero, $\psi_a(t^{(i)}) = 0$, and move the discussion of initial conditions to the end of this section. The stochastic noise $\eta_a(x)$ is drawn from a not necessarily Gaussian probability functional $\mathcal{P}[\eta(X)]$. Our goal will be to construct a functional representation of the time evolution of the field $\psi(X)$ evolving under the combined action of the space and time dependent force or drift term $F_a[\psi] = F_a(\psi(X), X)$ which contains linear and non-linear couplings of the fields, and the stochastic noise $\eta_a(x)$. We present here the compact, continuum-notation form of the derivation which conveys the key conceptual ideas of the subsequent construction. However, all functional treatments require a specific definition of the underlying discretization procedure in order to acquire a well-defined meaning. Therefore, we provide a rigorous discretized derivation of the functional integral in appendix B.

Following [21, 56], we first treat (3.53) as a deterministic equation of motion for with a given fixed realization of the noise $\eta_a(X)$. Let us therefore denote the general, η -dependent solution of (3.53) by $\psi_{a,\eta}(X)$. For a given function $\eta_a(X)$, the exact value of an observable $\mathcal{O}(\psi)$ is therefore given by $\mathcal{O}(\psi_n)$, which we write as

$$\mathcal{O}(\psi_{\eta}) = \int \mathcal{D}\psi \,\mathcal{O}(\psi) \,\delta_{\mathcal{D}} \left[\psi_{a}(X) - \psi_{a,\eta}(X)\right] , \qquad (3.54)$$

where the functional Dirac-delta distribution singles out the specific solution ψ_{η} . We can now insert the equation of motion (3.53), by performing a change of variables in the Dirac-delta distribution⁶,

$$\delta_{\mathrm{D}} \left[\psi_a(X) - \psi_{a,\eta}(X) \right] = \det \left[\frac{\delta \mathcal{E}_a[\psi]}{\delta \psi_b(X)} \right] \delta_{\mathrm{D}} \left[\mathcal{E}_a[\psi] \right]. \tag{3.56}$$

Here, ψ_{η} is the unique solution to

$$\mathcal{E}_a[\psi]\Big|_{\psi=\psi_\eta} = 0, \quad \text{with} \quad \mathcal{E}_a[\psi] := \frac{\partial}{\partial t}\psi_a(X) - F_a(\psi(X), X) - \eta_a(X).$$
 (3.57)

Inserted into (3.54), we find

$$\mathcal{O}(\psi_{\eta}) = \int \mathcal{D}\psi \,\mathcal{O}(\psi) \,\delta_{\mathcal{D}} \left[\mathcal{E}[\psi]\right] \,\det \left[\frac{\delta \mathcal{E}_{a}[\psi]}{\delta \psi_{b}(X)}\right] \,. \tag{3.58}$$

The determinant on the right-hand side represents the functional Jacobian that emerged form the above change of variables. Its explicit form is highly dependent on the underlying discretization procedure, and we refer to appendix B for a more

$$\delta(x - x_0) = \delta(f(x)) |f'(x)|, \tag{3.55}$$

which relates the composition of the Dirac-delta distribution with a function to the Dirac-delta distribution of the corresponding zero. In the functional case, the derivative gets promoted to a Jacobian determinant.

⁶This corresponds to a functional generalization of the familiar identity for real scalar functions $f: \mathbb{R} \to \mathbb{R}$ with a simple root at x_0 , given by

detailed discussion. From our functional approach, the ambiguity related to the functional Jacobian can be inferred from [24],

$$\det\left[\frac{\delta \mathcal{E}_a[\psi]}{\delta \psi_b(X)}\right] = \det\left[\delta_{ab}\frac{\partial}{\partial t} - \frac{\delta F_a[\psi(X), X]}{\delta \psi_b(X)}\right]$$
(3.59)

$$\sim \det \left[\delta_{ab} - \left[\frac{\partial}{\partial t} \right]^{-1} \frac{\delta F_a[\psi(X), X]}{\delta \psi_b(X)} \right],$$
 (3.60)

which can be rewritten as

$$\det \left[\frac{\delta \mathcal{E}_a[\psi]}{\delta \psi_b(X)} \right] \sim \exp \left[\operatorname{tr} \log \left[\delta_{ab} - \left[\frac{\partial}{\partial t} \right]^{-1} \frac{\delta F_a[\psi(X), X]}{\delta \psi_b(X)} \right] \right]. \tag{3.61}$$

The inverse of the time derivative operator is clearly given by the Heaviside function, since $\frac{\partial}{\partial t}\Theta(t-t')=\delta_{\rm D}(t-t')$. Thus, by replacing the logarithm by its series representation, only the first term gives a non-vanishing result, since $\Theta(t-t')\Theta(t'-t)=0$. We thus find

$$\det \left[\frac{\delta \mathcal{E}_a[\psi]}{\delta \psi_b(X)} \right] \sim \exp \left[-\Theta(0) \operatorname{Tr}_X \left[\frac{\delta F_a[\psi]}{\delta \psi_b(X)} \right] \right], \tag{3.62}$$

which clearly depends on the way how $\Theta(0)$ is regularized. This is tightly connected to the underlying stochastic discretization procedure. In the main text, we will adopt the convenient Itô discretization prescription which amounts to setting $\Theta(0) = 0$. In that case, the above determinant yields an irrelevant constant and can safely be absorbed into an overall normalization constant. We can now replace the functional Dirac-delta distribution $\delta_D \left[\mathcal{E}[\psi] \right]$ by its functional Fourier representation, and obtain

$$\mathcal{O}(\psi_{\eta}) = \mathcal{N} \int \mathcal{D}\psi_a \, \mathcal{D}\hat{\psi}_a \, \mathcal{O}(\psi) \, e^{i \int_X \, \hat{\psi}_a(X) \, \mathcal{E}_a[\psi]}$$
(3.63)

$$= \mathcal{N} \int \mathcal{D}\psi_a \mathcal{D}\hat{\psi}_a \,\mathcal{O}(\psi) e^{i\int_X \hat{\psi}_a(X) \left(\frac{\partial}{\partial t}\psi_a(X) - F_a[\psi(X), X] - \eta_a(X)\right)} \,. \tag{3.64}$$

The auxiliary field $\hat{\psi}$, which has been introduced as a Fourier conjugate field to ψ , clearly plays the same role as χ in the Koopman-von Neumann formalism and enforces the equations of motion. Indeed, it can be shown, that the kinetic coupling between $\hat{\psi}$ and $\dot{\psi}$ in the exponent translates into a commutator relation between the corresponding $\hat{\psi}$ and ψ operators in the respective operatorial theory. This was in fact the way MSR originally introduced the auxiliary field. In the above derivation we kept all fields deterministic. To obtain an expectation value for the observable $\mathcal{O}(\psi_n)$, we average over the respective probability distribution and obtain

$$\langle \mathcal{O}(\psi_{\eta}) \rangle = \int \mathcal{D}\psi_a \, \mathcal{D}\hat{\psi}_a \, \mathcal{D}\eta_a \, \mathcal{O}(\psi) \, e^{iS[\psi,\hat{\psi}]} \mathcal{P}[\eta] \,,$$
 (3.65)

where we identified the action

$$S[\psi, \hat{\psi}] = \int_{X} \hat{\psi}_{a}(X) \left(\frac{\partial}{\partial t} \psi_{a}(X) - F_{a}(\psi(X), X) - \eta_{a}(X) \right). \tag{3.66}$$

We will investigate the physical role of the auxiliary field $\hat{\psi}$ in the actual application in the next chapters. However, at this point we can already see that it plays an essential role in carrying the statistics of the theory, since the η -functional integration yields

$$\int \mathcal{D}\eta_a \,\mathrm{e}^{-\mathrm{i}\int_X \,\hat{\psi}_a(X)\eta_a(X)} \,\mathcal{P}[\eta] = \mathcal{Z}_{\eta}[\hat{\psi}_a] \,, \tag{3.67}$$

which is the moment-generating functional w.r.t. the probability distribution $\mathcal{P}[\eta]$. This will be exploited in chapters 5 and 6. Equation (3.65) can be used as a starting point for a functional treatment of the underlying stochastic theory. One therefore conveniently introduces the full moment-generating functional

$$\mathcal{Z}[J,\hat{J}] = \int \mathcal{D}\psi_a \, \mathcal{D}\hat{\psi}_a \, \mathcal{D}\eta_a \, e^{iS[\psi,\hat{\psi}] + i \int_X \hat{J}_a(X)\hat{\psi}_a(X) + i \int_X J_a(X)\psi_a(X)} \, \mathcal{P}[\eta] \,. \tag{3.68}$$

3.2.2. Stochastic Initial Conditions

Let us now turn to the case more relevant for our purposes, where the dynamics are purely deterministic, and the only source of randomness lies in the initial conditions. These are characterized by a probability distribution $\mathcal{P}[\psi^{(i)}]$, where $\psi^{(i)}$ denotes the initial configuration of the field. The associated initial value problem for the dynamical evolution is then given by

$$\begin{cases} \frac{\partial}{\partial t} \psi_a(t, x) = F_a[\psi] \\ \psi_a(t = t^{(i)}, x) = \psi_a^{(i)}(x) . \end{cases}$$
(3.69)

To make contact to the MSR/JD construction, we note that the above initial value problem is equivalent to

$$\begin{cases} \frac{\partial}{\partial t} \psi_a(t, x) = F_a[\psi] + \delta_D \left(t - t^{(i)} \right) \psi_a^{(i)}(x) \\ \psi_a(t < t^{(i)}, x) = 0. \end{cases}$$
(3.70)

This system has a jump discontinuity at $t = t^{(i)}$ initializing the desired value of the field ψ . The equivalence between both systems (3.69) and (3.70) can be seen by integrating the latter over a small interval $[t^{(i)} - \epsilon, t^{(i)} + \epsilon]$,

$$\int_{t^{(i)}-\epsilon}^{t^{(i)}+\epsilon} dt \frac{\partial}{\partial t} \psi_a(t,x) = \int_{t^{(i)}-\epsilon}^{t^{(i)}+\epsilon} dt F_a(\psi(t,x),t,x) + \int_{t^{(i)}-\epsilon}^{t^{(i)}+\epsilon} dt \delta_D(t-t^{(i)}) \psi_a^{(i)}(x), \quad (3.71)$$

from which we find

$$\psi_a(t^{(i)} + \epsilon, x) = \mathcal{O}(\epsilon) + \psi^{(i)}(x), \qquad (3.72)$$

where the force term contributes to order ϵ by the boundedness of F. In the limit $\epsilon \to 0$ we therefore recover the correct initial condition $\psi_a(t=t^{(i)},x)=\psi_a^{(i)}(x)$. We may thus follow the same steps as before to find the appropriate generating functional, simply by replacing the noise $\eta_a(t,x)$ by $\delta_D\left(t-t^{(i)}\right)\psi_a^{(i)}(x)$ which thus acts as a noise localized at initial time with space-dependent value $\psi^{(i)}(x)$. The result therefore is

$$\mathcal{Z}[J,\hat{J}] = \int \mathcal{D}\psi_a \, \mathcal{D}\hat{\psi}_a \, \mathcal{D}\psi_a^{(i)} \, e^{iS[\psi,\hat{\psi}]+i\int_X \, \hat{J}_a(X)\hat{\psi}_a(X)+i\int_X \, J_a(X)\psi_a(X)} \, \mathcal{P}[\psi^{(i)}] \,, \qquad (3.73)$$

with the associated action

$$S[\psi, \hat{\psi}] = \int_{X} \hat{\psi}_{a}(X) \left(\frac{\partial}{\partial t} \psi_{a}(X) - F_{a}(\psi(X), X) - \delta_{D} \left(t - t^{(i)} \right) \psi_{a}^{(i)}(x) \right). \tag{3.74}$$

This will be the starting point of our discussion in chapter 6.

We have now assembled all relevant pieces for a functional integral description of the N-particle system. In the next section, we will apply this framework directly to the microscopic trajectories to propagate the initial N-particle Liouville phase-space density evolving under a general time-dependent Hamiltonian. In particular, the MSR/JD formalism yields a functional representation of the N-particle time-evolution operator $\hat{U}(t^{(f)}, t^{(i)})$, suitable for systematic perturbative analyses.

4 Formal Solution to Liouville's Equation

In this chapter, we will present a formal solution to the Liouville equation based on the path-integral construction of chapter 3. A similar result was derived by [25] without the usage of path-integrals. The resulting perturbation theory will allow us to compute unequal-time correlation functions of the Klimontovich phase-space density in a perturbative manner. The general idea is based on propagating individual particles along their respective trajectories and to include interactions between particles order by order in the interaction Hamiltonian $H_{\rm int}$. Although using a slightly different approach, our results will be qualitatively and quantitatively similar to [31].

4.1. Dyson-Series Expansion of the Liouville Propagator

Having discussed the path-integral representation of the Liouville propagator for N-particle systems in chapter 3, we can now derive a formal solution to the Liouville equation which propagates the initial Liouville phase-space density to a final one. We start from (3.49),

$$\varrho_{N}(\mathbf{x}^{(f)}, t^{(f)}) = \int d\mathbf{x}^{(i)} U(\mathbf{x}^{(f)}, t^{(f)} | \mathbf{x}^{(i)}, t^{(i)}) \varrho_{N}^{(i)}(\mathbf{x}^{(i)})$$

$$= \int d\mathbf{x}^{(i)} \int_{\mathbf{x}^{(i)}}^{\mathbf{x}^{(f)}} \mathcal{D}\mathbf{x} \, \mathcal{D}\mathbf{\chi} \exp \left[\int_{t^{(i)}}^{t^{(f)}} dt \, \mathbf{\chi}(t)^{\top} \cdot \boldsymbol{\mathcal{E}}(\mathbf{x}, t) \right] \varrho_{N}^{(i)}(\mathbf{x}^{(i)})$$

$$= \int d\mathbf{x}^{(i)} \int_{\mathbf{x}^{(i)}}^{\mathbf{x}^{(f)}} \mathcal{D}\mathbf{x} \, \mathcal{D}\mathbf{\chi} \, e^{i\mathcal{S}[\mathbf{x}, \mathbf{\chi}]} \varrho_{N}^{(i)}(\mathbf{x}^{(i)}), \qquad (4.1)$$

where we have introduced the action $S[\mathbf{x}, \boldsymbol{\chi}]$ in the last line. In most cases, the path integral above cannot be solved exactly, as this would correspond to solving the N-body problem. We, therefore, must rely on approximation schemes. One such example is the perturbation theory around the free evolution, which we discuss in

the following. To that end, let us begin by splitting the equations of motion into a free and an interacting part,

$$\mathcal{E}(\mathbf{x},t) = \dot{\mathbf{x}} - \boldsymbol{\omega} \cdot \nabla_{\mathbf{x}} H_0(\mathbf{x},t) - \boldsymbol{\omega} \cdot \nabla_{\mathbf{x}} H_{\text{int}}(\mathbf{x},t) \equiv \mathcal{E}_0(\mathbf{x},t) + \mathcal{E}_{\text{int}}(\mathbf{x},t), \qquad (4.2)$$

where $H_0(\mathbf{x}, t)$ is the free Hamiltonian, generally defined by (2.19) and $H_{\text{int}}(\mathbf{x}, t)$ is the interacting Hamiltonian,

$$H_{\text{int}}(\mathbf{x},t) = \frac{1}{2} \sum_{i \neq j=1}^{N} v_2(x_i, x_j, t), \qquad (4.3)$$

which, for simplicity, contains only two-particle interactions. Accordingly, we define the free and interacting parts of the action as,

$$S_0[\mathbf{x}, \boldsymbol{\chi}] = \boldsymbol{\chi}^{\mathsf{T}}(t) \cdot \boldsymbol{\mathcal{E}}_0(\mathbf{x}, t) \quad \text{and} \quad S_{\mathrm{int}}[\mathbf{x}, \boldsymbol{\chi}] = \boldsymbol{\chi}^{\mathsf{T}}(t) \cdot \boldsymbol{\mathcal{E}}_{\mathrm{int}}(\mathbf{x}, t).$$
 (4.4)

Following the usual procedure from quantum mechanics, we replace the exponential containing the interaction part by its series expansion and find

$$U(\mathbf{x}^{(f)}, t^{(f)}|\mathbf{x}^{(i)}, t^{(i)}) = \int_{\mathbf{x}^{(i)}}^{\mathbf{x}^{(f)}} \mathcal{D}\mathbf{x} \, \mathcal{D}\mathbf{\chi} \, e^{i\mathcal{S}_0[\mathbf{x}, \chi] + i\mathcal{S}_{int}[\mathbf{x}, \chi]}$$

$$= \int_{\mathbf{x}^{(i)}}^{\mathbf{x}^{(f)}} \mathcal{D}\mathbf{x} \, \mathcal{D}\mathbf{\chi} \, e^{i\mathcal{S}_0[\mathbf{x}, \chi]} \sum_{n=0}^{\infty} \frac{(i\mathcal{S}_{int}[\mathbf{x}, \chi])^n}{n!}$$

$$\equiv \sum_{n=0}^{\infty} U_n(\mathbf{x}^{(f)}, t^{(f)}|\mathbf{x}^{(i)}, t^{(i)}), \qquad (4.5)$$

where U_n is referred to as the *n*-th order propagator and is defined as

$$U_n(\mathbf{x}^{(f)}, t^{(f)}|\mathbf{x}^{(i)}, t^{(i)}) = \frac{\mathrm{i}^n}{n!} \int_{\mathbf{x}^{(i)}}^{\mathbf{x}^{(f)}} \mathcal{D}\mathbf{x} \, \mathcal{D}\boldsymbol{\chi} \, \mathrm{e}^{\mathrm{i}\mathcal{S}_0[\mathbf{x}, \boldsymbol{\chi}]} \Big(\mathcal{S}_{\mathrm{int}}[\mathbf{x}, \boldsymbol{\chi}] \Big)^n$$
(4.6)

$$=rac{\mathrm{i}^n}{n!}\int\limits_{m{\chi}^{(\mathrm{i})}}^{m{\chi}^{(\mathrm{f})}}\mathcal{D}m{\chi}\,\mathcal{D}m{\chi}\,\mathrm{e}^{\mathrm{i}\mathcal{S}_0[m{x},m{\chi}]}\int\limits_{t^{(\mathrm{i})}}^{t^{(\mathrm{f})}}\mathrm{d}t_1\ldots\mathrm{d}t_n\left(m{\chi}_1^ opm{\mathcal{E}}_{\mathrm{int}}(m{x}_1,t_1)
ight)\ldots\left(m{\chi}_n^ opm{\mathcal{E}}_{\mathrm{int}}(m{x}_n,t_n)
ight)\,,$$

where we introduced the shorthand notation $\chi_a := \chi(t_a)$ and $\mathbf{x}_a := \mathbf{x}(t_a)$. The *n*-th order propagator can now be computed order by order in n.

4.1.1. Free Theory

The free theory is obtained by setting n = 0, for which we find

$$U_0(\mathbf{x}^{(f)}, t^{(f)} | \mathbf{x}^{(i)}, t^{(i)}) = \int_{\mathbf{x}^{(i)}}^{\mathbf{x}^{(f)}} \mathcal{D}\mathbf{x} \, \mathcal{D}\mathbf{\chi} \, \exp \left[i \int_{t^{(i)}}^{t^{(f)}} dt \, \, \mathbf{\chi}(t)^{\top} \cdot \boldsymbol{\mathcal{E}}_0(\mathbf{x}, t) \right]$$
(4.7)

$$= \int_{\mathbf{x}^{(i)}}^{\mathbf{x}^{(f)}} \mathcal{D}\mathbf{x} \, \delta_{\mathrm{D}} \left[\boldsymbol{\mathcal{E}}_{0}(\mathbf{x}, t) \right] = \, \delta_{\mathrm{D}} \left(\mathbf{x}^{(f)} - \mathbf{x}_{\mathrm{cl}}^{(0)}(t^{(f)}; \mathbf{x}^{(i)}, t^{(i)}) \right) \,. \tag{4.8}$$

In going from the first to the second line, we performed the functional χ -integration, which yields a Dirac-delta distribution enforcing the classical equations of motion $\mathcal{E}_0(\mathbf{x},t)$. We then replaced these equations by their solution, the free classical trajectory $\mathbf{x}_{\rm cl}^{(0)}(t^{\rm (f)};\mathbf{x}^{\rm (i)},t^{\rm (i)})$, according to (3.41) and (3.43). We, hence, find for the free propagator,

$$U_0(\mathbf{x}^{(f)}, t^{(f)}|\mathbf{x}^{(i)}, t^{(i)}) = \delta_D\left(\mathbf{x}^{(f)} - \mathbf{G}(t^{(f)}, t^{(i)}) \cdot \mathbf{x}^{(i)}\right) \Theta(t^{(f)} - t^{(i)}), \tag{4.9}$$

where we made use of the fact that the exact expression for the free trajectory is known, and given by (2.22), with the free particle retarded Green function $G(t^{(f)}, t^{(i)})$. The Heaviside function is included to ensure the causal propagation of the density. We can now exactly solve the freely evolved density,

$$\varrho_N^{(0)}(\mathbf{x}^{(f)}, t) = \int d\mathbf{x}^{(i)} U_0(\mathbf{x}^{(f)}, t^{(f)} | \mathbf{x}^{(i)}, t^{(i)}) \varrho_N^{(i)}(\mathbf{x}^{(i)})$$
(4.10)

$$= \varrho_N^{(i)}(\boldsymbol{G}_{fi}^{-1} \cdot \mathbf{x}^{(f)}), \qquad (4.11)$$

where we used $\det(\boldsymbol{G}) = 1$ to solve the argument of the Dirac-delta distribution for $\mathbf{x}^{(i)}$ and introduced the shorthand notation $\boldsymbol{G}_{ab} \equiv \boldsymbol{G}(t_a, t_b)$. The time-evolved density is obtained by evaluating the initial density $\varrho_N^{(i)}$ at the pre-image of the final phase-space point $\mathbf{x}^{(f)}$ under the map defined by the free particle propagator $\boldsymbol{G} : \mathbf{x}^{(i)} \mapsto \mathbf{x}^{(f)}$, i. e., by tracing the trajectories backwards in time to their initial positions. We note, that this is the Γ -space formulation of the free-streaming discussed in section 2.4.1.

4.1.2. Interacting Theory

For n > 0, we need to evaluate expressions of the form (4.6). We, therefore, note that the following holds:

$$i \int_{\mathbf{x}^{(i)}}^{\mathbf{x}^{(f)}} \mathcal{D}\mathbf{x} \, \mathcal{D}\boldsymbol{\chi} \, e^{i\mathcal{S}_0[\mathbf{x},\boldsymbol{\chi}]} \int_{t^{(i)}}^{t^{(f)}} dt_1 \left(\boldsymbol{\chi}_1^{\top} \cdot \boldsymbol{\mathcal{E}}_{int}(\mathbf{x}_1, t_1)\right) = \int d\mathbf{x}_1 dt_1 U_0(\mathbf{f}|\mathbf{1}) \hat{\mathcal{L}}_{int}(t_1) U_0(\mathbf{1}|\mathbf{i}), \tag{4.12}$$

where we identified the interaction Liouvillian defined in (2.45) and used the abbreviation $U(\mathbf{a}|\mathbf{b}) = U(\mathbf{x}_a, t_a|\mathbf{x}_b, t_b)$. This can be easily verified by discretizing the path integral, including a breakpoint at \mathbf{x}_1 , and replacing the auxiliary field $\mathbf{\chi}_1$ by

 $-i\nabla_x$ acting on the free propagator on its right. Repeating the steps for every action insertion in expression (4.6), we find

$$U_{n}(\mathbf{f}|\mathbf{i}) = \int_{t^{(i)}}^{t^{(f)}} d\mathbf{x}_{n} dt_{n} \dots \int_{t^{(i)}}^{t_{2}} d\mathbf{x}_{1} dt_{1} U_{0}(\mathbf{f}|\mathbf{n}) \hat{\mathcal{L}}_{int}(t_{n}) U_{0}(\mathbf{n}|\mathbf{n}-\mathbf{1}) \hat{\mathcal{L}}_{int}(t_{n-1}) \dots$$

$$\dots \hat{\mathcal{L}}_{int}(t_{1}) U_{0}(\mathbf{1}|\mathbf{i}).$$

$$(4.13)$$

Note that at n-th order there are n! possibilities of time-ordering n interactions which, thus, cancels the $\frac{1}{n!}$ prefactor in (4.6). We then obtain a *Born-type* series representation of the N-particle Liouville propagator. In particular, U_n is subject to the following recurrence relation,

$$U_n(\mathbf{f}|\mathbf{i}) = \int_{t^{(i)}}^{t^{(f)}} d\mathbf{x}_n dt_n U_0(\mathbf{f}|\mathbf{n}) \hat{\mathcal{L}}_{int}(t_n) U_{n-1}(\mathbf{n}|\mathbf{i}).$$
(4.14)

Inserted into the series representation of the propagator (4.5), we find the integral equation solved by the Liouville propagator,

$$U(\mathbf{f}|\mathbf{i}) = U_0(\mathbf{f}|\mathbf{i}) + \int_{t^{(i)}}^{t^{(f)}} d\mathbf{x}_1 dt_1 U_0(\mathbf{f}|\mathbf{1}) \hat{\mathcal{L}}_{int}(t_1) U(\mathbf{1}|\mathbf{i}).$$
(4.15)

Upon integration over the initial distribution, this leads to an integral equation of *Lippmann-Schwinger type* for the full phase-space density,

$$\varrho_N(\mathbf{x}^{(f)}, t^{(f)}) = \varrho_N^{(0)}(\mathbf{x}^{(f)}, t^{(f)}) + \int_{t^{(i)}}^{t^{(f)}} d\mathbf{x}_1 dt_1 U_0(\mathbf{x}^{(f)}, t^{(f)} | \mathbf{x}_1, t_1) \hat{\mathcal{L}}_{int}(t_1) \varrho_N(\mathbf{x}_1, t_1). \quad (4.16)$$

Integrating the above equation over the full final phase space and using the normalization of the ϱ_N and $\varrho_N^{(0)}$, we arrive at the normalization condition¹,

$$0 = \int_{t^{(i)}}^{t^{(f)}} d\mathbf{x}_1 dt_1 \,\hat{\mathcal{L}}_{int}(t_1) \,\varrho_N(\mathbf{x}_1, t_1) \,. \tag{4.17}$$

Furthermore, this condition has to hold for every individual particle and at any order of perturbation theory.

Since the free propagator consists of a Dirac-delta distributions, we can explicitly solve the integrals over the ensemble in (4.13). Consider, for instance, the first order

¹This equation can be equivalently verified upon integration by parts and making use of the anti-symmetry of the symplectic structure in combination with the fact that the phase-space density vanishes at the boundaries of phase space.

correction to the full Liouville density which, inserting $\hat{\mathcal{L}}_{int}(t)$, reads

$$\varrho_N^{(1)}(\mathbf{x}^{(f)},t) = \int d\mathbf{x}_1 \int_{t^{(i)}}^{t^{(f)}} dt_1 \delta_D \left(\mathbf{x}^{(f)} - \mathbf{G}_{f1} \cdot \mathbf{x}_1 \right) \nabla_{\mathbf{x}_1} H_{\text{int}}(\mathbf{x}_1, t_1) \cdot \boldsymbol{\omega} \cdot \nabla_{\mathbf{x}_1} \varrho_N^{(i)}(\mathbf{G}_{1i}^{-1} \cdot \mathbf{x}_1).$$

$$(4.18)$$

The gradient on the right-hand side acts on the inner argument \mathbf{x}_1 . We find

$$\left. \boldsymbol{\nabla}_{\mathbf{x}_{1}} \varrho_{N}^{(\mathrm{i})}(\boldsymbol{G}_{1i}^{-1} \cdot \mathbf{x}_{1}) = \boldsymbol{G}_{1i}^{-\top} \cdot \boldsymbol{\nabla}_{\mathbf{y}_{1}} \varrho_{N}^{(\mathrm{i})}(\mathbf{y}) \right|_{\mathbf{y} = \boldsymbol{G}_{1i}^{-1} \cdot \mathbf{x}_{1}} = \boldsymbol{G}_{1i}^{-\top} \cdot \overline{\boldsymbol{\nabla}}_{\mathbf{x}_{1}} \varrho_{N}^{(\mathrm{i})}(\boldsymbol{G}_{1i}^{-1} \cdot \mathbf{x}_{1}), \quad (4.19)$$

where the notation $\overline{\nabla}_{\mathbf{x}_1}$ indicates that the gradient acts on the full argument evaluated at $G_{1i}^{-1} \cdot \mathbf{x}_1$. A similar reasoning has been used by [25] in order to extract the inner derivative. The notation $G^{-\top}$ indicated that we are using the inverse transpose. Accordingly, equation (4.18) can be re-written as

$$\varrho_N^{(1)}(\mathbf{x}^{(f)},t) = \int_{t^{(i)}}^{t^{(f)}} dt_1 \overline{\nabla}_{\mathbf{x}^{(f)}} H_{\text{int}}(\boldsymbol{G}_{f1}^{-1} \cdot \mathbf{x}^{(f)}, t_1) \cdot \boldsymbol{\omega} \cdot \boldsymbol{G}_{1i}^{-\top} \cdot \overline{\nabla}_{\mathbf{x}^{(f)}} \varrho_N^{(i)}(\boldsymbol{G}_{fi}^{-1} \cdot \mathbf{x}^{(f)}), \qquad (4.20)$$

where we performed the integration over \mathbf{x}_1 using the Dirac-delta distribution on the left-hand side of $(4.18)^2$. We compactify the notation by introducing the operator

$$\hat{\boldsymbol{S}}_{ab}(\overline{\boldsymbol{\nabla}}_{\mathbf{x}_c}) \equiv \hat{\boldsymbol{S}}(t_a, t_b; \overline{\boldsymbol{\nabla}}_{\mathbf{x}_c}) \equiv \boldsymbol{\omega} \cdot \boldsymbol{G}_{ab}^{-\top} \cdot \overline{\boldsymbol{\nabla}}_{\mathbf{x}_c}, \qquad (4.21)$$

which, importantly, is defined to only act on objects with the same time-label t_b . The final first-order correction then reads

$$\varrho_N^{(1)}(\mathbf{x}^{(f)}, t^{(f)}) = \int_{t^{(i)}}^{t^{(f)}} dt_1 \overline{\nabla}_{\mathbf{x}^{(f)}} H_{\text{int}}(\boldsymbol{G}_{f1}^{-1} \cdot \mathbf{x}^{(f)}, t_1) \cdot \hat{\boldsymbol{S}}_{1i}(\overline{\nabla}_{\mathbf{x}^{(f)}}) \varrho_N^{(0)}(\mathbf{x}^{(f)}, t^{(f)}). \tag{4.22}$$

This equation can be interpreted as a scattering of the incoming free density with the interacting part of the Hamiltonian which carries the two-particle potential. The freely evolved density is, thus, deformed once by the interaction. The corresponding first order correction to the Liouville propagator, therefore, reads

$$U_{1}(\mathbf{x}^{(f)}, t^{(f)}|\mathbf{x}^{(i)}, t^{(i)}) = \int_{t^{(i)}}^{t^{(f)}} dt_{1} \overline{\nabla}_{\mathbf{x}^{(f)}} H_{\text{int}}(\boldsymbol{G}_{f1}^{-1} \cdot \mathbf{x}^{(f)}, t_{1}) \cdot \hat{\boldsymbol{S}}_{1i}(\overline{\nabla}_{\mathbf{x}^{(f)}}) U_{0}(\mathbf{x}^{(f)}, t^{(f)}|\mathbf{x}^{(i)}, t^{(i)}).$$

$$(4.23)$$

We can repeat similar steps for the second-order correction to the density, which is

²We also replaced $\nabla_{\mathbf{x}_1} H_{\text{int}}(\mathbf{x}_1, t_1)$ by $\overline{\nabla}_{\mathbf{x}_1} H_{\text{int}}(\mathbf{x}_1, t_1)$, which is trivial but makes sure to avoid collecting a matrix G_{f1} when applying the derivative.

given by

$$\varrho_N^{(2)}(\mathbf{x}^{(f)}, t^{(f)}) = \int d\mathbf{x}_2 \int_{t^{(i)}}^{t^{(f)}} dt_2 \delta_D \left(\mathbf{x}^{(f)} - \mathbf{G}_{f2} \cdot \mathbf{x}_2\right) \nabla_{\mathbf{x}_2} H_{\text{int}}(\mathbf{x}_2, t_2) \cdot \boldsymbol{\omega} \cdot \nabla_{\mathbf{x}_2} \varrho_N^{(1)}(\mathbf{x}_2, t_2).$$

$$(4.24)$$

This equation can now be solved similarly to the one above, however, care has to be taken when applying the phase-space gradient acting on $\varrho_N^{(1)}(\mathbf{x}_2, t_2)$, which can now either act on the interacting Hamiltonian H_{int} or the initial density in (4.22). For each case we collect a different particle propagator. The overall result may be brought into the form

$$\varrho_{N}^{(2)}(\mathbf{x}^{(f)}, t^{(f)}) = \int_{t^{(i)}}^{t^{(f)}} dt_{2} \int_{t^{(i)}}^{t_{2}} dt_{1} \left(\overline{\nabla}_{\mathbf{x}^{(f)}} H_{\text{int}}(\boldsymbol{G}_{f2}^{-1} \cdot \mathbf{x}^{(f)}, t_{2}) \cdot \left[\hat{\boldsymbol{S}}_{2i}(\overline{\nabla}_{\mathbf{x}^{(f)}}) + \hat{\boldsymbol{S}}_{21}(\overline{\nabla}_{\mathbf{x}^{(f)}}) \right] \right) \times \left(\overline{\nabla}_{\mathbf{x}^{(f)}} H_{\text{int}}(\boldsymbol{G}_{f1}^{-1} \cdot \mathbf{x}^{(f)}, t_{1}) \cdot \hat{\boldsymbol{S}}_{1i}(\overline{\nabla}_{\mathbf{x}^{(f)}}) \right) \varrho_{N}^{(0)}(\mathbf{x}^{(f)}, t^{(f)}). \tag{4.25}$$

Since the operators (4.21) can only act on an object with the same time-label t_b , in the above expression \hat{S}_{1i} and \hat{S}_{2i} both act on the initial phase-space density, while \hat{S}_{21} acts on the interacting Hamiltonian with the time argument t_1 . At second order, thus, two possible processes can occur: Either the classical evolution is affected twice by an interaction with an unperturbed trajectory resulting in a second order differential operator acting on $\varrho_N^{(0)}$, or the classical evolution is affected once by a perturbed trajectory that has already been deflected once due to a former interaction with H_{int} . This results in a single derivative acting on the free evolution and a single derivative acting on the interaction H_{int} itself. This can now be generalized to the following expression,

$$\varrho_{N}^{(n)}(\mathbf{x}^{(f)}, t^{(f)}) = \int_{t^{(i)}}^{t^{(f)}} dt_{n} \int_{t^{(i)}}^{t_{n}} dt_{n-1} \dots \int_{t^{(i)}}^{t_{2}} dt_{1} \times \\
\times \prod_{a=0}^{n-1} \left[\overline{\nabla}_{\mathbf{x}^{(f)}} H_{\text{int}}(\boldsymbol{G}_{f(n-a)}^{-1} \cdot \mathbf{x}^{(f)}, t_{n-a}) \cdot \sum_{b=0}^{n-a-1} \hat{\boldsymbol{S}}_{(n-a)b}(\overline{\nabla}_{\mathbf{x}^{(f)}}) \right] \varrho_{N}^{(0)}(\mathbf{x}^{(f)}, t^{(f)}).$$
(4.26)

We introduce the *n*-th order scattering operator \hat{S}_n given by

$$\hat{\mathcal{S}}_{n} := \int_{t^{(i)}}^{t^{(f)}} dt_{n} \int_{t^{(i)}}^{t_{n}} dt_{n-1} \dots \int_{t^{(i)}}^{t_{2}} dt_{1} \prod_{a=0}^{n-1} \left[\overline{\boldsymbol{\nabla}}_{\boldsymbol{\mathsf{x}}^{(f)}} H_{\text{int}}(\boldsymbol{G}_{f(n-a)}^{-1} \cdot \boldsymbol{\mathsf{x}}^{(f)}, t_{n-a}) \cdot \sum_{b=0}^{n-a-1} \hat{\boldsymbol{S}}_{(n-a)b}(\overline{\boldsymbol{\nabla}}_{\boldsymbol{\mathsf{x}}^{(f)}}) \right],$$

$$(4.27)$$

where $t_0 \equiv t^{(i)}$, which allows us to express the total Liouville phase-space density as

$$\varrho_N(\mathbf{x}^{(f)}, t^{(f)}) = \sum_{n=0}^{\infty} \hat{\mathcal{S}}_n \, \varrho_N^{(0)}(\mathbf{x}^{(f)}, t^{(f)}) \,. \tag{4.28}$$

The above equation shows how the total Liouville phase-space density arises from the free evolution as a deformation caused by interactions. It represents the general solution to the Liouville equation, reduced to all possible combinations of interaction processes that might happen at *n*-th order, yielding a series representation in terms of differential operators. The solution now only consists of evaluating time integrals for all possible interactions. Similarly, we find for the *n*-th order propagator

$$U_n(\mathbf{x}^{(f)}, t^{(f)}|\mathbf{x}^{(i)}, t^{(i)}) = \hat{\mathcal{S}}_n U_0(\mathbf{x}^{(f)}, t^{(f)}|\mathbf{x}^{(i)}, t^{(i)}). \tag{4.29}$$

4.2. Unequal-Time Correlation Functions

We are now ready to compute arbitrary expectation values by inserting the respective operators into the functional integration as shown in (3.50),

$$C_{f\dots f}(x_1, t_1, \dots, x_k, t_k) = \int d\mathbf{x}^{(i)} \int_{\mathbf{x}^{(i)}} \mathcal{D}\mathbf{x} \, \mathcal{D}\boldsymbol{\chi} \, \Phi_f(x_1, t_1) \cdots \Phi_f(x_k, t_k) \, e^{i\mathcal{S}[\mathbf{x}, \boldsymbol{\chi}]} \varrho_N^{(i)}(\mathbf{x}^{(i)}) \,.$$

$$(4.30)$$

There are, in principle, several ways to proceed now: The strategy pursued in [29, 31] is to define a generating functional by introducing external sources for the fields $\mathbf{x}(t)$ and $\chi(t)$ and to represent the observables as functional derivatives with respect to those sources. This allows the operators to be pulled out of the functional integration, in close analogy to how expectation values are obtained in quantum field theory. However, this method becomes cumbersome in our case, since the observables of interest—most notably the Klimontovich phase-space density—are non-polynomial functionals of the microscopic fields. In particular, the Klimontovich phase-space density is defined as a sum over Dirac-delta functions of the microscopic particles, which makes it non-analytic in the fundamental degrees of freedom. To apply the functional derivative technique, one must first express the Klimontovich density in terms of its Fourier representation, where each Dirac-delta function is written as an exponential function of the microscopic fields. These exponentials then act as translation operators on the sources in the generating functional, shifting the source fields at the point of insertion. This effectively re-introduces the operator insertions as modifications of the background source configuration.

We will, however, follow a different path more closely related to how unequal-time correlation functions of macroscopic quantities are computed in kinetic theory [26]. Let us therefore, again, split the functional integration (3.50) at the respective operator insertions. We find

$$C_{f...f}(x_1, t_1, \dots, x_k, t_k) = \int d\mathbf{x}_1 \cdots d\mathbf{x}_k d\mathbf{x}^{(i)} \Phi_f(x_1, t_1) U(\mathbf{x}_1, t_1 | \mathbf{x}_2, t_2) \dots$$

$$\dots U(\mathbf{x}_{k-1}, t_{k-1} | \mathbf{x}_k, t_k) \Phi_f(x_k, t_k) U(\mathbf{x}_k, t_k | \mathbf{x}^{(i)}, t^{(i)}) \varrho_N^{(i)}(\mathbf{x}^{(i)}).$$
(4.31)

The system is, thus, evolved from an initial configuration at time $t^{(i)}$ to each operator insertion, using the full N-particle propagator $U(\mathbf{x}_r, t_r | \mathbf{x}_{r-1}, t_{r-1})$. The perturbation

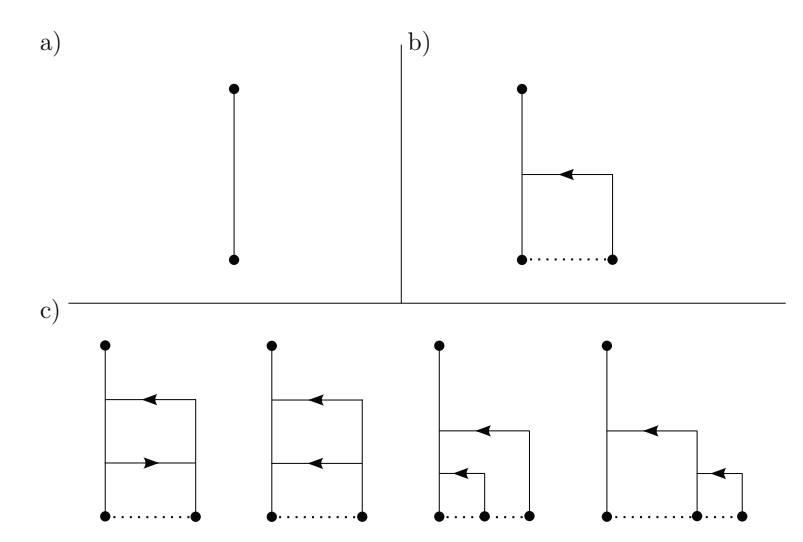


Figure 4.1.: A schematic diagram representation of the terms up to second order in perturbation theory for the mean Klimontovich phase space density $C_f(x_1, t_2)$ is given. In a) we present the free theory (4.32), in b) the first-order perturbation theory (4.35) and in c) the second-order perturbation theory. The filled circles represent positions in phase space. Interactions are depicted as arrows. The direction of the arrows indicates that, for instance, in b) a force is acting on the one-particle distribution at phase space position x_1 labeled 1. All phase space positions are connected by a dotted line, representing the respective initial s-particle phase space density. The two diagrams on the left in c) arise from the shot-noise contributions when evaluating the second-order expression. Figure taken from [57].

theory now consists of expanding the respective full propagators in a series expansion as discussed in the previous section and collecting the terms of a given order in the interaction. For instance, the one-point phase-space density correlation function at zeroth order, corresponding to free propagation, is trivially given by

$$C_f^{(0)}(x_1, t_1) = \int d\mathbf{x}_1 d\mathbf{x}^{(i)} \, \Phi_f(x_1, t_1) U_0(\mathbf{x}_1, t_1 | \mathbf{x}^{(i)}, t^{(i)}) \varrho_N^{(i)}(\mathbf{x}^{(i)})$$
(4.32)

$$=f_1^{(i)}(G_{1i}^{-1}\cdot x_1), \qquad (4.33)$$

which reproduces the standard result (2.90) and where $G_{ab} = G(t_a, t_b)$ is the 6-dimensional analogue to the shorthand notation introduced in (4.10). To first order in the interaction potential, we have to evaluate the expression

$$C_f^{(1)}(x_1, t_1) = \int d\mathbf{x}_1 d\mathbf{x}^{(i)} \, \Phi_f(x_1, t_1) U_1(\mathbf{x}_1, t_1 | \mathbf{x}^{(i)}, t^{(i)}) \varrho_N^{(i)}(\mathbf{x}^{(i)}) \,. \tag{4.34}$$

Inserting the definitions of Φ_f (2.52) and the first-order Liouville propagator U_1 (4.23), and solving the remaining integrals, we find

$$C_f^{(1)}(x_1, t_1) = \int dx_2 dt_2 \, \overline{\nabla}_{x_1} \, v_2(G_{12}^{-1} \cdot x_1, x_2, t_2) \cdot \hat{S}_{1i}(\overline{\nabla}_{x_1}) \, f_2^{(i)}(G_{1i}^{-1} \cdot x_1, G_{2i}^{-1} \cdot x_2) \,, \tag{4.35}$$

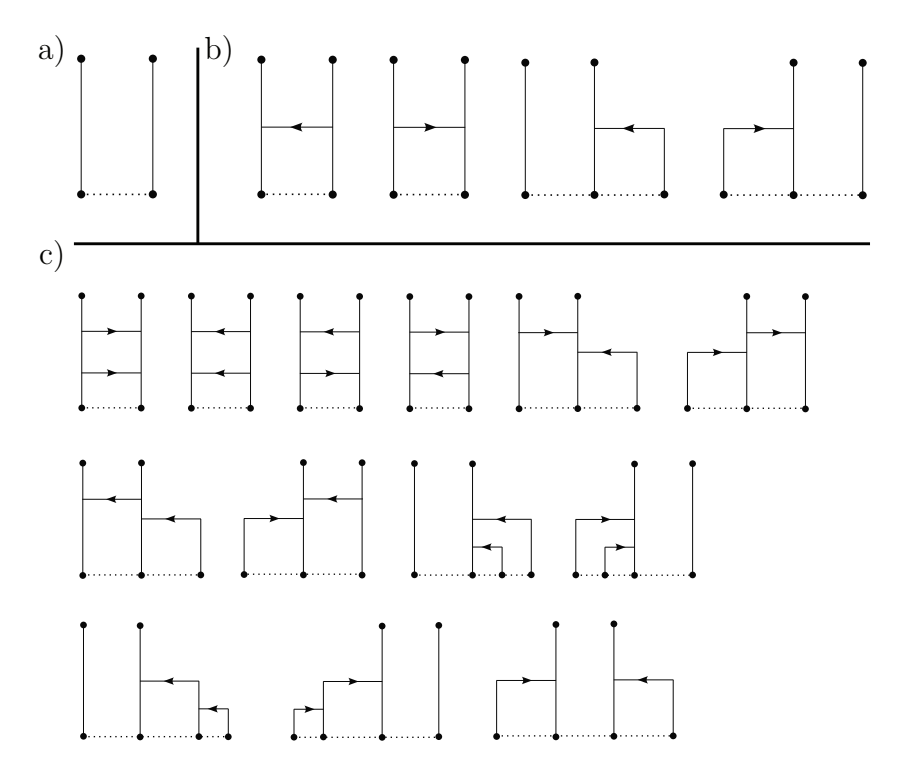


Figure 4.2.: All diagrams up to the second order in perturbation theory for the Klimontovich two-point correlation C_{ff} are represented. We list in a) the free theory (4.37), in b) the first-order perturbation theory (4.38) and in c) the second order perturbation theory.

where the operator

$$\hat{S}_{ab}(\overline{\nabla}_{x_c}) = \omega \cdot G_{ab}^{-\top} \cdot \overline{\nabla}_{x_c} \tag{4.36}$$

corresponds to (4.21) in μ -space. Although the resulting expression appears complex, its structure follows a systematic scheme: As expected, v_2 only couples two particles, such that of the full $\varrho_N^{(i)}$ only the two-particle reduced initial phase-space density remains after integration over the initial phase-space coordinates. The interaction describes how the free evolution of the particle at x_1 is affected by an interaction with a particle at x_2 at time t_2 . Note that particle 1 is evolved up to the final time t_1 , while particle 2 is only propagated up to the time of interaction t_2 inside t_2 . The latter particle position is then integrated over the whole phase-space volume. We illustrate the processes contained in (4.35) graphically in figure 4.1.

Analogously, the free evolution of the two-point phase-space density correlation is given by

$$C_{ff}^{(0)}(x_1, t_1, x_2, t_2) = \delta_{\mathcal{D}}(x_1 - G_{12} \cdot x_2) f_1^{(i)}(G_{1i}^{-1} \cdot x_1) + f_2^{(i)}(G_{1i}^{-1} \cdot x_1, G_{2i}^{-1} \cdot x_2), (4.37)$$

where both particles at x_1 and x_2 are freely evolved to their respective final times t_1 and t_2 . The first term corresponds to the one-particle contribution accounting for the possibility of picking the same particle, but at different times. For the first-order

correction to the two-point phase-space density we have to evaluate

$$\begin{split} C_{ff}^{(1)}(x_1, t_1, x_2, t_2) &= \\ & \int \mathrm{d}\mathbf{x}_1 \mathrm{d}\mathbf{x}_2 \mathrm{d}\mathbf{x}^{(i)} \, \Phi_f(x_1, t_1) U_1(\mathbf{x}_1, t_1 | \mathbf{x}_2, t_2) \Phi_f(x_2, t_2) U_0(\mathbf{x}_2, t_2 | \mathbf{x}^{(i)}, t^{(i)}) \varrho_N^{(i)}(\mathbf{x}^{(i)}) \\ &+ \int \mathrm{d}\mathbf{x}_1 \mathrm{d}\mathbf{x}_2 \mathrm{d}\mathbf{x}^{(i)} \, \Phi_f(x_1, t_1) U_0(\mathbf{x}_1, t_1 | \mathbf{x}_2, t_2) \Phi_f(x_2, t_2) U_1(\mathbf{x}_2, t_2 | \mathbf{x}^{(i)}, t^{(i)}) \varrho_N^{(i)}(\mathbf{x}^{(i)}) \,, \end{split}$$

which, after integration, can be brought into the form

$$C_{ff}^{(1)}(x_{1}, t_{1}, x_{2}, t_{2}) =$$

$$\int_{t^{(i)}}^{t^{(f)}} d\bar{t}_{1} \overline{\nabla}_{x_{1}} v_{2}(G_{1\bar{1}}^{-1} \cdot x_{1}, G_{2\bar{1}}^{-1} \cdot x_{2}, \bar{t}_{1}) \cdot \hat{S}_{1i}(\overline{\nabla}_{x_{1}}) f_{2}^{(i)}(G_{1i}^{-1} \cdot x_{1}, G_{2i}^{-1} \cdot x_{2})$$

$$+ (1 \leftrightarrow 2)$$

$$+ \int_{t^{(i)}}^{t^{(f)}} dt_{3} dx_{3} \overline{\nabla}_{x_{1}} v_{2}(G_{13}^{-1} \cdot x_{1}, x_{3}, t_{3}) \cdot \hat{S}_{1i}(\overline{\nabla}_{x_{1}}) f_{3}^{(i)}(G_{1i}^{-1} \cdot x_{1}, G_{2i}^{-1} \cdot x_{2}, G_{3i}^{-1} \cdot x_{3})$$

$$+ (1 \leftrightarrow 2),$$

$$(4.38)$$

where we have neglected the correction to the one-particle contribution. The first and second terms represent the interaction between the two external particles 1 and 2 and, therefore, correspond to a collision, i. e., a connected correlation that is being created due to an interaction. These terms arise due to the identification of the interacting particle index in the sum contained in $H_{\rm int}$ with one of the external particle indices. The third and fourth terms, on the other hand, correspond to interactions with an internal particle 3. We provide a graphical representation of these terms in figure 4.2. Going to second-order in perturbation theory, the number of terms increases rapidly. We therefore only give a graphic representation of the second-order perturbation theory in 4.1 and 4.2 to illustrate the different processes which can occur.

With the systematic approach presented in this chapter we could, in principle, compute unequal-time correlation functions to arbitrary order in the interaction potential. However, as we have just seen, the number of terms—and their combinatorial complexity—grows rapidly, even at low orders. Moreover, at higher orders, all contributions are treated on equal footing, without a natural hierarchy to distinguish physically relevant terms from subdominant ones. As we will see in chapter 11, this will lead to a very slow convergence of the perturbation series in practice, making this approach more valuable as a theoretical tool than as a method for efficient computation. However, the path-integral construction of the propagator and the representation of expectation values established here will serve as a foundation for the framework developed in the next chapter, where path integral methods are applied to systematically reorganize and resum the perturbation theory presented here.

5 Resummed Field Theory for Microscopic Particles

Despite being the most straightforward approach, the perturbation theory presented in chapter 4 is not very suitable for realistic applications due to the vast number of diagrams that have to be evaluated and the slow convergence of such a perturbative approach. The goal of this chapter is, therefore, to convert the particle-based description to a field theory which contains the full microscopic information. Such a field theory can either be obtained by artificially introducing new, macroscopic fields via a Dirac-delta function as shown in [34], or based on the Hubbard-Stratonovich transformation (HST), well-known from equilibrium statistical mechanics [57]. The latter approach, in addition, provides a physical understanding for the transition from the particle-based to a field-theory description. In order to perform the HST, we will first construct a generating functional and then bring it into a quadratic form. Similar approaches have already been successfully applied.

5.1. Construction of the Field Theory

Before we begin with the construction of the generating functional of the theory, let us introduce a compactified notation which will increase readability of lengthy expressions later on. First, let us introduce the combined variables X := (x, t), bundling the phase-space and time coordinates. We will also abbreviate

$$\int_{X} := \int d^{6}x \int_{t^{(i)}}^{\infty} dt.$$
 (5.1)

If the variable is indexed, we may also write $(1) := (X_1) = (x_1, t_1)$. In addition, we introduce the convention

$$A(1,2)B(2) := \int_{X_2} A(X_1, X_2)B(X_2),$$
 (5.2)

which implies the integration over variables of the same index. In the following we will further compactify the notation as needed. A summary of the notation used in this thesis can be found in Appendix A.

5.1.1. Construction via a Modified Hubbard-Stratonovich Transformation

Consider expression (3.50) for the computation of phase-space density correlation functions. Alternatively, these can also be obtained from the following generating functional,

$$\mathcal{Z}[J_f] := \int d\mathbf{x}^{(i)} \int_{\mathbf{x}^{(i)}} \mathcal{D}\mathbf{x} \mathcal{D}\boldsymbol{\chi} e^{i\mathcal{S}[\mathbf{x},\boldsymbol{\chi}] + J_f(X)\Phi_f(X)} \varrho_N^{(i)}(\mathbf{x}^{(i)}), \qquad (5.3)$$

such that the phase-space density correlation functions are given by

$$C_{f\dots f}(1,\dots,k) = \left. \frac{\delta^k \mathcal{Z}[J_f]}{\delta J_f(1)\dots\delta J_f(k)} \right|_{J_f=0}.$$
 (5.4)

However, in this form, the generating functional is not yet useful, since the Klimontovich phase-space density $\Phi_f(X)$ couples non-trivially to the microscopic degrees of freedom. We will, therefore, have to decouple the particle dynamics from the field itself. For this purpose, we introduce the *response field* Φ_B as a partner field to the Klimontovich phase-space density Φ_f . It is defined as

$$\Phi_B(1) := -i \sum_{i=1}^{N} \chi_i(t_1) \cdot \omega \cdot \nabla_{\mathsf{x}_i} \delta_{\mathrm{D}} \left(\mathsf{x}_i(t_1) - x_1 \right) . \tag{5.5}$$

With its help, we can bring the interaction part of $\mathcal{S}[\mathbf{x}, \boldsymbol{\chi}]$ into the more convenient form,

$$i \mathcal{S}_{int}[\mathbf{x}, \boldsymbol{\chi}] = -i \int_{t^{(i)}}^{\infty} \sum_{i \neq j=1}^{N} \chi_i \cdot \omega \cdot \nabla_{\mathbf{x}_i} v_2(\mathbf{x}_i, \mathbf{x}_j, t)$$

$$= \Phi_B(1) v_2(1, 2) \Phi_f(2)$$

$$= \Phi_B(1) \delta_D(1 - 2) \Phi_f(2),$$

$$(5.6)$$

where we defined $v_2(1,2) := v_2(x_1, x_2, t_1) \delta_D(t_1 - t_2)$ and the Dirac-delta function is written as $\delta_D(1-2) \equiv \delta_D(X_1 - X_2) \equiv \delta_D(x_1 - x_2) \delta_D(t_1 - t_2)$. In the last equality we, furthermore, introduced the dressed response field $\Phi_B([34])$ as

$$\Phi_{\mathcal{B}}(1) := \int_{X} \Phi_{B}(X) v_{2}(X, X_{1}). \tag{5.7}$$

We can now treat the fields Φ_f and Φ_B as components of a field doublet $\tilde{\Phi} = (\tilde{\Phi}_f, \tilde{\Phi}_B)^{\top} = (\Phi_B, \Phi_f)^{\top}$ where—for reasons that will become clear shortly—we interchanged the position of Φ_f and Φ_B . Similarly, we define a source doublet J, but place the source J_f in the first component, setting $J = (J_f, 0)^{\top}$, where $J_B = 0$, since there is no physical source for the \mathcal{B} -field. To keep the expressions compact, we introduce the Greek indices such that we can write the components as

$$A_{\alpha}(X)$$
, with $\alpha \in \{f, B\}$ (5.8)

for any field A(X). We can then rewrite the interaction term including the source as

$$e^{i\mathcal{S}_{int}[\mathbf{x},\mathbf{\chi}]+J_f(1)\Phi_f(1)} = e^{\frac{1}{2}(\tilde{\Phi}_{\alpha}(1)+J_{\alpha}(1))\sigma_{\alpha\beta}(1,2)(\tilde{\Phi}_{\beta}(2)+J_{\beta}(2))}$$

$$= e^{\frac{1}{2}(\tilde{\Phi}_a+J_a)\sigma_{ab}(\tilde{\Phi}_b+J_b)}.$$
(5.9)

with the self-inverse matrix $\sigma_{\alpha\beta}$ defined as

$$\sigma_{\alpha\beta}(1,2) = \begin{pmatrix} 0 & \delta_{\mathrm{D}}(1-2) \\ \delta_{\mathrm{D}}(1-2) & 0 \end{pmatrix}. \tag{5.10}$$

In the last line of (5.9), we have employed the *De Witt notation* which introduces the Latin index $a = (\alpha, X)$ such that we can compactly write

$$A_a \equiv A_\alpha(X) \,. \tag{5.11}$$

Having brought the generating functional into a quadratic form, we can now proceed with our main task to decouple the microscopic degrees of freedom from the fields. To this end, we employ a well-known procedure from condensed matter physics and equilibrium statistical mechanics. We, thus, perform a modified Hubbard-Stratonovich transformation¹, which essentially amounts to rewriting the above integral as a path integral over an auxiliary field $\Psi(X)$. This field will then be independent of the microscopic details. More precisely, we write,

$$e^{\frac{1}{2}(\tilde{\Phi}_a + J_a)\sigma_{ab}(\tilde{\Phi}_b + J_b)} = \mathcal{N} \int \mathcal{D}\Psi e^{-\frac{1}{2}\Psi_a[\sigma^{-1}]_{ab}\Psi_b + \Psi_a(J_a + \tilde{\Phi}_a)},$$

where the field doublet $\Psi_{\alpha}(X) = (\Psi_f(X), \Psi_{\mathcal{B}}(X))$, conjugate to $\tilde{\Phi}_{\alpha}(X)$, has been introduced. The full generating functional now reads

$$\mathcal{Z}[J_f] = \mathcal{N} \int \mathcal{D}\Psi \,e^{-\frac{1}{2}\Psi_a \left[\sigma^{-1}\right]_{ab}\Psi_b + J_a\Psi_a} \cdot \mathcal{Z}_{0,\tilde{\Phi}}[\Psi] , \qquad (5.12)$$

with

$$\mathcal{Z}_{0,\tilde{\Phi}}[\Psi] = \int d\mathbf{x}^{(i)} \varrho_N^{(i)}(\mathbf{x}^{(i)}) \int_{\mathbf{x}^{(i)}} \mathcal{D}\mathbf{x} \mathcal{D}\boldsymbol{\chi} \exp\left[i\mathcal{S}_0[\mathbf{x},\boldsymbol{\chi}] + \Psi_a \tilde{\Phi}_a\right].$$
 (5.13)

Note, that the macroscopic fields $\Psi_f(X)$ and $\Psi_{\mathcal{B}}(X)$ are independent of microscopic degrees of freedom, but couple linearly to $\tilde{\Phi}(X)$ and consequently to the Klimontovich phase-space density Φ_f and the response field $\Phi_{\mathcal{B}}$ in $\mathcal{Z}_{0,\tilde{\Phi}}$. This identifies $\mathcal{Z}_{0,\tilde{\Phi}}$ as the generating functional of free f- \mathcal{B} correlation functions, as one can easily verify by taking functional derivatives of $\mathcal{Z}_{0,\tilde{\Phi}}$ w.r.t. Ψ_f and $\Psi_{\mathcal{B}}$. The generating functional $\mathcal{Z}_{0,\tilde{\Phi}}$, thus, contains the full microscopic statistics. Introducing the associated

¹We call it a "modified" Hubbard-Stratonovich transformation since the conventional way to apply this transformation is to invert the potential to obtain a differential operator governing the dynamics of the conjugate field theory. Our approach, however, absorbs the potential into the field components such that the resulting dynamics for the new field are trivial.

cumulant generating functional

$$\mathcal{W}_{0, ilde{\Phi}}[\Psi] \equiv \ln \left[\mathcal{Z}_{0, ilde{\Phi}}[\Psi]
ight],$$

we can bring (5.12) into the compact form

$$\mathcal{Z}[J] = \mathcal{N} \int \mathcal{D}\Psi \,e^{-\frac{1}{2}\Psi_a \left[\sigma^{-1}\right]_{ab}\Psi_b + J_a \,\Psi_a + \mathcal{W}_{0,\tilde{\Phi}}[\Psi]} \,. \tag{5.14}$$

The functional $W_{0,\tilde{\Phi}}[\Psi]$ has the following series expansion,

$$\mathcal{W}_{0,\tilde{\Phi}}[\Psi] = \sum_{r,s=0}^{\infty} \frac{1}{r!s!} \left[\prod_{m=1}^{r} \Psi_{\mathcal{B}}(m) \right] \left[\prod_{n'=1}^{s} \Psi_{f}(n) \right] G_{f\cdots f\mathcal{B}\cdots\mathcal{B}}^{(0)}(1,\cdots r,1',\cdots s') \quad (5.15)$$

where integration over same indices is implied and which introduces the *free* mixed f- \mathcal{B} cumulants $G_{f\cdots f\mathcal{B}\cdots\mathcal{B}}^{(0)}$, containing r phase-space densities and s response fields,

$$G_{f\cdots f\mathcal{B}\cdots\mathcal{B}}^{(0)}(1,\cdots r,1',\cdots s') = \langle \Phi_f(1)\cdots \Phi_f(r)\Phi_{\mathcal{B}}(1')\cdots \Phi_{\mathcal{B}}(s')\rangle_c^{(0)}.$$
 (5.16)

Note, that the mean has to be taken w.r.t. the *free* microscopic action as is clear from (5.13). The $G_{f\cdots f\mathcal{B}\cdots\mathcal{B}}^{(0)}$ cumulants thus generalize the pure f cumulants discussed at the end of section 2.5 by including the response field. We discuss their form and physical meaning in section 5.2.1.

5.2. Resummed Field Theory

Together with (5.15), equation (5.14) defines the action of a statistical field theory where the generating functional has the form

$$\mathcal{Z}[J] = \mathcal{N} \int \mathcal{D}\Psi e^{-\mathcal{S}[\Psi] + J_a \Psi_a} = \mathcal{N} \int \mathcal{D}\Psi e^{-\mathcal{S}_0[\Psi] - \mathcal{S}_{int}[\Psi] + J_a \Psi_a}, \qquad (5.17)$$

where we defined the free action containing all² contributions up to quadratic order in the fields,

$$S_0[\Psi] = \Psi_{\mathcal{B}}(1) \left[\mathbb{1} - G_{f\mathcal{B}}^{(0)} \right] (1,2) \Psi_f(2) - \Psi_{\mathcal{B}}(1) G_f^{(0)}(1) - \frac{1}{2!} \Psi_{\mathcal{B}}(1) \Psi_{\mathcal{B}}(2) G_{ff}^{(0)}(1,2) .$$
(5.18)

The remaining terms define the self-interactions of the fields and are contained in the interacting part

$$S_{\text{int}}[\Psi] = -\sum_{r+s>2}^{\infty} \frac{1}{r!s!} \left[\prod_{m=1}^{r} \Psi_{\mathcal{B}}(m) \right] \left[\prod_{n'=1}^{s} \Psi_{f}(n') \right] G_{f\cdots f\mathcal{B}\cdots\mathcal{B}}^{(0)}(1, \dots, 1', \dots, s') . (5.19)$$

²Note that there exists no pure $\Phi_{\mathcal{B}}$ -field cumulant. See the following discussion for more details.

Introducing the inverse tree-level propagator,

$$\left[\Delta^{-1}\right]_{\alpha\beta}(1,2) = \begin{pmatrix} 0 & \mathbb{1} - G_{f\mathcal{B}}^{(0)} \\ \mathbb{1} - G_{\mathcal{B}f}^{(0)} & G_{ff}^{(0)} \end{pmatrix}(1,2), \text{ with } G_{\mathcal{B}f}^{(0)}(1,2) = G_{f\mathcal{B}}^{(0)}(2,1), (5.20)$$

we can write the quadratic part of the action (5.18) as

$$S_0[\Psi] = \frac{1}{2} \Psi_\alpha(1) \left[\Delta^{-1} \right]_{\alpha\beta} (1, 2) \Psi_\beta(2) - \Psi_\mathcal{B}(1) G_f^{(0)}(1) . \tag{5.21}$$

Note, that by construction we have the correspondence

$$\langle \Phi_f(1) \cdots \Phi_f(k) \rangle = \frac{\delta^k}{\delta J_f(1) \cdots \delta J_f(k)} \mathcal{Z}[J] \bigg|_{J=0}$$

$$= \langle \Psi_f(1) \dots \Psi_f(k) \rangle , \qquad (5.22)$$

which makes the contact between the Klimontovich phase-space density correlators and the correlation functions of the auxiliary fields. We may now apply the usual field theoretic methods in order to compute correlation functions. We therefore extend the source J to contain an additional response component, $J = (J_f, J_B)$ and replace the fields Ψ_f and Ψ_B in (5.19) by the functional derivative w.r.t. their respective source field, to find the usual expression

$$\mathcal{Z}[J] = \mathcal{N}' \exp \left[-\mathcal{S}_{I} \left[\frac{\delta}{\delta J_{f}}, \frac{\delta}{\delta J_{B}} \right] \right] \cdot \mathcal{Z}_{0}[J] ,$$
 (5.23)

where $\mathcal{Z}_0[J]$ is defined to contain the quadratic part of the action,³

$$\mathcal{Z}_0[J] = \mathcal{N}'' \int \mathcal{D}\Psi_f \mathcal{D}\Psi_{\mathcal{B}} e^{-\mathcal{S}_0[\Psi] + J_a \Psi_a}.$$
 (5.24)

The above path integration for the tree-level generating functional can be performed analytically and yields

$$\mathcal{Z}_0[J] = \exp\left[\frac{1}{2}J_{\alpha}(1)\Delta_{\alpha\beta}(1,2)J_{\beta}(2) + J_f(1)\Delta_{f\mathcal{B}}(1,2)G_f^{(0)}(2)\right],\tag{5.25}$$

where the tree-level propagator has the components

$$\Delta_{\alpha\beta}(1,2) = \begin{pmatrix} \Delta_{ff} & \Delta_{f\mathcal{B}} \\ \Delta_{\mathcal{B}f} & 0 \end{pmatrix} . \tag{5.26}$$

The inversion relation

$$\int_{\bar{X}} \left[\Delta^{-1} \right]_{\alpha \gamma} (X_1, \bar{X}) \Delta_{\gamma \beta} (\bar{X}, X_2) = \delta_{\mathcal{D}} (X_1 - X_2) \, \mathbb{1}_{2 \times 2} \,, \tag{5.27}$$

³The normalization $\mathcal{N} = \mathcal{N}'\mathcal{N}''$ is chosen such that $\mathcal{Z}[0] = 1 = \mathcal{Z}_0[0]$.

implies the following equations for the components of the tree-level propagator,

$$\Delta_{f\mathcal{B}}(1,2) = \left[\mathbb{1} - G_{f\mathcal{B}}^{(0)}\right]^{-1}(1,2) , \qquad (5.28)$$

$$\Delta_{\mathcal{B}f}(1,2) \equiv \Delta_{f\mathcal{B}}(2,1), \qquad (5.29)$$

$$\Delta_{ff}(1,2) = \Delta_{f\mathcal{B}}(1,\bar{1}) G_{ff}^{(0)}(\bar{1},\bar{2}) \Delta_{\mathcal{B}f}(\bar{2},2) . \tag{5.30}$$

We have thus developed a field-theoretic formulation of the N-particle system, in which the phase-space density and the response field (5.7) serve as the fundamental degrees of freedom. This framework is particularly well-suited for applying functional methods to compute the correlation functions of the Klimontovich phase-space density, using the correspondence relation (5.22). In the following, we will demonstrate how one-loop corrections are computed and examine the overall structure of the resulting field theory. Before proceeding, however, we first clarify the physical roles of both, the propagators and the interaction vertices, beginning with the latter.

5.2.1. Free Cumulants

As we have seen above, the free f- \mathcal{B} cumulants play the role of fundamental building blocks of the field theory, as they appear in both, the propagators and the vertices. They contain information on the microscopic degrees of freedom. Let us therefore illuminate their physical role in more detail.

The general f- \mathcal{B} cumulant is defined as the connected correlation function (5.16),

$$G_{f\cdots f\mathcal{B}\cdots\mathcal{B}}^{(0)}(1,\cdots r,1',s') = \langle \Phi_f(1)\cdots\Phi_f(r)\Phi_{\mathcal{B}}(1')\cdots\Phi_{\mathcal{B}}(s')\rangle_c^{(0)}. \tag{5.31}$$

The prescription of how these cumulants are computed is essentially described in chapter 4. Although, the computation appears to simplify at first glance, since the above cumulants are computed w.r.t. the free theory, it actually describes interaction processes, since the response field (5.7) contains the potential. The simplest cumulants to interpret are therefore clearly the pure Φ_f -field cumulants, as they correspond to freely evolved k-point density clusters propagating the initial correlations. If one or more $\Phi_{\mathcal{B}}$ -fields are present, however, the expressions become more involved. First, we note that in order to solve the respective path integral, we will have to replace the χ field contained in $\Phi_{\mathcal{B}}$ by the corresponding differential operator $-i\nabla_{\mathbf{x}}$, similarly to (4.12). It then follows from the normalization condition (4.17) that no $\Phi_{\mathcal{B}}$ -field may appear together with the latest time in (5.31). In particular, this implies that all pure $\Phi_{\mathcal{B}}$ -field cumulants must vanish identically,

$$G_{\mathcal{B}\dots\mathcal{B}}^{(0)}(1,\dots,s) = 0,$$
 (5.32)

and leads to the causality rule,

$$G_{f \dots f \mathcal{B} \dots \mathcal{B}}^{(0)}(1, \dots, r, 1', \dots, s') = 0, \quad \text{if} \quad \exists \ \bar{s} \in [1, \dots, s'] : t_{\bar{s}} \ge t_{\bar{r}} \ \forall \ \bar{r} \in [1, \dots, r].$$

$$(5.33)$$

The physical significance of the above rule and the role played by the mixed cumulants is best understood with a specific example at hand. Let us, therefore, discuss the free $G_{fB}^{(0)}$ cumulant since it appears in the propagator. By the above rule, we first find

$$G_{fB}^{(0)}(1,2) \propto \Theta(t_1 - t_2).$$
 (5.34)

Inserted into the respective path integral expression and after solving the Dirac-delta distributions similarly to the perturbative approach presented in chapter 4, we find the somewhat familiar expression

$$G_{f\mathcal{B}}^{(0)}(1,2) = \overline{\nabla}_{x_1} v_2(G_{12}^{-1} \cdot x_1, x_2, t_2) \cdot \hat{S}_{1i}(\overline{\nabla}_{x_1}) f_1^{(i)}(G_{1i}^{-1} \cdot x_1) \Theta(t_1 - t_2), \qquad (5.35)$$

where $\hat{S}_{1i}(\overline{\nabla}_{x_1})$ is the scattering operator in μ -space defined in (4.36). The above expression strongly resembles the first-order perturbative expression (4.35). Thus, $G_{fB}^{(0)}$ describes the microscopic process in which the freely evolved one-particle reduced density is deformed by an interaction originating from a particle at x_2 which is, importantly, not connected to the density at x_1 . In that sense, the cumulants act as building blocks, that have to be linked together in order to represent physical processes. The causality rule (5.33) states that interactions can only affect the future evolution of a phase-space density. If there is no density to act upon, the respective contribution vanishes. This can be generalized to higher-order mixed cumulants as follows: $G_{f\cdots fB\cdots B}^{(0)}(1,\cdots,s,1',\cdots,r')$ describes the response of the freely evolved s-point cumulant to r interactions at times $t_{1'},\cdots,t_{r'}$ with external particles located at $x_{1'},\cdots,x_{r'}$. The cumulant thus consists of a differential operator acting on the freely evolved pure f cumulant,

$$G_{f \cdots f \mathcal{B} \cdots \mathcal{B}}^{(0)}(1, \cdots, s, 1', \cdots, r') \simeq \hat{\mathcal{D}} \cdot G_{f \cdots f}^{(0)}(1, \cdots, s).$$
 (5.36)

Importantly, due to (5.33) the cumulant introduces a time flow from the external particles sourcing the interaction to the densities being deflected. We, therefore, find that the cumulants have an internal time-ordering, generalizing the time ordering enforced by the Heaviside function found in (5.35). The explicit form of the above differential operator is, of course, highly non-trivial, as the discussion in 4.1.2 suggests.

5.2.2. Propagators and Feynman Diagrams

We now turn to the interpretation of the propagator equations (5.28) and (5.30). We first note, that the inverse in (5.28) is to be understood in the functional sense, i. e., as the solution of the integral equation

$$\int_{\bar{X}_1} \left[\mathbb{1}(X_1, \bar{X}_1) - G_{f\mathcal{B}}^{(0)}(X_1, \bar{X}_1) \right] \Delta_{f\mathcal{B}}(\bar{X}_1, X_2) = \mathbb{1}(X_1, X_2). \tag{5.37}$$

By making the ansatz

$$\Delta_{fB}(X_1, X_2) = \mathbb{1}(X_1, X_2) + \widetilde{\Delta}_{fB}(X_1, X_2),$$
 (5.38)

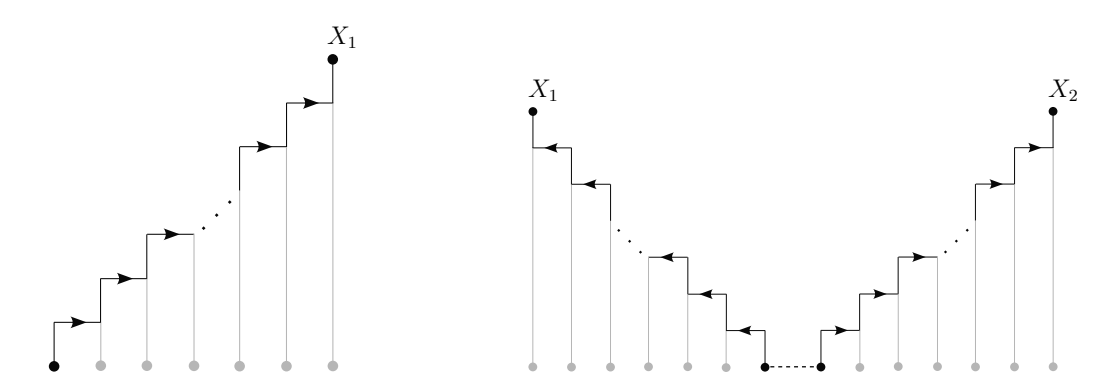


Figure 5.1.: Graphical illustration of the processes contributing to the causal propagator $\Delta_{f\mathcal{B}}$ (left panel) and to the statistical propagator Δ_{ff} (right panel). Phase-space densities sourcing the interactions are presented in gray. Dashed lines indicate the connected part of the correlation between these points.

we find that the corresponding integral equation for $\widetilde{\Delta}_{f\mathcal{B}}$ is given by

$$\widetilde{\Delta}_{f\mathcal{B}}(X_1, X_2) = G_{f\mathcal{B}}^{(0)}(X_1, X_2) + \int_{\bar{X}} G_{f\mathcal{B}}^{(0)}(X_1, \bar{X}) \widetilde{\Delta}_{f\mathcal{B}}(\bar{X}, X_2). \tag{5.39}$$

Due to the Heaviside function in (5.35) we also find $\widetilde{\Delta}_{f\mathcal{B}}(X_1, X_2) \propto \Theta(t_1 - t_2)$, which preserves the causal propagation. We therefore call $\Delta_{f\mathcal{B}}(1,2)$ and $\Delta_{\mathcal{B}f}(1,2)$ the retarded and advanced causal propagators, respectively, and define the Feynman diagrams,

$$\Delta_{fB}(1,2) \cong ---\cdots, \tag{5.40}$$

$$\Delta_{\mathcal{B}f}(1,2) \cong \cdots , \qquad (5.41)$$

where the direction of the time-flow is from the dotted end to the solid end. Equation (5.39) is of Volterra-Fredholm type and has to be solved numerically in general if no further symmetry assumptions are made. By iterating (5.39) we find the Neumann series representation of the causal propagator,

$$\Delta_{f\mathcal{B}}(1,2) = \mathbb{1}(1,2) + G_{f\mathcal{B}}^{(0)}(1,2) + G_{f\mathcal{B}}^{(0)}(1,\bar{1}) G_{f\mathcal{B}}^{(0)}(\bar{1},2) + \cdots$$
 (5.42)

$$= \sum_{n=0}^{\infty} \left[G_{f\mathcal{B}}^{(0)} \right]^n (1,2). \tag{5.43}$$

The interpretation of the causal propagators, therefore, is the following: each $G_{fB}^{(0)}$ describes how a one-point phase-space density responds to an incoming interaction, which is sourced by a phase-space density that has itself already been influenced by an earlier interaction. This process can repeat arbitrarily many times within the time interval $[t_1, t_2]$. Figure 5.1 provides a graphical representation of this iteration. Thus, objects involving Δ_{fB} propagators are, by construction, non-perturbative in terms of the microscopic interaction potential as they involve an analytical or a numerical

resummation of the interaction series (5.42). We have therefore found a systematic resummation of the perturbative expansion discussed in the previous chapter.

Similarly, we find an interpretation of the propagator (5.30): Two initially correlated phase-space densities, described by $G_{ff}^{(0)}$, source the interaction chain included in the Δ_{fB} propagators which we described above. The two external densities at X_1 and X_2 thus remain fully connected, see Figure 5.1. Since Δ_{ff} , thus, carries statistical information, we refer to it as the *statistical propagator* and equip it with its own Feynman diagram,

$$\Delta_{ff}(1,2) = \Delta_{f\mathcal{B}}(1,\bar{1}) G_{ff}^{(0)}(\bar{1},\bar{2}) \Delta_{\mathcal{B}f}(\bar{2},1) \cong ---- . \tag{5.44}$$

The $G_{ff}^{(0)}$ -cumulant is represented by the solid dot, and the two solid lines are shorthand representations of the retarded and advanced propagators Δ_{fB} and Δ_{Bf} . By means of (5.38), equation (5.30) can be expanded such that

$$\Delta_{ff}(1,2) = G_{ff}^{(0)}(1,2) + \tilde{\Delta}_{f\mathcal{B}}(1,\bar{1})G_{ff}^{(0)}(\bar{1},2) + G_{ff}^{(0)}(1,\bar{2})\tilde{\Delta}_{\mathcal{B}f}(\bar{2},2) + \tilde{\Delta}_{f\mathcal{B}}(1,\bar{1})G_{ff}^{(0)}(\bar{1},\bar{2})\tilde{\Delta}_{\mathcal{B}f}(\bar{2},2).$$
(5.45)

Since there is no pure $G_{\mathcal{BB}}^{(0)}$ -cumulant, we also have $\Delta_{\mathcal{BB}} = 0$.

Last but not least, the vertices $G_{f cdots f cdots cdots c}^{(0)}$ describe how r interactions affect the future evolution of a connected s-particle cluster. We, therefore, represent vertices by the following Feynman diagram,

$$G_{f...f\mathcal{B}...\mathcal{B}}^{(0)}(1,\ldots,r,1',\ldots,s') \cong \int_{r}^{1} \int_{s'}^{1'} .$$
 (5.46)

The solid line are attached to incoming interaction chains, while the dashed lines represent outgoing interactions, sourced by the cumulant itself. Importantly, due to the rule in (5.33) there has to be at least one outgoing line, representing the density that is being deflected, meaning that there is no sink in the time flow. Conversely, a pure phase-space density cumulant $G_{f\cdots f}^{(0)}$ will only source outgoing interaction chains. We can now understand the general construction of a Feynman diagram. All components of the diagram, i. e., propagators and vertices, are attached to each other such that the densities of one component act as sources for the response functions of another. This ensures a continuous time flow, which can only terminate at the external phase-space densities. Within vertices, the time flow can split or merge, indicating how a single density influences the future evolution of multiple densities or is affected through interactions with multiple densities from the past.

5.2.3. One Loop Corrections

With the generating functional (5.17) at hand, we can now compute loop-corrections to the propagators. The most straightforward approach is to use equation (5.23)

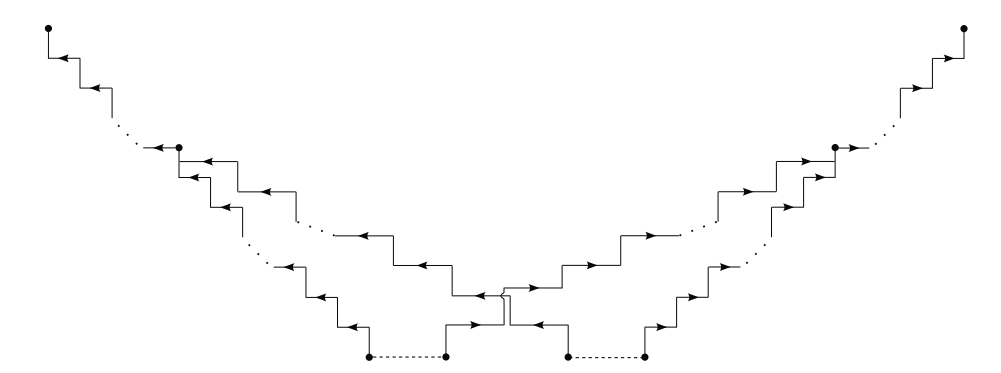


Figure 5.2.: A graphical representation of the first loop appearing in the one-loop self-energy contribution (5.49). The dashed lines connecting the phase-space points at the base of the diagram represent the connected part of the correlation between those points. For clarity, we do not explicitly depict the gray phase-space points taking part in the interactions.

and to apply the functional derivatives order by order in the couplings, i. e., the free cumulants. Note, that we have an infinite tower of mixed vertices. The only restriction is set by the causality rule (5.33). Neglecting all tadpole contributions⁴ we find that to one-loop order there exist two different topologies of diagrams that contribute to the loop correction coming from the three- and four-point self-interactions, given by

In fact, the highest vertex contributing to a loop correction at s-loop order is a 2s+2-point self-interaction, as it connects all propagator lines to the same vertex yielding generalizations of the diagram on the right in (5.47). Having determined the possible topologies at a given loop-level, one can now construct all contributing diagrams by inserting the respective vertices appearing in the action (5.19) and connecting them with the respective propagator. For our one-loop example, the three- and four point vertices are $G_{fff}^{(0)}$, $G_{ffB}^{(0)}$, $G_{fBB}^{(0)}$, $G_{ffBB}^{(0)}$, $G_{fBBB}^{(0)}$, $G_{fBBB}^{(0)}$. The one-loop corrected propagators are, thus, given by

$$G_{ff}^{1\text{loop}}(1,2) = \Delta_{ff}(1,2) + \Delta_{ff}(1,3) \Sigma_{\mathcal{B}f}^{1\text{loop}}(3,4) \Delta_{\mathcal{B}f}(4,2) + \Delta_{f\mathcal{B}}(1,3) \Sigma_{f\mathcal{B}}^{1\text{loop}}(3,4) \Delta_{ff}(4,2) + \Delta_{f\mathcal{B}}(1,3) \Sigma_{ff}^{1\text{loop}}(3,4) \Delta_{\mathcal{B}f}(4,2) ,$$

$$G_{f\mathcal{B}}^{1\text{loop}}(1,2) = \Delta_{f\mathcal{B}}(1,2) + \Delta_{f\mathcal{B}}(1,3) \Sigma_{f\mathcal{B}}^{1\text{loop}}(3,4) \Delta_{f\mathcal{B}}(4,2) ,$$
(5.48)

where we have defined the self-energy corrections $\Sigma_{f\mathcal{B}}^{1\text{loop}}$ and $\Sigma_{ff}^{1\text{loop}}$ at one-loop order. Keeping the above Feynman rules in mind, they can be expressed by the following

⁴These contributions are present in general. However, in [58] it was shown that such tadpoles vanish for homogeneous systems, which are our main systems of interest.

set of diagrams

$$\Sigma_{ff}^{1\text{loop}}(1,2) \cong \frac{1}{2} \cdots + \cdots + \frac{1}{2} \cdots + \frac{1}{2} \cdots$$

$$+ \frac{1}{2} \cdots + \frac{1}{2} \cdots + \cdots + \frac{1}{2} \cdots$$

$$(5.49)$$

$$\Sigma_{f\mathcal{B}}^{1\text{loop}}(1,2) \cong \cdots \longrightarrow + \frac{1}{2} \cdots \longrightarrow + \cdots \longrightarrow (5.50)$$

$$+ \frac{1}{2} \cdots \longrightarrow + \cdots \longrightarrow \cdots$$

As one can see, the number of diagrams contributing to a given loop order grows quickly. The physical process underlying a given diagram can be interpreted similarly to the tree-level propagators. In Figure 5.2 we show a schematic representation of the first loop-diagram in $\Sigma_{ff}^{1\text{loop}}$.

In conclusion, we have seen how an actual field theoretic formulation can be constructed out of the N-particle generating functional (5.3). In contrast to the latter, the fundamental degrees of freedom are the phase-space density Ψ_f and the response field Ψ_B , which have been decoupled from the microscopic particles by the modified Hubbard-Stratonovich transformation. The resulting tree-level and loop diagrams encode microscopic particle-interaction processes, where the simplest is being resummed withing the tree-level propagators. This offers a fundamental advantage over the perturbation theory presented in the previous chapter. However, the infinite tower of interaction vertices renders any approximation scheme highly non-trivial. Furthermore, as the cosmological application in chapter 11 shows, already the one-loop diagrams exhibit severe numerical cancellations among the different loop contributions. In the next chapter we will therefore present a different approach which restructures the physical processes in a more convenient way.

2

Path Integrals for Classical N-Particle Systems - Field Theory Picture

6 Statistical Field Theory Approach to the Klimontovich Equation

In the last chapter we have seen how to construct a field theoretic approach out of the N-particle description of the Liouville equation. However, due to the construction of the field theory, the particle interaction is encoded in an infinite tower of vertices. This is both, counterintuitive and impractical. Since we are ultimately interested in the dynamics of the Klimontovich phase-space density field, we will map the dynamics of microscopic particles to the dynamics of the field itself, given by the Klimontovich equation (2.78). This approach not only simplifies the vertex structure considerably, but also facilitates the comparison to conventional approaches. The basic concepts are covered by [59, 21].

6.1. The Klimontovich Equation as a Stochastic Differential Equation

Let us first recast the Klimontovich equation (2.78) into a form that is more suitable for our field-theoretic application. Since (2.78) is deterministic, specifying $\Phi_f^{(i)}(x) \equiv \Phi_f(x,t^{(i)})$ completely fixes its evolution in terms of the μ -space coordinates, and microscopic details enter only through the initial ensemble $\varrho_N^{(i)}(\mathbf{x}^{(i)})$. In that sense, the evolution is naturally decoupled from the microscopic degrees of freedom which therefore only enter the dynamics through the initial statistical distribution of the particles. To make this explicit, we introduce a new field variable $\Psi_f(X) \equiv \Psi_f(x,t)$, which evolves according to the Klimontovich equation, once its initial configuration is appropriately initialized as $\Phi_f^{(i)}$. Clearly, $\forall t > t^{(i)}$ we have $\Psi_f(x,t) \equiv \Phi_f(x,t)$ due to the uniqueness¹ of the solutions to (2.78). Using the same phase-space and time variables $(1) = X_1 = (x_1, t_1)$ as in chapter 5 and employing the condensed notation for integrals over X, as described in appendix A the stochastic evolution equation of

¹Although this redefinition of variables is trivial, it will make the comparison to the particle approach in chapter 5 easier, since the field Ψ_f exactly correspond to the auxiliary field Ψ_f after the Hubbard-Stratonovich transformation. We will postpone further discussion to the end of this chapter.

the phase-space density in μ -space is described by

$$\frac{\partial}{\partial t_1} \Psi_f(1) - U^{(0)}(1, 2) \Psi_f(2) = F[\Psi_f; 1] + \Phi^{(i)}(1), \qquad (6.1)$$

where we defined $\Phi^{(i)}(1) = \Phi^{(i)}(X_1) \equiv \delta_{\mathrm{D}}\left(t_1 - t^{(i)}\right)\Phi^{(i)}(x_1)$. The drift term $F[\Psi_f; 1]$ is a functional of Ψ and a function of the coordinates X and is defined by

$$F[\Psi_f, 1] = U^{(1)}(1, 2)\Psi_f(2) + U^{(2)}(1, 2, 3)\Psi_f(2)\Psi_f(3), \qquad (6.2)$$

where we recall that integrations are implied. Here, we formally decoupled the interaction operators defined in (2.78) from the field Ψ_f by including appropriate Dirac-delta distributions. In particular, we defined

$$U^{(0)}(X_1, X_2) := \hat{\mathcal{L}}_1^{(0)}(t_1) \delta_{\mathrm{D}} (X_1 - X_2)$$

$$U^{(1)}(X_1, X_2) := \hat{\mathcal{L}}_1^{(1)}(t_1) \delta_{\mathrm{D}} (X_1 - X_2)$$

$$U^{(2)}(X_1, X_2, X_3) := \hat{\mathcal{L}}_{12}^{(2)}(t_1) \delta_{\mathrm{D}} (X_1 - X_3) \delta_{\mathrm{D}} (t_1 - t_2) .$$

$$(6.3)$$

Since $\Phi_f^{(i)}(x_1) \equiv \sum_{i=1}^N \delta_D(x_1 - \mathsf{x}_i(t^{(i)})) = \sum_{i=1}^N \delta_D(x_1 - \mathsf{x}_i^{(i)})$ any solution to (6.1) will parametrically depend on all particle positions at the initial time, represented by $\mathbf{x}^{(i)}$. We will therefore denote the general solution to (6.1) by $\Psi_{f,\mathrm{sol}}(x_1,t_1;\mathbf{x}^{(i)})$. Once the solution $\Psi_{f,\mathrm{sol}}(X_1;\mathbf{x}^{(i)})$ is known, the correlation functions of the phase-space density are obtained as

$$C_{f\dots f}(X_1,\dots,X_k) = \left\langle \Psi_{f,\text{sol}}(X_1;\mathbf{x}^{(i)})\dots\Psi_{f,\text{sol}}(X_k;\mathbf{x}^{(i)}) \right\rangle$$
(6.4)

$$= \int d\mathbf{x}^{(i)} \varrho_N^{(i)}(\mathbf{x}^{(i)}) \Psi_{f,\text{sol}}(X_1; \mathbf{x}^{(i)}) \cdots \Psi_{f,\text{sol}}(X_k; \mathbf{x}^{(i)}).$$
 (6.5)

The form of equation (6.1) is now well suited for a functional treatment within the MSR/JD framework. This will be the main goal of the current chapter. Before that, however, let us discuss how perturbations in the field configuration affect the evolution of the system.

6.2. Response to Perturbations

Fluctuations arising from uncertainty in the initial field configuration propagate through the system and influence the evolution of the phase-space density. It is therefore essential to understand how the system responds to such perturbations. Let us therefore add a function K(1) on the right-hand side of (6.1), that serves as a small space and time dependent perturbation,

$$D_{0,R}^{-1}(1,2)\Psi_f(2) = F[\Psi_f, 1] + \Phi^{(i)}(1) + K(1).$$
(6.6)

We denote the general solution of (6.6) by $\Psi_{f,\text{sol}}^K(1;\mathbf{x}^{(i)})$ indicating, that it is also a functional of the perturbation K. The physical solution is ultimately recovered

setting K = 0. The free evolution is characterized by the linear differential operator on the left-hand side,

$$D_{0,R}^{-1}(X_1, X_2) := \left[\frac{\partial}{\partial t_1} - \hat{\mathcal{L}}^{(0)}(x_1, t_1) \right] \delta_{\mathcal{D}}(X_1 - X_2) . \tag{6.7}$$

The free retarded propagator of this theory, denoted as $D_{0,R}(1,2)$ is defined as the Green function to the above linear differential operator

$$D_{0,R}^{-1}(1,\bar{1})D_{0,R}(\bar{1},2) = \mathbb{1}(1,2), \qquad (6.8)$$

where of course, $\mathbb{1}(1,2) = \delta_D(X_1 - X_2)$. Clearly, the solution is given by

$$D_{0,R}(X_1, X_2) := \delta_{\mathcal{D}} (x_1 - G(t_1, t_2) \cdot x_2) \Theta(t_1 - t_2), \tag{6.9}$$

where G is the free particle propagator defined in (2.22). We can analogously define the *free advanced propagator* of this theory by interchanging the arguments of $D_{0,R}(1,2)$, i.e.,

$$D_{0,A}(1,2) := D_{0,R}(2,1). \tag{6.10}$$

Thus, under the free evolution, the density at x_2 evolves under its free trajectory up to x_1 at time t_1 . Retardation is again enforced by the Heaviside function. Equation (6.6) can now formally be solved by

$$\Psi_{f,\mathrm{sol}}^K(X_1;\mathbf{x^{(i)}}) = \Psi_f^{(0)}(X_1) + \int_{X_2} D_{0,R}(X_1,X_2) \Big[F\left[\Psi_{f,\mathrm{sol}}^K(X_2;\mathbf{x^{(i)}})\right] + K(X_2) \Big] \,, \ (6.11)$$

where $\Psi_f^{(0)}$ represents the free solution to the Klimontovich equation,

$$\Psi_f^{(0)}(X_1; \mathbf{x}^{(i)}) := \int_{X_2} D_{0,R}(X_1, X_2) \delta_{\mathcal{D}} \left(t_2 - t^{(i)} \right) \Phi_f^{(i)}(x_2)
= \Phi_f^{(i)} \left(G^{-1}(t_1, t^{(i)}) \cdot x_1 \right) \Theta(t_1 - t^{(i)}).$$
(6.12)

Equation (6.11) is a non-linear Volterra-Fredholm integral equation of the second kind². The causal structure of the linear Green function (6.9) implies that the time integration on the right-hand side of (6.11) represents a memory integral, i. e., the full solution $\Psi_{f,\text{sol}}^K(x_1,t_1;\mathbf{x}^{(i)})$ requires the knowledge of the full history of $\Psi_{f,\text{sol}}^K(x,t;\mathbf{x}^{(i)})$ for all times $t < t_1$. In order to understand how the perturbed solution $\Psi_{f,\text{sol}}^K(x_1,t_1;\mathbf{x}^{(i)})$ deviates from the unperturbed solution $\Psi_{f,\text{sol}}(x_1,t_1;\mathbf{x}^{(i)})$, we expand (6.11) in a *Volterra series*,

$$\Psi_{f,\text{sol}}^{K}(X;\mathbf{x}^{(i)}) = \sum_{n=0}^{\infty} \frac{1}{n!} \int_{X_1,\dots,X_n} \mathcal{R}^{(n)}(X;X_1,\dots,X_n;\mathbf{x}^{(i)})K(X_1)\dots K(X_n)$$
 (6.13)

in terms of the perturbation K(x,t). Equation (6.13) can be obtained by iterating (6.11) and represents a functional Taylor series expansion around K=0. The

²The Fredholm part, corresponding to the integration over the phase-space coordinates, can in principle be performed explicitly due to the Dirac-delta distribution in the free Green's function.

Volterra kernels $\mathcal{R}^{(n)}$ describe how the system at time t responds to perturbations at earlier times t_1, t_2, \ldots, t_n . They are therefore known as the response functions of the system and are defined as the n-th functional derivative of the perturbed solution w.r.t. to the perturbation K,

$$\mathcal{R}^{(n)}(X; X_1, \dots, X_n; \mathbf{x}^{(i)}) := \frac{\delta^n \Psi_{f, \text{sol}}^K(X; \mathbf{x}^{(i)})}{\delta K(X_1) \dots \delta K(X_n)} \bigg|_{K=0}.$$
(6.14)

Thus, they generally also depend on the initial field configuration. In particular, the lowest order

$$\mathcal{R}^{(0)}(X; \mathbf{x}^{(i)}) = \Psi_{f,\text{sol}}(X; \mathbf{x}^{(i)}), \qquad (6.15)$$

is the unperturbed solution. Because the evolution is causal, meaning that a perturbation at any given time can only influence the system's future, the response functions $\mathcal{R}^{(n)}$ naturally vanish for perturbations applied at times later than t. This causality ensures that the memory integrals in the Volterra series only involve past perturbations. If the perturbation is small (6.13) can be approximated by the lower-order response functions. For instance, we find³

$$\mathcal{R}^{(1)}(X_1; X_2; \mathbf{x}^{(i)}) = \frac{\delta \Psi_{f, \text{sol}}^K(X_1; \mathbf{x}^{(i)})}{\delta K(X_2)} \bigg|_{K=0} \propto \Theta(t_1 - t_2)$$
(6.16)

which describes the *linear response* of a perturbation at time t_1 to the solution at time t. The second order Volterra kernel

$$\mathcal{R}^{(2)}(X; X_1, X_2; \mathbf{x}^{(i)}) = \frac{\delta^2 \Psi_{f, \text{sol}}^K(X; \mathbf{x}^{(i)})}{\delta K(X_1) \delta K(X_2)} \bigg|_{K=0},$$
(6.17)

on the other hand, contains the information of how two perturbations at (x_1, t_1) and (x_2, t_2) affect the solution at time t. It thus describes a non-linear response of the system. Similar interpretations hold for the higher order response functions. Importantly, a given response function vanishes, if the time of a given perturbation is later than the time at which the density is evaluated,

$$\mathcal{R}^{(n)}(X; X_1, \dots, X_n; \mathbf{x}^{(i)}) = 0, \quad \text{if } \exists k \in \{1, \dots, n\} : t_k > t.$$
 (6.18)

For our statistical description we will be interested in the averaged response function which is defined as

$$\overline{\mathcal{R}}^{(n)}(X; X_1, \dots, X_n) := \left\langle \mathcal{R}^{(n)}(X; X_1, \dots, X_n; \mathbf{x}^{(i)}) \right\rangle, \tag{6.19}$$

³We recall that we are working in the Itô discretized theory, i. e., $\Theta(0) = 0$.

where the average is defined over the initial particle distribution. Most prominently, we define the *full retarded propagator* as the averaged linear response function⁴

$$G_R(X_1, X_2) := \overline{\mathcal{R}}^{(1)}(X_1; X_2) = \left\langle \frac{\delta \Psi_{f, \text{sol}}^K(X_1; \mathbf{x}^{(i)})}{\delta K(X_2)} \middle|_{K=0} \right\rangle \propto \Theta(t_1 - t_2). \tag{6.20}$$

It will play an essential role in the forthcoming discussion as it generalizes the free causal propagator (6.9) to the fully interacting statistical theory.

6.3. Generating Functional

With the above discussion we are now able to construct a field theoretic treatment of the Klimontovich equation (6.1). We are ultimately interested in the computation of unequal time correlators of the phase-space density, which are defined as

$$C_{f\dots f}(X_1,\dots,X_k) := \left\langle \Psi_{f,\text{sol}}^K(X_1;\mathbf{x}^{(i)}) \cdots \Psi_{f,\text{sol}}^K(X_k;\mathbf{x}^{(i)}) \right\rangle \bigg|_{K=0}$$

$$(6.21)$$

$$= \int d\mathbf{x}^{(i)} \varrho_N^{(i)}(\mathbf{x}^{(i)}) \Psi_{f,\text{sol}}^K(X_1; \mathbf{x}^{(i)}) \cdots \Psi_{f,\text{sol}}^K(X_k; \mathbf{x}^{(i)}) \bigg|_{K=0}, \quad (6.22)$$

where $\Psi_{f,\text{sol}}^K(X;\mathbf{x}^{(i)})$ represents the general solution to (6.6) as discussed in the previous section. While we could have immediately set K=0 and worked with the unperturbed solution of (6.1), temporarily retaining the perturbation K lets us give a clear physical interpretation to our fundamental fields. Only at the end do we send $K \to 0$ to recover the actual correlation functions. It is convenient to define the moment-generating functional $\mathcal{Z}[J_f, K]$ as

$$\mathcal{Z}[J_f, K] = \left\langle e^{J_f(1)\Psi_{f,\text{sol}}^K(1;\mathbf{x}^{(i)})} \right\rangle = \int d\mathbf{x}^{(i)} \varrho_N^{(i)}(\mathbf{x}^{(i)}) e^{J_f(1)\Psi_{f,\text{sol}}^K(1;\mathbf{x}^{(i)})}. \tag{6.23}$$

The above physical correlators of the phase-space density can now be obtained by taking functional derivatives of (6.23) w.r.t. $J_f(1)$ at vanishing source $J_f(1)$ and perturbation K,

$$C_{f\dots f}(1,\dots,k) = \frac{\delta^k \mathcal{Z}[J_f,K]}{\delta J_f(1)\dots\delta J_f(k)} \bigg|_{J_f=0=K}.$$
 (6.24)

Clearly, by the definition of (6.23) and the normalization of the initial phase-space density, $\int d\mathbf{x}^{(i)} \varrho_N^{(i)}(\mathbf{x}^{(i)}) = 1$, the generating functional is normalized according to

$$\mathcal{Z}[J_f = 0, K] \equiv 1, \qquad (6.25)$$

independent of the perturbation K. Following the procedure outlined in 3.2.2, we may now replace $\Psi_{f,\text{sol}}^K(1;\mathbf{x}^{(i)})$ in the exponential of (6.23) with a general field

⁴In the literature of solid state physics, G_R is called the susceptibility of the medium, describing the average responds to an external perturbation.

 $\Psi_f(1)$ by introducing the appropriate functional Dirac-delta distribution enforcing the equation of motion (6.1) to obtain the MSRJD functional integral of the Klimontovich equation,

$$\mathcal{Z}[J_f, K] = \int \mathcal{D}\Psi_f \mathcal{D}\Psi_B \exp\left[-\tilde{\mathcal{S}}[\Psi_f, \Psi_B] + J_f(1)\Psi_f(1) + K(1)\Psi_B(1)\right] \times \int d\mathbf{x}^{(i)} \int \varrho_N(\mathbf{x}^{(i)}) \exp\left[\Psi_B(1)\Phi_f^{(i)}(1)\right],$$
(6.26)

where we extracted the terms depending on the initial microscopic particle configuration $\Phi_f^{(i)}(1)$. The remaining terms containing the dynamics are stored in $\tilde{\mathcal{S}}$ and read

$$\widetilde{\mathcal{S}}[\Psi_f, \Psi_B] = \Psi_B(1) D_{0,R}^{-1}(1,2) \Psi_f(2) - \Psi_B(1) F[\Psi_f, 1]. \tag{6.27}$$

Note that the exponent in (6.26) differs from the exponent in (3.73) by a factor of (-i). Following [21] we conveniently absorbed this factor into the auxiliary field Ψ_B making it a genuinely imaginary field. For reasons that will become clear in the subsequent discussion we will refer to it as the *response field*. Next, we can write the remaining integral over the initial conditions as an exponential. Let us therefore expand the exponential according to,

$$\int d\mathbf{x}^{(i)} \int \varrho_N(\mathbf{x}^{(i)}) \exp\left[\Psi_B(1)\Phi_f^{(i)}(1)\right]$$
(6.28)

$$= \sum_{n=0}^{\infty} \frac{1}{n!} \Psi_B(1) \dots \Psi_B(n) \int d\mathbf{x}^{(i)} \varrho_N^{(i)}(\mathbf{x}^{(i)}) \Phi_f^{(i)}(1) \dots \Phi_f^{(i)}(n)$$
 (6.29)

$$= \sum_{n=0}^{\infty} \frac{1}{n!} \Psi_B(1) \dots \Psi_B(n) C_{f \dots f}^{(i)}(1, \dots, n)$$
(6.30)

$$\equiv \mathcal{Z}^{(i)}[\Psi_B] \,, \tag{6.31}$$

where we identified the series expansion of the generating functional of initial $\Phi_f^{(i)}$ correlators

$$C_{f...f}^{(i)}(X_1,...,X_n) := \left[\prod_{k=1}^n \delta_{\mathcal{D}}\left(t_k - t^{(i)}\right)\right] C_{f...f}^{(i)}(x_1,...,x_n), \qquad (6.32)$$

in the last line. Note that the Dirac-delta distributions localize the correlators at initial time. In principle, we could perform the time integration to obtain the initial value of the response field $\Psi_B^{(i)}$. However, it will be convenient to keep the general time dependence in Ψ_B while keeping the localization at initial time in mind. The response field Ψ_B thus acts as a conjugate field to the phase-space density Φ_f . Similarly, as in (5.14) we can use the associated cumulant generating functional $\mathcal{W}^{(i)}[\Psi_B]$ to write the entire integral over the initial conditions as an exponential,

$$\int d\mathbf{x}^{(i)} \int \varrho_N(\mathbf{x}^{(i)}) \exp\left[\Psi_B(1)\Phi_f^{(i)}(1)\right] = \mathcal{Z}^{(i)}[\Psi_B] = e^{\mathcal{W}^{(i)}[\Psi_B]}, \qquad (6.33)$$

where $\mathcal{W}^{(i)}[\Psi_B]$ is defined via its series representation,

$$W^{(i)}[\Psi_B] = \sum_{n=0}^{\infty} \frac{1}{n!} \Psi_B(1) \dots \Psi_B(n) G_{f\dots f}^{(i)}(1, \dots, n), \qquad (6.34)$$

with the initial phase-space density cumulants $G_{f...f}^{(i)}(1,...,n)$ defined analogously to (6.32),

$$G_{f...f}^{(i)}(X_1, \dots, X_n) := \left[\prod_{k=1}^n \delta_{\mathcal{D}}\left(t_k - t^{(i)}\right)\right] G_{f...f}^{(i)}(x_1, \dots, x_n). \tag{6.35}$$

It is clear from (6.26) that the perturbation K, introduced in equation (6.6), in order to study the system's response to local fluctuations, acts as a source for the response field. We therefore conveniently define $J_B = K$ and find the final expression for the generating functional for the Klimontovich equation,

$$\mathcal{Z}[J_f, J_B] = \int \mathcal{D}\Psi_f \mathcal{D}\Psi_B e^{-\mathcal{S}[\Psi_f, \Psi_B] + J_f(1)\Psi_f(1) + J_B(1)\Psi_B(1)}.$$
 (6.36)

This generating functional lays the cornerstone for the subsequent formalism. Writing out all the integrals, the associated action is defined as

$$S[\Psi_f, \Psi_B] = \int_{X_1, X_2} \Psi_B(X_1) \left[D_{0,R}^{-1} - U^{(1)} \right] (X_1, X_2) \Psi_f(X_2)$$

$$- \frac{1}{2} \int_{X_1, X_2, X_3} U_s^{(2)}(X_1, X_2, X_3) \Psi_B(X_1) \Psi_f(X_2) \Psi_f(X_3)$$

$$- \sum_{n=1}^{\infty} \frac{1}{n!} \int_{X_1, \dots, X_n} G_{f \dots f}^{(i)}(X_1, \dots, X_n) \Psi_B(X_1) \dots \Psi_B(X_n) .$$

$$(6.37)$$

We thus end up with a two-component field theory, where the coupling functions $U^{(1)}(1,2)$ and $U_s^{(2)}(1,2,3)$ carry the external potential and the two-particle interactions and thus couple to one and two phase-space densities, respectively. For convenience, we have symmetrized the latter and defined

$$U_s^{(2)}(1,2,3) = U^{(2)}(1,2,3) + U^{(2)}(1,3,2)$$
 (6.38)

The pure Ψ_B -field couplings in the last line of (6.37) define a possibly infinite tower of spurious vertices that are due to the arbitrarily complicated structure of the initial conditions, which describe how a given set of densities is connected by the cumulants of the initial statistics. The Dirac-delta distributions in (6.35) ensure that the spurious interactions are localized at the initial time $t^{(i)}$. Note, that only response fields are attached to the initial couplings, which will restrict the possible diagrams emerging from the above field theory. Furthermore, there is no pure Ψ_f -field coupling, which is due to the causal structure of the theory as will become clear in the next sections.

Since the initial vertices also contain terms that are linear and quadratic in the fields, it will be convenient for the later discussion to separate those terms from the

higher order initial cumulants. We therefore define the dynamical action $\mathcal{S}_{\mathcal{D}}[\Psi]$ as

$$S_{\mathcal{D}}[\Psi] = \Psi_B(1) \left[D_{0,R}^{-1} - U^{(1)} \right] (1,2) \Psi_f(2)$$

$$- U_s^{(2)}(1,2,3) \Psi_B(1) \Psi_f(2) \Psi_f(3)$$

$$- G_f^{(i)}(1) \Psi_B(1) - \frac{1}{2!} G_{ff}^{(i)}(1,2) \Psi_B(1) \Psi_B(2) .$$
(6.39)

The residual couplings, containing the initial non-Gaussian structure are collected in $\mathcal{S}_{\mathcal{I}}[\Psi]$,

$$S_{\mathcal{I}}[\Psi] = -\sum_{n=3}^{\infty} \frac{1}{n!} G_{f...f}^{(i)}(1, ..., n) \Psi_B(1) ... \Psi_B(n), \qquad (6.40)$$

such that the total action splits into

$$S[\Psi] = S_{\mathcal{D}}[\Psi] + S_{\mathcal{I}}[\Psi]. \tag{6.41}$$

Let us briefly summarize and comment on the above construction. Starting from the exact Klimontovich field equation (6.6) which contains the full information of the N-particle statistics, we were able to construct an action from which correlation functions can be derived in the usual (quantum) statistical field theoretic way, i. e., as averages weighted by a factor e^{-S} . The price we have to pay, however, is a doubling of the fundamental degrees of freedom: instead of a single field Ψ_f , we now have both Ψ_f and Ψ_B . This doubling also increases the number of fundamental correlators, for instance, we now encounter mixed correlation functions such as $\langle \Psi_f \dots \Psi_B \rangle$. Note also, that the interpretation of the action (6.37) as an actual action for the dynamics of Ψ_f and Ψ_B has to be taken with a grain of salt as the field Ψ_B does not represent a physical degree of freedom. Its role will be clarified in the next section and relates, as already suspected, to the system's response properties. Furthermore, the action (6.37) is generally complex due to its origin in the Dirac-delta distribution enforcing the classical evolution equation, such that the factor e^{-S} is neither real nor non-negative. However, integrating out the response field, results in a well-defined probability distribution for Ψ_f .

6.4. Mixed Correlation Functions and Cumulants

Before continuing the technical development of the field theory, let us take a moment to discuss the physical properties of the correlation functions derived from the above generating functional. Clearly, the pure f-correlation functions are those of the physical phase-space density. We therefore have to understand the role of the response field Ψ_B . As already mentioned, the field Ψ_B does not represent a physical degree of freedom. This is clear from the observation that (6.25) implies that

$$\langle \Psi_B(X_1) \dots \Psi_B(X_n) \rangle \Big|_{J_f=0} = 0.$$
 (6.42)

In particular, the expectation value for Ψ_B vanishes, $\langle \Psi_B(X_1) \rangle \Big|_{J_f=0} = 0$, and it has no own independent dynamics. However, despite the fact that it has only been introduced as a Lagrangian multiplier in order to enforce the dynamics for Ψ_f , it allows for a clear interpretation in terms of the system's response functions, as discussed in section 6.2. Restoring the perturbation $K = J_B$ (see the discussion above (6.36)), we find for the expectation value of the phase-space density with perturbation K,

$$\left\langle \Psi_{f,\text{sol}}^K(1; \mathbf{x}^{(i)}) \right\rangle = \left. \frac{\delta \mathcal{Z}[J_f, K]}{\delta J_f(1)} \right|_{J_f=0}$$
(6.43)

$$= \int \mathcal{D}\Psi_f \mathcal{D}\Psi_B \,\Psi_f(1) \,\mathrm{e}^{-\mathcal{S}[\Psi_f, \Psi_B] + K \cdot \Psi_B}$$
(6.44)

$$= \int \mathcal{D}\Psi_f \mathcal{D}\Psi_B \,\Psi_f(1) \,e^{-\mathcal{S}[\Psi_f, \Psi_B]} \left(1 + K(1)\Psi_B(1) + \frac{1}{2!} \left(K(1)\Psi_B(1) \right)^2 + \dots \right).$$
(6.45)

We thus obtain a series expansion similar to (6.13). Taking functional derivatives w.r.t. K, we find

$$\left\langle \frac{\delta^n \Psi_{f,\text{sol}}^K(1)}{\delta K(1') \dots \delta K(n')} \right\rangle \bigg|_{K=0} = \int \mathcal{D}\Psi_f \mathcal{D}\Psi_B \, e^{-\mathcal{S}[\Psi_f, \Psi_B]} \, \Psi_f(1) \Psi_B(1') \dots \Psi_B(n') \,, \quad (6.46)$$

and thus the interpretation of the mixed $C_{fB...B}$ correlation function in terms of the response functions (6.19),

$$C_{fB...B}(1, 1', ..., n') \equiv \overline{\mathcal{R}}^{(n)}(1; 1', ..., n'),$$
 (6.47)

describing the averaged influence of n fluctuations at X_1 to X_n onto the phase-space density at X. The generalization to arbitrary mixed cumulants is straightforward: The mixed correlation function

$$C_{f\dots fB\dots B}(1,\dots,n_f,1',\dots,n_B') \coloneqq \frac{\delta^{n_f+n_B} \mathcal{Z}[J_f,J_B]}{\delta J_f(1)\dots\delta J_f(n_f)\delta J_B(1')\dots\delta J_B(n_B')}\bigg|_{J=0}$$

represents the averaged influence of n_B fluctuations on n_f densities. The causality rule (6.18) now translates into the statement

$$C_{f...fB...B}(1,...,n_f,1',...,n_B') = 0 \text{ if } \exists k \in \{1,...,n_B\} : t_k > t_s \forall s \in \{1,...,n_f\}.$$

$$(6.48)$$

Most prominently, the mixed two-point correlation function corresponds to the full retarded propagator,

$$\langle \Psi_f(1)\Psi_B(2)\rangle = G_R(1,2) \propto \Theta(t_1 - t_2).$$
 (6.49)

We can now naturally define the general mixed *cumulant* as the connected part of the above correlation functions,

$$G_{f...fB...B}(1,\ldots,n_f,1',\ldots,n_B') = \langle \Psi_f(1)\ldots\Psi_f(n_f)\Psi_B(1')\ldots\Psi_B(n_B')\rangle_c$$
 (6.50)

Clearly, by (6.42) only the Ψ_f part of a given correlation function decomposes. Having the above discussion in mind, we can, from this point on, treat Ψ_f and Ψ_B on equal footing and analyze the field theory defined by the generating functional (6.36) by standard procedures. As a reminder, we will make use of DeWitt's condensed notation defined in appendix A and already used in chapter 5 and write $a = (\alpha, X_a)$ where Greek indices refer to the respective density or response component of Ψ_{α} , with $\alpha = \{f, B\}$.

6.5. Bare Theory

We start by discussing the general properties and physical implications of the field theory defined by the generating functional (6.36),

$$\mathcal{Z}[J] = \int \mathcal{D}\Psi \exp\left[-\mathcal{S}[\Psi] + J_a \Psi_a\right], \qquad (6.51)$$

where the action admits the formal expansion around⁵ $\Psi = 0$,

$$\mathcal{S}[\Psi] = \sum_{n=0}^{\infty} \frac{1}{n!} \mathcal{S}_{a_1 \dots a_n}^{(n)} \Psi_{a_1} \dots \Psi_{a_n}, \quad \text{with} \quad \mathcal{S}_{a_1 \dots a_n}^{(n)} := \frac{\delta^n \mathcal{S}[\Psi]}{\delta \Psi_{a_1} \dots \delta \Psi_{a_n}} \bigg|_{\Psi=0}, \quad (6.52)$$

and we define the bare n-point vertices by its coefficients $\mathcal{S}_{a_1...a_n}^{(n)}$. More precisely, we distinguish between the bare n-point dynamical vertices $\mathcal{S}_{\mathcal{D},a_1...a_n}^{(n)}$ and the bare n-point initial vertices $\mathcal{S}_{\mathcal{I},a_1...a_n}^{(n)}$, corresponding to contributions from the dynamics and the non-Gaussian initial conditions, respectively. We define the $free^6$ propagator Δ_0 as the inverse of the functional Hessian of the above action,

$$S_{ac}^{(2)} \Delta_{0,cb} = \delta_{ab} \,. \tag{6.53}$$

In order to systematically organize the theory, it will be convenient to split the dynamical action even further, such that,

$$S[\Psi] = S_0[\Psi] + S_{int}[\Psi] + S_{\mathcal{I}}[\Psi]. \qquad (6.54)$$

The free action S_0 is defined to contain the above inverse free propagator and the initial mean field. Explicitly, it reads

$$S_0[\Psi] := \frac{1}{2} \Psi_a \left[\Delta_0^{-1} \right]_{ab} \Psi_b + S_{\mathcal{D},a}^{(1)} \Psi_a ,$$
 (6.55)

⁵We emphasize this because, in what follows, we will distinguish between expansions around zero and non-trivial field configurations.

⁶Even though the propagator receives contributions from the external potential, we will refer to it as the free propagator.

where

$$S_{\mathcal{D},\alpha}^{(1)}(X_1) = \begin{pmatrix} 0\\ -G_f^{(i)}(X_1) \end{pmatrix}$$
 (6.56)

The interaction action $\mathcal{S}_{\mathrm{int}}$ contains the two-particle interactions and is defined as

$$S_{\text{int}}[\Psi] := \frac{1}{3!} S_{\mathcal{D},abc}^{(3)} \Psi_a \Psi_b \Psi_c. \tag{6.57}$$

Inserting this decomposition into the generating functional, enables us to rewrite the latter in the usual way

$$\mathcal{Z}[J] = \int \mathcal{D}\Psi \,e^{-\mathcal{S}_0[\Psi] - \mathcal{S}_{int}[\Psi] - \mathcal{S}_{\mathcal{I}}[\Psi] + J_i \,\Psi_i}$$
(6.58)

$$= e^{-(\hat{\mathcal{S}}_{int} + \hat{\mathcal{S}}_{\mathcal{I}})} \int \mathcal{D}\Psi e^{-\mathcal{S}_0[\Psi] + J_i \Psi_i}$$
(6.59)

$$= e^{-(\hat{\mathcal{S}}_{int} + \hat{\mathcal{S}}_{\mathcal{I}})} \mathcal{Z}_0[J], \qquad (6.60)$$

where \hat{S}_{int} and $\hat{S}_{\mathcal{I}}$ denote the corresponding operators obtained by replacing the fields Ψ_a by functional derivatives with respect to the source J. The free generating functional is Gaussian and can be solved analytically,

$$\mathcal{Z}_0[J] = \mathcal{N} e^{\frac{1}{2}(J_a - \mathcal{S}_{\mathcal{D},a}^{(1)})\Delta_{0,ab}(J_b - \mathcal{S}_{\mathcal{D},b}^{(1)})}, \qquad (6.61)$$

where \mathcal{N} is a normalization constant. In order to study the above generating functional (6.58), whether perturbatively or non-perturbatively, it is essential to understand the precise structure of the free propagators, as it encodes the fundamental dynamical properties of the field theory.

6.5.1. Free Propagators and Resummation of the External Potential

Let us start by analyzing the simple case of the free theory, where only the external potential is present, and particle interactions are neglected, that is, $S_{\rm int} \to 0$, or equivalently, $U^{(2)} \to 0$. Although this case is principally trivial, it will serve as an intuitive toy example to build up physical intuition for the more general formalism introduced in the later chapters. In this limit, the generating functional becomes exactly solvable by analytical methods, even if we allow for arbitrary initial conditions.

The associated generating functional is

$$\mathcal{Z}[J] = e^{-\hat{\mathcal{S}}_{\mathcal{I}}} \mathcal{Z}_0[J], \qquad (6.62)$$

with \mathcal{Z}_0 given by (6.61). The inverse free propagator can be obtained from (6.37)

upon functional differentiation around vanishing field Ψ and has the components

$$\left[\Delta_0^{-1}\right]_{\alpha\beta}(1,2) = \begin{pmatrix} 0 & D_{0,R}^{-1} - U^{(1)} \\ D_{0,A}^{-1} - U^{(1)} & -G_{ff}^{(i)} \end{pmatrix} (1,2). \tag{6.63}$$

The inversion can be performed by solving the functional matrix equation

$$\int_{X} \Delta_{0}^{-1}(X_{1}, X) \cdot \Delta_{0}(X, X_{2}) = \delta_{D}(X_{1} - X_{2}) \, \mathbb{1}_{2 \times 2}.$$
(6.64)

The matrix structure of Δ_0 is clearly given by

$$\Delta_0 = \begin{pmatrix} \Delta_{0,ff} & \Delta_{0,fB} \\ \Delta_{0,Bf} & 0 \end{pmatrix} = \begin{pmatrix} \Delta_{0,ff} & \Delta_{0,R} \\ \Delta_{0,A} & 0 \end{pmatrix}, \tag{6.65}$$

where the coefficients are subject to the evolution equations

$$\left[D_{0,R}^{-1} - U^{(1)}\right](1,\bar{1})\Delta_{0,R}(\bar{1},2) = \mathbb{1}(1,2), \qquad (6.66)$$

$$\Delta_{0,A}(1,2) = \Delta_{0,R}(2,1), \qquad (6.67)$$

$$\left[D_{0,R}^{-1} - U^{(1)}\right](1,\bar{1})\Delta_{0,ff}(\bar{1},2) = G_{ff}^{(i)}(1,\bar{2})\Delta_{0,A}(\bar{2},2). \tag{6.68}$$

Since $D_{0,R}^{-1}$ describes the free time evolution, these equations can be seen as averaged equations of motion. The first equation identifies $\Delta_{0,R}$ as the retarded Green function to the differential operator $\left[D_{0,R}^{-1} - U^{(1)}\right]$, i.e., the free evolution with external potential. The causal structure of $D_{0,R}$ is thus inherited by $\Delta_{0,R}$, and we will therefore refer to $\Delta_{0,R}$ and $\Delta_{0,A}$ as the free retarded and free advanced causal propagators respectively. On the other hand, the equation of motion for Δ_{ff} can be solved by multiplication from the left with $\Delta_{0,R}$

$$\Delta_{0,ff}(1,2) = \Delta_{0,R}(1,\bar{1})G_{ff}^{(i)}(\bar{1},\bar{2})\Delta_{0,A}(\bar{2},2). \tag{6.69}$$

Thus, $\Delta_{0,ff}$ arises as the propagation of an initial two-point fluctuation under the influence of an external potential. We will therefore refer to $\Delta_{0,ff}$ as the *free statistical propagator*.

With the explicit structure of the propagators at hand, we can evaluate the Gaussian part of the generating functional $\mathcal{Z}_0[J]$,

$$\mathcal{Z}_0[J] = \exp\left[\frac{1}{2}J_{\alpha}(1)\Delta_{0,\alpha\beta}(1,2)J_{\beta}(2) + J_f(1)\Delta_{0,R}(1,2)G_f^{(i)}(2)\right]. \tag{6.70}$$

The source for the response field J_B only appears to linear order in the generating functional. This, together with the fact that only J_B -derivatives appear in the action $S_{\mathcal{I}}$, make the structure quite remarkable, since the full non-Gaussian theory is exactly solvable. Every functional derivative w.r.t. J_B in $S_{\mathcal{I}}$ brings down a term $J_f \cdot \Delta_{0,fB}$ from \mathcal{Z}_0 , effectively replacing the derivative operator in $S_{\mathcal{I}}$. We find for the full

generating functional

$$\mathcal{Z}[J] = \exp\left[\frac{1}{2}J^{\top} \cdot \Delta_0 \cdot J - J_f \cdot \Delta_{0,R} \cdot \mathcal{S}_{\mathcal{D},B}^{(1)} + S_{\mathcal{I}}[J_f \cdot \Delta_{0,R}]\right]. \tag{6.71}$$

It is worthwhile to briefly analyze equation (6.66) in more detail, as it exhibits a form that will reappear throughout our discussion. Rewriting (6.66), we find

$$\Delta_{0,R}^{-1}(1,2) = D_{0,R}^{-1}(1,2) - U^{(1)}(1,2),, \tag{6.72}$$

which can be recognized as a Dyson-type equation for the retarded propagator. Suppressing the explicit phase-space and time indices for brevity, its formal solution can be expressed as

$$\Delta_{0,R}(1,2) = D_{0,R}(1,2) + D_{0,R}(1,\bar{1}) U^{(1)}(\bar{1},\bar{2}) \Delta_{0,R}(\bar{2},2)$$

$$= D_{0,R} \cdot \sum_{n=0}^{\infty} \left(U^{(1)} \cdot D_{0,R} \right)^{n}, \qquad (6.73)$$

where the second line shows the resummation of an infinite series of multiple scatterings off the external potential. The crucial observation is that the causal propagator $\Delta_{0,R}$ non-perturbatively resums all orders of the external potential $U^{(1)}$. Consequently, $\Delta_{0,R}$ provides an exact solution for the full response of the system to the presence of an external field. Equation (6.73) is a prototypical non-perturbative equation and will reappear frequently throughout the following chapters. In general, one has to rely on numerical methods to solve such equations.

6.5.2. Bare Feynman Diagrams

It will be convenient to introduce Feynman diagrams in order to schematically represent equations. The basic building blocks are given by the free propagators and the bare vertices. Since we have two fundamental fields, there will be two types of lines. In general, we will represent the response field Ψ_B by a dashed line and the phase-space density field Ψ_f by a solid line. The diagrammatic representation of a bare vertex with r density and s response field is in general given by

$$S_{f...fB...B}^{(r+s)}(1, ...r, 1', ...s') = \sum_{r=s'}^{1} \sum_{s'}^{1'}, \qquad (6.74)$$

where the gray lines are truncated propagators, indicating which end of a respective propagator is attached. In particular, the non-vanishing vertices are given by

$$S_{fB}^{(2)}(1,2) = 1 \longrightarrow 2 \qquad S_{BB}^{(2)}(1,2) = 1 \longrightarrow 2$$
 (6.75)

for the inverse free causal and statistical propagators,

$$\mathcal{S}_B^{(1)}(1) = 1 \cdots \bullet \tag{6.76}$$

for the initial mean field, and

for the interaction vertex. All higher order initial vertices are analogously represented by

$$S_{B...B}^{(k)}(1,...,k) = \frac{1}{k} ...$$
(6.78)

Next, the free causal propagators have the representation

$$\Delta_{0,R}(1,2) \equiv \Delta_{0,fB}(1,2) = 1 - 2 , \qquad (6.79)$$

$$\Delta_{0,A}(1,2) \equiv \Delta_{0,Bf}(1,2) = 1 - 2$$
, (6.80)

where the dashed and solid ends indicate the response and phase-space density field, respectively. The time flow in a causal propagator is thus always from the dashed end to the solid end. We note, that the inversion relation between the free causal propagator $\Delta_{0,fB}$ and $S_{\mathcal{D},Bf}^{(2)}$ can be represented as

$$- \bullet - = 1 \tag{6.82}$$

Last but not least, we represent the statistical propagator by

$$\Delta_{0.ff}(1,2) = 1 \longrightarrow 2 = 1 \longrightarrow 2, \qquad (6.83)$$

where the left-hand side diagrammatically illustrates its decomposition into causal propagators: a Gaussian initial fluctuation, represented by the vertex, is propagated forward in time along both branches. As a result, the time flow in $\Delta_{0,ff}$ is outward-oriented at both ends.

When constructing a given diagram, the legs of the free propagators are connected to the appropriate legs of the interaction vertices. The causal structure of the theory is encoded in the orientation of the free propagator, which flows from its dashed to its solid end, representing the causal propagation of a perturbation from an earlier to a later time. Importantly, since the interaction vertices never contain only Ψ_f -legs, there is always at least one outgoing dashed line. This ensures that perturbations cannot simply disappear within a diagram—any perturbation that enters must propagate further. In this way, the structure of the vertices and propagators enforces

a continuous causal time flow, consistent with the causality rule described by (6.48).

6.6. The Background Field Approximation

We yet have to incorporate the missing two-particle interaction vertex $\mathcal{S}_{Bff}^{(3)}$, neglected in the above description. This term will induce a non-trivial coupling between the response field Ψ_B and the phase-space density Ψ_f , such that the full generating functional will no longer be analytically solvable. Nonetheless, in order to study an ensemble of N mutually interacting particles, we will have to develop methods in order to describe the whole system.

The most naive approach would be to pull the $S_{\rm int}$ interaction part out of the functional integration by replacing the fields with appropriate functional derivatives as indicated in (6.60). Expanded in this way, the interactions are treated as small fluctuations around the free dynamics with an external potential discussed in the previous section. However, this would neglect the possible back-reaction of the manifestly non-trivial mean background, $\overline{\Psi}_f := \langle \Psi_f \rangle \neq 0$, to the dynamics. Already at initial time we evidently have a non-trivial mean background which is hidden in $G_f^{(i)} \neq 0$. This background will therefore evolve in time, and is expected to affect the evolution of the fields themselves, similarly to an external potential, discussed in section 6.5.1. In order to incorporate those effects into our description we perform a background field approximation which is sometimes also called mean field approximation. Let us therefore expand the system around the classical mean by writing

$$\Psi_{\alpha}(X) = \overline{\Psi}_{\text{EoM},\alpha}^{(0)}(X) + \Psi_{\alpha}^{\delta}(X), \qquad (6.84)$$

where $\overline{\Psi}^{(0)}_{\text{EoM},\alpha}$ is the classical⁷ expectation value and $\Psi^{\delta}_{\alpha}(X)$ is the fluctuation around it. The former is defined by the stationarity requirement

$$0 \stackrel{!}{=} \frac{\delta \mathcal{S}[\Psi]}{\delta \Psi_{\alpha}(X)} \bigg|_{\Psi = \overline{\Psi}_{\text{EoM}}^{(0)}}, \tag{6.85}$$

and describes the deterministic evolution of the initial mean field. The variation with respect to Ψ_f leads to a simple constraint,

$$0 = \overline{\Psi}_{\text{EoM},B}^{(0)}, \qquad (6.86)$$

which states that the classical response field vanishes in accordance with (6.42).

⁷In this context, "classical" refers to the deterministic solution of the underlying statistical theory, analogous to the classical limit in quantum field theory—that is, the solution obtained without incorporating statistical fluctuations. We have added the subscript "EoM" here to indicate that the solution satisfies the classical equation of motion, where the right-hand side of the stationarity condition vanishes. While this distinction is not strictly necessary at this point, it will become important later, when we introduce background fields in the presence of external sources. The "EoM" label will then serve to distinguish the source-free solution from the general mean field.

On the other hand, the functional derivative with respect to Ψ_B yields the actual evolution equation for the mean field $\overline{\Psi}_{\mathrm{EoM},f}^{(0)}$,

$$0 = \Delta_{0,Bf}^{-1}(1,2)\overline{\Psi}_{\mathrm{EoM},f}^{(0)}(2) + \mathcal{S}_{\mathcal{D},B}^{(1)}(1) + \frac{1}{2}\,\mathcal{S}_{\mathcal{D},Bff}^{(3)}(1,2,3)\,\overline{\Psi}_{\mathrm{EoM},f}^{(0)}(2)\,\overline{\Psi}_{\mathrm{EoM},f}^{(0)}(3)\,, \ (6.87)$$

which represents a non-linear equation for the classical phase-space density. In general, this equation cannot be solved analytically, and one must rely on numerical methods. However, in chapter 8, we consider a special class of systems that admits an analytical solution.

The bare theory in section 6.5 was defined as an expansion around vanishing fields in (6.52). Let us thus now expand the action analogously in a Taylor series around the non-vanishing classical expectation value $\overline{\Psi}_{\rm EoM}^{(0)}$,

$$\mathcal{S}\left[\overline{\Psi}_{\text{EoM}}^{(0)} + \Psi^{\delta}\right] = \frac{1}{2} \overline{\mathcal{S}}_{\mathcal{D},ab}^{(2)} \Psi_{a}^{\delta} \Psi_{b}^{\delta} + \sum_{n=3}^{\infty} \frac{1}{n!} \overline{\mathcal{S}}_{\mathcal{D},a_{1}...a_{n}}^{(n)} \Psi_{a_{1}}^{\delta} \dots \Psi_{a_{n}}^{\delta} + \sum_{n=3}^{\infty} \frac{1}{n!} \overline{\mathcal{S}}_{\mathcal{I},a_{1}...a_{n}}^{(n)} \Psi_{a_{1}}^{\delta} \dots \Psi_{a_{n}}^{\delta}$$

$$(6.88)$$

$$= \mathcal{S}_0[\Psi^{\delta}; \overline{\Psi}_{EoM}^{(0)}] + \mathcal{S}_{int}[\Psi^{\delta}; \overline{\Psi}_{EoM}^{(0)}] + \mathcal{S}_{\mathcal{I}}[\Psi^{\delta}; \overline{\Psi}_{EoM}^{(0)}], \qquad (6.89)$$

where we defined

$$\overline{\mathcal{S}}_{a_1...a_n}^{(n)} := \frac{\delta^n \mathcal{S}[\Psi]}{\delta \Psi_{a_1} \dots \delta \Psi_{a_n}} \bigg|_{\Psi = \overline{\Psi}^{(0)}}, \tag{6.90}$$

as the n-th order functional derivative w.r.t. the fields evaluated at the non-vanishing mean background. This stands in contrast to the bare vertices (6.52). In general, $\overline{\mathcal{S}}^{(n)}$ will functionally depend on the mean background, which is crucial for the upcoming analysis. In (6.88) we used that $\overline{\mathcal{S}}$ and $\overline{\mathcal{S}}^{(1)}$ vanish according to the first and the second equation in (6.85), respectively. Furthermore, we again decomposed the action into three parts: the quadratic part \mathcal{S}_0^8 , the term containing the interaction vertex $\overline{\mathcal{S}}_{\mathcal{D}}^{(3)}$, denoted by \mathcal{S}_{int} , and the infinite tower of initial vertices, denoted by $\mathcal{S}_{\mathcal{I}}$. We can now proceed in the same way as in 6.5. The three parts explicitly read

$$S_0[\Psi^{\delta}; \overline{\Psi}_{\text{EoM}}^{(0)}] = \frac{1}{2} \Psi_a^{\delta} \left[\Delta^{-1} \right]_{ab} \Psi_b^{\delta}, \qquad (6.91)$$

$$S_{\text{int}}[\Psi^{\delta}; \overline{\Psi}_{\text{EoM}}^{(0)}] = \frac{1}{3!} \overline{S}_{\mathcal{D},abc}^{(3)} \Psi_a^{\delta} \Psi_b^{\delta} \Psi_c^{\delta}, \qquad (6.92)$$

$$\mathcal{S}_{\mathcal{I}}[\Psi^{\delta}; \overline{\Psi}_{\text{EoM}}^{(0)}] = \sum_{n=3}^{\infty} \frac{1}{n!} \overline{\mathcal{S}}_{\mathcal{I}, a_1 \dots a_n}^{(n)} \Psi_{a_1}^{\delta} \dots \Psi_{a_n}^{\delta}, \qquad (6.93)$$

⁸We use the same notation as the free action discussed earlier.

where we defined the inverse tree-level propagator

$$\left[\Delta^{-1}\right](1,2) = \begin{pmatrix} 0 & \Delta_{0,A}^{-1} - \Sigma_A^{(0),H} \\ \Delta_{0,R}^{-1} - \Sigma_R^{(0),H} & \overline{\mathcal{S}}_{\mathcal{D},BB}^{(2)} \end{pmatrix}(1,2), \qquad (6.94)$$

which will be analyzed in the next section. In the above equation, the mean field $\overline{\Psi}^{(0)}_{{\rm EoM},f}$ enters via

$$\Sigma_R^{(0),H}(1,2) = \overline{\mathcal{S}}_{\mathcal{D},Bff}^{(3)}(1,2,3)\overline{\Psi}_{\text{EoM},f}^{(0)}(3),$$
 (6.95)

which represents the first approximation to the *Hartree self-energy* as indicated by the superscript "H" and which will be discussed in general in the next chapter. It describes the direct influence of the mean field to the evolution. Inserting the above decomposition of the action into the generating functional and using the invariance of the path integral measure under the shift (6.84) from $\Psi \to \Psi^{\delta}$, we find

$$\mathcal{Z}[J] = e^{J_a \overline{\Psi}_{\text{EoM},a}^{(0)}} \int \mathcal{D}\Psi^{\delta} e^{-\mathcal{S}_0[\Psi^{\delta}; \overline{\Psi}_{\text{EoM}}^{(0)}] - \mathcal{S}_{\text{int}}[\Psi^{\delta}; \overline{\Psi}_{\text{EoM}}^{(0)}] - \mathcal{S}_{\mathcal{I}}[\Psi^{\delta}; \overline{\Psi}_{\text{EoM}}^{(0)}] + J_a \Psi_a^{\delta}}.$$
(6.96)

This generating functional now includes all statistical fluctuations that induce deviations from the classical mean $\overline{\Psi}_{\rm EoM}^{(0)}$ defined by the classical equations of motion (6.85). If a non-vanishing background is present—as is clearly the case in our system—then incorporating a background field into the approximation improves the convergence of the perturbative expansion compared to a naive approach that starts from the generating functional expanded around a vanishing background. This is due to the fact that in this construction, we explicitly capture part of the interaction within the quadratic part of the action as can be seen from (6.94). From that point on, we can either expand the generating functional in a usual perturbative expansion as we will discuss in the subsequent sections, or follow a more systematic procedure and derive full equations of motion discussed in detail in chapter 7. For the former approach, the generating functional is formally written as an asymptotic series by expanding the exponential containing $S_{\rm int}$ in a series expansion and pulling it out of the functional integration by replacing the fields with appropriate functional derivatives. We obtain

$$\mathcal{Z}[J] = \sum_{n=0}^{\infty} \frac{1}{n!} \mathcal{Z}_n[J], \qquad (6.97)$$

where the n-th order generating functional is defined as

$$\mathcal{Z}_{n}[J] = e^{J_{a}\overline{\Psi}_{\text{EoM},a}^{(0)}} \left(-S_{\text{int}} \left[\frac{\delta}{\delta J}; \overline{\Psi}_{\text{EoM}}^{(0)} \right] \right)^{n} \int \mathcal{D}\Psi^{\delta} e^{-S_{0}[\Psi^{\delta}; \overline{\Psi}_{\text{EoM}}^{(0)}] - S_{\mathcal{I}}[\Psi^{\delta}; \overline{\Psi}_{\text{EoM}}^{(0)}] + J_{a}\Psi_{a}^{\delta}}.$$
(6.98)

For the perturbative approach we can then analyze the resulting expressions order by order in n.

6.6.1. Tree-Level Theory

As a first step let us study the lowest order approximation that arises from the n=0 term in the above expansion. We therefore define the *tree-level generating functional* as,

$$\mathcal{Z}_0[J] = e^{J_a \overline{\Psi}_{\text{EoM},a}^{(0)}} e^{-S_{\mathcal{I}}\left[\frac{\delta}{\delta J}; \overline{\Psi}_{\text{EoM}}^{(0)}\right]} \int \mathcal{D}\Psi^{\delta} e^{-S_0\left[\Psi^{\delta}; \overline{\Psi}_{\text{EoM}}^{(0)}\right] + J_a \Psi_a^{\delta}}, \tag{6.99}$$

where we pulled the terms containing the initial conditions out of the Gaussian functional integration. Importantly, the functional derivatives w.r.t. J do not act on the first exponential. We define the *tree-level propagator* Δ_{ab} as the inverse of (6.94). It has the same qualitative structure as the propagator in 6.5, however it now contains contributions from the mean background $\overline{\Psi}^{(0)}$. It reads

$$\Delta_{\alpha\beta}(1,2) = \begin{pmatrix} \Delta_{ff} & \Delta_{fB} \\ \Delta_{Bf} & 0 \end{pmatrix} (1,2) = \begin{pmatrix} \Delta_{ff} & \Delta_{R} \\ \Delta_{A} & 0 \end{pmatrix} (1,2), \qquad (6.100)$$

where, demanding

$$\overline{\mathcal{S}}_{ab}^{(2)} \Delta_{bc} = \delta_{ac} \,, \tag{6.101}$$

the components fulfill a similar set of equations as in (6.66), namely

$$\left[\Delta_{0,R}^{-1} - \Sigma_R^{(0),H}\right](1,\bar{1})\Delta_R(\bar{1},2) = \mathbb{1}(1,2), \qquad (6.102)$$

$$\left[\Delta_{0,A}^{-1} - \Sigma_A^{(0),H}\right](1,\bar{1})\Delta_A(\bar{1},2) = \mathbb{1}(1,2), \qquad (6.103)$$

$$\left[\Delta_{0,R}^{-1} - \Sigma_R^{(0),H}\right](1,\bar{1})\Delta_{ff}(\bar{1},2) = G_{ff}^{(i)}(1,\bar{2})\Delta_A(\bar{2},2). \tag{6.104}$$

The first two equations define the causal tree-level propagator as the Green function to the differential operator that extends the one in (6.66) by the classical mean field. More precisely, Δ_R is the retarded causal tree-level propagator and Δ_A the advanced one. The third equation defines an equation of motion for the statistical tree-level propagator. Again, the latter can be solved upon multiplication from the left with Δ_R ,

$$\Delta_{ff}(1,2) = \Delta_R(1,\bar{1})G_{ff}^{(i)}(\bar{1},\bar{2})\Delta_A(\bar{2},2). \tag{6.105}$$

For later purpose, it will be convenient to further simplify the equation for the retarded tree-level propagator. Since Δ_R will contain one contribution of pure free-propagation, it will be sensible to decouple it from those which contain at least one contribution from the mean background. We make the ansatz,

$$\Delta_R(1,2) = \Delta_{0,R}(1,2) + \Omega_R(1,\bar{1})\Delta_{0,R}(\bar{1},2)$$
(6.106)

where Ω_R now contains at least one contribution from the mean background. Plugged into the above equation we find the respective equation for Ω_R , given by

$$\Omega_R(1,2) = \Delta_{0,R}(1,\bar{1})\Sigma_R^{(0),H}(\bar{1},2) + \Delta_{0,R}(1,\bar{1})\Sigma_R^{(0),H}(\bar{1},\bar{2})\Omega_R(\bar{2},2)$$
(6.107)

$$= \mathcal{V}_R^{(0)}(1,2) + \mathcal{V}_R^{(0)}(1,\bar{1})\Omega_R(\bar{1},2), \qquad (6.108)$$

where we defined

$$\mathcal{V}_{R}^{(0)}(1,2) = \Delta_{0,R}(1,\bar{1})\Sigma_{R}^{(0),H}(\bar{1},2) \tag{6.109}$$

which describes the free evolution of the mean background interaction. From the free propagator it inherits a Heaviside function such that we added the subscript "R" to account for this retardation. Thus, once the mean field equation (6.87) is solved, one proceeds by computing $\mathcal{V}_R^{(0)}$, Ω_R and eventually Δ_R . Following the same steps that led to (6.71), the tree-level generating functional now assumes the form

$$\mathcal{Z}_0[J_f, J_B] = \exp\left[\frac{1}{2}J^{\top} \cdot \Delta \cdot J + J_f \cdot \overline{\Psi}_f^{(0)} + S_{\mathcal{I}}[J_f \cdot \Delta_{fB}]\right]. \tag{6.110}$$

6.6.2. Feynman Diagrams for the Tree-Level Theory

We now need to introduce Feynman diagrams for the theory in presence of a non-trivial background. To distinguish these diagrams from those with a trivial background as in 6.5, we represent the vertices with non-trivial background by

$$\overline{\mathcal{S}}_{f\dots fB\dots B}^{(r+s)}(1,\dots r,1',\dots s') = \sum_{r=s'}^{1} \sum_{s'}^{1'} , \qquad (6.111)$$

where the black dot indicates the presence of the background. However, the only vertex that differs from the bare theory defined in (6.52) is the inverse tree-level propagator itself, given by

$$-\bullet \cdots = -\bullet \cdots - - - \cdots, \qquad (6.112)$$

where the second diagram on the right-hand side represents the mean interaction potential \mathcal{V}_{Bf} where we indicated the mean field

$$\overline{\Psi}_f^{(0)} \cong \longrightarrow, \tag{6.113}$$

coupling to the two-particle interaction vertex. The mean field can be obtained as the formal solution to equation (6.87), which may be represented as

$$\longrightarrow = \longrightarrow + \frac{1}{2} \longrightarrow (6.114)$$

We can now introduce analogous diagrammatic representations for the tree-level propagators,

$$\Delta_{fB} \cong ---- ,$$

$$\Delta_{Bf} \cong ---- ,$$
(6.115)

such that

$$\cdots \bullet - \cdots = 1 \tag{6.116}$$

$$-----=1 (6.117)$$

With those rules, equation (6.112) can be rearranged to the following Dyson-Schwinger like equation,

$$\underline{\hspace{1cm}} = \underline{\hspace{1cm}} + \underline{\hspace{1cm}} \qquad (6.118)$$

Confirming our expectation, we observe that the mean background is resummed in the same way as the external potential in (6.73). Given a solution for $\overline{\Psi}_f^{(0)}$, equation (6.118) is again a non-perturbative equation resumming *part* of the contributions from the two-particle potential,

Importantly, though being a non-perturbative equation, Δ_{fB} still contains only tree-level diagrams. All corrections are due to the direct influence of the mean background to the evolution. This justifies calling it the tree-level propagator. The inclusion of loop-corrections to Δ_{fB} will be discussed in section 6.6.3.

The equation of motion (6.102) for Δ_R suggests that Δ_R corresponds to the retarded Green function of the Klimontovich equation, *linearized* about the classical solution $\overline{\Psi}_f^{(0)}$, for a given initial density. The statistical objects derived from \mathcal{Z}_0 are therefore computed in this linearized limit. For instance, the connected part of the two-point function is given by

$$\langle \Psi_f(X_1)\Psi_f(X_2)\rangle_c^{\text{tree}} = \Delta_{ff} \equiv ----$$
 (6.120)

Thus, the statistical tree-level propagator corresponds to the linearized system's response to an initial two-point fluctuation, since by (6.105) we find

Similar equations hold for all higher-order statistical cumulants. We may thus summarize the discussion by stating that the tree-level theory corresponds to the bare theory taking into account the non-trivial mean background. Importantly, the only object that receives contributions from the mean field is the (inverse) free propagator. For this reason, we will distinguish only between the free propagator and the bare (or tree-level) propagator. It should thus be understood that, from

this point onward, we are always working in the presence of a non-trivial mean background, and that bare quantities refer to their definitions as derived directly from the classical action \mathcal{S} .

6.6.3. Loop Expansion and Perturbation Theory

With the tree-level generating functional at hand, we can now extend the discussion in order to incorporate higher-order loop corrections. We, therefore, have to apply the functional derivatives arising in the series expansion (6.97) order by order in n. Apart from being a tedious calculation, this poses no further conceptual difficulty.

With the Feynman diagrams introduced above, the obtained corrections can be represented in a simple way, by connecting the statistical and causal tree-level propagators Δ_{ff} and Δ_{fB} appropriately to the vertices. The interaction vertex $S_{Bff}^{(3)}$ couples two Ψ_f fields represented by solid lines to a single response field, represented by a dashed line. In contrast, the initial vertices only couple to Ψ_B fields, since they source initial fluctuation. Therefore, they can only couple to the response end of a Δ_{fB} propagator. Keeping these rules in mind, we find for the expansion of the full mean background, showing only the terms up to one-loop order,

$$G_f(1) \cong \longrightarrow +\frac{1}{2} \longrightarrow \longrightarrow + \dots$$
 (6.122)

The first diagram represents the tree-level value of the mean field, i. e., the classical solution, while the second diagram corresponds to the one-loop correction to the classical solution. Importantly, it contains a tree-level propagator, which indicates the back-reaction of the statistical fluctuations onto the mean field. Of course, the new mean field is not a solution to the equations (6.85) anymore. In the next chapter we will study how the action has to be modified in order to obtain the corrected mean field as a stationarity condition similar to the tree-level case.

We now turn to the loop corrections of the causal tree-level propagator. As expected from the tree-level analysis, corrections to the mean field will also influence the response function, which already accounts for the non-vanishing mean field. Indeed, we find for the lowest order terms,

$$G_{fB}(1,2) \cong -----+ \frac{1}{2} ------+ \dots$$
 (6.123)

The second diagram on the right-hand side enters the one-loop correction to the propagator in the same way as the classical mean field does in the tree-level propagator. As we will see in chapter 7 those contributions correspond to the evaluation of the propagator on a slightly corrected mean background. It represents a local correction to the propagator. The third diagram on the other hand, is a non-local correction

and represents a coupling between different scales of the theory. In chapter 8 when considering homogeneous systems, those types of diagrams will contain convolutions that effectively re-distribute structures between different scales and thus modify the system's response to perturbations in a non-linear way.

Note, that a diagram of the type

$$-----, \qquad (6.124)$$

is forbidden by causality. The upper propagator in the loop is accompanied by $\Theta(t_1 - t_2)$, while the lower propagator comes with $\Theta(t_2 - t_1)$. Since the vertices are local in time, the full loop will be proportional to $\Theta(t_1 - t_2)\Theta(t_2 - t_1) = 0$ indicating a closed time loop and thus vanishes.

Last but not least, the loop corrections to the connected two-point phase space density, i. e., the one-loop statistical propagator, are given by

They can be divided into three groups. The first two loop-diagrams correspond to the one-loop corrections of the causal propagator that transports the information of an initial two-point fluctuation, $G_{ff}^{(i)}$, represented by the dot on the left leg of the diagrams. The next two diagrams represent the same structure but symmetrized on the two external legs. The last three diagrams in contrast, contain the one-loop corrections to the true statistical fluctuations. They represent vertex corrections to the bare $\mathcal{S}_{BB}^{(2)}$ vertex that are transported with causal tree-level propagators. In particular the two diagrams in the last line include higher-order contributions from the initial fluctuations. The ellipses on the right-hand side of (6.122), (6.123) and (6.125) stand for all higher-order loop-corrections. Clearly, with increasing order of the perturbative expansion, the number of diagrams to be evaluated quickly becomes

very large, such that this approach soon becomes impractical. In chapter 7 we will, therefore, construct a more systematic approach that will allow for a more controlled approximation.

6.7. Comparison to the Microscopic Picture

Let us recall that the construction of the generating functional (5.14) in chapter 5 was based on the evolution of particle trajectories in Γ -space. Thus, the interaction potential does not directly affect the macroscopic fields, but its effect is instead transmitted through interactions between different particle trajectories to the fields. This leads to a complicated structure of the theory where (nearly all) the vertices are functions of the interaction potential. There is, a priori, no apparent hierarchy among those vertices that would suggest an appropriate truncation scheme. In fact, we will see in our application in Section 11.2 that the complicated vertex structure will lead to cancellations between loop diagrams, indicating that the perturbation theory should be restructured.

The generating functional (6.96) constructed in this chapter, on the other hand, is based on the evolution of the macroscopic field itself. Thus, the interaction potential directly affects the field which is reflected in the vertex structure of the theory. It has only a single dynamical vertex which carries the interaction potential, while the rest of the vertices carry only information on initial correlations present in the system. It is reasonable to expect that interactions will dominate the system, so that we can neglect all but the dynamical vertex of the theory, and thus truncate the hierarchy. Later, in our application in section 11.3.1, we will see that this is in fact a valid assumption.

6.8. (Un)avoidable non-Gaussianity of Initial Conditions – Vlasov Limit

Up to now we have kept our discussion completely general without making any assumptions on the explicit form of the initial conditions that define the possibly infinite tower of spurious initial vertices. From a field-theoretic perspective, this structure is difficult to handle, as it leads to infinitely many interaction terms and a rapidly growing number of diagrams at higher orders in the loop expansion. We are thus led to ask, under which conditions this tower of initial vertices can be truncated. To be more specific, these vertices encode the connected n-point correlations of the initial one-particle phase-space density distribution functional $\mathcal{P}[f^{(i)}]$ from which the realizations are drawn (see Section 2.6). In many physical systems, it is reasonable to assume that the cumulants of this distribution become negligible beyond a certain order. Most prominently, a Gaussian distribution is fully characterized by its first two cumulants, the mean $C_{\mathcal{P}}^{(1)}$ and the covariance $G_{\mathcal{P}}^{(2)}$, with all higher-order cumulants vanishing. The Gaussian distribution plays a special role because the central limit theorem suggests that if the initial density

arises as a superposition of many statistically independent physical processes, the resulting distribution is Gaussian. Small deviations from Gaussianity can then be systematically incorporated using an Edgeworth expansion, if necessary. Let us therefore, for the moment, adopt the reasonable assumption that $\mathcal{P}[f^{(i)}]$ is Gaussian, with only $C_{\mathcal{P}}^{(1)}$ and $G_{\mathcal{P}}^{(2)}$ non-vanishing.

In order to understand the implication on the initial vertices, let us recall that those are given by the initial cumulants of the Klimontovich phase-space density Φ_f , see equation (6.35). Even if the *continuous* density $f_1^{(i)}(x)$ is exactly Gaussian, the *discrete* phase-space density $\Phi_f^{(i)}$ has non-zero cumulants at *every order* of the cumulant expansion, due to the trivial particle self-correlation. Thus, $\Phi_f^{(i)}$ is manifestly non-Gaussian. Consider for instance, the three-point cumulant $G_{fff}^{(i)}(X_1, X_2, X_3)$, which at initial time is given by

$$G_{fff}^{(i)}(x_1, x_2, x_3) = \delta_{\mathcal{D}}(x_1 - x_2) \, \delta_{\mathcal{D}}(x_1 - x_3) \, C_{\mathcal{P}}^{(1)}(x_1) + \, \delta_{\mathcal{D}}(x_1 - x_2) \, G_{\mathcal{P}}^{(2)}(x_2, x_3)$$

$$+ \, \delta_{\mathcal{D}}(x_2 - x_3) \, G_{\mathcal{P}}^{(2)}(x_3, x_1) + \, \delta_{\mathcal{D}}(x_3 - x_1) \, G_{\mathcal{P}}^{(2)}(x_1, x_2) \,, (6.126)$$

none of which vanishes. Clearly, $G_{fff}^{(i)}$ cannot even be assumed to be small, as it is of the same order as $C_{\mathcal{P}}^{(1)}$ and $G_{\mathcal{P}}^{(2)}$. Thus, the cumulants of higher order of the initial Klimontovich phase-space density $\Phi_f^{(i)}$ cannot simply be neglected due to the shot-noise or particle-noise contributions. It can furthermore be shown [60], that neglecting those higher order contributions leads to inconsistencies in the cumulant description of the evolution and thus possibly to poor approximations of the system's behavior. This is intuitively clear, as the shot-noise contributions arise due to the discrete particle nature of the system that is necessary to describe collisional processes. To see this, consider the Klimontovich equation (2.78),

$$\left[\partial_{t_1} - \hat{\mathcal{L}}_1^{(0)}\right] \Phi_f(x_1, t_1) = \int d^6 \bar{x}_2 \, \hat{\mathcal{L}}_{1\bar{2}}^{(2)} \, \Phi_f(x_1, t_1) \, \Phi_f(\bar{x}_2, t_1) \,, \tag{6.127}$$

where $\hat{\mathcal{L}}^{(2)}$ is the two-particle interaction operator. By means of the Green function (6.9) it can formally be solved generating an integral equation of the form

$$\Phi_{f}(x_{1}, t_{1}) = \Phi_{f}^{(0)}(x_{1}, t_{1})
+ \int d^{6}\bar{x}_{1} d\bar{t}_{1} d^{6}\bar{x}_{2} D_{0,R}(x_{1}, t_{1}, \bar{x}_{1}, \bar{t}_{1}) \hat{\mathcal{L}}_{\bar{1}\bar{2}}^{(2)} \Phi_{f}(\bar{x}_{1}, \bar{t}_{1}) \Phi_{f}(\bar{x}_{2}, \bar{t}_{1}),$$
(6.128)

where $\Phi_f^{(0)}$ is the free solution. Higher order cumulants, $G_{f...f}$, can now be built by multiplying several copies of this equation and averaging over the initial density. Upon iteration, one then encounters different combinations of averaged products of Φ_f containing the respective Dirac-delta distributions, each of these collapsing one of the interaction integrals by identifying two of the densities. The resulting term will then yield a non-vanishing connected correlation between the external densities in $G_{f...f}$, which exactly reproduces the collision terms that appears in the BBGKY hierarchy. Thus, the Dirac-delta distributions and therefore the shot-

noise contributions are essential to describe particle collisions. If one drops all shot-noise contributions from the initial vertices, and hence neglects all collision terms, the perturbative expansion reduces to the collisionless Vlasov limit: the system then evolves in a smooth mean-field potential generated by the continuous density f_1 (see our discussion in section 2.4.2). Conversely, keeping those shotnoise terms restores the full, microscopic dynamics governed by the Klimontovich equation, in which discreteness and two-body encounters are present. This combined treatment is of course built on the fact that both the microscopic and macroscopic descriptions obey a structurally equivalent dynamical equation. Consequently, our unified formalism simply interpolates between the Vlasov, i.e., mean-field, and Klimontovich, i.e., collisional, descriptions by turning shot-noise on or off in the initial cumulants. In what follows we will refer to the "microscopic picture" as the Klimontovich description, and to the "macroscopic, mean-field picture" as the Vlasov description, where in the latter case only the continuous cumulants of $f_1^{(i)}$ appear in the vertices, making any truncation of the hierarchy much more straightforward. In particular, if the initial density f_1 is Gaussian, no additional initial vertex arises apart from those absorbed into the free action. Last but not least, we mention that the Klimontovich description can be refined even further by only including certain classes of shot-noise terms. In that way, one can reproduce familiar descriptions of kinetic theory as those mentioned in section 2.4.3. A detailed analysis of this has been done in [37].

Formal Development - Full Statistical Equations of Motion

In the last chapter we have constructed a generating functional $\mathcal{Z}[J]$ that enables us to compute general arbitrary time correlation functions of the Klimontovich phase-space density. In section 6.6.3 we have then seen, how corrections to the classical theory in the presence of a mean background can be organized in a loop expansion. The goal of this chapter will be to formalize the functional treatment in a non-perturbative way by working with the full statistical theory without making any a priori truncation. We will then ultimately derive equations of motion for the full statistical correlation functions. We follow [61].

7.1. Generating Functionals for the Full Theory

We begin with a brief and structured recap of the key generating functionals in our statistical field theory. This will prepare for the formal developments in the subsequent sections.

7.1.1. Correlation Functions and Cumulants

Let us first recap the main objects of interest from which the formal development is constructed. The generating functional (6.36) has the form

$$\mathcal{Z}[J] = \int \mathcal{D}\Psi e^{-\mathcal{S}[\Psi] + J_a \Psi_a}, \qquad (7.1)$$

where the action can be expanded around a general non-vanishing background $\overline{\Psi}$,

$$S\left[\Psi\right] = \sum_{n=1}^{\infty} \frac{1}{n!} \overline{S}_{a_1...a_n}^{(n)} \left(\Psi_{a_1} - \overline{\Psi}_{a_1}\right) \dots \left(\Psi_{a_n} - \overline{\Psi}_{a_n}\right) , \qquad (7.2)$$

with the bare vertices defined as the coefficients $\overline{\mathcal{S}}_{a_1...a_n}^{(n)}$. For the following formal treatment it will be necessary to define all objects more generally with non-vanishing external current J. We therefore define correlation functions in the presence of an

external source as

$$C_{a_1...a_n} := \frac{1}{\mathcal{Z}[J]} \frac{\delta^n \mathcal{Z}[J]}{\delta J_{a_1} \dots \delta J_{a_n}}, \tag{7.3}$$

where the $\frac{1}{\mathcal{Z}[J]}$ prefactor ensures the correct normalization of the general J-dependent correlation function¹. The *physical* correlation functions of the phase-space density and response functions are then obtained at vanishing current, i. e.,

$$C_{a_1...a_n} = C_{a_1...a_n} \bigg|_{J=0}$$
 (7.4)

In the following we will refer to the physical objects as to *lie on the equations* of motion for reasons that will become clear in the subsequent discussion. The source J will be used to probe the statistical fluctuations around the "true" physical configuration. In particular, higher order correlation functions can be generated from lower order correlation functions. To see this, let us define the full mean field in the presence of an external source as

$$\overline{\Psi}_a := \langle \Psi_a \rangle^J = \frac{1}{\mathcal{Z}[J]} \frac{\delta \mathcal{Z}[J]}{\delta J_a}, \quad \text{with} \quad \overline{\Psi}_{\text{EoM}} := \overline{\Psi} \Big|_{J=0},$$
 (7.5)

where $\overline{\Psi}_{\text{EoM}}$ refers to the physical, observable mean field² at vanishing current. Note, that $\overline{\Psi}$ is a functional of J. We can now apply a further functional derivative w.r.t. J to find the relation

$$C_{ab} = \left[\frac{\delta}{\delta J_a} + \overline{\Psi}_a \right] \overline{\Psi}_b \,, \tag{7.6}$$

where the mean field inside the square brackets compensates for the normalization factor. This relation can be generalized to

$$C_{a_1...a_n} = \prod_{i=1}^n \left[\frac{\delta}{\delta J_{a_i}} + \overline{\Psi}_{a_i} \right] \cdot 1, \qquad (7.7)$$

where the 1 on the right-hand side has been added to capture the functional field derivatives that do not hit the mean field $\overline{\Psi}$ and therefore vanish. We can apply the above reasoning to expectation values $\langle \mathcal{O}[\Psi] \rangle$ of arbitrary operators $\mathcal{O}[\Psi]$. Provided these operators admit a well-defined series expansion in terms of the fields, we find

$$\langle \mathcal{O}[\Psi] \rangle = \mathcal{O}\left[\Psi_a = \frac{\delta}{\delta J_a} + \overline{\Psi}_a\right] \cdot 1.$$
 (7.8)

Similarly to the discussion in 2.2.2, the above correlation functions are decomposable into connected and disconnected pieces. The disconnected parts are simply products of connected parts of lower degree that do not interact with each other.

¹It can be shown that the normalization $\frac{1}{\mathcal{Z}[J]}$ eliminates so-called *vacuum bubbles* that have not external legs attached to a source J

²The tree-level mean field $\overline{\Psi}_{\rm EoM}^{(0)}$ is thus only the lowest order approximation to the full mean field.

Consequently, the correlation functions carry redundant information and one is typically interested in the study of the connected correlation functions, i.e., the cumulants³. These can be obtained from a generating functional, which is typically referred to as the *Schwinger functional*, defined as

$$W[J] = \ln \left[\mathcal{Z}[J] \right] . \tag{7.9}$$

It can be readily verified that the above definition of the Schwinger functional only produces connected correlators, e.g., for the two-point function we find

$$\langle \Psi_{a_1} \Psi_{a_2} \rangle_c \equiv \frac{\delta^2 \mathcal{W}[J]}{\delta J_{a_1} \delta J_{a_2}} = \mathcal{C}_{a_1 a_2} - \mathcal{C}_{a_1} \mathcal{C}_{a_2}. \tag{7.10}$$

We therefore define

$$\mathcal{G}_{a_1...a_n} := \frac{\delta^n \mathcal{W}[J]}{\delta J_{a_1} \dots \delta J_{a_n}}, \tag{7.11}$$

$$G_{a_1...a_n} := \frac{\delta^n \mathcal{W}[J]}{\delta J_{a_1} \dots \delta J_{a_n}} \bigg|_{J=0}, \tag{7.12}$$

where the first expression refers to the cumulants in the presence of an external current J, while the latter represents the physical cumulant at vanishing source. We will represent the full cumulants by the following diagram,

$$\mathcal{G}_{f\dots fB\dots B}(1,\dots,r,1',\dots,s') \cong \bigcap_{r} \bigcap_{s'} \bigcap_{s'} (7.13)$$

and similarly for the physical cumulants. Note, that we will make no difference between the \mathcal{G} 's and the \mathcal{G} 's on a diagrammatic level. Of particular interest will be the two-point cumulant \mathcal{G}_{ab} , which we call the *full* propagator of the system in the presence of external sources. The full physical propagator has the component decomposition

$$G_{ab} = \begin{pmatrix} G_{ff} & G_{fB} \\ G_{Bf} & 0 \end{pmatrix} \cong \begin{pmatrix} - \bullet & - \bullet \cdots \\ \cdots & 0 \end{pmatrix}, \qquad (7.14)$$

with the components G_{ff} , G_{fB} , and G_{Bf} , to which we refer as the full statistical propagator and the full causal propagators, respectively. Here, G_{fB} represents the retarded propagator and G_{Bf} the advanced one. Clearly, by (6.42) the physical component $G_{BB} = 0$. Note, that the propagator \mathcal{G}_{ab} can be generated from the mean field $\overline{\Psi}$, since

$$\mathcal{G}_{ab} = \frac{\delta^2 \mathcal{W}[J]}{\delta J_a \delta J_b} = \frac{\delta \overline{\Psi}_b}{\delta J_a}.$$
 (7.15)

³In older literature the cumulants are often referred to as the *Ursell functions*, in honor to Harold Ursell, who introduced them first in 1927 [62].

7.1.2. The One-Particle Irreducible Effective Action

Importantly, the Schwinger functional still contains redundant information. Consider for instance the following two diagrams that contribute to the two-loop correction of the statistical propagator, in 6.6.3

$$-\cdots$$
, and $-\cdots$ (7.16)

The diagram on the left consists of two one-loop subdiagrams connected by a tree-level propagator. Since both subdiagrams have already been considered at one-loop level, this composite diagram does not introduce any new information. In contrast, the diagram on the right cannot be decomposed into known one-loop subdiagrams, therefore it represents a genuinely new two-loop structure. This brings us to the concept of one-particle irreducibility. A diagram is called one-particle irreducible (1PI) if it cannot be separated into two disconnected pieces and one-particle reducible (1PR) if it can. Thus, in (7.16) the diagram on the left is 1PR while the diagram on the right side is 1PI. It will therefore be sensible to include this distinction in the following considerations. The generating functional for 1PI correlation functions is denoted by Γ and is referred to as the (statistical) effective action⁴. It is a functional of the mean field with external currents ψ and defined as the Legendre-Fenchel transformation⁵ of the Schwinger functional w.r.t. the currents J_a ,

$$\Gamma[\overline{\Psi}] := \sup_{J} \left\{ \int_{X} J_{\alpha}(X) \overline{\Psi}_{\alpha}(X) - \mathcal{W}[J] \right\} = \int_{X} J_{\alpha}^{\overline{\Psi}}(X) \overline{\Psi}_{\alpha}(X) - \mathcal{W}[J^{\overline{\Psi}}]. \tag{7.17}$$

Here $J_a^{\overline{\Psi}}$ is a $\overline{\Psi}$ -dependent current defined by the above supremum requirement. If the Schwinger functional is a convex, differentiable functional, the supremum is attained and given by the maximum of the right-hand side of (7.17) which is found by demanding

$$0 \stackrel{!}{=} \frac{\delta}{\delta J_{\alpha}(X)} \left\{ \int_{Y} J_{\beta}(Y) \overline{\Psi}_{\beta}(Y) - \mathcal{W}[J] \right\} \bigg|_{J = J^{\overline{\Psi}}} = \overline{\Psi}_{\alpha}(X) - \frac{\delta \mathcal{W}[J]}{\delta J_{\alpha}(X)} \bigg|_{J = J^{\overline{\Psi}}}. \quad (7.18)$$

The maximizing current $J^{\overline{\Psi}}$ is then found by solving

$$\overline{\Psi}_{\alpha}(X) = \frac{\delta \mathcal{W}}{\delta J_{\alpha}(X)} \bigg|_{J_{\alpha} = J_{\alpha}^{\overline{\Psi}}}$$
(7.19)

for J in terms of $\overline{\Psi}$. Henceforth, we will simply write J_a instead of $J_a^{\overline{\Psi}}$, with the understanding that it is always the current which solves (7.19). The above equation shows that Γ is indeed a functional of the mean background $\overline{\Psi}$ with external current. This stands in contrast to the functionals $\mathcal{Z}[J]$ and $\mathcal{W}[J]$ which are functionals of

 $^{^4}$ In literature Γ is often called the quantum effective action.

⁵When W is differentiable and strictly convex, the supremum in (7.17) is attained and reduces to the usual (smooth) Legendre transform.

the source itself. This will turn out to be a major advantage for our treatment. In order to switch the description from J to $\overline{\Psi}$, we will have to express the functional derivatives w.r.t. J as those w.r.t. $\overline{\Psi}$. This can be done using the chain rule,

$$\frac{\delta}{\delta J_a} = \frac{\delta \overline{\Psi}_b}{\delta J_a} \frac{\delta}{\delta \overline{\Psi}_b} = \mathcal{G}_{ab} \frac{\delta}{\delta \overline{\Psi}_b}$$
 (7.20)

where we used (7.15) in order to insert the source-dependent propagator \mathcal{G} .

To understand the physical significance of Γ , we start by taking a functional derivative of (7.17) w.r.t. $\overline{\Psi}_a$ and find

$$\frac{\delta\Gamma[\overline{\Psi}]}{\delta\overline{\Psi}_{\alpha}(X)} = J_{\alpha}(X), \qquad (7.21)$$

which yields an equation of motion for the source dependent mean field $\overline{\Psi}$. It is therefore referred to as the statistical equation of motion in the presence of an external current. This equation will enable us to derive relations between the cumulants and the 1PI correlation functions. In contrast, the physical or observable mean field, $\overline{\Psi}_{\rm EoM}$ is defined as the configuration at which the external source vanishes, i. e., J=0. Thus, evaluating (7.21) at $\overline{\Psi}_a = \overline{\Psi}_{{\rm EoM},a}$, we obtain

$$\frac{\delta\Gamma[\overline{\Psi}]}{\delta\overline{\Psi}_{\alpha}(X)}\bigg|_{\overline{\Psi}=\overline{\Psi}_{\text{EoM}}} = 0, \qquad (7.22)$$

which is the statistical equation of motion for the physical mean field $\overline{\Psi}_{EoM}$. Accordingly, the exact physical field configurations are given by stationary points of the functional $\Gamma[\overline{\Psi}]$, showing that Γ indeed generalizes the classical action \mathcal{S} to the full statistical theory. The current independent equations of motion (7.22) generalize the tree-level or classical equations of motion (6.85). All objects that are derived from Γ contain the full statistical information. For instance, the coefficients of the series expansion of \mathcal{S} in (7.2), which define the bare vertices of the classical theory generalize to

$$\Gamma_{a_1...a_n}^{(n)} := \frac{\delta^n \Gamma[\overline{\Psi}]}{\delta \overline{\Psi}_{a_1} \dots \delta \overline{\Psi}_{a_n}}, \qquad (7.23)$$

$$\overline{\Gamma}_{a_1...a_n}^{(n)} := \frac{\delta^n \Gamma[\overline{\Psi}]}{\delta \overline{\Psi}_{a_1} \dots \delta \overline{\Psi}_{a_n}} \bigg|_{\overline{\Psi} = \overline{\Psi}_{\text{FoM}}}, \tag{7.24}$$

which define the full vertex functions and contain all statistical corrections to the bare vertices involving n fields. In the presence of a non-trivial mean field, the physical vertex functions (7.24) functionally depend on $\overline{\Psi}_{\rm EoM}$ similarly to the $\overline{\Psi}_{\rm EoM}^{(0)}$ dependence of the tree-level vertices in the background field approximation 6.6. It can be shown, that only 1PI processes contribute to $\Gamma_{a_1...a_n}^{(n)}$ and $\overline{\Gamma}_{a_1...a_n}^{(n)}$. Similarly to

the cumulants, we will represent the full vertices by the following Feynman diagram,

$$\Gamma_{f...fB...B}^{(r+s)}(1,\ldots,r,1',\ldots,s') \cong \prod_{r=s}^{1} \prod_{s'}^{1'} .$$
 (7.25)

The coefficients can be used to define the *vertex expansion* of Γ around the physical saddle point at $\overline{\Psi}_{EoM}$ in analogy to the expansion of the bare action in (7.2),

$$\Gamma[\overline{\Psi}] = \sum_{n=0}^{\infty} \frac{1}{n!} \overline{\Gamma}_{a_1...a_n}^{(n)} \left(\overline{\Psi}_{a_1} - \overline{\Psi}_{\text{EoM},a_1} \right) ... \left(\overline{\Psi}_{a_n} - \overline{\Psi}_{\text{EoM},a_n} \right) .$$
 (7.26)

In particular, the physical equations of motion (7.22) imply,

$$\overline{\Gamma}_{\alpha}^{(1)}(X) = 0. \tag{7.27}$$

While the above discussion has been kept completely general, we can already deduce an important property of the physical vertices $\overline{\Gamma}^{(n)}$: The normalization of the generating functional (6.25) implies $\mathcal{W}[J_f=0,J_B]=0$ independent of the value of J_B . Since the physical, source free mean field satisfies

$$\overline{\Psi}_{\text{EoM},f} \neq 0, \qquad \overline{\Psi}_{\text{EoM},B} = 0,$$
 (7.28)

the definition of the effective action as the Legendre transform (7.17) immediately gives

$$\Gamma[\overline{\Psi}_{\rm EoM}] \equiv 0, \qquad (7.29)$$

and hence all its physical vertex functions involving only phase-space densities vanish,

$$\overline{\Gamma}_{f-f}^{(n)}(1,\dots,n) \equiv 0. \tag{7.30}$$

In other words, statistical fluctuations do not generate any effective physical vertices composed solely of phase-space density fields. The structure of the classical action S, in which every vertex necessarily includes at least one response field, is therefore inherited by the full statistical theory. This ensures that the causality built into the classical description is preserved. As we will see, this constraint imposes important restrictions on the class of diagrams that can contribute in the full theory. For instance, the physical two-point vertex function has the components

$$\overline{\Gamma}_{ab}^{(2)} = \begin{pmatrix} 0 & \overline{\Gamma}_{fB}^{(2)} \\ \overline{\Gamma}_{Bf}^{(2)} & \overline{\Gamma}_{BB}^{(2)} \end{pmatrix} \cong \begin{pmatrix} 0 & -\bullet \cdot \\ \cdot \cdot \bullet - \cdot \cdot \bullet \cdot \end{pmatrix} . \tag{7.31}$$

Another important property can be deduced from the fact that Γ and W are related by a Legendre transform. Taking a functional derivative of (7.21) w.r.t. J,

we find

$$\frac{\delta}{\delta J_a} \frac{\delta \Gamma[\overline{\Psi}]}{\delta \overline{\Psi}_b} = \mathcal{G}_{ac} \frac{\delta^2 \Gamma[\overline{\Psi}]}{\delta \overline{\Psi}_c \delta \overline{\Psi}_b} = \mathcal{G}_{ac} \Gamma_{cb}^{(2)} = \delta_{ab} , \qquad (7.32)$$

where the chain rule (7.20) has been used. We thus found the important relation

$$\mathcal{G}_{ab} = \left[\frac{1}{\Gamma^{(2)}}\right]_{ab},\tag{7.33}$$

i. e., the 1PI two-point vertex function is the inverse of the full propagator of the theory in the presence of an external current. Evaluated at the physical field configuration, J=0 and $\overline{\Psi}=\overline{\Psi}_{\rm EoM}$ we find analogously

$$G_{ab} = \left[\frac{1}{\overline{\Gamma}^{(2)}}\right]_{ab}.\tag{7.34}$$

This relation now implies a set of equations for the components of G_{ab} and $\overline{\Gamma}_{ab}^{(2)}$. We find

$$\overline{\Gamma}_{Bf}^{(2)}(1,\bar{1}) G_{fB}(\bar{1},2) = \mathbb{1}(1,2) ,$$

$$\overline{\Gamma}_{fB}^{(2)}(1,\bar{1}) G_{Bf}(\bar{1},2) = \mathbb{1}(1,2) ,$$

$$\overline{\Gamma}_{Bf}^{(2)}(1,\bar{1}) G_{fB}(\bar{1},2) = -\overline{\Gamma}_{BB}^{(2)}(1,\bar{2}) G_{Bf}(\bar{2},2) ,$$
(7.35)

or, on a diagrammatic level

between the physical propagators and vertices, which generalize the corresponding relations of the bare and tree-level theory to the full theory. Again, the equation for the full physical statistical propagator can be solved and yields

$$G_{ff}(1,2) = -G_{fB}(1,\bar{1}) \, \overline{\Gamma}_{BB}^{(2)}(\bar{1},\bar{2}) \, G_{Bf}(\bar{2},2) \,, \tag{7.37}$$

or, diagrammatically

Grounded on these equations, we can now derive similar relations for higher n-point vertex functions. For instance, taking a further functional derivative of (7.33) w.r.t. J, yields

$$\mathcal{G}_{a_1 a_2 a_3} = -\mathcal{G}_{a_1 b_1} \mathcal{G}_{a_2 b_2} \Gamma_{b_1 b_2 b_3}^{(3)} \mathcal{G}_{b_3 a_3}. \tag{7.39}$$

The three-point cumulant thus corresponds to full propagators attached to all truncated irreducible three-point processes represented by the three-point vertex function $\Gamma^{(3)}$. Similarly, one can construct higher order cumulants in terms of vertex functions and lower order cumulants. On the basis of the above discussion, we will construct an exact systematic treatment in section 7.3 by deriving equations of motion for each vertex function.

7.2. One-Loop Effective Action

Let us now study the relationship between the full statistical effective action Γ and the classical action \mathcal{S} , by computing a first approximation to Γ . By its definition, we can rewrite Γ as

$$\Gamma[\overline{\Psi}] = J_a \,\overline{\Psi}_a - \ln\left[\int \mathcal{D}\Psi \,\mathrm{e}^{-\mathcal{S}[\Psi] + J_a \,\Psi_a}\right] \,. \tag{7.40}$$

We can now perform a shift inside the functional integration, $\Psi = \overline{\Psi} + \Psi^{\delta}$ and expand the action around the *true* mean-field $\overline{\Psi}$ in the presence of an external source,

$$\mathcal{S}[\overline{\Psi} + \Psi^{\delta}] = \mathcal{S}[\overline{\Psi}] + \mathcal{S}_{a}^{(1)}[\overline{\Psi}] \Psi_{a}^{\delta} + \frac{1}{2} \mathcal{S}_{ab}^{(2)}[\overline{\Psi}] \Psi_{a}^{\delta} \Psi_{b}^{\delta} + \mathcal{O}\left(\left(\Psi^{\delta}\right)^{3}\right). \tag{7.41}$$

Inserted into (7.40), we find

$$\Gamma[\overline{\Psi}] = \mathcal{S}[\overline{\Psi}] - \ln \left[\int \mathcal{D}\Psi \, e^{-\left[\mathcal{S}_a^{(1)} - \Gamma_a^{(1)}\right]\Psi_a^{\delta} - \frac{1}{2}\,\mathcal{S}_{ab}^{(2)}\Psi_a^{\delta}\Psi_b^{\delta} + \mathcal{O}\left(\left(\Psi^{\delta}\right)^3\right)} \right]$$
(7.42)

$$= \mathcal{S}[\overline{\Psi}] + \mathcal{K}[\overline{\Psi}]. \tag{7.43}$$

Thus, Γ corresponds to lowest-order to the classical action. The solution to the effective equations of motion (7.22) in this approximation clearly matches the tree-level equations of motion discussed in (6.85). In order to find the first non-trivial correction to Γ , we need to solve a functional integro-differential equation for the correction \mathcal{K} ,

$$\mathcal{K}[\overline{\Psi}] = -\ln\left[\int \mathcal{D}\Psi \,e^{-\frac{\delta\mathcal{K}}{\delta\overline{\Psi}_a}\Psi_a^{\delta} - \frac{1}{2}\,\mathcal{S}_{ab}^{(2)}\Psi_a^{\delta}\Psi_b^{\delta} + \mathcal{O}\left(\left(\Psi^{\delta}\right)^3\right)}\right] \,. \tag{7.44}$$

This equation has in principle to be solved perturbatively, as \mathcal{K} appears on both sides. However, since \mathcal{K} is already of one-loop order at least, we can neglect its contribution to the path integral on the right-hand side. Neglecting all higher orders in the fluctuation as well, yields a pure Gaussian functional integral that can be solved directly,

$$\mathcal{K}[\overline{\Psi}] = -\ln\left[\det\left(\mathcal{S}^{(2)}\right)^{-\frac{1}{2}}\right] = \frac{1}{2}\ln\left[\det\left(\mathcal{S}^{(2)}\right)\right] = \frac{1}{2}\mathrm{Tr}\left[\ln\left(\mathcal{S}^{(2)}\right)\right], \quad (7.45)$$

and thus the well-known expression for the one-loop effective action,

$$\Gamma[\overline{\Psi}] = \mathcal{S}[\overline{\Psi}] + \frac{1}{2} \text{Tr} \left[\ln \left(\mathcal{S}^{(2)} \right) \right].$$
 (7.46)

In the above equation, the trace runs over all degrees of freedom in $\mathcal{S}^{(2)}$. Importantly, $\mathcal{S}^{(2)}$ functionally depends on the general mean field $\overline{\Psi}$. We can now compute corrections to the bare vertices by taking functional derivatives of the above expression and evaluating on the equation of motion. We find

$$\Gamma_a^{(1)}[\overline{\Psi}] = \mathcal{S}_a^{(1)}[\overline{\Psi}] + \frac{1}{2} \operatorname{Tr} \left[\mathcal{S}_a^{(3)} \cdot \left[\mathcal{S}^{(2)} \right]^{-1} \right], \tag{7.47}$$

$$\Gamma_{ab}^{(2)}[\overline{\Psi}] = \mathcal{S}_{ab}^{(2)}[\overline{\Psi}] - \frac{1}{2} \text{Tr} \left[\mathcal{S}_a^{(3)} \cdot \left[\mathcal{S}^{(2)} \right]^{-1} \cdot \mathcal{S}_b^{(3)} \cdot \left[\mathcal{S}^{(2)} \right]^{-1} \right] . \tag{7.48}$$

These equations contain all one-loop processes that contribute to the given vertices. A discussion of how these equations can be solved for a specific system at hand will be given in the next chapter. For the remaining of the present chapter, we will generalize the above logic to find exact equations of motion for the full effective vertices.

7.3. The Master Dyson-Schwinger Equation

Similar to the BBGKY hierarchy, which couples the s-particle reduced correlation functions to an infinite⁶ tower of coupled equations, (see section 2.3), a hierarchy between the full correlation functions and cumulants can be established. This hierarchy roots in the functional identity

$$0 = \int \mathcal{D}\Psi \frac{\delta}{\delta \Psi_b} \exp \left[-\mathcal{S}[\Psi] + \int_X J_a \Psi_a \right], \qquad (7.49)$$

i. e., the vanishing of the functional integral over a total functional derivative. It can be seen as a general symmetry identity related to the translational invariance of the functional measure $\mathcal{D}\Psi$, i. e., the invariance under a shift in field space⁷ $\Psi_a \to \Psi_a + \phi_a$. Applying the above functional derivative on the exponential, we find the relation

$$0 = \left\langle \frac{\delta \mathcal{S}[\Psi]}{\delta \Psi_b} - J_b \right\rangle, \tag{7.50}$$

which enforces the classical equations of motion in the presence of an external current to hold on average. Following the functional treatment for the computation of expectation values (7.8), this equation can be written entirely in terms of functional derivatives,

$$J_a = \frac{\delta S}{\delta \Psi_a} \left[\Psi_b = \frac{\delta}{\delta J_b} + \overline{\Psi}_b \right] \cdot 1.$$
 (7.51)

⁶The tower is infinite in the thermodynamic limit.

⁷This symmetry requires the measure to be flat, meaning that under the given shift the functional Jacobian is trivial. This property may fail in cases where the measure is non-flat, for instance when the field space has a nontrivial metric.

Inserting (7.21) on the left-hand side and the chain rule (7.20) on the right-hand side, we find the corresponding equation in the Legendre transformed picture,

$$\frac{\delta\Gamma[\overline{\Psi}]}{\delta\overline{\Psi}_{\beta}(X)} = \frac{\delta\mathcal{S}}{\delta\Psi_{\beta}(X)} \left[\Psi_{\alpha}(Y) = \int_{Z} \mathcal{G}_{\alpha\gamma}(Y, Z) \frac{\delta}{\delta\overline{\Psi}_{\gamma}(Z)} + \overline{\Psi}_{\alpha}(Y) \right] \cdot 1, \quad (7.52)$$

which we will refer to as the (statistical) master Dyson-Schwinger equation [63, 64] for the 1PI vertex functions. Applying functional derivatives w.r.t. $\overline{\Psi}_{\alpha}$, we can derive a coupled tower of equations for the effective vertices $\Gamma^{(n)}$, which in turn by the correspondence (7.33) and (7.39) can be used to derive equations for the full cumulants themselves. The resulting equations of motion for the full physical cumulants are then obtained by evaluating the respective Dyson-Schwinger equation on the equations of motion. As the Dyson-Schwinger equations represent an infinite tower of coupled equations, exact solutions are almost never possible. Therefore, one has to rely on approximation procedures. We will discuss these in the next chapter. However, it is instructive to study the general structure of the Dyson-Schwinger equations in more detail for our particular theory at hand.

7.4. Dyson-Schwinger Equations for Cumulants of the Klimontovich Equation

Let us now explicitly compute the right-hand side of (7.52). It will be convenient to separate the initial vertices from the dynamical vertices in order to easily distinguish between the Klimontovich description and the special case of a Gaussian Vlasov description. Let us therefore expand the action as in (6.41),

$$S[\Psi] = S_{\mathcal{D},a}^{(1)} \Psi_a + \frac{1}{2!} S_{\mathcal{D},ab}^{(2)} \Psi_a \Psi_b + \frac{1}{3!} S_{\mathcal{D},abc}^{(3)} \Psi_a \Psi_b \Psi_c + S_{\mathcal{I}}[\Psi], \qquad (7.53)$$

where again $\mathcal{S}_{\mathcal{I}}[\Psi]$ contains all three-point and higher initial cumulants. In the case of an initially Gaussian Vlasov fluid, this term vanishes. Taking a functional derivative w.r.t. Ψ_a gives

$$S_a^{(1)}[\Psi] = S_{\mathcal{D},a}^{(1)} + S_{\mathcal{D},ab}^{(2)} \Psi_b + \frac{1}{2!} S_{\mathcal{D},abc}^{(3)} \Psi_b \Psi_c + S_{\mathcal{I},a}^{(1)}[\Psi]. \tag{7.54}$$

Under the averaging process on the left-hand side of (7.52), the product $\Psi_a\Psi_b$ becomes

$$\Psi_a \Psi_b \Big|_{\Psi = \mathcal{G} \cdot \frac{\delta}{\delta \overline{\Psi}} + \overline{\Psi}} = \overline{\Psi}_a \, \overline{\Psi}_b + \, \mathcal{G}_{ab} \,, \tag{7.55}$$

and similarly for all higher order monomials in $\mathcal{S}_{\mathcal{I}}[\Psi]$. The master Dyson-Schwinger equation can thus be written as

$$\Gamma_a^{(1)}[\overline{\Psi}] = \mathcal{S}_{\mathcal{D},a}^{(1)} + \mathcal{S}_{\mathcal{D},ab}^{(2)} \overline{\Psi}_b + \frac{1}{2!} \mathcal{S}_{\mathcal{D},abc}^{(3)} \left(\overline{\Psi}_b \overline{\Psi}_c + \mathcal{G}_{bc} \right) + \left\langle \mathcal{S}_{\mathcal{I},a}^{(1)}[\Psi] \right\rangle$$
 (7.56)

or, using the more compact matrix notation,

$$\Gamma_a^{(1)}[\overline{\Psi}] = \mathcal{S}_{\mathcal{D},a}^{(1)}[\overline{\Psi}] + \frac{1}{2!} \operatorname{Tr} \left[\mathcal{S}_{\mathcal{D},a}^{(3)} \cdot \mathcal{G} \right] + \left\langle \mathcal{S}_{\mathcal{I},a}^{(1)}[\Psi] \right\rangle. \tag{7.57}$$

This equation is the starting point of the Dyson-Schwinger hierarchy. The first term on the right-hand side contains the purely classical evolution of the mean field, as discussed in 6.6. The second term represents loop corrections thereof that arise from the trace and the full propagator \mathcal{G} . It represents a back reaction of the statistical fluctuation onto the evolution of the mean itself. The third term represents all higher order statistical fluctuations that arise from the higher order vertices due to the initial conditions. It generalizes the second term to more complicated loop topologies. Since it only contains $\overline{\Psi}_B$ couplings, it vanishes when evaluated on the equations of motion. However, it generates non-trivial contributions upon taking functional derivatives. For instance, we consider the next order Dyson-Schwinger equation for the two-point vertex function that arises by taking a functional derivative w.r.t. Ψ_b ,

$$\Gamma_{ab}^{(2)}[\overline{\Psi}] = \mathcal{S}_{\mathcal{D},ab}^{(2)}[\overline{\Psi}] - \frac{1}{2!} \text{Tr} \left[\mathcal{S}_{\mathcal{D},a}^{(3)} \cdot \mathcal{G} \cdot \Gamma_b^{(3)} \cdot \mathcal{G} \right] + \Gamma_b^{(2)} \cdot \left\langle \Psi \mathcal{S}_{\mathcal{I},a}^{(1)}[\Psi] \right\rangle. \tag{7.58}$$

This equation equivalently establishes a relation between the full inverse propagator on the left-hand side with the inverse tree-level propagator on the right-hand side, together with the loop correction that involves a full three-point vertex function. The latter therefore requires the knowledge of the Dyson-Schwinger equation for $\Gamma^{(3)}$. The last term describing the influence of the initial cumulants now contains an additional field insertion in the expectation value, which is due to the functional derivative w.r.t. the mean field⁸. Importantly, the Ψ_f component of the inserted field now yields a non-vanishing expectation value, when evaluated on the equations of motion, as we will discuss momentarily. The Dyson-Schwinger equation for the three-point vertex function now arises similarly upon taking a further functional derivative w.r.t. $\overline{\Psi}_c$,

$$\Gamma_{abc}^{(3)}[\overline{\Psi}] = \mathcal{S}_{\mathcal{D},abc}^{(3)}[\overline{\Psi}] + \frac{1}{2!} \operatorname{Tr} \left[\mathcal{S}_{\mathcal{D},a}^{(3)} \cdot \mathcal{G} \cdot \Gamma_b^{(3)} \cdot \mathcal{G} \cdot \Gamma_c^{(3)} \cdot \mathcal{G} \right]
+ \frac{1}{2!} \operatorname{Tr} \left[\mathcal{S}_{\mathcal{D},a}^{(3)} \cdot \mathcal{G} \cdot \Gamma_c^{(3)} \cdot \mathcal{G} \cdot \Gamma_b^{(3)} \cdot \mathcal{G} \right] - \frac{1}{2!} \operatorname{Tr} \left[\mathcal{S}_{\mathcal{D},a}^{(3)} \cdot \mathcal{G} \cdot \Gamma_{bc}^{(4)} \cdot \mathcal{G} \right]
+ \Gamma_{bc}^{(3)} \cdot \left\langle \Psi \mathcal{S}_{\mathcal{I},a}^{(1)}[\Psi] \right\rangle + \Gamma_b^{(2)} \cdot \left\langle \Psi \mathcal{S}_{\mathcal{I},a}^{(1)}[\Psi] \Psi \right\rangle \cdot \Gamma_c^{(2)} .$$
(7.59)

As expected, this equation now introduces the effective four-point vertex function. This infinite hierarchy now extends to all higher vertex-functions. In particular, for Gaussian initial conditions, the n-th order vertex function $\Gamma^{(n)}$ couples to the (n+1)-order vertex function $\Gamma^{(n+1)}$. The initial vertices introduce even higher vertex

$$\frac{\delta}{\delta \overline{\Psi}_a} \left\langle \mathcal{O}(\Psi) \right\rangle = \Gamma_{ab}^{(2)} \frac{\delta}{\delta J_b} \left\langle \mathcal{O}(\Psi) \right\rangle = \Gamma_{ab}^{(2)} \left\langle \Psi_b \, \mathcal{O}(\Psi) \right\rangle \,.$$

⁸More precisely, using the inverse chain rule (7.20), one finds

functions.

Finally, let us explicitly state the equations of motion for the key physical quantities, the physical mean phase-space density $\overline{\Psi}_{\text{EoM},f}$, the physical causal propagator G_{fB} and the physical statistical propagator G_{ff} , corresponding respectively to the system's linear response function, and its two-point density fluctuation function. The physical mean field $\overline{\Psi}_{\text{EoM}}$ is obtained by evaluating (7.57) on the equations of motion. Clearly, the f-component of $\Gamma_a^{(1)}$ vanishes identically on both sides. By the statistical equations of motion (7.22) we are thus left with

$$0 = \overline{\Gamma}_B^{(1)}(1) = \overline{\mathcal{S}}_{\mathcal{D},B}^{(1)}(1) + \frac{1}{2!} \, \overline{\mathcal{S}}_{\mathcal{D},Bff}^{(3)}(1,2,3) \, G_{ff}(2,3) \,, \tag{7.60}$$

since $\mathcal{S}_{\mathcal{D},Bff}^{(3)}$ is the only three-point coupling in the action $\mathcal{S}_{\mathcal{D}}$ and the $\mathcal{S}_{\mathcal{I}}$ -term drops out because it only contains $\overline{\Psi}_B$ -field correlators whose physical expectation values vanish identically by (6.42). Inserting the expression for the action $\mathcal{S}_{\mathcal{D}}$, one finds

$$0 = \cdots \bullet = \cdots \bullet + \cdots \bullet + \frac{1}{2!} \cdots \bullet + \frac{1}{2!} \cdots \bullet . \tag{7.61}$$

This generalizes the tree-level equation (6.87) or its diagrammatic form (6.114) for the mean background to the full statistical theory. As we can see, its solution is not independently solvable anymore, but requires knowledge of the full statistical propagator, to which we turn in the following. Consider next the Dyson-Schwinger equation for the mixed, two-point vertex function $\overline{\Gamma}_{Bf}^{(2)}$, which can be obtained from the Bf-component of (7.58) evaluated on the equations of motion,

$$\overline{\Gamma}_{Bf}^{(2)}(1,2) = \overline{\mathcal{S}}_{\mathcal{D},Bf}^{(2)}(1,2) - \left[\overline{\mathcal{S}}_{\mathcal{D},Bff}^{(3)}(1,\bar{1},\bar{2})G_{ff}(\bar{1},\bar{3})G_{fB}(\bar{2},\bar{4})\overline{\Gamma}_{fBf}^{(3)}(\bar{3},\bar{4},2) \right] - \frac{1}{2!} \left[\overline{\mathcal{S}}_{\mathcal{D},Bff}^{(3)}(1,\bar{1},\bar{2})G_{fB}(\bar{1},\bar{3})G_{fB}(\bar{2},\bar{4})\overline{\Gamma}_{BBf}^{(3)}(\bar{3},\bar{4},2) \right] .$$
(7.62)

Diagrammatically, this equation can be visualized to

$$\cdots \bullet - = \cdots \bullet - \frac{1}{2!} \cdots \bullet - \frac{1}{$$

The first diagram represents the bare two-point vertex. As we have seen in section 6.6 evaluated on a non-trivial mean background, $\overline{\mathcal{S}}_{\mathcal{D},Bf}^{(2)}(1,2)$ contains the inverse free propagator and a contribution from the *full* mean field coupling to the three-point vertex, i.e.,

$$\cdots \bullet = \cdots \bullet - \cdots , \qquad (7.64)$$

which generalizes Equation (6.112). Accordingly, we separate the two terms, each

contributing differently to the full inverse causal propagator, and find

$$\cdots \bullet - = \cdots \bullet - \cdots \bullet - \frac{1}{2!} \cdots \bullet - \frac{1}{2!} \cdots \bullet (7.65)$$

The difference between the full inverse causal propagator $\overline{\Gamma}_{Bf}^{(2)}$ and the inverse free propagator $\overline{\mathcal{S}}_{\mathcal{D},Bf}^{(2)}[0]$ defines the so-called *causal self-energy* Σ_{Bf} , which is given by

$$\Sigma_{Bf} \cong \cdots + \frac{1}{2!} \cdots (7.66)$$

As one can see, the causal self-energy splits into two parts. The first, containing the first diagram on the right-hand side, arises from the full mean field and is local in time due to the time-local nature of the three-point interaction vertex. The second, containing the remaining two diagrams, represents a non-local, non-linear correction to the full causal propagator, such that the total causal self energy decomposes as

$$\Sigma_{Bf} = \Sigma_{Bf}^H + \Sigma_{Bf}^F, \tag{7.67}$$

where we defined the *Hartree self-energy* as

$$\Sigma_{Bf}^{H} \cong \dots \tag{7.68}$$

and the Fock self-energy as

$$\Sigma_{Bf}^F \cong \cdots \longrightarrow + \frac{1}{2!} \cdots \longrightarrow \cdots$$
 (7.69)

The nomenclature is based on the respective contributions in quantum field theory. We will discuss their physical meaning at the end of this section and in the next chapter. As one can see, the causal self-energy Σ_{Bf} depends on the full propagators themselves and additionally the higher order three-point vertices $\overline{\Gamma}_{fBf}^{(3)}$ and $\overline{\Gamma}_{BBf}^{(3)}$. While the former has a classical counterpart in $\mathcal{S}_{fBf}^{(3)}$, the latter is not present in the bare theory. It is effectively generated and of pure statistical nature, i.e., at least of one-loop order. The explicit equations of motion for the exact linear response function of the system can be obtained upon multiplication from the right with G_{fB} and using the appropriate relation from (7.36). We find

$$\left(\Delta_{0,Bf}^{-1} - \Sigma_{Bf}\right)(1,\bar{1}) G_{fB}(\bar{1},2) = \mathbb{1}(1,2), \qquad (7.70)$$

where $\Delta_{0,Bf}^{-1}$ is the inverse free propagator. The formal solution of (7.70) arises upon multiplication with $\Delta_{0,fB}$ from the left, and yields the Dyson-Schwinger equation for the causal G_{fB} propagator,

$$G_{fB} = \Delta_{0,fB} + \Delta_{0,fB} \cdot \Sigma_{Bf} \cdot G_{fB} \tag{7.71}$$

or diagrammatically,

A similar reasoning can be applied for the advanced propagator G_{Bf} , such that the relation $G_{fB}(1,2) = G_{Bf}(2,1)$ holds. Last, but not least, the statistical propagator G_{ff} obeys a similar equation. The BB-component of (7.58) is given by

$$\overline{\Gamma}_{BB}^{(2)}(1,2) = \overline{S}_{\mathcal{D},BB}^{(2)}(1,2) - \frac{1}{2!} \left[\overline{S}_{\mathcal{D},Bff}^{(3)}(1,\bar{1},\bar{2}) G_{ff}(\bar{1},\bar{3}) G_{ff}(\bar{2},\bar{4}) \overline{\Gamma}_{ffB}^{(3)}(\bar{3},\bar{4},2) \right]
- \left[\overline{S}_{\mathcal{D},Bff}^{(3)}(1,\bar{1},\bar{2}) G_{fB}(\bar{1},\bar{3}) G_{ff}(\bar{2},\bar{4}) \overline{\Gamma}_{BfB}^{(3)}(\bar{3},\bar{4},2) \right]
- \frac{1}{2!} \left[\overline{S}_{\mathcal{D},Bff}^{(3)}(1,\bar{1},\bar{2}) G_{fB}(\bar{1},\bar{3}) G_{fB}(\bar{2},\bar{4}) \overline{\Gamma}_{BBB}^{(3)}(\bar{3},\bar{4},2) \right] (7.73)
- \sum_{n'=2}^{\infty} \frac{1}{n'!} S_{\mathcal{I}}^{(n'+1)}(1,1',\ldots,n') G_{B\ldots Bf}(1',\ldots,n',\bar{1}) \overline{\Gamma}_{fB}^{(2)}(\bar{1},2) .$$

Importantly, only in the BB-component do the terms arising from the initial conditions in $\mathcal{S}_{\mathcal{I}}$ contribute. Diagrammatically, we can represent this equation as

As we can see, the loop diagrams correct the initial two-point fluctuations represented by the first diagram on the right-hand side. We therefore define the *statistical self-energy* Σ_{BB} as

$$\Sigma_{BB} \cong \frac{1}{2!} \cdots + \cdots + \frac{1}{2!} \cdots + \cdots + \frac{1}{2!} \cdots$$

$$+ \sum_{n=2}^{\infty} \frac{1}{n!} \cdots \cdot \vdots n \cdot \cdots$$

$$(7.75)$$

The solution for the full propagator is then given by the relation (7.37), i.e., by connecting the statistical self-energy with two causal propagators from the left and from the right. In order to give a physical interpretation, it is useful to further decompose the statistical self-energy into two contributions, which we call Σ_{BB} and $\Sigma_{BB}^{(p)}$, defined as

$$\widetilde{\Sigma}_{BB} \cong \frac{1}{2!} \cdots + \cdots + \frac{1}{2!} \cdots$$
 (7.76)

and

$$\Sigma_{BB}^{(p)} \cong \sum_{n=2}^{\infty} \frac{1}{n!} \cdots \underbrace{: n \overset{\bullet}{\bullet} \bullet \cdots}_{(7.77)}$$

such that

$$\Sigma_{BB} = \widetilde{\Sigma}_{BB} + \Sigma_{BB}^{(p)}. \tag{7.78}$$

In summary, we have decomposed our system into the causal and statistical selfenergies Σ_{Bf} and Σ_{BB} (c.f. for similar treatments [21, 60, 65]). The former represents a renormalization of the time-evolution operator, i. e., the Klimontovich operator itself. Importantly, it inherits the causal structure, such that $\Sigma_{Bf}(1,2) \propto \Theta(t_1-t_2)$. It is responsible for the growth and decay of structures. In particular, the Hartree selfenergy is a time-local instantaneous back reaction of the mean background onto the evolution of the perturbations. On the other hand, the Fock self-energy represents the non-Markovian property of the out-of-equilibrium ensemble and consists of causal memory integrals, that "remember" the full history of the system. In the plasma physical context, the causal self-energy is also referred to as a resonance broadening term which can be understood when analyzed in time-frequency domain as it affects the dispersion relation of the plasma. The statistical self-energy can be interpreted as a dynamically generated effective perturbation that adds to the initial perturbation $G_{ff}^{(i)}$. The total fluctuation is then propagated by the linear response function G_{fB} . Thus, the statistical self-energy is responsible for mode-coupling and describes the redistribution of matter. Following the literature, we separated the initial vertices into the term $\Sigma_{BB}^{(p)}$. If the initial particle ensemble is drawn from a Gaussian random field, this term vanishes in the Vlasov description, where particle collisions are neglected. In contrast, $\Sigma_{BB}^{(p)}$ appears in the Klimontovich description, where it describes random particle noise arising from particle collisions, and thus generating additional fluctuations. However, if the initial fluid is non-Gaussian, then $\Sigma_{BB}^{(p)}$ also contributes in the Vlasov description, capturing how higher-order initial correlations source two-point fluctuations. There is of course a lot more to say about the physical role played by the self-energies. In particular, in equilibrium they play an important role in the derivation of fluctuation-dissipation relations [18, 19, 66].

Because each self-energy involves the full three-point effective vertices, which in turn involve the next higher-order vertices, one must truncate the Dyson-Schwinger hierarchy. In the next chapter, we consider a special class of systems that allows for an even more extensive analytical description, and we will develop methods to systematically approximate this infinite hierarchy of equations.

Statistically Homogeneous and Isotropic Systems

Finding non-trivial analytic solutions to the above equations is, in almost all physically relevant cases, impossible. However, as in many physical systems, symmetry assumptions offer a powerful tool to reduce the number of degrees of freedom and thus simplifying the mathematical description. In this chapter, we focus on the scenario where the statistical properties of the system are invariant under translations and rotations in physical space. While not fully general, these assumptions hold in many realistic situations, most notably in cosmic structure formation, as discussed in Chapter 11.

8.1. Statistical and Dynamical Setup

We begin by specifying the fundamental ingredients of our statistically homogeneous and isotropic system. As established in earlier sections, the statistical properties of our ensemble are encoded in the initial conditions, which we now revisit under the constraints of spatial homogeneity and isotropy. We then introduce the class of interaction potentials, which we will be dealing with and which must be compatible with these symmetries. Finally, we discuss the particles' free Green function around which the approximations are built.

8.1.1. Statistically Homogeneous and Isotropic Initial Conditions

For our analytical model, we assume that the initial fluid from which our particles' initial coordinates are sampled is a Gaussian random field. That is, the probability distribution functional $\mathcal{P}[f_1^{(i)}]$ is completely characterized by its mean $C_{\mathcal{P}}^{(1)}$ and covariance $G_{\mathcal{P}}^{(2)}$, defined by

$$C_{\mathcal{P}}^{(1)}(x) = \left\langle f_1^{(i)}(x) \right\rangle_{\mathcal{P}} = \int \mathcal{D}f_1^{(i)} f_1^{(i)}(x) \mathcal{P}[f_1^{(i)}], \qquad (8.1)$$

$$G_{\mathcal{P}}^{(2)}(x_{1}, x_{2}) = \left\langle f_{1}^{(i)}(x_{1}) f_{1}^{(i)}(x_{2}) \right\rangle_{c, \mathcal{P}}$$

$$= \int \mathcal{D} f_{1}^{(i)} f_{1}^{(i)}(x_{1}) f_{1}^{(i)}(x_{2}) \mathcal{P}[f_{1}^{(i)}] - \left\langle f_{1}^{(i)}(x_{1}) \right\rangle_{\mathcal{P}} \left\langle f_{1}^{(i)}(x_{2}) \right\rangle_{\mathcal{P}}.$$
(8.2)

All higher order cumulants are set to zero. In addition to Gaussianity, we further assume that the initial statistics of the one-particle phase-space density distribution $f_1^{(i)}$ is statistically homogeneous and isotropic in physical space. These symmetry requirements are motivated both, by simplicity, as they considerably constrain the form of the correlation functions, and by the commonly made assumption that there is no preferred position or direction in space, when averaged over multiple realizations of $f_1^{(i)}(x)$. Technically, we define $\mathcal{P}[f_1^{(i)}]$ to be statistically homogeneous in space, if all its correlation functions are invariant under arbitrary spatial translations,

$$C_{\mathcal{P}}^{(n)}(\vec{q}_1 + \vec{a}, \vec{p}_1, \dots, \vec{q}_n + \vec{a}, \vec{p}_n) = C_{\mathcal{P}}^{(n)}(\vec{q}_1, \vec{p}_1, \dots, \vec{q}_n, \vec{p}_n) \ \forall n, \ \forall \vec{a} \in \mathbb{R}^3.$$
 (8.3)

Analogously, we define statistical spatial isotropy for $\mathcal{P}[f_1^{(i)}]$, if all its correlation functions are invariant under arbitrary spatial rotations,

$$C_{\mathcal{P}}^{(n)}(\hat{R}\cdot\vec{q_1},\vec{p_1},\ldots,\hat{R}\cdot\vec{q_n},\vec{p_n}) = C_{\mathcal{P}}^{(n)}(\vec{q_1},\vec{p_1},\ldots,\vec{q_n},\vec{p_n}) \ \forall n, \ \forall \hat{R} \in SO(3).$$
 (8.4)

In combination with statistical homogeneity, this implies for the correlation functions that they can only depend on relative distances $q_{ij} = |\vec{q}_i - \vec{q}_j|$.

For the resulting particle theory, we find that the only non-vanishing s-particle reduced initial correlation functions are given by

$$f_1^{(i)}(x) = C_{\mathcal{P}}^{(1)}(x) \tag{8.5}$$

$$g_2^{(i)}(x) = G_P^{(2)}(x_1, x_2).$$
 (8.6)

The requirement of homogeneity and isotropy further implies, that $f_1^{(i)}$ is independent of the spatial coordinate while g_2 may only depend on the relative separation of the spatial coordinates. We may therefore write

$$f_1^{(i)}(\vec{q}, \vec{p}) \equiv \bar{\rho} \,\varphi^{(i)}(\vec{p}) \tag{8.7}$$

$$g_2^{(i)}(\vec{q}_1, \vec{p}_1, \vec{q}_2, \vec{p}_2) \equiv \bar{\rho}^2 \, \tilde{g}_2^{(i)}(|\vec{q}_1 - \vec{q}_2|, \vec{p}_1, \vec{p}_2).$$
 (8.8)

Here, $\bar{\rho} = \frac{N}{V}$ is the mean particle density and V is the volume to which the particles are confined in configuration space. For normalization reasons, we have pulled a factor of $\bar{\rho}^2$ out of g_2 . Furthermore, we introduced the initial momentum distribution function which describes the average number density of particles in momentum space at initial time. From the normalization (2.54), we have that $\varphi^{(i)}$ is normalized to unity, $\int d^3p \, \varphi^{(i)}(\vec{p}) = 1$. A typical example would be a Maxwell-Boltzmann momentum statistics for particles of mass m at temperature T,

$$\varphi^{(i)}(\vec{p}) = \frac{1}{(2\pi m k_B T)^{3/2}} e^{-\frac{\vec{p}^2}{2m k_B T}}.$$
 (8.9)

8.1.2. Homogeneous and Isotropic Potentials

Next, we turn to the dynamical part of the system and specify the interactions. As an external potential would spoil homogeneity and in certain cases also isotropy, we are only left with a two-particle interaction v_2 . As above, we demand it to respect spatial homogeneity and isotropy, such that it does not induce preferred positions or directions throughout all realizations. We will furthermore focus on the important class of momentum independent interactions. This leaves us with two-particle interactions of the form

$$v_2(x_1, x_2, t) = v_2(|\vec{q}_1 - \vec{q}_2|, t),$$
 (8.10)

where we kept a general time dependence. We will specify to time independent potentials when appropriate, as time-translationally invariant systems allow for further analytical treatments. The Fourier transform of the above potential is then given by

$$v_2(\vec{k}_1, \vec{k}_2, t) = (2\pi)^3 \delta_{\rm D} \left(\vec{k}_1 + \vec{k}_2 \right) v_2(k_1, t).$$
 (8.11)

In real space, we require that the potential decays fast enough towards infinity, such that the Fourier transform of the two-particle potential does not become singular as \vec{k} goes to zero. Equivalently, the integral of the force over real-space must vanish,

$$0 \stackrel{!}{=} \vec{k} v(k) \Big|_{\vec{k}=0} = -i \int d^3 q \, \nabla_{\vec{q}} v(q) \,, \tag{8.12}$$

which, by angular integration, is satisfied. Physically, this equation expresses that the total force derived from the potential vanishes when integrated over all space, implying the absence of any residual net force.

8.1.3. A Note on Long-Range Interaction Potentials

We are furthermore interested in a special class of systems, namely those governed by long-range interaction potentials. These systems are characterized by interactions that decay slowly with distance, such that they are sensitive to the global configuration of the system. Typical examples are the Coulomb interaction for plasmas or the Newtonian gravitational potential describing the dynamics of self-gravitating systems. As the latter describes the evolution of cosmic structures, which we will be dealing with in chapter 10 and 11, we very briefly mention their main physical properties and implications here, referring to the vast existing literature [67, 68, 69, 70, 71, 72, 73, 74, 75, 76, 77] for detailed studies of their thermodynamical properties. We call a system long-range interacting, if the system's total energy scales super-extensively with the number of particles N. This can be understood as follows: Consider the potential energy of particle j, $U_j \sim \sum_{i=1}^N v_2(|\vec{q}_i - \vec{q}_j|)$. If the potential has only a finite radius of convergence, only a finite number of particles will contribute to the above energy. Provided, that the mean particle number density stays constant, the above potential energy is independent of the particle number N. In contrast, if the potential is longrange, every particle will contribute a non-trivial amount to U_j , such that $U_j \sim N$. The total energy of the system will therefore scale as $E \sim \sum_{j=1}^{N} U_j \sim N^2$ and is thus super-extensive. Since extensivity is required to have a well-defined thermodynamic

limit, this poses a problem. To guarantee the existence of the thermodynamical limit in those cases, one usually employs Kac's prescription [78] and demands that the coupling of the potential scales as $\sim \frac{1}{N}$, such that $E \sim \frac{1}{N} \sum_{i,j=1}^{N} v_{ij} \sim N$, which restores extensivity. In the case of a self-gravitating fluid, one typically demands that the mass of the individual particles that sample the fluid, scales as $m \propto \frac{1}{N}$ at a fixed volume V, such that the mean mass density of the fluid stays constant. We can then define the thermodynamic limit such that

$$\bar{\rho} = \frac{N}{V} \sim N \to \infty$$
, while $\bar{\rho}_m = m\bar{\rho} = \text{const.}$ (8.13)

This will be the thermodynamic limit we will be working with. Importantly, using the Kac prescription, the potential energy of the individual particle contributions becomes arbitrarily weak. It can then be shown [77] that the dynamics of the system approaches the Vlasov dynamics, where the particles only evolve under the influence of a smooth mean field. Collisional effects scale as $g_2 \sim \frac{1}{N}$ and only become important for finite composite systems. Thus, from here on, we will adopt the Vlasov description and neglect all shot-noise contributions.

Another important property of such systems is that the potential decay is given by

$$v_2(r) \sim \frac{1}{r^{\alpha}}, \quad \text{with} \quad \alpha < d,$$
 (8.14)

where d is the spatial dimension. This is thus too slow to ensure convergence of the integral (8.12), and therefore formally violates the condition. In the case of the Coulomb interaction, however, the presence of both positive and negative charges leads to screening effects that effectively render the potential short-ranged, thereby restoring the condition. In contrast, gravity involves only attractive interactions between positive masses, and no such screening mechanism exists. As we will see, the condition can nonetheless be recovered by subtracting the contribution of the homogeneous mean background, as discussed in Section 10.1.

8.1.4. Free Particle Green Function

By a similar logic as above, the free part of the Hamiltonian function, defined by (2.19), should also respect the symmetries of the system. For that reason, $H_0(\mathbf{x}, t)$ cannot be a function of the configuration space coordinates $\vec{\mathbf{q}}$. The only remaining degree of freedom of the matrix A(t) is thus a possibly time-dependent mass m(t),

$$A(t) = \begin{pmatrix} 0 & 0 \\ 0 & \frac{1}{m(t)} \end{pmatrix} . {8.15}$$

Putting all things together, the total Hamiltonian function of the homogeneous and isotropic system is given by

$$H(\mathbf{x},t) = \sum_{i=1}^{N} \frac{\vec{\mathsf{p}}_{i}^{2}}{2 m(t)} + \sum_{i \neq j=1}^{N} v_{2}(|\vec{\mathsf{q}}_{i} - \vec{\mathsf{q}}_{j}|, t).$$
 (8.16)

The associated free equations of motion are given by (2.21). Importantly, the matrix $\boldsymbol{\omega} \cdot \boldsymbol{A}(t)$ is *nilpotent*, so its commutator vanishes, $[\boldsymbol{\omega} \cdot \boldsymbol{A}(t_1), \boldsymbol{\omega} \cdot \boldsymbol{A}(t_2)] = 0 \ \forall t_1, t_2$. Following the general derivation in 2.1.1 that led to the form of the free particle Green function (2.33), we find

$$G(t,t') = \begin{pmatrix} g_{qq}(t,t') \, \mathbb{1}_{3\times 3} & g_{qp}(t,t') \, \mathbb{1}_{3\times 3} \\ \mathbb{0}_{3\times 3} & g_{pp}(t,t') \, \mathbb{1}_{3\times 3} \end{pmatrix} \, \Theta(t-t') \,, \tag{8.17}$$

where the non-vanishing components are given by

$$g_{qq}(t,t') = 1, \quad g_{pp}(t,t') = 1, \quad g_{qp}(t,t') = \int_{t'}^{t} d\bar{t} \frac{1}{m(\bar{t})}.$$
 (8.18)

Consequently, the solution to the free classical trajectory is given by

$$\mathbf{x}_{i}(t) = G(t, t^{(i)}) \cdot \mathbf{x}_{i}^{(i)} = \begin{pmatrix} \vec{\mathbf{q}}_{i}^{(i)} + g_{qp}(t, t^{(i)}) \, \vec{\mathbf{p}}_{i}^{(i)} \\ \vec{\mathbf{p}}_{i}^{(i)} \end{pmatrix} \Theta(t - t^{(i)}). \tag{8.19}$$

8.1.5. Fourier-Space Treatment of Correlation Functions

The Hamiltonian function is constructed such that the evolution respects the initial symmetries of statistical spatial homogeneity and isotropy. As a consequence the full phase-space density correlation functions exhibit the same shift and rotational symmetry requirements as defined for the initial state. These symmetries imply that most integrals we encounter will be convolutions, which naturally motivates a Fourier space formulation where such expressions reduce to products. We therefore adopt the Fourier conventions defined in Appendix A and find for the Fourier transform of the Klimontovich phase-space density,

$$\Phi_f(\vec{k}_1, \vec{\ell}_1, t_1) = \sum_{i=1}^N e^{-i\vec{k}_1^\top \cdot \vec{\mathbf{q}}_i(t_1) - i\vec{\ell}_1^\top \cdot \vec{\mathbf{p}}_i(t_1)}.$$
 (8.20)

We will use similar condensed notation for the field theory summarized in the appendix. In particular, we have the Fourier variables $s = (\vec{k}, \vec{\ell})$ conjugate to $x = (\vec{q}, \vec{p})$, which we extend to S = (s, t). Importantly, the symmetries imply for the Fourier transformation of the full phase-space density cumulants

$$G_{f...f}(S_1,...,S_n) \propto (2\pi)^3 \delta_D \left(\vec{k}_1 + ... + \vec{k}_n\right).$$
 (8.21)

This property is inherited by all expectation values that are derived from the $G_{f...f}$'s. Another reason, why the Fourier space treatment is particularly convenient is that the moments of the momentum statistics (2.99) can now easily be computed by applying appropriate derivatives to the general cumulant,

$$\left\langle \mathcal{O}_1(\vec{k}_1, t_1) \dots \mathcal{O}_n(\vec{k}_n, t_n) \right\rangle = \left. F_{\mathcal{O}_1}(i \nabla_{\vec{\ell}_1}) \dots F_{\mathcal{O}_n}(i \nabla_{\vec{\ell}_n}) G_{f \dots f}(S_1, \dots, S_n) \right|_{\ell=0}, \quad (8.22)$$

and setting all $\vec{\ell}$ -vectors to zero afterwards.

Let us consider the following important example. We define the density fluctuation as

$$\delta(\vec{q},t) = \frac{\rho(\vec{q},t) - \bar{\rho}}{\bar{\rho}}, \qquad (8.23)$$

which measures the local deviation from the homogeneous mean background. To understand how such local fluctuations at different positions in physical space are related, we compute its correlation function

$$\langle \delta(\vec{q}_1, t_1) \delta(\vec{q}_2, t_2) \rangle = \frac{G_{\rho\rho}(\vec{q}_1, t_1, \vec{q}_2, t_2)}{\bar{\rho}^2} = \frac{1}{\bar{\rho}^2} \int d^3 p_1 d^3 p_2 G_{ff}(X_1, X_2), \qquad (8.24)$$

since by definition $\langle \rho(\vec{q},t)\rangle = \bar{\rho}$. In Fourier-space, we then find the relation

$$(2\pi)^{3}\delta_{D}\left(\vec{k}_{1}+\vec{k}_{2}\right)P_{\delta}(k_{1},t_{1},t_{2}) := \left\langle\delta(\vec{k}_{1},t_{1})\delta(\vec{k}_{2},t_{2})\right\rangle = \frac{1}{\bar{\rho}^{2}}G_{ff}(\vec{k}_{1},0,t_{1},\vec{k}_{2},0,t_{2}).$$
(8.25)

Where we defined the density fluctuation power spectrum $P_{\delta}(\vec{k}, t_1, t_2)$. This will be our main object of interest.

8.2. Field Theory

Let us now collect the main ingredients for our field theoretic treatment of statistically homogeneous and isotropic systems. Applied to the Klimontovich equation (2.78) it reads

$$\left[\frac{\partial}{\partial t_1} + \frac{\vec{p_1}}{m(t_1)} \cdot \nabla_{\vec{q_1}}\right] \Phi_f(x_1, t_1) - \int d^6 x_2 \, \Phi_f(x_2, t_1) \hat{\mathcal{L}}_{12}^{(2)} \Phi_f(x_1, t_1) = 0, \qquad (8.26)$$

where the two-particle interaction operator is given by

$$\hat{\mathcal{L}}_{12}^{(2)}(\cdot) = \nabla_{\vec{q}_1} v_2(|\vec{q}_1 - \vec{q}_2|, t_1) \cdot \nabla_{\vec{p}_1}(\cdot). \tag{8.27}$$

As already indicated, homogeneity and isotropy will make it convenient to work in Fourier space from the beginning. The Fourier transform of the Klimontovich equation (8.26) therefore reads

$$\left[\frac{\partial}{\partial t_{1}} - \frac{\vec{k}_{1}}{m(t_{1})} \cdot \nabla_{\vec{\ell}_{1}}\right] \Phi_{f}(s_{1}, t_{1})
+ \int \frac{d^{3}k_{2}}{(2\pi)^{3}} (\vec{k}_{2} \cdot \vec{\ell}_{1}) v_{2}(\vec{k}_{2}, t_{1}) \Phi_{f}(\vec{k}_{2}, 0, t_{1}) \Phi_{f}(\vec{k}_{1} - \vec{k}_{2}, \vec{\ell}_{1}, t_{1}) = 0.$$
(8.28)

Note, that the density sourcing the interaction has vanishing momentum mode, as the potential is independent of the momenta. Furthermore, we see how the symmetry restrictions reduce the number of integrals in the interaction. These characteristics will simplify the computations considerably. Nevertheless, for the construction it is more convenient to restore all missing Fourier integrals for a symmetric field-theoretic treatment. Defining the inverse free retarded propagator in Fourier space as

$$D_{0,R}^{-1}(\hat{1},\hat{2}) = \left[\frac{\partial}{\partial t_1} - \frac{\vec{k}_1}{m(t_1)} \cdot \nabla_{\vec{\ell}_1} \right] \mathbb{1}(\hat{1},\hat{2}), \tag{8.29}$$

we easily find

$$D_{0,R}(\hat{1},\hat{2}) = \delta_{D} \left(s_1 + G^{-\top}(t_1, t_2) \cdot s_2 \right) \Theta(t_1 - t_2), \qquad (8.30)$$

such that

$$D_{0,R}^{-1}(\hat{1},\hat{3}) D_{0,R}(\hat{3},\hat{2}) = \mathbb{1}(\hat{1},\hat{2}), \tag{8.31}$$

where the identity in Fourier space is defined as $\mathbb{1}(\hat{1},\hat{2}) = \delta_{\mathrm{D}}(s_1 + s_2) \delta_{\mathrm{D}}(t_1 - t_2)$. We furthermore used the notation $G^{-\top}$ for the inverse transposed particle Green function. The advanced propagator is again given by $D_{0,A}(\hat{1},\hat{2}) = D_{0,R}(\hat{2},\hat{1})$. Furthermore, we find the symmetric two-particle coupling function given by

$$U_s^{(2)}(\hat{1}, \hat{2}, \hat{3}) = \frac{1}{2} \left(U^{(2)}(\hat{1}, \hat{2}, \hat{3}) + U^{(2)}(\hat{1}, \hat{3}, \hat{2}) \right), \tag{8.32}$$

with

$$U^{(2)}(\hat{1},\hat{2},\hat{3}) = (2\pi)^{3} \delta_{D} \left(\vec{k}_{1} + \vec{k}_{2} + \vec{k}_{3} \right) (2\pi)^{3} \delta_{D} \left(\vec{\ell}_{1} + \vec{\ell}_{3} \right) (2\pi)^{3} \delta_{D} \left(\vec{\ell}_{2} \right) \times \times b(\vec{\ell}_{1},\vec{k}_{2},t_{2}) \delta_{D} \left(t_{1} - t_{2} \right) \delta_{D} \left(t_{2} - t_{3} \right)$$
(8.33)

$$b(\vec{\ell}_1, \vec{k}_2, t_2) := (\vec{k}_2 \cdot \vec{\ell}_1) v_2(\vec{k}_2, t_1). \tag{8.34}$$

With those definitions, we can set up the MSRJD action as described in 6.3,

$$S[\Psi] = \Psi_B(-\hat{1}) D_{0,R}^{-1}(\hat{1}, \hat{2}) \Psi_f(-\hat{2}) - \frac{1}{2} U^{(2)}(\hat{1}, \hat{2}, \hat{3}) \Psi_B(-\hat{1}) \Psi_f(-\hat{2}) \Psi_f(-\hat{3}) - \Psi_B(-\hat{1}) G_f^{(i)}(\hat{1}) - \frac{1}{2} \Psi_B(-\hat{1}) G_{ff}^{(i)}(\hat{1}, \hat{2}) \Psi_B(-\hat{2}),$$
(8.35)

with the two relevant initial cumulants given by

$$G_f^{(i)}(\hat{1}) = f_1^{(i)}(\vec{k}_1, \vec{\ell}_1) = \bar{\rho} (2\pi)^3 \delta_D (\vec{k}_1) \varphi^{(i)}(\vec{\ell}_1)$$
(8.36)

$$G_{ff}^{(i)}(\hat{1},\hat{2}) = g_2^{(i)}(\vec{k}_1,\vec{\ell}_1,\vec{k}_2,\vec{\ell}_2) = \bar{\rho}^2 (2\pi)^3 \,\delta_{\rm D} \left(\vec{k}_1 + \vec{k}_2\right) \,\tilde{g}^{(i)}(k_1,\vec{\ell}_1,\vec{\ell}_2) \,. \tag{8.37}$$

All terms in the action respect the conservation of \vec{k} -modes, as enforced by the respective Dirac-delta distributions. This is an important feature of our system, which can be compared to momentum conservation in quantum field theory. Therefore, all mixed cumulants derived from the above action will respect the symmetry¹. The resulting action, corresponds to a field theory with three-point interaction vertex.

¹This can be shown as a Ward identity related to the symmetry transformations described in section 8.1.1.

All higher-order cumulants vanish, since we are working in the Vlasov description and therefore neglect all shot-noise contributions to the initial vertices. Our main goal will be the computation of the two-point functions for this theory.

8.2.1. Tree-Level Propagators

At tree-level the mean field equation is given by the stationarity condition of the classical action itself. We find

$$0 = \frac{\delta \mathcal{S}[\Psi]}{\delta \Psi_B(\hat{1})} = D_{0,R}^{-1}(\hat{1}, \hat{2}) \, \overline{\Psi}_{f,\text{EoM}}^{(0)}(\hat{2}) - G_f^{(i)}(\hat{1}) \,. \tag{8.38}$$

Importantly, compared to the mean background equation (6.87) for the general system, the non-linear term vanishes in our present case. By homogeneity, the mean field must be independent of the position in real space, or $\overline{\Psi}_{f,\text{EoM}}(\vec{k}_1,\vec{\ell}_1,t_1) \propto (2\pi)^3 \, \delta_{\text{D}}\left(\vec{k}_1\right)$ in Fourier space. Thus, by the condition (8.12) there cannot be two mean fields coupling to the two-particle interaction vertex, i. e., diagrams of the form

$$\cdots <$$
 (8.39)

must vanish. The solution to equation (8.38) is clearly given by

$$\overline{\Psi}_{f,\text{EoM}}^{(0)}(\vec{k}_1, \vec{\ell}_1, t_1) = \int \frac{\mathrm{d}^3 k_2}{(2\pi)^3} \frac{\mathrm{d}^3 \ell_2}{(2\pi)^3} \int_{t^{(i)}}^{t_1} \mathrm{d}t_2 D_{0,R}(\vec{k}_1, \vec{\ell}_1, t_1, \vec{k}_2, \vec{\ell}_2, t_2) G_f^{(i)}(\vec{k}_2, \vec{\ell}_2, t_2)$$
(8.40)

$$=G_f^{(i)}(G^{\top}(t_1, t^{(i)}) \cdot s_1) \tag{8.41}$$

$$=:G_f^{(0)}(\vec{k}_1, \vec{\ell}_1, t_1). \tag{8.42}$$

Thus, the tree-level mean field corresponds to the freely evolved initial mean field. Next, we turn to the computation of the tree-level propagators. From the discussion at the end of (6.6.1), we have to find expressions for $\mathcal{V}_R^{(0)}$ and Ω_R . The former can be computed from the first order approximation to the Hartree self-energy (c.f. equation (6.109)), and reads

$$\mathcal{V}_{R}^{(0)}(S_{1}, S_{2}) = (2\pi)^{3} \delta_{D} \left(\vec{k}_{1} + \vec{k}_{2}\right) (2\pi)^{3} \delta_{D} \left(\vec{\ell}_{2}\right) \tilde{\mathcal{V}}_{R}^{(0)}(\vec{k}_{1}, \vec{\ell}_{1}, t_{1}, t_{2}) \tag{8.43}$$

$$\tilde{\mathcal{V}}_{R}^{(0)}(\vec{k_{1}}, \vec{\ell_{1}}, t_{1}, t_{2}) := -\bar{\rho} b(\vec{\ell_{1}} + g_{qp}(t_{1}, t_{2}) \vec{k_{1}}, \vec{k_{1}}, t_{2}) \varphi^{(i)}(\vec{\ell_{1}} + g_{qp}(t_{1}, t_{2}) \vec{k_{1}}) \Theta(t_{1} - t_{2}),$$
(8.44)

where we extracted the Delta-distributions set by the symmetries. The defining equation for Ω_R reads

$$\Omega_R(S_1, S_2) = \mathcal{V}_R^{(0)}(S_1, S_2) + \int_{\bar{S}} \mathcal{V}_R^{(0)}(S_1, \bar{S}) \,\Omega_R(\bar{S}, S_2) \,. \tag{8.45}$$

Due to the structure of $\mathcal{V}_{R}^{(0)}$ it is sensible to similarly decompose Ω_{R} as

$$\Omega_R(S_1, S_2) = (2\pi)^3 \delta_D \left(\vec{k}_1 + \vec{k}_2 \right) (2\pi)^3 \delta_D \left(\vec{\ell}_2 \right) \tilde{\Omega}_R(\vec{k}_1, \vec{\ell}_1, t_1, t_2). \tag{8.46}$$

Inserted into equation (8.45) we finally end up with an integral equation for $\tilde{\Omega}_R$, which reads

$$\tilde{\Omega}_{R}(\vec{k_{1}}, \vec{\ell_{1}}, t_{1}, t_{2}) = \tilde{\mathcal{V}}_{R}^{(0)}(\vec{k_{1}}, \vec{\ell_{1}}, t_{1}, t_{2}) + \int_{t_{2}}^{t_{1}} d\bar{t} \,\tilde{\mathcal{V}}_{R}^{(0)}(\vec{k_{1}}, \vec{\ell_{1}}, t_{1}, t_{2}) \,\tilde{\Omega}_{R}(\vec{k_{1}}, 0, t_{1}, t_{2}) \quad (8.47)$$

Remarkably, the Dirac-delta distributions have completely removed the spatial part of the integral equation. The solution algorithm is now to first solve the above integral equation for vanishing $\vec{\ell}$ -vectors,

$$\tilde{\Omega}_{R}(\vec{k_{1}}, 0, t_{1}, t_{2}) = \tilde{\mathcal{V}}_{R}^{(0)}(\vec{k_{1}}, 0, t_{1}, t_{2}) + \int_{t_{2}}^{t_{1}} d\bar{t} \, \tilde{\mathcal{V}}_{R}^{(0)}(\vec{k_{1}}, 0, t_{1}, t_{2}) \, \tilde{\Omega}_{R}(\vec{k_{1}}, 0, t_{1}, t_{2}) \,. \tag{8.48}$$

Homogeneity has thus reduced the complexity to a one-dimensional integral equation. This is as far as we can get analytically, in general, for a homogeneous system. Equation (8.48) is a Volterra integral equation of the second kind. The causal structure ensured by the Heaviside function enables a very efficient numerical solution, as, upon time discretization, we simply have to invert a lower triangular matrix via forward substitution.

In certain rare cases, (8.48) can even be solved analytically. The basic requirement for this to be possible is that the objects appearing in (8.48) are time-translation invariant, i. e., only depend on time differences. This requirement is typically fulfilled if the potential is time independent as well as the Hamiltonian function in (8.16), which is thus a conserved quantity. In such cases, the integral in (8.48) becomes a Laplace convolution and may be diagonalized by means of a Laplace transformation. Defining $\tau = t_1 - t_2$, we write

$$\tilde{\Omega}_{R}(\vec{k_{1}},\tau) = \tilde{\mathcal{V}}_{R}^{(0)}(\vec{k_{1}},\tau) + \int_{t_{2}}^{t_{1}} d\bar{t} \,\tilde{\mathcal{V}}_{R}^{(0)}(\vec{k_{1}},\tau) \,\tilde{\Omega}_{R}(\vec{k_{1}},\tau) \,. \tag{8.49}$$

Applying a Laplace transform on both sides and using the Laplace convolution theorem, we find

$$\mathcal{L}\Big[\tilde{\Omega}_R(\vec{k}_1,\tau)\Big](z) = \mathcal{L}\Big[\tilde{\mathcal{V}}_R^{(0)}(\vec{k}_1,\tau)\Big](z) + \mathcal{L}\Big[\tilde{\mathcal{V}}_R^{(0)}(\vec{k}_1,\tau)\Big](z) \,\mathcal{L}\Big[\tilde{\Omega}_R(\vec{k}_1,\tau)\Big](z) \,, \quad (8.50)$$

where z is the Laplace conjugate variable to τ and \mathcal{L} is the Laplace transformation operator. The above equation can be solved algebraically. Transforming the equation

back yields the final result for $\tilde{\Omega}_R$

$$\tilde{\Omega}_{R}(\vec{k_{1}},\tau) = \mathcal{L}^{-1} \left[\frac{\mathcal{L}\left[\tilde{\mathcal{V}}_{R}^{(0)}(\vec{k}_{1},\tau)\right](z)}{1 - \mathcal{L}\left[\tilde{\mathcal{V}}_{R}^{(0)}(\vec{k}_{1},\tau)\right](z)} \right] (\tau).$$
(8.51)

Having obtained an expression for $\tilde{\Omega}_R$, either analytically or numerically, we can now insert it back into Equation (8.47) to derive the general form of Ω_R for non-vanishing $\vec{\ell}$. The retarded tree-level propagator then follows from

$$\Delta_R(\hat{1}, \hat{2}) = D_{0,R}(\hat{1}, \hat{2}) + \Omega_R(\hat{1}, \hat{3})D_{0,R}(\hat{3}, \hat{2}). \tag{8.52}$$

Last but not least, we obtain the statistical propagator by the solution of the integrals (6.105)

$$\Delta_{ff}(\hat{1}, \hat{2}) = \Delta_R(\hat{1}, \hat{3}) G_{ff}^{(i)}(\hat{3}, \hat{4}) \Delta_A(\hat{4}, \hat{2}), \qquad (8.53)$$

which can either be done analytically or numerically.

8.2.2. Analytical Toy Model

Let us briefly discuss a model that admits an analytical solution for the tree-level propagators. We consider the initial mean and covariance to be independent of the momenta. This corresponds to the low-temperature limit of the above-mentioned Boltzmann distribution in (8.9). We therefore find

$$G_f^{(i)}(S_1) = (2\pi)^3 \delta_{\rm D} \left(\vec{k_1}\right) \bar{\rho}$$
 (8.54)

$$G_{ff}^{(i)}(S_1, S_2) = (2\pi)^3 \delta_{\rm D} \left(\vec{k_1} + \vec{k_2} \right) \bar{\rho}^2 P_{\delta}^{(i)}(k_1)$$
 (8.55)

where only the initial power spectrum $P_{\delta}^{(i)}(k_1)$ contains non-trivial statistics. Next, we assume our potential and the mass to be time-independent, such that

$$v_2(k,t) = v_2(k) (8.56)$$

$$g_{qp}(t_1, t_2) = \frac{t_1 - t_2}{m}, (8.57)$$

where m is the constant particle mass. We then find

$$\tilde{\mathcal{V}}_{R}^{(0)}(\vec{k}_{1}, \vec{\ell}_{1}, t_{1}, t_{2}) = -\bar{\rho}k_{1}^{2}v_{2}(k_{1})\left(\frac{t_{1} - t_{2}}{m} + \frac{\vec{k}_{1} \cdot \vec{\ell}_{1}}{k_{1}^{2}}\right)\Theta(t_{1} - t_{2}). \tag{8.58}$$

8.2. Field Theory

Solving first for $\vec{\ell} = 0$, we find the Laplace transform

$$\mathcal{L}\left[\tilde{\mathcal{V}}_{R}^{(0)}(\vec{k}_{1},0,t_{1}-t_{2})\right](z) = \mathcal{L}\left[-\frac{\bar{\rho}\,k_{1}^{2}\,v_{2}(k_{1})\,(t_{1}-t_{2})}{m}\right](z) \tag{8.59}$$

$$= -\frac{\bar{\rho}}{m} k_1^2 v_2(k_1) \frac{1}{z^2} \tag{8.60}$$

Using the inverse Laplace transform of the form

$$\mathcal{L}^{-1}\left[\frac{-A}{s^2+A}\right](t) = -\sqrt{A}\sin\left(\sqrt{A}t\right)\,,\tag{8.61}$$

we get a closed expression for (8.51) given by

$$\tilde{\Omega}_R(\vec{k}, 0, t_1 - t_2) = -\omega(k) \sin\left(\omega(k)(t_1 - t_2)\right), \tag{8.62}$$

with the k-dependent frequency

$$\omega(k) = \sqrt{\frac{\bar{\rho}k^2v_2(k)}{m}} \,. \tag{8.63}$$

Inserted back into (8.47), we get the general result

$$\tilde{\Omega}_{R}(\vec{k}, \vec{\ell}, t_{1} - t_{2}) = -\left[\omega(k)\sin\left(\omega(k)(t_{1} - t_{2})\right) + m\omega(k)^{2}\cos\left(\omega(k)(t_{1} - t_{2})\right)\frac{\vec{k}_{1} \cdot \vec{\ell}_{1}}{k_{1}^{2}}\right]\Theta(t_{1} - t_{2}).$$
(8.64)

Equation (8.64) is the general solution of the causal tree-level propagator in the low-temperature limit of a Boltzmann gas. Interestingly, we see that if the potential is repulsive, i. e., $v_2(k) > 0$, $\tilde{\Omega}_R$ and thus Δ_R exhibit oscillatory behavior with frequency $\omega(k)$. This can be understood, since in a homogeneous system where the thermal motion of the particles is negligible, a repulsive inter-particle potential will lead to a collective oscillating behavior within the system. It arises due to the system's response to a local perturbation as it tries to restore homogeneity. For instance, consider the Coulomb potential,

$$v_C(|\vec{q}_1 - \vec{q}_2|) = \frac{e^2}{4\pi\varepsilon_0} \frac{1}{|\vec{q}_1 - \vec{q}_2|},$$
 (8.65)

whose Fourier transform is

$$v_C(k) = \frac{e^2}{\epsilon_0} \frac{1}{k^2} \,. \tag{8.66}$$

Inserting this into (8.63) we recover the well-known plasma frequency (or Langmuir frequency),

$$\omega(k) = \sqrt{\frac{\bar{\rho}e^2}{m\epsilon_0}} \equiv \omega_P \,. \tag{8.67}$$

The charged particles, thus, oscillate around their equilibrium position, which is famously known as plasma oscillations.

On the other hand, if the potential is attractive, $v_2(k) < 0$, we find

$$\omega(k) = i\sqrt{\frac{\bar{\rho}k^2|\tilde{v}(k)|}{m}} = i|\omega(k)|, \qquad (8.68)$$

and thus

$$\tilde{\Omega}_{R}(\vec{k}, \vec{\ell}, t_{1} - t_{2}) = \left[|\omega(k)| \sinh\left(|\omega(k)|(t_{1} - t_{2})\right) + m|\omega(k)|^{2} \cosh\left(|\omega(k)|(t_{1} - t_{2})\right) \frac{\vec{k}_{1} \cdot \vec{\ell}_{1}}{k_{1}^{2}} \right] \Theta(t_{1} - t_{2})^{2}.$$

In this case, the propagator consists of an exponentially growing and an exponentially decaying part. This is also intuitively clear, as a small deviation from homogeneity leads to a collapse of structures. Most prominently, consider the attractive Newtonian gravitational potential,

$$v_G(|\vec{q}_1 - \vec{q}_2|) = -\frac{Gm^2}{|\vec{q}_1 - \vec{q}_2|},$$
 (8.70)

with Fourier transform

$$v_G(k) = -\frac{4\pi Gm^2}{k^2} \,. ag{8.71}$$

We find the growth rate

$$\omega(k) = \sqrt{4\pi G m \bar{\rho}} \equiv \omega_G. \tag{8.72}$$

In a homogeneous system with negligible thermal motion, attractive forces such as the Newtonian gravitational potential lead to exponentially growing structures due to local perturbations. On a physical level, a local over density in a self-gravitating gas leads to a collapse of the whole surrounding system and thus to an exponentially growing perturbation. This result is famously known as Jeans instability. The frequency we recovered in (8.72) is related to the characteristic timescale of collapse for a collisionless fluid τ by $\tau = \frac{1}{\omega_G}$ and is usually referred to as the free-fall collapse time.

We can finally solve for the statistical propagator (6.105) and find

$$\Delta_{ff}(S_1, S_2) = (2\pi)^3 \delta_{\rm D} \left(\vec{k}_1 + \vec{k}_2 \right) \bar{\rho}^2 P_{\delta}^{(i)}(k_1) F(S_1) F(S_2), \qquad (8.73)$$

with

$$F(\vec{k}_1, \vec{\ell}_1, t_1) = \cos\left(\omega(k_1)(t_1 - t^{(i)})\right) - m\omega(k)\sin\left(\omega(k)(t_1 - t_2)\right) \frac{\vec{k}_1 \cdot \vec{\ell}_1}{k_1^2}.$$
 (8.74)

Since, at tree-level we have $G_{ff} = \Delta_{ff}$ as a first approximation to the two-point phase-space density correlation function, the time evolution of the power spectrum can be read off directly from equation (8.25),

$$P_{\delta}(k, t_1, t_2) = P_{\delta}^{(i)}(k_1) \cos\left(\omega(k_1)(t_1 - t^{(i)})\right) \cos\left(\omega(k_1)(t_2 - t^{(i)})\right). \tag{8.75}$$

8.3. Truncated Dyson-Schwinger Equations

We now briefly turn to the most commonly used truncation schemes of the Dyson-Schwinger hierarchy as encountered in quantum field theory. Unlike the perturbative expansion discussed in section 6.6.3, these provide non-perturbative approximations that can capture phenomena beyond the reach of perturbative methods. For our present case, the Dyson-Schwinger equations read

$$0 = \cdots \bullet + \cdots \bullet + \frac{1}{2!} \cdots \bullet ,$$

$$\cdots \bullet \cdots = \cdots \bullet \cdots - \frac{1}{2!} \cdots \bullet \cdots - \frac{1}{2!} \cdots \bullet \cdots - \frac{1}{2!} \cdots \bullet \cdots$$

$$(8.76)$$

8.3.1. 1PI Resummation and One-Loop Effective Action

Clearly, the most straightforward non-perturbative approximation beyond the treelevel theory, is given by the one-loop effective action, discussed in 7.2. This amounts to solving the equations (7.47) and (7.48), which clearly corresponds to closing the hierarchy (8.76) by replacing all full statistical objects on the right-hand side by their bare quantities. The solution to the upper equation corresponds to the formal resummation of the causal one-loop self energies,

$$G_{fB}^{\text{1lp.}} = \Delta_{fB} + \Delta_{fB} \cdot \Sigma_{Bf}^{\text{1lp.}} \cdot G_{fB}^{\text{1lp.}}$$

$$(8.77)$$

$$= \Delta_{fB} \cdot \sum_{n=0}^{\infty} \left(\Sigma_{Bf}^{\text{1lp.}} \cdot \Delta_{fB} \right)^{n} . \tag{8.78}$$

This naturally extends the tree-level resummation by capturing the next to leading order corrections in a non-perturbative way. However, we have to remark that only the causal self-energy is resummed in this procedure. We will therefore expect an oscillatory behavior of the full result, depending on the sign of the self energy. Indeed,

similar procedures in the hydrodynamical approaches to the Vlasov equation have shown that this type of resummation leads to damping effects that, depending on the particular resummation procedure, arise from Bessel functions or Gaussian damping on small scales. From a numerical perspective, equation (8.77) again corresponds to a linear Volterra integral equation for the resummed one-loop causal propagator. Since, by homogeneity, we find

$$\Sigma_{ab}(1,2) \propto (2\pi)^3 \,\delta_{\rm D} \left(\vec{k}_1 + \vec{k}_2\right) \,\Theta(t_1 - t_2) \,,$$
 (8.79)

the integral equation can be solved numerically upon discretization in time. The only numerical issue is to solve the inner loop integrations. Once the self-energy is known for all times, one can use a similar algorithm as for the solution of the tree-level propagator (8.47). Note, that this procedure will only perform a partial resummation of the *causal* self-energies, as the solution for the statistical one-loop 1PI propagator is given by

$$G_{ff}^{\text{1lp.}} = -G_{fB}^{\text{1lp.}} \cdot \mathcal{S}_{BB}^{(2)} \cdot G_{Bf}^{\text{1lp.}} + G_{fB}^{\text{1lp.}} \cdot \Sigma_{BB} \cdot G_{Bf}^{\text{1lp.}}.$$
(8.80)

Thus, the present procedure does not capture the back-reaction of the statistical self-energy to the propagation and the mean background. We therefore cannot describe further mode-coupling effects that are not already present at the perturbative one-loop level. We will therefore have to extend the approximation scheme.

8.3.2. Self Consistent Hartree-Fock Approximation

We can now extend the previous method such that the back-reaction of the propagator to the background and vice versa is treated self-consistently meaning, that the value of the propagator depends on its own history, such that it feeds back onto itself. The corresponding equations of motion are obtained from the Dyson-Schwinger equations by replacing the higher-order effective vertices, i. e., $\Gamma^{(3)}$, by their tree-level value, while keeping the propagators exact to this approximation. We thus obtain a self-consistent feedback mechanism in which the full statistical propagator is dynamically computed and reenters the evolution equations through the Hartree and Fock contributions to the causal and statistical self-energies, which in turn drive the evolution of the propagator. This scheme is commonly referred to as the self-consistent Hartree-Fock approximation [79, 80, 81]. In that way, the statistical self-energies are resummed in a non-trivial way. The above system of equations is more intricate to solve than the previously discussed 1PI resummation, as it constitutes a set of coupled, non-linear Volterra-Fredholm integral equations. Their numerical solution therefore requires discretization in both time and Fourier mode \vec{k} .

8.3.3. Beyond Hartree-Fock - 2PI Loop Expansion

Last, but not least, let us sketch which further procedures exist beyond the above-mentioned. One well established formalism known as the *Cornwall-Jackiw-Tomboulis*-or 2PI-formalism [82, 83] directly extends the above self-consistent Hartree-Fock method, and generalizes the 1PI effective action introduced in 7.2. Let us briefly

summarize the main ideas.

Similarly to the generating functional (7.1) that generates expectation values of the field Ψ , one can introduce a bilocal source $K_{\alpha\beta}(X,Y)$ such that

$$\mathcal{Z}[J,K] = \int \mathcal{D}\exp\left[-S[\Psi] + J_a\Psi_a + \frac{1}{2}\Psi_a K_{ab}\Psi_b\right]$$
(8.81)

$$W[J, K] = \ln \left[\mathcal{Z}[J, K] \right], \tag{8.82}$$

with

$$\frac{\delta \mathcal{W}[J,K]}{\delta J_a} = \overline{\Psi}_a, \qquad \frac{\delta \mathcal{W}[J,K]}{\delta K_{ab}} = \frac{1}{2} \left[\mathcal{G}_{ab} + \overline{\Psi}_a \overline{\Psi}_b \right]. \tag{8.83}$$

One then defines the 2PI-effective action in analogy to the 1PI effective action as a double Legendre transform w.r.t. the sources J and K,

$$\Gamma_{2PI}[\overline{\Psi}, \mathcal{G}] := J_a \overline{\Psi}_a + \frac{1}{2} K_{ab} \left[\mathcal{G}_{ab} + \overline{\Psi}_a \overline{\Psi}_b \right] - \mathcal{W}[J, K]. \tag{8.84}$$

By making a saddle-point approximation one can show, that Γ_{2PI} can be brought into the form

$$\Gamma_{2PI}[\overline{\Psi}, \mathcal{G}] = \mathcal{S}[\overline{\Psi}] - \frac{1}{2} \operatorname{Tr} \ln \left[\mathcal{G}^{-1} \right] - \frac{1}{2} \operatorname{Tr} \left[\Delta^{-1}[\overline{\Psi}] - \mathbb{1} \right] + \Gamma_{2}[\overline{\Psi}, \mathcal{G}], \qquad (8.85)$$

where $\mathcal{S}[\overline{\Psi}]$ is the classical action evaluated at the mean field, $\Delta^{-1}[\overline{\Psi}]$ is the inverse classical propagator in the presence of the full mean field, and importantly, $\Gamma_2[\overline{\Psi}, \mathcal{G}]$ is the sum of all 2PI vacuum diagrams, with classical vertices and full propagators running inside the diagrams. The stationarity conditions for Γ_{2PI} , similar to (7.22) then imply

$$0 = \frac{\delta\Gamma_{2PI}[\overline{\Psi}, \mathcal{G}]}{\delta\overline{\Psi}}\bigg|_{\substack{\overline{\Psi} = \overline{\Psi}_{EoM} \\ \mathcal{G} = G}}, \qquad 0 = \frac{\delta\Gamma_{2PI}[\overline{\Psi}, \mathcal{G}]}{\delta\mathcal{G}}\bigg|_{\substack{\overline{\Psi} = \overline{\Psi}_{EoM} \\ \mathcal{G} = G}}.$$
 (8.86)

While the left-hand equation yields an equation of motion for the mean field, the right-hand equation yields

$$0 = -G^{-1} + \Delta^{-1}[\overline{\Psi}] + \frac{\delta\Gamma_2}{\delta\mathcal{G}} \bigg|_{\substack{\overline{\Psi} = \overline{\Psi}_{\text{EoM}} \\ \mathcal{G} = G}}$$
(8.87)

$$\Leftrightarrow G = \Delta^{-1}[\overline{\Psi}] + \Sigma[\overline{\Psi}_{EoM}, G],$$

i. e., the Dyson-Schwinger equation for the exact propagator, where the self-energy is defined by

$$\Sigma[\overline{\Psi}_{\text{EoM}}, G] := 2 \frac{\delta \Gamma_2[\overline{\Psi}, \mathcal{G}]}{\delta \mathcal{G}} \bigg|_{\substack{\overline{\Psi} = \overline{\Psi}_{\text{EoM}} \\ \mathcal{G} = G}}.$$
 (8.88)

We now expand $\Gamma_2[\overline{\Psi}, \mathcal{G}]$ and consequently $\Sigma[\overline{\Psi}_{EoM}, G]$ in a loop expansion. Because each loop involves the full propagator G, the resulting equations are non-perturbative self-consistency conditions for the full propagator G. At lowest (one-loop) order this yields the Hartree-Fock approximation discussed above. In this way, the 2PI formalism systematically extends our previous resummations to arbitrary loop topologies. Equivalently, one could have derived the same truncated self-consistent system from the Dyson-Schwinger hierarchy, by retaining only classical vertices in the higher-order equations for the 1PI effective vertices and then back-substituting them into the lower equations, thereby generating every diagram topology up to the chosen loop order.

Let us close the theoretical treatment of our formalism by mentioning that the 2PI formalism may be extended to higher nPI vertex functions [82]. This amounts to including higher-order Dyson-Schwinger equations. We expect the dominant contribution to arise from the vertex correction to the 2-particle potential interaction $S_{Bff}^{(3)}$. The leading orders to the Dyson-Schwinger equation (7.59) are in that case given by

The first diagram on the right-hand side corresponds to the classical two-particle interaction vertex which is being renormalized by the two leading order diagrams containing only the Γ_{Bff} vertices. Hence, we expect that these contributions dominate the next higher order corrections.

3

Application to Cosmic Large Scale Structure Formation

9

Cosmology

In the following chapters we will present the application of the theoretical framework developed in Part I and Part II of this thesis to the large-scale structure formation in the Universe. In this chapter, we aim to provide the basis for understanding the later results, but also to provide insights into the problems faced in the field of cosmic large-scale structure formation. Throughout this chapter we follow [84, 85, 86, 87, 4, 5].

9.1. Cosmological Standard Model

Let us begin by discussing the standard model of cosmology which establishes the accepted views on the physics governing the evolution of the Universe and its matter-energy content. Cosmology is the study of the Universe and its contents as a whole. Since the scales which are considered in this field are so vast, the dominant force in the Universe is gravity.

9.1.1. Lovelock's Theorem and Einstein's Field Equations

In order to describe the dynamical evolution of the Universe, we must turn to a theoretical framework that accounts not only for the dynamics of the energy and matter content, but also for the dynamics of spacetime itself. Therefore, instead of considering a static background as in the Newtonian approach, one promotes space-time to a four dimensional Lorentzian manifold \mathcal{M}^4 , i. e., a smooth manifold equipped with a non-degenerate metric of signature (-,+,+,+), whose metric tensor $g_{\mu\nu}(x)$ is a dynamical field. Consequently, the notion of distance is intrinsically local: at each point $x \in \mathcal{M}^4$, lengths are measured by the infinitesimal line element

$$ds^2 = g_{\mu\nu}(x) \mathrm{d}x^{\mu} \mathrm{d}x^{\nu} \tag{9.1}$$

which defines how distances are measured in a neighborhood of x. Here $x^{\mu}=(x^0,x^1,x^2,x^3)$ is a four-vector with the Greek index μ running from 0 to 3, where x^0 denotes the time and x^i (i=1,2,3) denotes the spatial coordinates. To determine how this dynamical metric responds to and is sourced by the energy density, we search for appropriate field equations of the form

$$\mathcal{D}_{\mu\nu}[g] = T_{\mu\nu} \,, \tag{9.2}$$

9. Cosmology

where $\mathcal{D}_{\mu\nu}[g]$ is some yet to be specified symmetric second rank tensorial functional of the metric and its derivatives, and $T_{\mu\nu}$ is the energy-momentum tensor describing the energy and matter content of space-time. Physically, this equation states that the gravitational field dynamics encoded in $\mathcal{D}_{\mu\nu}[g]$ is generated by the energy-momentum tensor of all matter and energy present in spacetime. Although the space of possible forms seems vast at first sight, we can significantly constrain the form of $\mathcal{D}_{\mu\nu}[g]$ by imposing a few physically and mathematically well-motivated requirements. In particular, we demand that the field equations are local and second-order in the metric derivatives, ensuring that the dynamics is governed by well-posed differential equations. Furthermore, we demand that $\mathcal{D}_{\mu\nu}[g]$ is identically divergence-free, which is a mathematical consequence of general covariance under coordinate transformations¹, and necessary for the energy-momentum tensor to be divergence-free. It then follows from Lovelock's theorem that in four² dimensions the most general symmetric, divergence-free, second-rank tensor constructed solely from the metric $g_{\mu\nu}$ and its derivatives up to second order is a linear combination of the Einstein tensor $G_{\mu\nu}$ and the metric itself,

$$\mathcal{D}_{\mu\nu}[g] \equiv \alpha G_{\mu\nu} + \beta g_{\mu\nu} := \alpha \left(R_{\mu\nu}[g] - \frac{1}{2} R[g] g_{\mu\nu} \right) + \beta g_{\mu\nu}, \qquad (9.3)$$

where $\alpha, \beta \in \mathbb{R}$ are the only degrees of freedom in the construction of $\mathcal{D}_{\mu\nu}[g]$. In the above equation, $R_{\mu\nu}[g]$ is the *Ricci curvature tensor* and $R[g] = g^{\mu\nu}R_{\mu\nu}$ is the *Ricci scalar*. Matching the correct Newtonian limit for weak gravitational fields, finally yields the well-known *Einstein field equations*

$$G_{\mu\nu} + \Lambda g_{\mu\nu} = \frac{8\pi G_{\rm N}}{c^4} T_{\mu\nu},$$
 (9.4)

where Λ is the cosmological constant, c is the speed of light and G_N is the Newtonian gravitational constant. These field equations, first derived by Albert Einstein from the equivalence principle, lie at the heart of the general theory of relativity. They describe the inherent coupling and mutual influence of spacetime geometry and its energy and matter content: the energy and matter content evolves according to the underlying geometry, while the geometry changes according to the energy and matter distribution. Importantly, Lovelock's theorem states that the above field equations are unique up to the choice of the two coupling parameters G_N and Λ . While the former is well-known already in Newtonian theory and describes the strength of the gravitational coupling, the role of the cosmological constant Λ is less obvious and will become important in the subsequent cosmological application.

¹To be more specific, this follows from the invariance of the corresponding gravitational action under diffeomorphisms, and can thus be seen as a *Noether identity* [88].

²Indeed, the number of dimensions is crucial for Lovelock's theorem to hold in this form. At higher dimensions, additional degrees of freedom arise in the form of higher-order curvature invariants, such as the Gauss-Bonnet term, $G = R^2 - 4R_{\mu\nu}R^{\mu\nu} + R_{\mu\nu\alpha\beta}R^{\mu\nu\alpha\beta}$, which reduces to the topological Euler-Characteristic in four dimensions. However, they may nonetheless play a significant role in quantum corrections to the Einstein equations at short distances, as suggested by their appearance in low-energy effective actions derived from string theory. [89]

9.1.2. Space-Time Dynamics of the Universe

The Einstein field equations (9.4) represent a set of coupled, non-linear hyperbolicelliptic partial differential equations, that describe the dynamics of the ten metric degrees of freedom in four dimensions. As such, they are extremely complicated to solve, unless symmetry restrictions are made.

We assume that our spacetime (M, g) is spatially homogeneous, meaning that M can be foliated by a one-parameter family of spacelike hypersurfaces Σ_t such that at each t and for any two points $x, y \in \Sigma_t$ there exists an isometry f of g which maps x onto y. Simply put, the geometry is the same at every point on the hypersurface. We further assume that our spacetime is spatially isotropic around a point x, if there exists a congruence of time-like geodesics through it with tangent vector u, such that any two vectors $v_1, v_2 \in T_p M$ which are orthogonal to u in x can be mapped onto each other through an isometry f of g while leaving u and x invariant. This means that if the spacetime is spatially isotropic, observers with four-velocities ucannot identify a preferred direction. If the spacetime is spatially isotropic around each point, it is also homogeneous. Together these imply that each Σ_t is a maximally symmetric 3-manifold. It is then a mathematical theorem that these spaces have constant sectional curvature k, and can thus be split into three classes: spherical or elliptical geometry, Euclidean geometry and hyperbolic geometry. The respective line element is then given by the famous Friedmann-Lemaître-Robertson-Walker metric, which in local spherical coordinates reads

$$ds^{2} = -c^{2}dt^{2} + a(t)^{2} \left[d\chi^{2} + \mathcal{S}_{k}(\chi) d\Omega^{2} \right], \qquad (9.5)$$

where $d\Omega^2 = d\theta^2 + \sin^2(\theta)d\phi^2$ is the usual surface element of the 2-sphere and the function $S_k(\chi)$ is given by

$$S_k(\chi) = \begin{cases} \frac{1}{\sqrt{k}} \sin(\sqrt{k}\chi) & \text{for } k > 0 \text{ (spherical)} \\ \chi & \text{for } k = 0 \text{ (Euclidean)} \\ \frac{1}{\sqrt{|k|}} \sinh(\sqrt{|k|}\chi) & \text{for } k < 0 \text{ (hyperbolic)} \end{cases}$$
(9.6)

Here, χ is the radial coordinate with units of length, such that the curvature parameter k has units of (length)⁻². The scale function a(t) controls how these spatial hypersurfaces expand or shrink over time.

We can now connect to physics by making two fundamental assumptions about our Universe, known as the cosmological principle: When averaged over sufficiently large scales, our Universe is spatially homogeneous and isotropic. While isotropy can be tested through observations, homogeneity cannot and thus relies on the assumption that our position in the Universe is by no means preferred. If both hold, the large-scale geometry and evolution of the Universe are described by the line element (9.5). In order to solve Einstein's equations, we need to specify the energy and matter content of our Universe. To satisfy Einstein's field equations, the symmetries imply that it must be possible to find local coordinates such that

9. Cosmology

the energy-momentum tensor is diagonal. In order to comply with the cosmological principle, its components cannot depend on the spatial coordinates, which leads to the conclusion that $T_{\mu\nu}$ corresponds to the energy-momentum tensor of an ideal fluid. For a comoving observer for whom the symmetries are preserved, this implies $T_{\mu\nu} = \text{diag}(\bar{\rho}c^2, \bar{P}, \bar{P}, \bar{P})$, where $c^2\bar{\rho}$ and \bar{P} are the mean energy density and the mean pressure of the cosmic fluid. With the homogeneous and isotropic metric (9.5) and the respective energy momentum tensor, the Einstein field equations reduce to a set of two simple equations, that can be brought into the form

$$\left(\frac{\dot{a}}{a}\right)^2 = \frac{8\pi G_{\rm N}}{3}\bar{\rho} - \frac{kc^2}{a^2} + \frac{\Lambda c^2}{3} \tag{9.7}$$

$$\frac{\ddot{a}}{a} = -\frac{4\pi G_{\rm N}}{3} \left(\bar{\rho} + \frac{3\bar{P}}{c^2} \right) + \frac{\Lambda c^2}{3} \,.$$
 (9.8)

These are the well-known *Friedmann equations* that govern the evolution of the scale factor a(t) in dependence of the matter content of our Universe. Typically, the scale factor is normalized to $a(t_0) = 1$ today.

9.1.3. Cosmic Expansion

The divergence-free nature of the Einstein field equations implies the local conservation of energy and momentum in general relativity. In the context of a homogeneous and isotropic FLRW Universe, this conservation law takes the form of the adiabatic equation,

$$\frac{\mathrm{d}}{\mathrm{d}t}(a(t)^{3}\,\bar{\rho}(t)\,c^{2}) = -\bar{P}(t)\frac{\mathrm{d}}{\mathrm{d}t}(a(t)^{3})\,,\tag{9.9}$$

which can easily be verified using Friedmann's equations. The meaning of (9.9) is clear, as the left-hand side represents the change of internal energy within a comoving volume, while the right-hand side accounts for the work associated with pressure as the Universe expands or contracts. It thus corresponds to the cosmological version of the first law of thermodynamics and describes the dilution of energy due to the cosmic expansion. Assuming a constant equation of states connecting the mean energy density with the mean pressure of the cosmic fluid,

$$\bar{P} = \omega \,\bar{\rho} \,c^2 \,, \tag{9.10}$$

(9.9) yields the general solution

$$\bar{\rho}(t) = \bar{\rho}(t_0) a(t)^{-3(1+\omega)}$$
. (9.11)

The most relevant cases to us are non-relativistic matter, i. e., cold dust with $\omega_m = 0$ and ultra-relativistic radiation with $\omega_r = \frac{1}{3}$, such that

$$\bar{\rho}_m(t) = \bar{\rho}_m(t_0) a(t)^{-3}, \qquad \bar{\rho}_r(t) = \bar{\rho}_r(t_0) a(t)^{-4}.$$
 (9.12)

Both equations describe how the mean density decreases with cosmic expansion. Physically, the a^{-3} scaling of non-relativistic matter can be explained as a pure

dilution of particle number as the volume grows. The additional factor of a^{-1} for radiation is a consequence an increase or decrease of the radiation wavelength due to cosmic expansion. The relative change in wavelength of radiation emitted at time $t_{\rm e}$ and measured at time $t_{\rm o}$ is given by the redshift

$$z := \frac{\lambda_0 - \lambda_e}{\lambda_e} = \frac{a(t_0)}{a(t_e)} - 1 = \frac{\nu(t_e)}{\nu(t_0)} - 1, \qquad (9.13)$$

and thus $\nu \propto a^{-1}$. Since the energy of a photon is given by $E_{\nu} = h\nu$ with h being Planck's constant, we find the additional factor of a^{-1} . Consequently, at very early times, i.e., small a, radiation dominates the total energy, while at later times matter takes over.

It is convenient to define the *Hubble function*,

$$H(t) := \frac{\dot{a}}{a}, \tag{9.14}$$

representing the relative expansion rate. Today's value is given by the *Hubble* constant, $H_0 := H(t_0)$. Furthermore, we define the critical density as

$$\rho_{\rm cr}(t) := \frac{3H(t)^2}{8\pi G_{\rm N}}, \qquad \rho_{\rm cr,0} := \rho_{\rm cr}(t_0) = \frac{3H_0^2}{8\pi G_{\rm N}}.$$
(9.15)

Assuming that the total density of the Universe is given by a sum over individual contributions X, with mean density $\bar{\rho}_X$, such that the total mean density is given by $\bar{\rho}_{\text{tot}} = \sum_X \bar{\rho}_X$, and assuming a constant equation of state $\bar{P}_X = \omega_X \bar{\rho}_X c^2$, it is often convenient to introduce the dimensionless (time-dependent) density parameters

$$\Omega_X(t) = \frac{\bar{\rho}_X(t)}{\rho_{\rm cr}(t)} = \frac{8\pi G_{\rm N}}{3H(t)^2} \bar{\rho}_{X,0} a(t)^{-3(1+\omega_X)}, \qquad \Omega_k(t) = -\frac{k c^2}{H(t)^2 a(t)^2},
\Omega_{\Lambda}(t) = \frac{\Lambda c^2}{3H(t)^2} = \frac{8\pi G_{\rm N}}{3H(t)^2} \frac{\Lambda c^2}{8\pi G_{\rm N}} = \frac{\bar{\Lambda}}{\rho_{\rm cr}(t)}.$$
(9.16)

The last equation already suggests that the cosmological constant Λ , introduced earlier as a purely geometrical degree of freedom can in principle be seen as a contribution to the energy density of the Universe. With these definitions the first Friedmann equation can be reexpressed purely in terms of the density parameters, which for H(a=1) obey the relation

$$1 = \sum_{X} \Omega_X(t) + \Omega_k(t) + \Omega_{\Lambda}(t). \qquad (9.17)$$

The second equation on the other hand can be brought into the form

$$\frac{\dot{H}}{H^2} = -\Omega_k - \frac{3}{2} \sum_X (1 + \omega_X) \,\Omega_X \,,$$
 (9.18)

and describes the acceleration and deceleration of the Universe. Expressed in terms

9. Cosmology

of today's values of the density parameters, the first equation reads

$$H(t)^{2} = H_{0}^{2} \left(\sum_{X} \Omega_{X,0} a(t)^{-3(1+\omega_{X})} + \Omega_{k,0} a^{-2} + \Omega_{\Lambda,0} \right).$$
 (9.19)

It is instructive to study a special case, where the above equations are analytically solvable. We define the *Einstein-de Sitter Cosmology* as a Universe filled only with pressureless dust, $\Omega_{m,0} = 1$. Equation (9.19) then yields

$$H(t) = H_0 \sqrt{\Omega_{m,0}} \, a^{-\frac{3}{2}} \,. \tag{9.20}$$

From $H = \frac{\dot{a}}{a}$ it then follows

$$a(t) = \left(\frac{3}{2}\sqrt{\Omega_{m,0}}H_0\,t\right)^{\frac{2}{3}} \propto t^{\frac{2}{3}} \tag{9.21}$$

for the scale factor. This analytically solvable cosmology is often used as a toy model and, as we will see, can in certain circumstances be used to approximate the realistic case.

9.1.4. The Λ CDM Paradigm

To our current knowledge, the Universe is exceptionally well described by a spatially flat (k = 0) FLRW-metric, with dynamics set by a cosmological constant Λ , radiation Ω_r and matter Ω_m . In this setting, the expansion history obeys

$$H(a)^{2} = H_{0}^{2} \left(\Omega_{r,0} a^{-4} + \Omega_{m,0} a^{-3} + \Omega_{\Lambda,0} \right).$$
 (9.22)

One further assumes two contributions to $\Omega_{m,0}$. One is ordinary matter, usually referred to as baryonic matter, whose density parameter is denoted by $\Omega_{b,0}$. The other, describes a form of matter, to which one usually refers to as cold dark matter, whose existence is postulated, in order to explain the observed structures³ of the Universe. Dark matter is assumed to only interact gravitationally, making it "dark" to our observation. Furthermore, the attribute "cold" is used to distinguish those models of non-relativistic dark matter, from models of "warm" dark matter, describing relativistic constituents. Observational data prefer cold dark matter, and also indicate that its density parameter $\Omega_{c,0}$ is by far the larger contribution to $\Omega_{m,0}$. Furthermore, it appears that the Universe has recently $(z \simeq 1)$ entered a phase of accelerated expansion, which is assigned to the influence of the cosmological constant Λ . Although there exist models that introduce an additional dynamical fluid to account for the accelerated expansion of the Universe, we have seen that Lovelock's theorem provides a natural explanation in the form of a geometrical

³For instance, gravitational lensing suggests the existence of matter at place where no ordinary matter is observed.

Parameters	Planck2018	This Thesis
$H_0 [{\rm km s^{-1} Mpc^{-1}}]$	67.66 ± 0.42	70
$\Omega_{m,0}$	0.3111 ± 0.0056	0.345
$\Omega_{\Lambda,0}$	0.6889 ± 0.0056	0.655
$\Omega_{b,0}$	0.0489 ± 0.0059	0.045
$\Omega_{c,0}$	0.2607 ± 0.0061	0.3
n_s	0.9665 ± 0.0038	1

Table 9.1.: List of cosmological parameters as measured by the Planck stellite [90] and the set of parameters used throughout this thesis. Since we will compare our results with those of simulations run with the same parameters and not observation we are free to deviate from the measurements of [90]. For instance, we choose a higher value for the Hubble constant as it is favored by local probes [91].

parameter. We will refer to this contribution as dark energy⁴, which constitutes by far the dominant contribution to today's energy content. This model is referred to as the Λ CDM-model. Measurements of the Cosmic Microwave Background (CMB) indicate the set of cosmological parameters given in 9.1.

9.2. From Inflation to Today's Large-Scale Structures

Up to now, we described our Universe as a perfect homogeneous and isotropic fluid. However, the Universe as we observe it today is rich in complex large-scale structures such as galaxies, galaxy clusters, and vast cosmic filaments. Those structures have evolved over billions of years from small-scale density inhomogeneities. Thus, to understand how today's structures emerged, one must understand the physics behind their original seeding and subsequent growth.

9.2.1. Inflation and the Seeds for Initial Structures

It is now widely believed and part of the cosmological standard model that during the very early epochs, the Universe underwent a phase of rapid accelerated expansion, known as *cosmic inflation*. Originally introduced to explain among other conceptual problems the next-to-perfect flatness and isotropy of the Universe, it also provides an explanation for small scale initial density perturbations.

During inflation (approximately from $10^{-36}s$ to $10^{-33}s$ after the Big Bang), the Universe undergoes an accelerated expansion $\ddot{a} > 0$, which leads to a shrinking comoving Hubble radius r_H ,

$$\dot{r}_H = \frac{\mathrm{d}}{\mathrm{d}t} \left(\frac{c}{a H(a)} \right) < 0, \qquad (9.23)$$

⁴In some contexts, a distinction is made between a true cosmological constant and more general dark energy models with dynamical behavior.

9. Cosmology

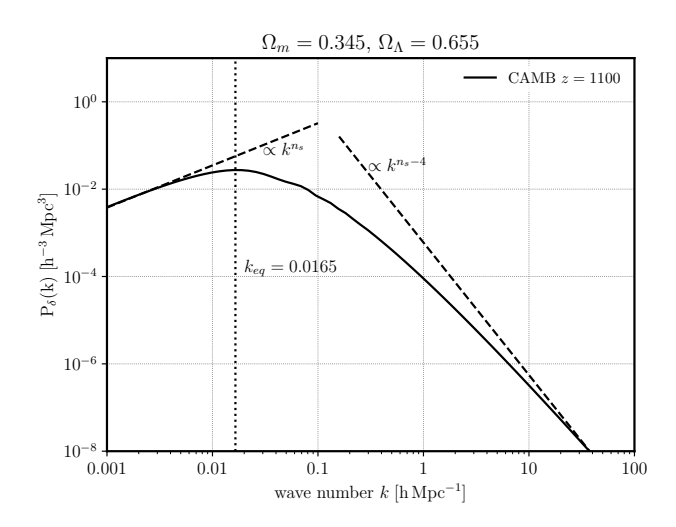


Figure 9.1.: This figure illustrates the scaling of the power spectrum shortly after Recombination (z=1100) for a Λ CDM cosmology generated with CAMB [92]. The limits (9.27) for the large- and small scale behavior of the initial power spectrum are represented by dashed lines. The matter-radiation equality scale k_{eq} is indicated by the dotted line. The wiggles in the dark-matter power spectrum around $k=0.3\,\mathrm{h\,Mpc^{-1}}$ are imprints of baryonic acoustic oscillations (BAOs).

which characterizes the scale of the observable Universe. If the Hubble radius shrinks enough, it can explain both the flatness and the isotropy of the Universe we observe today. If the Hubble radius shrinks below the particle horizon, which defines the maximum distance that particles can travel during the lifetime of the Universe, then the observable Universe would have been in causal contact. This would explain why the Cosmic Microwave Background radiation corresponds to a (near perfect) black-body radiation with only tiny temperature fluctuations of the order of 10^{-5} K. A shrinking Hubble horizon, would also cause $\Omega_k(t) \propto \frac{1}{a(t)^2 H(t)^2}$ to shrink drastically in time. As a result, any initial curvature is exponentially suppressed, driving the Universe towards flatness, without the need for fine-tuned initial conditions. In addition to solving these important theoretical problems, inflation also provides a mechanism for generating the primordial density fluctuations which allow structures to form at later times. The simplest model for this inflationary phase is that of a scalar quantum field, the inflaton, which slowly settles into a minimum of its potential⁵. As a quantum field, the inflaton is subject to microscopic quantum fluctuations before inflation. During the inflationary phase, quantum fluctuations whose wavelengths exceed the rapidly shrinking Hubble radius are "frozen" outside the Hubble horizon as they lose their causal connection. These fluctuations of the inflaton field translate into curvature perturbations, since space-time is distorted by its energy content. They can be described by the comoving curvature perturbations \mathcal{R} which is conserved outside the horizon for adiabatic perturbations and is proportional to the gravitational potential Φ in Newtonian gauge. For slow-roll inflation, the

⁵These models are generally known as slow roll models.

power spectrum of the comoving curvature perturbations is nearly scale invariant,

$$P_{\mathcal{R}}(k) \propto k^{n_s - 1} \,, \tag{9.24}$$

with spectral index n_s which is determined by the slow-roll parameters and is expected to be very close to one. For $n_s = 1$ one arrives at the perfectly scale-free Harrison-Zel'dovich power spectrum. Current observations indicate that $n_s = 0.9665$, confirming a slight deviation from scale invariance. Since \mathcal{R} is proportional to the gravitational potential, we can finally relate the power spectrum of the comoving curvature perturbations $P_{\mathcal{R}}$ to the primordial power spectrum of density fluctuations P_{δ}^{prim} using Poisson's equation,

$$P_{\delta}^{\text{prim}}(k) \propto k^4 P_{\mathcal{R}}(k) \propto k^{n_s+3}$$
. (9.25)

After inflation ends, the comoving Hubble radius increases and modes which were "frozen" outside the horizon, re-enter the horizon during the subsequent radiation and matter dominated era⁶. Since the primordial density perturbations in and outside the horizon grow differently during the radiation dominated era, the initially nearly scale-free power spectrum (9.25) is changed. While perturbations outside the horizon continue to grow, perturbations entering the horizon during radiation domination cannot grow efficiently: they either undergo oscillations in baryonic matter, or remain nearly constant in dark matter. During matter domination, there is nothing to suppress growth and matter perturbations grow equally in- and outside the horizon. A characteristic scale is, thus, set by the comoving wave number at radiation-matter equality,

$$k_{eq} = 2\pi \frac{H_0}{c} \sqrt{\frac{2\Omega_{m,0}}{a_{eq}}}$$
 (9.26)

The dark-matter power spectrum well after radiation-matter equality at $z \approx 3528$, can be approximated by

$$P_{\delta}^{(i)}(k) = \begin{cases} k^{n_s} & k \ll k_{eq} \\ k^{n_s - 4} & k \gg k_{eq} \end{cases}$$
 (9.27)

In figure 9.1 the initial power spectrum which will be used throughout this thesis is shown, which follows the characteristic form described by (9.27).

9.3. Cosmic Structure Formation

Having discussed the formation of initial perturbations, we can now turn to their evolution within the matter dominated epoch at late times. In this section we present the most conventional approaches to which we will compare our results in the next chapters. Most of these models rely on a *coarse-grained*, *continuous*

⁶Actually, inflation is followed by a phase called *reheating*, during which the inflaton field decays into other fields in order to fill the Universe with the known types of matter. However, this mechanism is not well understood today.

9. Cosmology

hydrodynamical description of matter, typically treating the cosmic medium as an ideal and pressureless, self-gravitating fluid. This assumption is justified, if the system is close to local equilibrium at sufficiently early times, and that local particle velocities with respect to this equilibrium state are non-relativistic. Given that cold dark matter dominates the energy density of the Universe throughout most of its history, and that baryonic physics becomes relevant mostly on small scales, we restrict our attention here to dark-matter-only models. This simplification allows us to focus on the pure gravitational dynamics that drive the formation of large-scale structures.

9.3.1. Eulerian Standard Perturbation Theory

The starting point of standard perturbation theory (SPT) is the Vlasov equation (2.92),

$$\partial_t f_1(x,t) + \frac{\vec{p}}{m} \cdot \nabla_{\vec{r}} f_1(x,t) - [\nabla_{\vec{r}} \Phi_G(\vec{r},t)] \cdot \nabla_{\vec{p}} f_1(x,t) = 0, \qquad (9.28)$$

describing the motion of a collisionless fluid subject to the gravitational potential $\Phi_{G}(\vec{r},t)$ which is sourced by the Newtonian Poisson equation,

$$\Delta_r \Phi_G(\vec{r}, t) = 4 \pi G_N \rho_m(\vec{r}, t) - \Lambda c^2, \qquad \rho_m(\vec{r}, t) = \int d^3 p \, m \, f_1(x, t), \qquad (9.29)$$

where $\rho_m(\vec{r},t)$ is the local mass density of the fluid. Here $x=(\vec{r},\vec{p})$ are the physical phase-space coordinates. By now it should be clear that the above equation with its non-linearity introduced by the gravitational interaction in the last term on the right-hand side of (9.28) is highly non-trivial to solve. The standard approach is to further reduce the amount of information by taking the first few moment equations of (9.28). The moments are defined in (2.56), (2.57) and (2.58). In particular, taking the zeroth and first order moment of (9.28), one arrives at the *continuity equation* and the *Euler equation*,

$$\partial_t \rho_m(\vec{r}, t) + \frac{1}{m} \nabla_{\vec{r}} \cdot \vec{\Pi}(\vec{r}, t) = 0,$$

$$\partial_t \vec{\Pi}(\vec{r}, t) + \frac{1}{m} \nabla_{\vec{r}} \cdot \hat{T}(\vec{r}, t) + \frac{1}{m} \rho_m(\vec{r}, t) \nabla_{\vec{r}} \Phi_G(\vec{r}, t) = 0,$$
(9.30)

where $\vec{\Pi}(\vec{r},t)$ is the momentum density and $\hat{T}(\vec{r},t)$ is the stress-energy tensor. These equations appear in the treatment of hydrodynamics and are therefore called *fluid equations*. As one can see, the free-streaming term $\frac{\vec{p}}{m} \cdot \nabla_{\vec{r}} f_1(x,t)$ in (9.28) leads to each moment equation depending on the next higher-order moment, thereby again generating an infinite hierarchy that must be truncated to achieve a closed system of equations. Thus, to find an appropriate truncation to the system (9.30), one combines the moments $\rho_m(\vec{r},t)$ and $\vec{\Pi}(\vec{r},t)$ to a velocity field $\vec{v}(\vec{r},t)$ and a velocity

dispersion tensor $\hat{\sigma}(\vec{r},t)$, defined as

$$\vec{v}(\vec{r},t) := \frac{\vec{\Pi}(\vec{r},t)}{\rho_m(\vec{r},t)},$$

$$\hat{\sigma}(\vec{r},t) := \frac{1}{m \, \rho_m(\vec{r},t)} \hat{T}(\vec{r},t) - \vec{v}(\vec{r},t) \otimes \vec{v}(\vec{r},t).$$
(9.31)

 $\vec{v}(\vec{r},t)$ describes the velocity-field of a mean flow of the fluid and $\hat{\sigma}(\vec{r},t)$ measures deviations from it. Inserting those definitions into the fluid equations (9.30), we find

$$\partial_{t} \rho_{m}(\vec{r}, t) + \frac{1}{m} \nabla_{\vec{r}} \cdot (\rho_{m}(\vec{r}, t) \, \vec{v}(\vec{r}, t)) = 0,$$

$$\partial_{t} \vec{v}(\vec{r}, t) + (\vec{v}(\vec{r}, t) \cdot \nabla_{\vec{r}}) \, \vec{v}(\vec{r}, t) + \frac{1}{m} \nabla_{\vec{r}} \Phi_{G}(\vec{r}, t) + \frac{\nabla_{\vec{r}} \cdot (\rho_{m}(\vec{r}, t) \hat{\sigma}(\vec{r}, t))}{\rho_{m}(\vec{r}, t)} = 0.$$
(9.32)

The simplest possible truncation of this system arises by the *single-stream approximation* (SSA) in which the effect of the velocity dispersion tensor is neglected, $\hat{\sigma}(\vec{r},t) \equiv 0$. Thus, one discards all deviations from the mean macroscopic flow. One then finds a closed system described by

$$\partial_{t} \rho_{m}(\vec{r}, t) + \frac{1}{m} \nabla_{\vec{r}} \cdot (\rho_{m}(\vec{r}, t) \, \vec{v}(\vec{r}, t)) = 0,$$

$$\partial_{t} \, \vec{v}(\vec{r}, t) + (\vec{v}(\vec{r}, t) \cdot \nabla_{\vec{r}}) \, \vec{v}(\vec{r}, t) + \frac{1}{m} \nabla_{\vec{r}} \Phi_{G}(\vec{r}, t) = 0.$$
(9.33)

In the cosmological context, we are working on an expanding background. It is thus convenient to introduce *comoving coordinates* \vec{q} defined by $\vec{r}(t) = a(t)\vec{q}(t)$, in order to separate the background movement of the flow. The velocity field thus splits into two components,

$$\vec{v}(\vec{r},t) = \partial_t \vec{r}(t) = \dot{a}\vec{q} + a\dot{\vec{q}} = \vec{v}_{\text{Hubble}}(\vec{q},t) + a\vec{v}_{\text{pec}}(\vec{q},t), \qquad (9.34)$$

where we defined the *Hubble flow* $\vec{v}_{\text{Hubble}}(\vec{q},t) = H(t)\vec{r}$, capturing the background motion, and the peculiar velocity field $\vec{v}_{\text{pec}}(\vec{q},t)$, describing the intrinsic motion of the fluid. The perturbation theory now arises by describing the density as a fluctuation field $\delta(\vec{q},t)$ over a mean background $\bar{\rho}_m(t)$, with

$$\rho_m(\vec{q}, t) = \bar{\rho}_m(t) (1 + \delta(\vec{q}, t)). \tag{9.35}$$

Additionally, we also split the potential into a mean background density contribution and a fluctuation, $\Phi_{\rm G}(\vec{q},t) = \bar{\Phi}_{\rm G}(\vec{q},t) + \Phi_{\rm G}^{\delta}(\vec{q},t)$, demanding that the fluctuation $\Phi_{\rm G}^{\delta}(\vec{q},t)$ is sourced by the density fluctuations $\delta(\vec{q},t)$ via the Poisson equation

$$\Delta_q \, \Phi_{\rm G}^{\delta}(\vec{q}, t) = 4 \, \pi \, G_{\rm N} \, a^2 \, \bar{\rho}_m(t) \, \delta(\vec{q}, t) = \frac{3}{2} \, a^2 \, H^2 \, \Omega_m(t) \, \delta(\vec{q}, t) \,, \tag{9.36}$$

9. Cosmology

where we inserted the evolution (9.12) for the mean background matter density. Inserting (9.35) and (9.34) into (9.33) and subtracting the background evolution equations, one finally arrives at

$$\partial_{t} \, \delta(\vec{q}, t) + \nabla_{\vec{q}} \cdot ((1 + \delta(\vec{q}, t)) \, \vec{v}_{\text{pec}}(\vec{q}, t)) = 0 \,,$$

$$\partial_{t} \, \vec{v}_{\text{pec}}(\vec{q}, t) + 2 \, H \, \vec{v}_{\text{pec}}(\vec{q}, t) + (\vec{v}_{\text{pec}}(\vec{q}, t) \cdot \nabla_{\vec{q}}) \, \vec{v}_{\text{pec}}(\vec{q}, t) + \frac{1}{a^{2}} \nabla_{\vec{q}} \, \Phi_{G}^{\delta}(\vec{q}, t) = 0 \,.$$
(9.37)

This is the final set of equations from which one can start a perturbation theory. We have to emphasize again that there has already been made an approximation in the derivation of (9.37) by assuming $\hat{\sigma} = 0$ in (9.32). Thus, even when we achieve a full solution to the above system, we would still rely on the validity of the single-stream approximation.

Let us now analyze the linear order resulting from the above set of equations, i.e., we assume $\delta \ll 1$ and $|\vec{v}_{\rm pec}| \ll 1$. The corresponding equations are

$$\partial_{t} \, \delta(\vec{q}, t) + \nabla_{\vec{q}} \cdot \vec{v}_{\text{pec}}(\vec{q}, t) = 0 \,,$$

$$\partial_{t} \, \vec{v}_{\text{pec}}(\vec{q}, t) + 2 \, H \, \vec{v}_{\text{pec}}(\vec{q}, t) + \frac{1}{a^{2}} \nabla_{\vec{q}} \, \Phi_{G}^{\delta}(\vec{q}, t) = 0 \,. \tag{9.38}$$

Taking a further time derivative of the first equation and combining it with the second one, we arrive at

$$\partial_t^2 \delta(\vec{q}, t) + 2 H(t) \partial_t \delta(\vec{q}, t) - \frac{3}{2} H^2(t) \Omega_m^2(t) \delta(\vec{q}, t) = 0, \qquad (9.39)$$

which is the growth equation of linear SPT. It is a linear, second order ODE, where the coefficients only depend on time. We can therefore make the separation ansatz $\delta(\vec{q},t) = D(t) \, \delta(\vec{q},t^{(i)})$, to find the corresponding equations for the linear growth factor D(t),

$$\ddot{D}(t) + 2H(t)\dot{D}(t) - \frac{3}{2}H^{2}(t)\Omega_{m}^{2}(t)D(t) = 0.$$
 (9.40)

As a second order differential equation, the general solution for D(t) consists of two linearly independent modes. A faster growing mode $D_+(t)$ describing the amplification of density perturbations, which is the physically relevant solution for the study of structure formation and the slower growing mode $D_-(t)$, which rapidly becomes negligible compared to $D_+(t)$. For an Einstein-de Sitter Universe with $\Omega_m = 1$, we find

$$D_{+}(a) = a$$
, $D_{-}(a) = a^{-\frac{3}{2}}$. (9.41)

For a Λ CDM cosmology with exactly vanishing radiation contribution, $\Omega_r = 0$, there also exists an analytical solution [93], given by

$$D_{+}(a) = a \frac{{}_{2}F_{1}\left(\frac{1}{3}, 1; \frac{11}{6}; -a^{3}w\right)}{{}_{2}F_{1}\left(\frac{1}{3}, 1; \frac{11}{6}; -w\right)}, \qquad D_{-}(a) = a^{-\frac{3}{2}} \frac{{}_{2}F_{1}\left(-\frac{1}{2}, \frac{1}{6}; \frac{1}{6}; -a^{3}w\right)}{{}_{2}F_{1}\left(-\frac{1}{2}, \frac{1}{6}; \frac{1}{6}; -w\right)}, \quad (9.42)$$

where ${}_2F_1(a,b;c;z)$ is the Gaussian hypergeometric function, and $w=\frac{1-\Omega_{m,0}}{\Omega_{m,0}}$ is the fraction of matter energy density at present time. It is furthermore convenient to define the logarithmic derivative of the growth factor w.r.t. the scale factor a as

$$f := \frac{\mathrm{d}\ln(D(a))}{\mathrm{d}\ln(a)} = \frac{a}{D(a)}\frac{\mathrm{d}D}{\mathrm{d}a}, \tag{9.43}$$

which describes how fast density perturbations grow relative to the scale factor. Clearly in an Einstein-de Sitter Universe, we find $\frac{\Omega_m}{f^2} = 1$ exactly. For a more general Λ CDM model, this is no longer true. However, one can show empirically [94], that $\frac{\Omega_m}{f^2} \simeq 1$ holds approximately to within 10% accuracy for a long time period. Thus, setting $\frac{\Omega_m}{f^2} = 1$ maps a general Λ CDM cosmology to a simpler Einstein-de Sitter one, which is a useful approximation for many analytical applications [95].

9.3.2. Path-Integral Formulation of SPT

The path-integral approach presented in chapter 3, can also be used to construct a generating functional based on the hydrodynamical equations (9.38), as was shown by [6]. Introducing the rescaled peculiar velocity field $\vec{u}_{pec} := \vec{v}_{pec}/H$ and transforming to the time-coordinate $\eta := \ln(a)$, we can write (9.37) as

$$\partial_{\eta} \delta(\vec{q}, \eta) + \nabla_{\vec{q}} \cdot ((1 + \delta(\vec{q}, \eta)) \, \vec{u}_{pec}(\vec{q}, \eta)) = 0 \,, (9.44)$$

$$\partial_{\eta} \vec{u}_{pec}(\vec{q}, \eta) + 2 \, \vec{u}_{pec}(\vec{q}, \eta) + (\vec{u}_{pec}(\vec{q}, \eta) \cdot \nabla_{\vec{q}}) \, \vec{u}_{pec}(\vec{q}, \eta) + \frac{3}{2} \Omega_m(\eta) \, \delta(\vec{q}, \eta) = 0 \,. (9.45)$$

After taking the divergence of Euler's equation (9.45), hence dropping any curl contribution and transforming to Fourier space, and introducing the field doublet

$$\varphi_a(\vec{k}, \eta) \equiv \begin{pmatrix} \delta(\vec{k}, \eta) \\ -\theta(\vec{k}, \eta) \end{pmatrix}, \qquad (9.46)$$

where we defined the velocity divergence field $\theta := \nabla \cdot \vec{u}_{pec}$, we can bring the equations of motion into the compact form

$$(\delta_{ab}\partial_{\eta} + \Omega_{ab}(\eta))\varphi_b(\vec{k},\eta) - \int_{\vec{k}_1,\vec{k}_2} \delta_D\left(\vec{k} - \vec{k}_1 - \vec{k}_2\right)\gamma_{abc}\left(\vec{k}_1,\vec{k}_2\right)\varphi_b(\vec{k}_1,\eta)\varphi_c(\vec{k}_2,\eta) = 0.$$
(9.47)

The linear equations of motion are defined by the matrix

$$\Omega_{ab}(\eta) = \begin{pmatrix} 0 & -1\\ -\frac{3}{2}\Omega_m(\eta) & 1 + \frac{H'(\eta)}{H(\eta)} \end{pmatrix} , \qquad (9.48)$$

where the prime denotes a derivative with respect to η . The non-zero elements of

9. Cosmology

 γ_{abc} are given by

$$\gamma_{121}(\vec{k}_2, \vec{k}_1) = \gamma_{112}(\vec{k}_1, \vec{k}_2) = \frac{(\vec{k}_1 + \vec{k}_2) \cdot \vec{k}_2}{2 k_2^2} ,$$

$$\gamma_{222}(\vec{k}_1, \vec{k}_2) = \frac{(\vec{k}_1 + \vec{k}_2)^2 (\vec{k}_1 \cdot \vec{k}_2)}{2 k_1^2 k_2^2} .$$
(9.49)

For an EdS cosmology with $\Omega_m(\eta) = 1$ and $\frac{H'}{H} = -\frac{1}{2}$, the solution of the linear equations of motion is particularly simple. As discussed in the previous section, any Λ CDM cosmology can be mapped to EdS through an appropriate change of variables to a very good approximation. In this simple case, the linear retarded propagator $g_{ab}^{\rm R}$ can be explicitly calculated by solving

$$(\delta_{ac}\partial_{\eta} + \Omega_{ac}(\eta)) g_{cb}^{R}(\eta, \eta') = \delta_{ab}\delta_{D}(\eta - \eta')$$
(9.50)

for $\eta > \eta'$. It is given by

$$g_{ab}^{R}(\eta, \eta') = \frac{e^{\eta - \eta'}}{5} \begin{pmatrix} 3 & 2\\ 3 & 2 \end{pmatrix} \Theta(\eta - \eta') - \frac{e^{\frac{3}{2}(\eta - \eta')}}{5} \begin{pmatrix} -2 & 2\\ 3 & -3 \end{pmatrix} \Theta(\eta - \eta')$$
(9.51)

where $\Theta(\eta - \eta')$ is the Heaviside function ensuring causality. The decaying mode given by the second term can be neglected for large $(\eta - \eta')$. Following the same procedure detailed in section 3.2.2, the generating functional can be written as [5]

$$Z[J,K] = \exp\left\{-i \int d\eta \,\gamma_{abc} \left(\frac{-i\delta}{\delta K_a} \frac{-i\delta}{\delta J_b} \frac{-i\delta}{\delta J_c}\right)\right\} Z_0[J,K]$$
 (9.52)

with the generating functional of the free theory given by

$$Z_{0}[J,K] = \exp\left\{-\int_{\eta',\eta''} \left[\frac{1}{2}J_{a}(-\vec{k},\eta')P_{ab}^{L}(k,\eta',\eta'')J_{b}(\vec{k},\eta'') + iJ_{b}(-\vec{k},\eta')g_{ab}^{R}(\eta',\eta'')K_{b}(\vec{k},\eta'')\right]\right\},$$
(9.53)

where appropriate source fields K_a and J_a were introduced and P_{ab}^L corresponds to the initial power spectrum evolved at linear order,

$$P_{ab}^{L}(k,\eta,\eta') = g_{ac}^{R}(\eta,0)g_{bd}^{R}(\eta',0)P_{cd}^{(i)}(k).$$
(9.54)

As usual perturbative corrections to the free theory are obtained by expanding the exponential in powers of γ_{abc} . We can now read off the Feynman rules from the generating functional for the three fundamental building blocks of the theory which

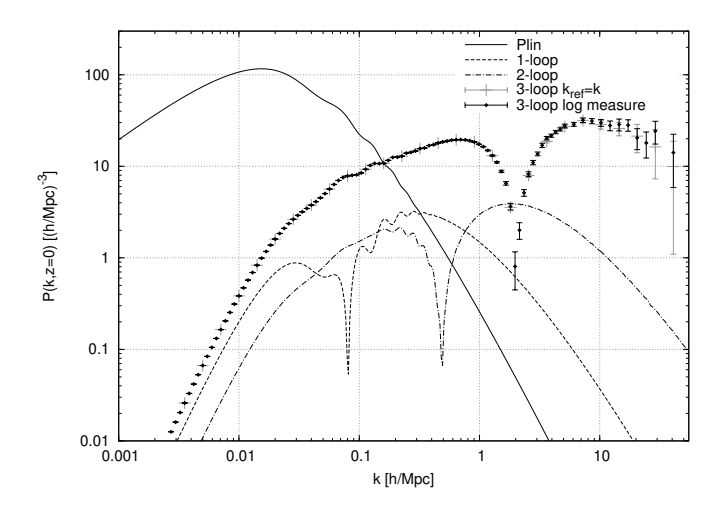


Figure 9.2.: This figure was taken from Blas et al. 2014 [96] and shows the loop-contributions up to third-loop order for SPT. The two-loop contribution on small scales exceeds the one-loop contribution. The three-loop contribution finally confirms the suspicion that the loop expansion in SPT is divergent.

can be represented by the following Feynman diagrams,

$$= -ig_{ab}^{R}(\eta_a, \eta_b), \qquad = P_{ab}^{L}(k, \eta_a, \eta_b),$$

$$= -i\gamma_{abc}(\vec{k}_b, \vec{k}_c)\delta_{D}\left(\vec{k}_a - \vec{k}_b - \vec{k}_c\right).$$

$$(9.55)$$

At one-loop order we then find the following diagrams,

However, it has been shown [96] that the perturbative loop expansion does not converge. Already at second loop-order, the two-loop contribution exceeds the amplitude of the one-loop correction on small scales. Evaluating the three-loop correction has confirmed that the perturbation series is divergent. This can be seen from figure 9.2. Therefore, most effort has gone into finding a better (non-perturbative) resummation scheme and to go beyond the truncation imposed by the SSA.

9.3.3. Lagrangian Perturbation Theory

In contrast to Eulerian Standard Perturbation Theory, which deals with continuous fields such as density and velocity, Lagrangian Perturbation Theory (LPT) is built on the premises of following the trajectories of particles or fluid elements. The central

9. Cosmology

object of LPT is the displacement field $\vec{\Psi}(\vec{q},t)$ which maps the initial particle position in Lagrangian coordinates $\vec{q}^{(i)}$ onto the Eulerian particle position \vec{x} at some later time t,

$$\vec{x}(t) = \vec{q}^{(i)} + \vec{\Psi}(\vec{q}^{(i)}, t)$$
 (9.57)

Starting from the equations for motion for the particle positions (9.57), an evolution equation for the displacement field $\vec{\Psi}(\vec{q},t)$ can be derived, which can then be solved perturbatively. To linear order in PT, the following solution can is obtained

$$\vec{\nabla}_{\vec{q}^{(i)}} \cdot \vec{\Psi}^{(1)}(\vec{q}^{(i)}, t) = -D_{+}(t) \, \delta(\vec{q}^{(i)}) \,, \tag{9.58}$$

where $D_{+}(t)$ is the linear growth factor obeying (9.40) and $\delta(\vec{q}^{(i)})$ is the initial density contrast. In modern cosmology LPT, and especially second order LPT (2LPT), is widely used to generate the initial conditions for large numerical N-body simulations. In fact, we will use this approach to set up the initial conditions for our theoretical description of large-scale structure formation in chapter 10.

9.3.4. State of the Art in Cosmic Structure Formation

Standard Perturbation Theory as well as Lagrangian Perturbation Theory fail to correctly describe large-scale structure formation where linear theory is no longer sufficient. The perturbation series of SPT, for instance, start to diverge at three-loop order. In addition, both suffer from the so-called *shell-crossing problem*, which manifests itself in different ways. In SPT the problem occurs due to the SSA which implies that the system can be described by smooth density and velocity fields. However, this assumption breaks down once different streams start to cross. This, of course, severely limits the range of validity of SPT in the context of non-linear cosmic structure formation.

Although LPT is technically free of the SSA, it still breaks down once shell-crossing becomes important. The problem arises due to the computation of the forces acting on a trajectory in regions where multiple streams cross at the same Eulerian position. The total gravitational force acting on a fluid element at this position should, therefore, be the sum of the individual contributions from each stream. The fluid element should then be accelerated by this total force. Instead, the LPT solutions only accelerate fluid elements with the gravitational force field of their individual stream even after shell-crossing [97]. Attempts at rectifying this issue have, so far, not produced quantitative results which could indicate their success.

Today, numerical N-body simulations provide the most reliable results for cosmic large-scale structure formation. However, they come with a high computational cost. In addition, it is not possible to provide a complete coverage of the relevant range of scales with a satisfactory resolution. And last but not least, numerical simulations offer only limited insight into the underlying physical processes governing cosmic structure formation. It is, therefore, inevitable to develop viable analytical methods for this task.

10 Newtonian Dynamics of Correlated Particles on an Expanding Space-Time

We will now specialize the theoretical frameworks discussed in Part I and II to the case of cosmic structure formation. We will model the dark matter distribution in the universe as a self-gravitating ensemble of N classical particles evolving on an expanding background. The true nature of dark matter particles is hereby irrelevant. First, we define the appropriate Hamilton function and interaction potential which describe the evolution of individual particles on an expanding background. Once the Hamilton function is defined, the trajectories of the particles are fixed, and the behavior of the particle ensemble—whether in equilibrium or out-of-equilibrium—is only determined by its initial state [98, 28, 27, 99]. For self-gravitating systems, the out-of-equilibrium case is generally the more appropriate description [67, 100, 68]. Influenced by the gravitational potential, the initial state will evolve over time. We set up a suitable initial phase-space density, which shall contain all relevant correlations needed for the analysis of cosmic structure formation. We will follow the derivations presented in [58, 29].

10.1. Particle Trajectories on an Expanding Background

We begin by describing the dynamics of a point-like test particle of mass m which move under the influence of gravitational interaction with a density field. The density field itself consists of N individual particles of the same mass. The derivation follows similar steps as the one presented in section 9.3.1. In physical coordinates, the corresponding Lagrange function reads

$$\mathcal{L}(\vec{r}, \dot{\vec{r}}, t) = \frac{1}{2} m \dot{\vec{r}}^2 - m \Phi_{G}(\vec{r}, t), \qquad (10.1)$$

where the Newtonian gravitational potential $\Phi_{G}(\vec{r},t)$ is sourced by the mass density $\rho_{m}(\vec{r},t)$ through Poisson's equation (c.f. equation (9.29)),

$$\Delta_r \Phi_G(\vec{r}, t) = 4\pi G_N \rho_m(\vec{r}, t) - \Lambda c^2, \qquad (10.2)$$

with the gravitational constant G_N and the cosmological constant Λ . In order to separate the background expansion from the peculiar particle motion, we switch to comoving coordinates $\vec{r}(t) = a(t)\vec{q}(t)$, where the cosmological scale factor a(t) derives from Friedmann's second equation (9.8), for a pressureless fluid

$$\frac{\ddot{a}(t)}{a(t)} = -\frac{4\pi G_{\rm N}}{3} \bar{\rho}_m(t) + \Lambda c^2.$$
 (10.3)

Here, $\bar{\rho}_m(t)$ denotes the mean mass density, governing the background expansion. In comoving coordinates the Langrange function (10.1) takes on the form

$$\mathcal{L}(\vec{q}, \dot{\vec{q}}, t) = \frac{1}{2} m \left(\dot{a}\vec{q} + a\dot{\vec{q}} \right)^2 - m\Phi_{G}(\vec{q}, t). \tag{10.4}$$

We apply a gauge transformation by adding a total time-derivative of a function f(t) to the Lagrange function in order to bring it into a more convenient form. Specifically, we choose $f(t) = \frac{1}{2}ma\dot{a}\vec{q}^2$, leading to

$$\mathcal{L}'(\vec{q}, \dot{\vec{q}}, t) = \mathcal{L}(\vec{q}, \dot{\vec{q}}, t) + \frac{\mathrm{d}}{\mathrm{d}t} f(t)$$

$$= \frac{1}{2} m a^2 \dot{\vec{q}}^2 - m \varphi_{\mathrm{G}}(\vec{q}, t), \qquad (10.5)$$

where the gravitational potential is redefined as

$$\varphi_{G}(\vec{q},t) = \Phi_{G}(\vec{q},t) + \frac{1}{2}a\ddot{a}\vec{q}^{2}.$$
(10.6)

Its physical interpretation can be inferred from the corresponding Poisson equation,

$$\Delta_q \varphi_{\mathcal{G}}(\vec{q}, t) = \frac{4\pi G_{\mathcal{N}}}{a(t)} \left(\rho_m(\vec{q}, t) - \bar{\rho}_m \right) = \frac{4\pi G_{\mathcal{N}}}{a(t)} \bar{\rho}_m \, \delta(\vec{q}, t) \,. \tag{10.7}$$

In the above, we inserted Friedmann's equation (10.3) and used that the mean density in comoving coordinates is constant in time. Furthermore, the density contrast δ is defined as $\delta(\vec{q},t) = \frac{\rho_m(\vec{q},t) - \bar{\rho}_m}{\bar{\rho}_m}$. Thus, $\varphi_G(\vec{q},t)$ is only sourced by density fluctuations which corresponds exactly to the Newtonian limit of general relativity¹. Since we model the density field by N individual particles, the comoving mass density is given

¹This is the so-called *Jeans swindle*. By "artificially" dropping the infinite contribution from the mean background, we render the self-gravitating system well-defined. This can be argued for, as by isotropy, the homogeneous background does not exhibit a force on a test particle. However, viewed from the perspective of general relativity, this problem does not arise, because the homogeneous background is itself a solution of the field equations with its own dynamics, incorporated in the scale factor a, which is not true in the Newtonian case.

by

$$\rho_m(\vec{q}, t) = m \sum_{i=1}^{N} \delta_{\rm D} (\vec{q} - \vec{q}_i(t)) . \qquad (10.8)$$

We can, therefore, find the explicit solution for $\varphi(\vec{q},t)$, given by

$$\varphi_{\rm G}(\vec{q},t) = -\frac{mG_{\rm N}}{a(t)} \sum_{i=1}^{N} \frac{1}{|\vec{q} - \vec{q}_i(t)|} = -\frac{3}{8\pi\bar{\rho}} a(t)^2 H(t)^2 \Omega_m(t) \sum_{i=1}^{N} \frac{1}{|\vec{q} - \vec{q}_i(t)|}. (10.9)$$

For later convenience we have expressed the result in terms of the matter-density parameter Ω_m and the Hubble function $H = \frac{\dot{a}}{a}$. Note, that the dependence on the particle mass has been replaced by a dependence on the inverse mean particle-number density. For numerical as well as analytical reasons, it is advantageous to use the logarithm of the scale factor as the time coordinate. Therefore, we perform the transformation

$$\eta = \ln(a(t)), \quad d\eta = H(t)dt,$$
(10.10)

which, applied to the Lagrange function (10.5), yields

$$\mathcal{L}\left(\vec{q}, \frac{d\vec{q}}{d\eta}, \eta\right) = \frac{1}{2} m e^{2\eta} H(\eta) \left(\frac{d\vec{q}}{d\eta}\right)^2 - m \widetilde{\varphi}_{G}(\vec{q}, \eta),
\widetilde{\varphi}_{G}(\vec{q}, \eta) := \frac{1}{H(\eta)} \varphi_{G}(\vec{q}, \eta).$$
(10.11)

We can now construct the corresponding Hamiltonian function for N mutually interacting particles of equal mass m on this expanding background. We find

$$\mathcal{H}(\mathbf{q}, \mathbf{p}, \eta) = \sum_{i=1}^{N} \frac{\vec{\mathsf{p}}_{i}^{2}}{2 m(\eta)} + \frac{1}{2} \sum_{i \neq j=1}^{N} v_{G}(|\vec{\mathsf{q}}_{i} - \vec{\mathsf{q}}_{j}|, \eta) ,$$

$$\vec{\mathsf{p}}_{i}(\eta) \coloneqq m(\eta) \frac{d\vec{\mathsf{q}}}{d\eta} ,$$

$$m(\eta) \coloneqq m e^{2\eta} H(\eta) ,$$

$$(10.12)$$

where $m(\eta)$ can be interpreted as a time-dependent mass whose time dependence arises from the expanding background and the factor of $\frac{1}{2}$ in (10.12) ensures that each particle pair contributes only once to the total energy of the system. The pair potential $v_G(|\vec{\mathbf{q}}_i - \vec{\mathbf{q}}_j|, \eta)$ derives from (10.9) and reads

$$v_{\rm G}(|\vec{\mathsf{q}}_i - \vec{\mathsf{q}}_j|, \eta) = -\frac{3 \, m(\eta) \, \Omega_m(\eta)}{8 \, \pi \, \bar{\rho}} \, \frac{1}{|\vec{\mathsf{q}}_i - \vec{\mathsf{q}}_j|} \,. \tag{10.13}$$

This is our final result. The scaling of $v_{\rm G} \sim \frac{1}{\bar{\rho}} \sim \frac{1}{N}$ is consistent with the Kacprescription of a long-range interacting potential (c.f. section 8.1.3 and [78, 77]). Thus, in the thermodynamic limit of infinitely many particles, the Vlasov description will be the appropriate one for our formalism. As expected, the gravitational interaction couples to the time-dependent mass factor. Furthermore, in this framework, the strength of the gravitational interaction is set by the matter density parameter $\Omega_m(\eta)$, as only matter sources Newtonian gravity. Consequently, its time dependence reflects the evolution of other components in the universe that dilute the relative strength of the matter contribution. In a purely matter-dominated universe (Einstein-de Sitter with $\Omega_m = 1$), the only time dependence arises from the friction-like effect of the expanding background, encoded in $m(\eta)$. However, when additional components such as a cosmological constant are present, as in Λ CDM cosmology, $\Omega_m(\eta) < 1$, and the effective interaction weakens over time, suppressing gravitational clustering at late times.

We recognize the structure of the general homogeneous Hamiltonian function with time-dependent mass and potential, discussed in section 8.1.4. We can therefore directly read off the particle Green function as

$$G(\eta, \eta') = \begin{pmatrix} g_{qq}(\eta, \eta') \, \mathbb{1}_{3 \times 3} & g_{qp}(\eta, \eta') \, \mathbb{1}_{3 \times 3} \\ \mathbb{0}_{3 \times 3} & g_{pp}(\eta, \eta') \, \mathbb{1}_{3 \times 3} \end{pmatrix} \, \Theta(\eta, \eta') \,, \tag{10.14}$$

with

$$g_{qq}(\eta, \eta') = 1, \quad g_{pp}(\eta, \eta') = 1, \quad g_{qp}(\eta, \eta') = \int_{\eta'}^{\eta} d\bar{\eta} \frac{1}{m(\bar{\eta})}.$$
 (10.15)

10.2. Initial Conditions for Cosmic Structure Formation

Having discussed the trajectories of the individual particles, we will now define a suitable initial phase-space density $\varrho_N^{(i)}(\mathbf{q}^{(i)},\mathbf{p}^{(i)}) \equiv \varrho_N(\mathbf{q}^{(i)},\mathbf{p}^{(i)},\eta^{(i)})$ describing the probabilistic distribution of the initial particle positions and velocities for our statistical system in the cosmological context. As this derivation has already been presented in [29], we simply state the result here and focus on the relevant discussion for our application.

We start from a continuous mass-density field in the early matter-dominated epoch. The central objects describing the state of a system are the mass density field $\rho_m^{(i)}(\vec{q})$ and the peculiar velocity-density field $\vec{\Pi}^{(i)}(\vec{q})$. The cosmological principle, homogeneity and isotropy on large scales suggests that the statistics of both fields can be described by a statistically homogeneous and isotropic probability distribution (c.f. chapter 8). We, therefore, find a constant mean background mass-density and a vanishing mean velocity of the system. It is suitable to describe the mass-density field by its fluctuation around the mean background,

$$\rho_m^{(i)}(\vec{q}) = \bar{\rho}_m^{(i)}(1 + \delta^{(i)}(\vec{q})), \text{ with } \langle \delta^{(i)}(\vec{q}) \rangle = 0.$$
 (10.16)

As predicted by inflationary models and confirmed to high accuracy by observations

of the temperature fluctuations in the CMB, we assume that the tuple

$$d^{(i)}(\vec{q}) := \begin{pmatrix} \delta^{(i)}(\vec{q}) \\ \vec{\Pi}^{(i)}(\vec{q}) \end{pmatrix}$$
 (10.17)

follows a combined multivariate Gaussian distribution²,

$$\mathcal{P}(d^{(i)}) = \frac{1}{\sqrt{(2\pi)^4 \det(C^{(i)})}} e^{-\frac{1}{2}d^{(i)^\top} \cdot C^{(i)^{-1}} \cdot d^{(i)}}, \qquad (10.18)$$

where the covariance matrix is the single parameter characterizing the distribution. It reads

$$C^{(i)} = \begin{pmatrix} C_{\delta\delta}^{(i)} & \vec{C}_{\delta\vec{\Pi}}^{(i)} \\ \vec{C}_{\vec{\Pi}\delta}^{(i)} & C_{\vec{\Pi}\otimes\vec{\Pi}}^{(i)} \end{pmatrix} = \begin{pmatrix} \left\langle \delta^{(i)}(\vec{q}_1)\delta^{(i)}(\vec{q}_2) \right\rangle & \left\langle \delta^{(i)}(\vec{q}_1)\vec{\Pi}^{(i)}(\vec{q}_2) \right\rangle^{\top} \\ \left\langle \vec{\Pi}^{(i)}(\vec{q}_1)\delta^{(i)}(\vec{q}_2) \right\rangle & \left\langle \vec{\Pi}^{(i)}(\vec{q}_1)\otimes\vec{\Pi}^{(i)}(\vec{q}_2) \right\rangle \end{pmatrix}. \quad (10.19)$$

All the above correlation functions are, due to homogeneity and isotropy, functions of the relative distance $|\vec{q}_1 - \vec{q}_2|$ only. Furthermore, they can all be related to the same initial matter-density power spectrum, which is defined as the Fourier transform of $C_{\delta\delta}^{(i)}(r)$,

$$P_{\delta}^{(i)}(k) = \int d^{3}\vec{r} C_{\delta\delta}^{(i)}(r) e^{-i\vec{k}\cdot\vec{r}}.$$
 (10.20)

We now have to map the probability distribution (10.18) of the continuous fields $\delta^{(i)}(\vec{q})$ and $\vec{\Pi}^{(i)}(\vec{q})$ to the corresponding initial phase-space distribution of the canonical positions and momenta of particles that sample the density field. This follows along the same lines as described in section 2.6. Note, however, that we are describing the continuous initial fluid not in terms of the full phase-space density $f_1^{(i)}(\vec{q}, \vec{p})$ but in terms of its first two momentum moments, $\delta^{(i)}(\vec{q})$ and $\vec{\Pi}^{(i)}(\vec{q})$. The logic, however, stays the same, and we use appropriate conditional probabilities of finding the respective particle at a certain phase-space position, given a value of the density and velocity field at that point. The analysis is performed in detail in [29, 58], and we find

$$\varrho_N^{(i)}(\mathbf{q}^{(i)}, \mathbf{p}^{(i)}) = V^{-N} \int \frac{\mathrm{d}\mathbf{t}_p^{(i)}}{(2\pi)^{3N}} \mathcal{C}(\mathbf{q}^{(i)}, \mathbf{t}_p^{(i)}) \, \exp\left(-\frac{1}{2}\mathbf{t}_p^{(i)} \cdot \mathbf{C}_{pp}^{(i)} \cdot \mathbf{t}_p^{(i)} + \mathrm{i}\mathbf{t}_p^{(i)} \cdot \mathbf{p}^{(i)}\right) \,, \quad (10.21)$$

where, for convenience, we have chosen to represent it as the Fourier transform of the characteristic function w.r.t. the momentum variables. The function $\mathcal{C}(\mathbf{q}^{(i)}, \mathbf{t}_p^{(i)})$, furthermore, contains all initial density-density and density-momentum correlations

²Technically, this is due to both fields being related to the Laplacian and the gradient of the same primordial velocity potential which is, in turn, assumed to be a Gaussian random field.

and reads

$$\mathcal{C}(\mathbf{q}^{(i)}, \mathbf{t}_{p}^{(i)}) = \prod_{j=1}^{N} \left(1 - i\vec{\mathsf{C}}_{\delta_{j}p_{s}}^{(i)} \cdot \vec{\mathsf{t}}_{p_{s}}^{(i)} \right) + \sum_{\substack{j,k=1\\j\neq k}}^{N} \mathsf{C}_{\delta_{j}\delta_{k}}^{(i)} \prod_{\substack{l=1\\l\neq j,k}}^{N} \left(1 - i\vec{\mathsf{C}}_{\delta_{l}p_{s}}^{(i)} \cdot \vec{\mathsf{t}}_{p_{s}}^{(i)} \right) \\
+ \sum_{\substack{j,k=1\\j\neq k}}^{N} \mathsf{C}_{\delta_{j}\delta_{k}}^{(i)} \sum_{\substack{a,b=1\\a\neq b\\a,b\neq j,k}}^{N} \mathsf{C}_{\delta_{a}\delta_{b}}^{(i)} \prod_{\substack{l=1\\l\neq j,k,a,b}}^{N} \left(1 - i\vec{\mathsf{C}}_{\delta_{l}p_{s}}^{(i)} \cdot \vec{\mathsf{t}}_{p_{s}}^{(i)} \right) + \cdots, \tag{10.22}$$

where a sum over same indices is implied. The correspondence between the particle correlations $C_{\delta_j\delta_k}^{(i)}$, $\vec{C}_{\delta_jp_k}^{(i)}$, $C_{p_jp_k}^{(i)}$ and the covariance matrix (10.19) is established in [29, 58] and reads

$$C_{\delta_{j}\delta_{k}}^{(i)} := C_{\delta\delta}(|\vec{q}_{j}^{(i)} - \vec{q}_{k}^{(i)}|) = C_{\delta\delta}(|\vec{q}_{j}^{(i)} - \vec{q}_{k}^{(i)}|),
\vec{C}_{\delta_{j}p_{k}}^{(i)} := \vec{C}_{\delta p}(|\vec{q}_{j}^{(i)} - \vec{q}_{k}^{(i)}|) = m(\eta^{(i)}) \vec{C}_{\delta\vec{\Pi}}(|\vec{q}_{j}^{(i)} - \vec{q}_{k}^{(i)}|),
C_{p_{j}p_{k}} := C_{pp}(|\vec{q}_{j}^{(i)} - \vec{q}_{k}^{(i)}|) = m(\eta^{(i)})^{2} C_{\vec{\Pi}\otimes\vec{\Pi}}(|\vec{q}_{j} - \vec{q}_{k}|),
\mathbf{C}_{pp}^{(i)} := C_{p_{j}p_{k}}^{(i)} \otimes (e_{j} \otimes e_{k}).$$
(10.23)

The time-dependent particle mass, evaluated at the initial time, appears because it relates the initial velocity field to the canonical momenta of the particle ensemble.

From the distribution (10.21) we can now deduce the three lowest-order particlereduced phase-space densities, which we represent in Fourier space. We find for the initial one-particle reduced phase-space density

$$f_1^{(i)}(s_1) = \bar{\rho}(2\pi)^3 \delta_D(\vec{k}_1) \varphi^{(i)}(\vec{\ell}_1),$$
 (10.24)

where the initial momentum distribution function is given by

$$\varphi^{(i)}\left(\vec{\ell}_1\right) = \exp\left(-\frac{1}{2}m(\eta^{(i)})\,\sigma_p^2\vec{\ell}_1^2\right) \tag{10.25}$$

and has the same qualitative structure as the Maxwell-Boltzmann distribution (8.9). Here, we have defined the initial momentum dispersion

$$\sigma_p^2 \equiv \mathsf{C}_{pp}^{(\mathsf{i})}(0) = \frac{1}{3} \int \frac{\mathrm{d}^3 \vec{k}}{(2\pi)^3} \frac{P_\delta^{(\mathsf{i})}(k)}{k^2} \,. \tag{10.26}$$

For the two-particle reduced correlation function g_2 we find analogously,

$$g_2^{(i)}(s_1, s_2) = \bar{\rho}^2 (2\pi)^3 \,\delta_{\mathcal{D}} \left(\vec{k}_1 + \vec{k}_2\right) \,\mathcal{C}_2(\vec{k}_1, \vec{\ell}_1, \vec{\ell}_2) \,\varphi^{(i)}(\vec{\ell}_1) \,\varphi^{(i)}(\vec{\ell}_2) \,. \tag{10.27}$$

We have introduced the functions C_n describing all connected phase-space correlations between n particles at initial time which are obtained from the general expression (10.22). For n=1, this function clearly reduces to $\mathcal{C}_1(\vec{\ell}_1)=1$. For n=2 we get

$$\mathcal{C}_{2}(\vec{k}_{1}, \vec{\ell}_{1}, \vec{\ell}_{2}) = \int d^{3}\vec{r}_{12} e^{-i\vec{k}_{1} \cdot \vec{r}_{12}} \left[\left(1 + \mathsf{C}_{\delta\delta}^{(i)}(r_{12}) - i\mathsf{C}_{\delta p}^{(i)}(r_{12}) \cdot \left(\vec{\ell}_{1} - \vec{\ell}_{2} \right) + \left(\mathsf{C}_{\delta p}^{(i)}(r_{12}) \cdot \vec{\ell}_{1} \right) \left(\mathsf{C}_{\delta p}^{(i)}(r_{12}) \cdot \vec{\ell}_{2} \right) \right] e^{-\vec{\ell}_{1} \cdot \mathsf{C}_{pp}^{(i)}(r_{12}) \cdot \vec{\ell}_{2}} - 1 \right].$$
(10.28)

Analogous expressions can be derived for the initial three-particle reduced correlations functions $g_3^{(i)}$ and \mathcal{C}_3 respectively. Note, that the existence of a non-vanishing $g_3^{(i)}$ is not related to the notion of primordial non-Gaussianities in the density and velocity fields. Instead, it is the consequence of mapping the initial conditions of $\rho^{(i)}$ and $\vec{\Pi}^{(i)}$ to the continuous initial phase-space density $f_1^{(i)}$ on which the formalism is built. The expansion of (10.22)—or \mathcal{C}_2 and \mathcal{C}_3 respectively—strongly resembles a Mayer-cluster expansion. In fact, it has been shown in [30] that the initial distribution can be constructed diagrammatically by considering all possible density-density, density-momentum and momentum-momentum correlations between N-particles. In the absence of those correlations, the initial distribution reduces to an uncorrelated Boltzmann gas, putting the system in thermal equilibrium initially. The interaction potential will then drive the system out of equilibrium, which is what we are going to study next.

11 Results for Cosmic Large-Scale Structure Formation

Having introduced the theoretical framework based on the particle picture in Part I and the field theory approach based on the Klimontovich equation in Part II, we now turn to the discussion of the results for cosmic large-scale structure within these two descriptions. As we have already established on a theory level, the field theory description developed in Part II bears a considerable advantage over the particle-based description in Part I, we primarily present our results in that framework. However, we will discuss the results for the particle-based approach in order to point out the difference on a quantitative level.

We will begin by presenting the results for the tree-level theory for the density-fluctuation power and bispectrum. While the tree-level descriptions will be identical, we will see that for the bispectrum both frameworks will differ in the number of diagrams which need to be evaluated. This is, of course, due to the property of the field theory approach in terms of the Klimontovich equation which contains only one vertex containing the interaction due to the potential. In contrast, the approach in Part I has an infinite tower of vertices with no clear hierarchy. This difference will be even more evident for the one-loop corrections to the power spectrum.

11.1. Tree-Level Results for Cosmic *n*-Point Statistics

Before presenting the full numerical result, we will consider a case for which analytical expressions for the tree-level propagators can be found. In this limit, we will also be able to recover results known from SPT.

In the following derivation we will follow the same lines as in section 8.2.1. Therefore, we will need the corresponding expression for the freely evolved background interaction potential $\tilde{\mathcal{V}}_{R}^{(0)}$. It can be obtained from the general expression (8.44), in which we insert the respective potential and momentum distribution function derived

in the previous chapter. The result is

$$\tilde{\mathcal{V}}_{R}^{(0)}(\vec{k_{1}}, \vec{\ell_{1}}, \eta_{1}, \eta_{2}) = \frac{3}{2}m(\eta_{2})\Omega_{m}(\eta_{2})\left(\frac{\vec{k_{1}} \cdot \vec{\ell_{1}}}{k_{1}^{2}} + g_{qp}(\eta_{1}, \eta_{2})\right) \times \exp\left[-\frac{1}{2}m(\eta^{(i)})\sigma_{p}^{2}(\vec{\ell_{1}} + g_{qp}(\eta_{1}, \eta_{2})\vec{k_{1}})^{2}\right]$$
(11.1)

with g_{qp} given by equation (10.15). From this, we can derive the Volterra integral equation for $\tilde{\Omega}_R$, which reads

$$\tilde{\Omega}_{R}(\vec{k_{1}}, 0, \eta_{1}, \eta_{2}) = \tilde{\mathcal{V}}_{R}^{(0)}(\vec{k_{1}}, 0, \eta_{1}, \eta_{2}) + \int_{\eta_{2}}^{\eta_{1}} d\bar{\eta} \, \tilde{\mathcal{V}}_{R}^{(0)}(\vec{k_{1}}, 0, \eta_{1}, \eta_{2}) \, \tilde{\Omega}_{R}(\vec{k_{1}}, 0, \eta_{1}, \eta_{2}) \,. \tag{11.2}$$

We further need $G_f^{(i)}$ and $G_{ff}^{(i)}$ which are given by the initial reduced distributions $f_1^{(i)}$ and $g_2^{(i)}$ since we are working in the Vlasov description and thus neglect the shot-noise contributions. We stress that $\tilde{\mathcal{V}}_R^{(0)}$ corresponds to the mixed $G_{f\mathcal{B}}^{(0)}$ cumulant in the resummed particle field theory of chapter 5. Thus, at tree-level we will obtain the same analytical as well as numerical results.

Setting the interaction potential $v(\vec{k}, \eta) \equiv 0$, we recover the density-fluctuation power spectrum in the free theory given by,

$$P_{\delta}^{(0)}(\vec{k}_1, t_1, t_2) = \mathcal{C}_2(\vec{k}_1, T_1 \vec{k}_1, -T_2 \vec{k}_1) e^{-\frac{1}{2}m(\eta^{(i)})^2 \sigma_p^2 \vec{k}_1^2 \left(T_1^2 + T_2^2\right)}, \tag{11.3}$$

where T_1 and T_2 are defined as

$$T_1 = g_{qp}(\eta_1, \eta^{(i)}), \quad T_2 = g_{qp}(\eta_2, \eta^{(i)}).$$
 (11.4)

11.1.1. Analytical Solution for an Einstein-de Sitter Cosmology in the Large-Scale Limit

In an Einstein-de Sitter (EdS) cosmology ($\Omega_m = 1$) our system simplifies considerably, and we can perform most of the integrations analytically as has been shown in [34]. We briefly present the calculations for this special case in order to illustrate the structure of the theory in more detail. For instance, we find

$$H(\eta) = H_0 e^{-\frac{3}{2}\eta}, \qquad f(\eta) = H_0 e^{\frac{1}{2}\eta},$$
 (11.5)

which implies,

$$g_{qp}(\eta_1, \eta_2) = -\frac{2H_0}{m} \left(e^{-\frac{1}{2}\eta_1} - e^{-\frac{1}{2}\eta_2} \right). \tag{11.6}$$

In order to solve the Volterra integral equation, we perform a similar approximation as in the toy model described in section 8.2.2 and assume that we are only interested in scales for which $k^2 \ll \frac{1}{\sigma_p^2}$. We can then approximate the exponential in $G_f^{(i)}$ and $G_{ff}^{(i)}$ by 1, and thus neglect the small scale damping. Furthermore, we linearize C_2 in

 $G_{ff}^{(i)}$ in terms of the initial power spectrum as higher order effects will also only be relevant on smaller scales. In this *large-scale limit* we can now solve the Volterra integral equation as described in section 8.2.1 and obtain

$$\tilde{\Omega}_{R}^{(0,\text{LS})}(\vec{k}_{1}, \vec{\ell}_{1}, \eta_{1}, \eta_{2}) = \frac{3}{5} \left(e^{\eta_{1} - \eta_{2}} - e^{-\frac{3}{2}(\eta_{1} - \eta_{2})} + m \frac{\vec{k}_{1} \cdot \vec{\ell}_{1}}{k^{2}} \left[e^{\frac{3}{2}(\eta_{1} - \eta_{2})} + \frac{3}{2} e^{\frac{3}{2}(\eta_{2} - \eta_{1})} \right] \right) \Theta(\eta_{1} - \eta_{2}).$$
(11.7)

Solving the remaining integrals we find for the statistical propagator

$$\Delta_{ff}^{(LS)}(S_1, S_2) = \bar{\rho}^2 (2\pi)^3 \delta_D \left(\vec{k}_1 + \vec{k}_2 \right) \tilde{\Delta}_{ff}^{(LS)}(\vec{k}_1, \vec{\ell}_1, \vec{\ell}_2, \eta_1, \eta_2) , \qquad (11.8)$$

where we defined

$$\tilde{\Delta}_{ff}^{(LS)}(\vec{k}_{1}, \vec{\ell}_{1}, \vec{\ell}_{2}, \eta_{1}, \eta_{2}) = e^{\eta_{1} + \eta_{2} - 2\eta^{(i)}} P_{\delta}^{(i)}(k_{1}) \left(1 + e^{\frac{1}{2}\eta_{1}} \frac{\vec{k}_{1} \cdot \vec{\ell}_{1}}{k_{1}^{2}} \right) \times \left(1 - e^{\frac{1}{2}\eta_{2}} \frac{\vec{k}_{1} \cdot \vec{\ell}_{1}}{k_{1}^{2}} \right).$$
(11.9)

The tree-level two-point cumulant is then given by

$$G_{ff}^{\text{(tree, LS)}}(\vec{k}_1, \vec{\ell}_1, \vec{\ell}_2, \eta_1, \eta_2) \equiv \Delta_{ff}^{\text{(LS)}}(\vec{k}_1, \vec{\ell}_1, \vec{\ell}_2, \eta_1, \eta_2),$$
 (11.10)

which yields the density-fluctuation power spectrum at tree-level upon setting $\vec{\ell}_1 = \vec{\ell}_2 = 0$. We find

$$P_{\delta}^{\text{(tree, LS)}}(\vec{k}_1, \eta_1, \eta_2) = e^{\eta_1 + \eta_2 - 2\eta^{(i)}} P_{\delta}^{(i)}(k).$$
 (11.11)

For equal times, i. e., $\eta = \eta_1 = \eta_2$, we can bring (11.11) into the more familiar form,

$$P_{\delta}^{\text{(tree,LS)}}(\vec{k},\eta) = \frac{D_{+}^{2}(\eta)}{D_{+}^{2}(\eta^{(i)})} P_{\delta}^{(i)}(k), \qquad (11.12)$$

by using that for an EdS cosmology the linear growth factor known from Eulerian SPT is given by $D_{+}(\eta) = e^{\eta}$. The fact, that we reproduce the standard SPT result is of course no surprise, since we have shown that the tree-level description corresponds to solving the linearized Vlasov equation over the free evolution, which, as described earlier, is the approach followed by Eulerian SPT.

Having the full phase-space information at hand in (11.10), we can just as easily obtain velocity power spectra by taking appropriate derivatives with respect to the conjugate velocity variables $\vec{\ell}$, as described in section 8.1.5. For instance, we directly

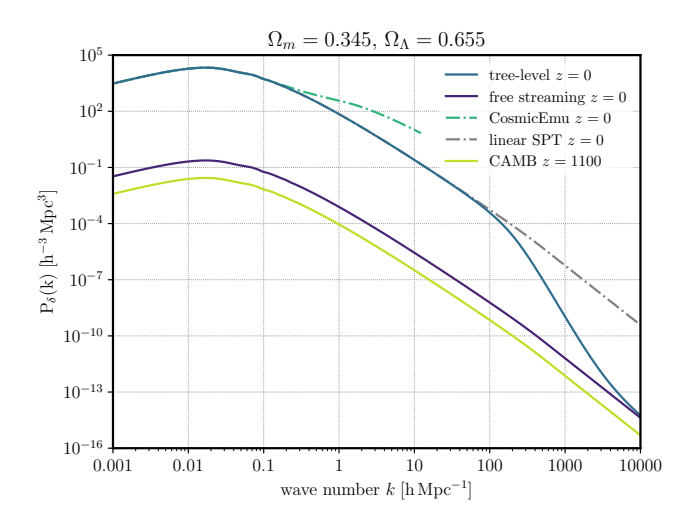


Figure 11.1.: The tree-level result for the density-fluctuation power spectrum $P_{\delta}(k)$ for a standard Λ CDM cosmology is shown and compared to the result obtained with linear SPT (11.15). The initial power spectrum was generated with CAMB [92] at z=1100 and evolved to z=0 according to the tree-level theory. For reference, the non-linear power spectrum as predicted by numerical simulations (Cosmic Emulator [101]) is shown.

find the expression for the velocity-density power spectrum,

$$P_{\vec{\Pi}}^{(\text{tree,LS})}(\vec{k}_{1}, \eta_{1}, \eta_{2}) = \frac{i\nabla_{\vec{\ell}_{1}} \cdot i\nabla_{\vec{\ell}_{2}} G_{ff}^{(\text{tree, LS})}(\vec{k}_{1}, \vec{\ell}_{1}, \vec{\ell}_{2}, \eta_{1}, \eta_{2})}{\bar{\rho}} \Big|_{\vec{\ell}_{1} = \vec{\ell}_{2} = 0}$$

$$= e^{\eta_{1} + \eta_{2} - 2\eta^{(i)}} \frac{P_{\delta}^{(i)}(k_{1})}{\vec{k}_{1}^{2}}.$$
(11.13)

Expressing the above relation in terms of the growth factor for an EdS cosmology, we again find the familiar result which corresponds to the solution found in Eulerian SPT for equal times,

$$P_{\vec{\Pi}}^{\text{(tree,LS)}}(\vec{k}_1, \eta) = \frac{D_+^2(\eta)}{D_+^2(\eta^{(i)})} \frac{P_\delta^{(i)}(k)}{\vec{k}_1^2}.$$
 (11.14)

However, it should be noted that these results are only obtained in the large-scale. Without this simplifying assumption the evolution of structures is a highly non-linear process, already at tree-level. In this case, a fully analytical solution is no longer possible and the integral equations for the causal and statistical propagators have to be solved numerically as described in the following section.

11.1.2. Numerical Results for the Power Spectrum at Tree Level

In general, the Volterra integral equation (11.2) has to be solved numerically upon time-discretisation. The causal structure of $\mathcal{V}_{R}^{(0)}$ reduces the matrix equation to

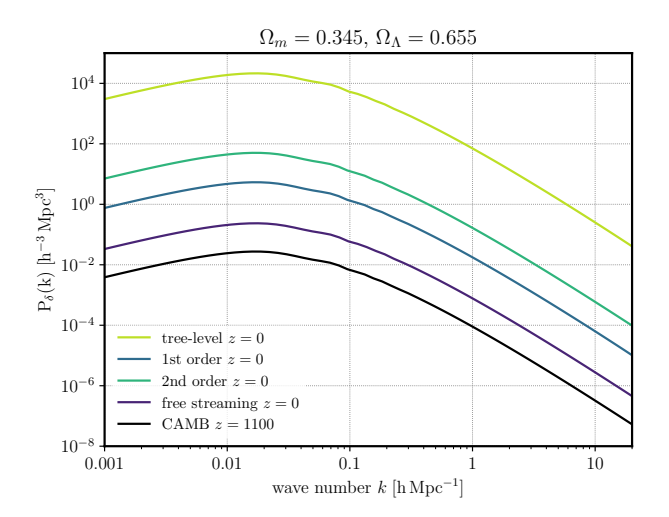


Figure 11.2.: We show the results for the free evolution as well as the first- and secondorder perturbation theory presented in 4 for the density-fluctuation power spectrum $P_{\delta}(k)$ for a standard Λ CDM cosmology. For comparison, the tree-level result is shown whose amplitude is several orders of magnitude higher than that of second-order PT. The initial power spectrum was generated with CAMB [92] at z=1100.

a lower triangular matrix, which can be inverted by forward substitution. After numerically solving the time-integrals, we find the full tree-level result for the statistical propagator $\Delta_{ff}(\vec{k}_1, \vec{\ell}_1, \vec{\ell}_2, \eta_1, \eta_2)$ and thus $G_{ff}^{(\text{tree})}(\vec{k}_1, \vec{\ell}_1, \vec{\ell}_2, \eta_1, \eta_2)$ from which we obtain the density-fluctuation power spectrum $P_{\delta}^{(\text{tree})}(\vec{k}_1, \eta_1, \eta_2)$ according to (8.25).

In figure 11.1 we show the numerical tree-level result for an equal-time density-fluctuation power spectrum $P_{\delta}^{(\text{tree})}(\vec{k},\eta)$ for a standard ΛCDM cosmology, evolved from the time of CMB decoupling at redshift z=1100 to the present at z=0 which was also found in [34, 58]. We compare our result to the free evolution given by (11.3) and the power spectrum obtained from numerical simulations. For reference, we also include the linear power spectrum given by

$$P_{\delta}^{(\text{lin})}(\vec{k},\eta) = \frac{D_{+}^{2}(\eta)}{D_{+}^{2}(\eta^{(i)})} P_{\delta}^{(i)}(k), \qquad (11.15)$$

where $D_+(\eta)$ is the linear growth factor for a Λ CDM cosmology. For wave numbers $k \leq 100 \,\mathrm{h\,Mpc^{-1}}$, the tree-level result exactly follows the linear power spectrum $P_{\delta}^{(\mathrm{lin})}$. On these scales $\sigma_p \sim 10^{-5}$ and we are well within the regime which is well described by the large-scale limit $k^2 \ll \frac{1}{\sigma_p^2}$. In this regime, the effects of the exponential damping are negligible and $\Omega_R^{(0)}$ as well as the causal propagator Δ_R are independent of k and only a time dependent scaling function. On these scales, the amplitudes of initial density-fluctuations simply grow as a function of time only. In general, however, the integral equation which is solved in order to find the tree-level evolution, incorporates non-linear effects in k, leading to deviations from the linear growth on smaller scales.

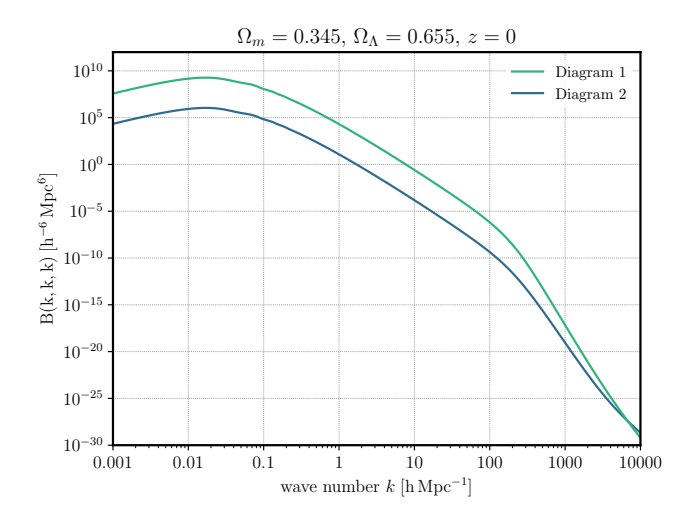


Figure 11.3.: The tree-level result for the two diagram contribution (11.16) to the density-fluctuation bispectrum B(k, k, k) for an equilateral configuration and a standard Λ CDM cosmology are shown. The order corresponds to the order of appearance in (11.16). The initial power spectrum was generated with CAMB [92] at z=1100.

For $k \geq 100 \, \mathrm{h} \, \mathrm{Mpc}^{-1}$, the large-scale limit can no longer be applied, and the tree-level power spectrum is dominated by the exponential damping due to the initial velocity dispersion, which prevents structures from growing. As $k \to \infty$, the tree-level power spectrum approaches the free evolution described by (11.3). In Figure 11.2 we present results from the microscopic perturbation theory described in chapter 4 up to second order for comparison¹. Clearly, such a perturbative expansion is not suitable to capture relevant effects, as the convergence is too slow. As discussed in chapter 6 the tree-level theory resums all contributions from a non-vanishing background field described by $G_f^{(0)}$.

While the tree-level result correctly reproduces the shape and amplitude of the power spectrum from numerical N-body simulation on large scales, its amplitude falls below the N-body results on scales $k \geq 0.1 \,\mathrm{h\,Mpc^{-1}}$. The tree-level theory fails to capture sufficient gravitational interactions to describe the growth of structures on smaller scales.

11.1.3. Numerical Results for the Bispectrum at Tree Level

Analogously to the density-fluctuation power spectrum at tree level, we obtain the tree-level bispectrum by taking appropriate functional derivatives of the tree-level

¹See the end of section 2.2 and [57, 102, 31] for technical details and cosmological application.

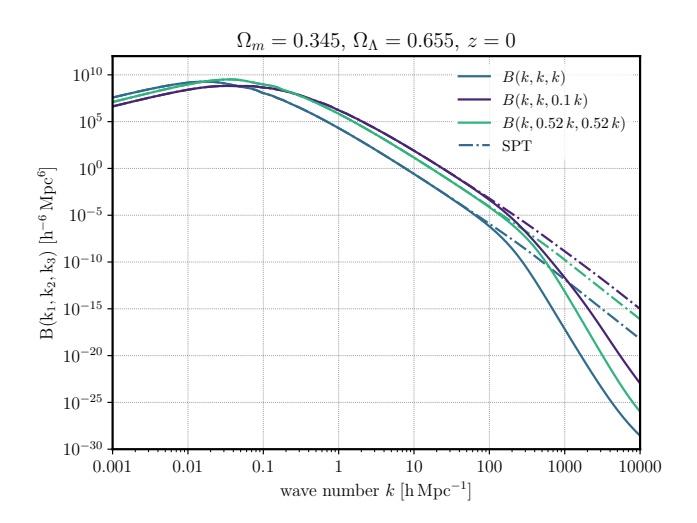


Figure 11.4.: The tree-level result for the total density-fluctuation bispectrum B(k,k,k) for an equilateral, squeezed and flattened configuration for a standard Λ CDM cosmology are shown. The results are compared to the SPT bispectra (dashed-dotted) given by (11.17) for the same configurations. The initial power spectrum was generated with CAMB [92] at z=1100.

generating functional (6.110), which corresponds to the following two diagrams

While the first diagram contains the dynamical vertex $\bar{S}_{\mathcal{D},Bff}^{(3)}$, the second diagram contains the initial vertex $\bar{S}_{\mathcal{I},fff}^{(3)}$. The numerical results for both diagrams are shown in figure 11.3 for an equilateral configuration, and it is immediately obvious that the contribution due to the initial vertex $\bar{S}_{\mathcal{I},fff}^{(3)}$ is subdominant and can easily be neglected. Thus, as expected, the bispectrum is dominated by the interaction potential. In figure 11.4 the total bispectrum is shown for the three typical (equilateral, squeezed and flattened) configurations. The results are compared to the respective tree-level bispectra of Eulerian SPT given by [4],

$$B_{\text{SPT}}(\vec{k}_1, \vec{k}_2, \vec{k}_3, \eta) = 2 F_2(\vec{k}_1, \vec{k}_2) P_{\delta}^{(\text{lin})}(k_1, \eta) P_{\delta}^{(\text{lin})}(k_2, \eta) + 2 \text{ cycl. perm.}, \quad (11.17)$$

where

$$F_2(\vec{k}_1, \vec{k}_2) = \frac{5}{7} + \frac{1}{2} \left(\frac{\vec{k}_1 \cdot \vec{k}_2}{k_1^2} + \frac{\vec{k}_1 \cdot \vec{k}_2}{k_1^2} \right) + \frac{2}{7} \frac{\left(\vec{k}_1 \cdot \vec{k}_2 \right)^2}{k_1^2 k_2^2}.$$
 (11.18)

As for the tree-level power spectrum, we observe a damping on small scales, $k > 100 \,\mathrm{h\,Mpc^{-1}}$, which asymptotically approaches the evolution described by the free

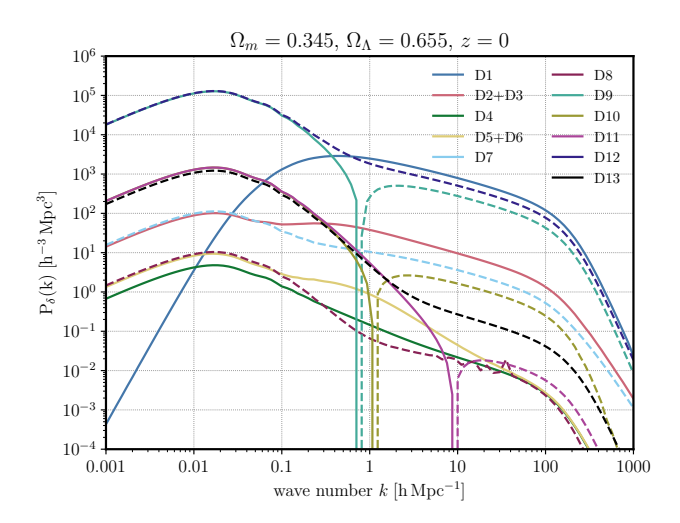


Figure 11.5.: The thirteen individual one-loop contributions are shown here, labelled by D1 to D13 in the same order as they appear in (5.49) and (5.50). Dashed lines indicate negative values The initial power spectrum was generated with CAMB [92] at z=1100.

cumulant $G_{\rho\rho\rho}^{(0)}$.

At this point we should note the important difference between the Klimontovich field theory approach presented in Part I and the particle-based approach of section 5.1: while in the Klimontovich field theory description, we only have two diagram contributions to the bispectrum, in the particle approach, we find three diagrams, which correspond to the $G_{\rho\rho\rho}^{(0)}$, $G_{\rho\rho\rho}^{(0)}$ and $G_{\rho\rho\rho}^{(0)}$ vertex, respectively. While we can identify that the contribution of the $G_{\rho\rho\rho}^{(0)}$ is attributed to the initial $G_{fff}^{(i)}$ cumulant, the other two vertices are contained in the single dynamical vertex of the Klimontovich field theory. This property of having only a single dynamical vertex will prove to be an enormous advantage of the Klimontovich field theory as we shall see in the next sections where we will consider one-loop contributions to the power spectrum.

11.2. Loop Corrections to the Power Spectrum in the Particle Picture

Let us first discuss the one-loop corrections in the particle picture introduced in chapter 5. In order to compute the full one-loop correction to the two-point phase-space density cumulant, one has to evaluate thirteen diagrams that appear in the self-energy (5.49) and (5.50). This is tedious work, as on top of the thirteen diagrams that have to be evaluated, each Δ_{fB} propagator appearing in the loops or in the outer legs, consists of two terms, according to (5.38), that have to be integrated separately. Each self-energy consists of one or two propagators, which are attached to higher-order cumulants, in a similar manner as in the tree-level computation of Δ_{ff} . We present the result for all individual loop diagrams in Figure 11.5. First of

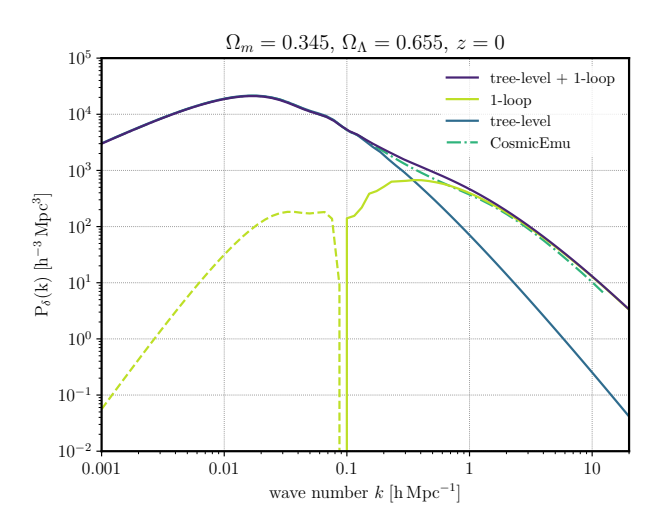


Figure 11.6.: The tree-level and one-loop contributions for the density-fluctuation power spectrum $P_{\delta}(k)$ for a standard Λ CDM cosmology at z=0 are shown. The initial power spectrum was generated with CAMB [92] at z=1100. We compare the full result (tree-level + one-loop) to the non-linear power spectrum expected from simulations generated with Cosmic Emulator [101]. Dashed lines indicate negative values.

all, we observe that several diagrams lead to significant corrections on larger scales which exceed the amplitude of tree-level contribution by an order of magnitude. This is surprising, as we have seen in section 11.1 that structure growth on larger scales is fully described by the tree-level theory. However, the one-loop corrections involve finely tuned cancellations between different diagrams, such that the overall contribution to the large-scale amplitude shown in figure 11.6 is several magnitudes below the tree-level contribution.

The loop contributions in figure 11.5 appear in groups which are separated by orders of magnitude. It is, however, in general not possible to neglect contributions with lower amplitude, specifically because of the finely tuned cancellations. The strong cancellations indicate that the perturbative loop-expansion in this approach is not well-suited to capture the relevant processes and that some kind of resummation procedure is required. Typically, non-perturbative resummation schemes would be applied. However, due to the very fine cancellations, the precision which is needed to evaluate the eight-dimensional one-loop diagrams leads to prohibitively long computation times and sometimes cannot be reached at all. This leads to numerical instabilities in the application of (non-perturbative) resummation schemes. Even going to second-loop order in this approach is numerically challenging.

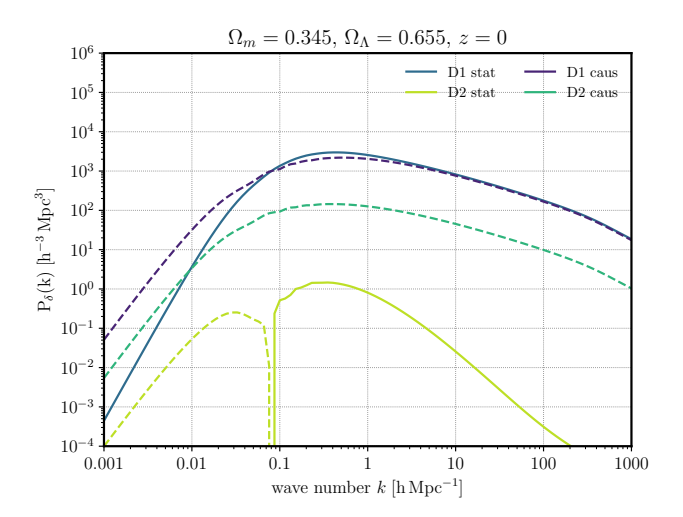


Figure 11.7.: The four one-loop contributions containing the self-energy contributions in (11.19), (11.20) and (11.21) are shown. 'D1 stat' refers to the statistical self-energy (11.20). 'D1 caus' and 'D2 caus' refer to the two diagrams resulting from the causal self-energies, in the order they are displayed in (11.19). Finally, 'D2 stat' refers to the diagram associated with (11.21). The results have been obtained using the analytical propagators derived in section 11.1.1 where we mapped the EdS cosmology to Λ CDM. Dashed lines indicate negative values. The initial power spectrum was generated with CAMB [92] at z=1100.

11.3. Cosmic Structure Formation in Klimontovich Field Theory

It now becomes very clear why the single dynamical vertex of the Klimontovich field theory poses an enormous advantage over the particle-based field theory of chapter 5. The number of diagrams reduces considerably and, although there are cancellations between diagrams, they are much less severe. In the following, we will present the one-loop results for the power spectrum in the framework introduced in chapters 6 and 7. We will also discuss the application of non-perturbative resummation schemes and the expected results.

11.3.1. Results for the Power Spectrum at One-Loop Order

At one loop-order, there are only four distinct diagrams which have to be evaluated. Their contributions can be split into the causal self-energy,

$$\Sigma_{\mathcal{D},fB}^{(1-\text{lp.})} \cong \frac{1}{2} - \cdots + - \cdots , \qquad (11.19)$$

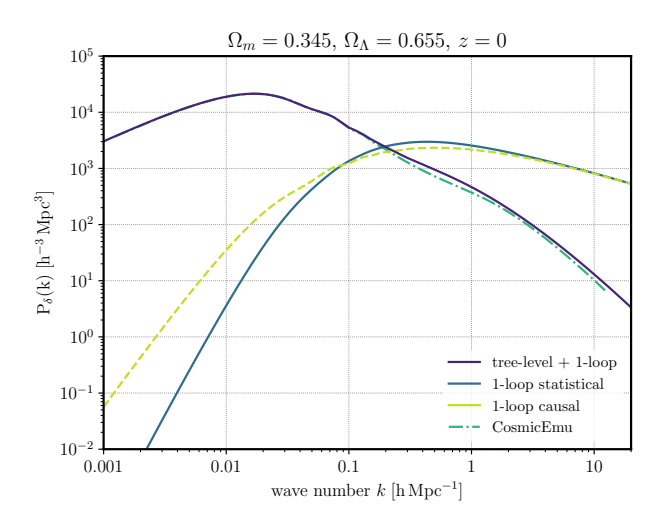


Figure 11.8.: The full tree-level + one-loop result for the density-fluctuation power spectrum $P_{\delta}(k)$ for a standard Λ CDM cosmology at z=0 is shown and compared to the non-linear power spectrum expected from simulations generated with Cosmic Emulator [101]. One-loop contributions from the statistical ((11.20) and (11.21)) and causal self-energy (11.19) contributions are shown separately. The results have been obtained using the analytical propagators derived in section 11.1.1 where we mapped the EdS cosmology to Λ CDM. The initial power spectrum was generated with CAMB [92] at z=1100. Dashed lines indicate negative values.

and the statistical self-energy,

$$\Sigma_{\mathcal{D},ff}^{(1-\text{lp.})} \cong \frac{1}{2} \cdots$$
 (11.20)

from the dynamical part of the action. In addition, there is another contribution to the self-energy which is due to the initial three-point vertex of the action,

$$\Sigma_{\mathcal{I},ff}^{(1-\text{lp.})} \cong \frac{1}{2} \cdots + \frac{1}{2} \cdots$$
 (11.21)

In figure 11.7 all four loop-contributions are presented. As expected, the loop-contribution containing the initial non-Gaussian three-point statistics is negligible. It can also be observed that the amplitudes of the loop-contributions are well below that of the tree-level power spectrum on large scales where the evolution is fully captured by the tree-level theory. As we can see in figure 11.8, the contribution from the first two diagrams in (11.19) is cancelled by the contribution from (11.20) on small scales, such that the resulting power spectrum at one-loop order correctly reproduces the shape of the non-linear power spectrum. Importantly, while the statistical loop corrections are proportional to convolutions of the initial power spectrum, the causal

corrections contain products of it, which compete against each other very similarly to the contributions in standard perturbation theory. Comparing our result against numerical simulations in figure 11.8 we find deviations of the order of 10% - 20% on scales $k > 0.2 \,\mathrm{h\,Mpc^{-1}}$. The result is, of course, identical to the one-loop result in 11.2, since both approaches are exact reformulations of the same underlying microscopic physics.

At the one-loop level our numerical results are identical to those of Eulerian SPT on all relevant scales². This is, however, not surprising since deviations from the SSA should appear at second loop-order for the first time. We do not expect that solely the inclusion of the full-phase space information will be able to close the gap between numerical simulations and analytical results found at $k > 0.2 \,\mathrm{h\,Mpc^{-1}}$. Instead, it is far more likely that the physics on these scales is the result of non-perturbative effects as suggested by [5, 36, 103, 15].

²Taking the damping due to the initial velocity dispersion discussed in 11.1 into account, one would, of course, observe a damping on small scales for the one-loop result. However, scales with $k > 100 \,\mathrm{h\,Mpc^{-1}}$ are typically not of interest in cosmology.

12 Conclusion

Starting from the path-integral construction for classical mechanics based on the KvN formalism and the MSR/JD formalism, we were able to derive a perturbative solution for the Liouville equation based on particle trajectories in phase-space. However, as we know from similar approaches, such a perturbation theory is not applicable to realistic systems since the convergence is too poor and, typically, relevant physical effects cannot be captured well enough. This perturbation theory is not new and has been extensively studied in [29, 102, 31]. The goal was, therefore, to find a resummation scheme which could, at least partly, resum relevant effects.

In a second step we, therefore, reformulated this particle-based perturbation theory into a field theory which still contained the full phase-space information of the particle ensemble using a modified Hubbard-Stratonovich transformation. We also found that our derivation leads to the same formulation as first found by [34, 35]. In this field theory formulation we were indeed able to resum parts of the microscopic dynamics. With the resummed field theory at hand, we were able to set up a perturbative loop expansion and to produce numerical results for the cosmic density-fluctuation power spectrum up to one-loop order [58]. Although, we were able to quantitatively reproduce the one-loop result from Eulerian SPT, we encountered a concerning feature of the resummed field theory, which is rooted in its very construction. Since the resummed field theory is merely a reformulation of a perturbative expansion based on particle-trajectories in Γ -space, it is based on resumming perturbations of particle trajectories that cumulatively lead to a perturbation of the field. This feature manifests itself in the form of an infinite tower of vertices which contain the interaction potential. We found—as did [35]—that at one-loop order we already have to take thirteen loop diagrams into account. The number of diagrams also grows rapidly with increasing loop order. What is even more concerning, however, are the finely tuned cancellations between these diagrammatic contributions which we demonstrated in our cosmological application. These do not allow for a systematic truncation of the tower of vertices of the resummed field theory. They further introduce a numerical challenge since the eight-dimensional integrals have to be evaluated to a very high precision. In addition, we found that the amplitude of several one-loop diagram contributions exceeds the amplitude of the tree-level contribution even on scales where the system is already fully described by the tree-level theory. Our findings, thus, suggest that the resummed field theory has to be restructured in order to avoid cancellations and ideally to reduce the number of diagrams.

178 12. Conclusion

In Part II of this thesis, we present a new field theory formulation which is no longer based on the evolution of individual particle trajectories, but on the evolution of the field, i.e., the Klimontovich phase-space density, itself. By construction, the perturbative expansion now describes the effect of the interaction potential directly on the field. We gradually build up the field theory in chapter 6 and show the connection to the particle picture of chapter 5. In this new formulation we can also show that the tree-level solution corresponds to the solution of the linearized Klimontovich equation. We have shown that the particle-noise contributions to the initial phase-space density cumulants are directly related to particle collisions in the kinetic sense. Therefore, neglecting those terms reduces the Klimontovich description to the Vlasov description. Having provided an intuition for the theory in chapter 6, we present a complete and formal development of the field theory in chapter 7. The novel element of the theory, is that the mean field itself receives corrections due to interactions during the evolution of the system. We show in chapter 7 that the most natural formulation of this approach is in terms of an effective action. The Dyson-Schwinger equations then allows us to obtain n-point correlation functions in a self-consistent manner.

The vertex structure of this field theory is quite simple, since there is only one dynamical vertex containing the interaction potential. There is, however, an infinite tower of vertices which are attributed to initial correlations present in the system, and are relevant for the description of particle collisions. We can then differentiate between the Klimontovich and the Vlasov description. The latter describes the evolution of a collisionless system. If Gaussian initial conditions for this system can be assumed, the initial vertices stemming from higher order statistics vanish and only the interaction vertex survives. This is a valid assumption for many systems that are dominated by the interaction potential. It is, therefore, possible to truncate the infinite hierarchy by taking only the contributions from the dynamical vertices into account that are up to quadratic order in the initial statistics. In general, however, we can treat arbitrarily complicated systems in this manner. Compared to the approach of chapter 5, the number of diagrams is drastically reduced—even if the initial vertices are taken into account. At one-loop order, for instance, four diagrams in total have to be evaluated.

In Part III, we present the application of the formalism of Part I and II to cosmic large-scale formation. We derive the results for the Klimontovich field theory of Part II, as it is our main focus. It should be stressed, that the results of the resummed field theory for microscopic particles and those of the Klimontovich field theory agree, since they describe the same exact phase-space evolution. However, the latter field theory offers—at least in the author's opinion—a better framework for obtaining them. In section 11.1 we present the tree-level results for the cosmic density-fluctuation power spectrum and bispectrum. Up to $k < 100 \,\mathrm{h\,Mpc^{-1}}$ the numerical results agree with those obtained from linear Eulerian SPT. This is not surprising, as we have shown, that the tree-level description corresponds to the linearized Vlasov equation, in the absence of collisions. On smaller scales, $k > 100 \,\mathrm{h\,Mpc^{-1}}$, however, we observe a damping which is due to the velocity dispersion present in the initial conditions that

are not incorporated in Eulerian SPT. Our main result is the density-fluctuation power spectrum to first order in the loop expansion. We present them first in the scope of the resummed field theory of chapter 5 in order to showcase the finely tuned cancellations between different loop diagrams. Finally, we present the one-loop results in the framework developed in chapters 6 and 7. We demonstrate that—for this system—the contribution from the initial three-point vertex can in fact be neglected, thus offering a systematic truncation of the tower of vertices. The one-loop results agree with those obtained with one-loop Eulerian SPT. This is not surprising, since deviations from SPT in the single-stream approximation will start to appear only at two-loop order. We compare our results from those obtained from numerical simulations and find very good agreement on large scales, while on smaller scales $k > 0.2 \,\mathrm{h\,Mpc^{-1}}$ our results deviate by 10 - 20%. It is clear that higher-order corrections are required to correctly reproduce the power spectrum on these scales. An obvious next step would be, therefore, to compute the next order in the loop expansion. It is useful in order to quantify the deviations from two-loop Eulerian SPT, but we do not expect that a simple loop expansion will provide the desired results. It is far more likely that the missing power on intermediate and small scales is the result of non-perturbative effects which are not captured by this expansion.

The tree-level approach already suggests that non-perturbative descriptions lie at heart of structure formation of classical ensembles. Since in contrast to most quantum field theories, there is no small coupling parameter, a perturbative loop expansion is difficult to justify, if even possible. The apparent divergence of the Eulerian SPT approach supports this idea. We have therefore presented the most natural improvements to the naive loop expansion and hope that in the near future these will prove fruitful and help describing the evolution of cosmic structures.

 $"Are \ You \ Not \ Entertained?"$

- Maximus Decimus Meridius

4 Appendices

A Summary of Field Theory Notation

In this appendix we shortly summarize the notations used throughout this work.

A.1. Condensed Notation

Since the equations tend to become very cumbersome, we introduce a unified index notation to simplify our expressions. We bundle the phase-space coordinates together with the time variable to a phase space-time coordinate X = (x, t). Integrals over the whole phase-space and time will be abbreviated as

$$\int_{X} := \int d^{6}x \int_{t^{(i)}}^{\infty} dt.$$
 (A.1)

Next, our fields will involve two components, $A_f(X)$ and $A_B(X)$. We therefore accumulate both into a field doublet $A_{\alpha}(X)$ whose components will be denoted by Greek indices, $\alpha \in \{f, B\}$. To further compactify our notation, we adopt the *DeWitt* notation by letting Latin indices represent both the continuous space-time coordinate and the discrete field index, $a = (X, \alpha)$ and write

$$A_a \equiv A_\alpha(X) \,. \tag{A.2}$$

Scalar products will involve integrals and summations over phase space-time X and components α , which we will abbreviate using the Einstein sum convention,

$$A_a B_a \equiv \sum_{\alpha \in \{f, B\}} \int_X A_\alpha(X) B_\alpha(X) . \tag{A.3}$$

If we further need to integrate only over a subset of the components and therefore cannot employ the DeWitt notation, we will shorten the equations by implicitly writing the integrals as

$$\int_{X_1} A(X_1)B(X_1) = A(1)B(1), \qquad (A.4)$$

where $(1) = X_1 = (x_1, t_1)$. Similar rules hold in Fourier space, where we generally write $(\hat{1}) = (S_1) = (s_1, t_1)$.

Furthermore, we define the following shorthand notation for functional derivatives of a functional F[h] w.r.t. to its argument $h_{\alpha}(X)$ as

$$F_{a_1...a_n}^{(n)} \equiv \frac{\delta^n F[h]}{\delta h_{a_1} \dots \delta h_{a_n}}.$$
 (A.5)

B Discretized Stochastic Evolution Equations

In this appendix we discuss in more detail the discretization procedure leading to the MSR/JD generating functional discussed in section 3.2 and used throughout this work. We essentially follow [104, 21, 19, 59, 105]. To keep the concepts as simple as possible, we consider a one-dimensional problem, described by the stochastic differential equation

$$\frac{\mathrm{d}\psi(t)}{\mathrm{d}t} = F[\psi(t)] + \eta(t), \qquad (B.1)$$

where $F[\psi(t)]$ is the locally Lipschitz continuous drift term, and $\eta(t)$ is the random noise, possibly describing the random initial distribution $\psi(t=0) = \psi^{(i)}$.

B.1. Itô vs. Stratonovich in the Linear Case

As the transition form a continuous to a discretized description leads necessarily to ambiguities that have to be treated carefully, we begin our discussion with an exactly solvable toy model that already exhibits all features relevant to our discussion. Specifically, we consider the linear process,

$$\frac{\mathrm{d}\psi(t)}{\mathrm{d}t} = -\mu\psi(t) + K(t) + \eta(t), \qquad (B.2)$$

where, as in the main text, we included a source K(t) in order to probe the response to fluctuations. The advantage of this model is that it has an analytical solution $\psi_{\text{sol}}^{K}(t)$ given by

$$\psi_{\text{sol}}^{K}(t) = e^{-\mu t} \psi^{(i)} + \int_{0}^{t} dt' e^{-\mu (t-t')} \left[\eta(t) - K(t) \right].$$
 (B.3)

As discussed in the main text, the linear response function of this system is given by

$$R(t,t') = \frac{\delta \psi_{\text{sol}}^{K}(t)}{\delta K(t')}\Big|_{K=0} = e^{-\mu(t-t')}\Theta(t-t') = \begin{cases} e^{-\mu(t-t')} & t > t' \\ \Theta(t) & t = 0 \\ 0 & t < t' \end{cases}$$
(B.4)

The ambiguity now arises, since the value of $\Theta(0)$ is a priori undefined, and so is the value of R(t,t), which has a jump discontinuity for equal times. In order to physically understand the origin of this ambiguity, let us define the associated discretized theory, by splitting the time interval $[0,t^{(f)}]$ into N steps of size $\epsilon = \frac{t^{(f)}}{N}$, such that $t_n = n\epsilon$, for $n = 1, \ldots, N$. We abbreviate $\psi_n = \psi(t_n)$ and $F_n = F(\psi(t_n))$ and similarly for K(t). Defining $\eta_n = \int_{t_{n-1}}^{t_n} \eta(t) dt$ and setting $\psi_0 \equiv \psi^{(i)}$ we find for the discretized version of (B.2),

$$\frac{\psi_n - \psi_{n-1}}{\epsilon} = (1 - a) \left(-\mu \psi_{n-1} + K_{n-1} \right) + a \left(-\mu \psi_n + K_n \right) + \frac{\eta_n}{\epsilon} . \tag{B.5}$$

There is an ambiguity that arises during the discretization of the dynamical equation (B.2), since it is a priori not clear at which end of the interval $[t_{n-1}, t_n]$ the force term F(t) and the perturbation K(t) on the right-hand side of (B.2) have to be evaluated. We have therefore introduced the parameter $a \in [0, 1]$ in order to interpolate between both ends and thus to track the ambiguity till the end. Equation (B.5) can easily be solved for ψ_n yielding the updating prescription

$$\psi_n = \frac{1 + (a-1)\mu\epsilon}{1 + a\mu\epsilon} \psi_{n-1} + \frac{\epsilon[(1-a)K_{n-1} + aK_n] + \eta_n}{1 + a\mu\epsilon}$$
(B.6)

$$= c \psi_{n-1} + \frac{\epsilon[(1-a)K_{n-1} + aK_n] + \eta_n}{1 + a\mu\epsilon},$$
 (B.7)

with

$$c := \frac{1 + (a - 1)\mu\epsilon}{1 + a\mu\epsilon}.$$
 (B.8)

This recurrence relation can be iterated to yield the following discretized solution

$$\psi_{\text{sol},n}^{K} = c^{n} \psi^{(i)} + \sum_{k=0}^{n-1} c^{n-1-k} \frac{\epsilon[(1-a)K_k + aK_{k+1}] + \eta_n}{1 + a\mu\epsilon}.$$
 (B.9)

The continuum limit is the obtained by letting $\epsilon \to 0$ and $N \to \infty$. In this limit, the discretized solution (B.9) converges to the solution (B.3), which can be shown using the identity

$$e^x = \lim_{N \to \infty} \left(1 - \frac{x}{N} \right)^N. \tag{B.10}$$

The discretized version of the linear response function can be computed to

$$R_{nm} := \frac{\partial \psi_{\text{sol},n}^K}{\partial (\epsilon K_m)} = \begin{cases} \frac{c^{n-m}}{(1+a\mu\epsilon)(1+(a-1)\mu\epsilon)} & n > m \\ \frac{a}{1+a\mu\epsilon} & n = m \\ 0 & n < m \end{cases}$$
(B.11)

In the continuum limit, we obtain

$$R(t,t') = \frac{\delta \psi_{\text{sol}}^{K}(t)}{\delta K(t')}\Big|_{K=0} = e^{-\mu(t-t')}\Theta(t-t') = \begin{cases} e^{-\mu(t-t')} & t > t' \\ a & t = 0 \\ 0 & t < t' \end{cases}$$
(B.12)

which shows that the ambiguity in choosing the value of $\Theta(0)$ corresponds to choosing a specific discretization procedure for the underlying discrete time evolution. Thus, the value of the response function for equal times depends on the convention employed when evaluating the right-hand side of (B.2) during the discretization. The most important conventions are $It\hat{o}$, with a=0 and Stratonovich with $a=\frac{1}{2}$. The Itô prescription is sometimes called pre-point prescription because the force terms are evaluated on the earlier time of the interval $[t_{n-1}, t_n]$, while the Stratonovich prescription amounts to evaluating the forces in the middle of the interval. It is therefore referred to as mid-point prescription. Throughout the main text we use the Itô convention which amounts to set $a = \Theta(0) = 0$, which has important advantages as we will see.

B.2. The Discretized MSR/JD-Path Integral

We are now ready to turn to the more general case (B.1), whose discretized version reads

$$\frac{\psi_n - \psi_{n-1}}{\epsilon} = (1 - a) \left(F_{n-1} - K_{n-1} \right) + a \left(F_n - K_n \right) + \frac{\eta_n}{\epsilon} , \qquad (B.13)$$

where we choose to keep the parameter a general in order to see how the different discretization prescriptions affect the path integral construction. The associated generating functional is defined as

$$\mathcal{Z}[J,K] = \left\langle \exp\left[\sum_{n=1}^{N} \epsilon J_n \psi_{\text{sol},n}^K\right] \right\rangle_{\mathcal{P}}, \tag{B.14}$$

where $\langle \cdot \rangle_{\mathcal{P}}$ indicates averaging w.r.t. $\mathcal{P}[\eta]$. Ignoring for the moment this averaging process, we can write the exponential as

$$\exp\left[\sum_{n=1}^{N} \epsilon J_n \psi_{\text{sol},n}^K\right] = \left[\prod_{n=1}^{N} \int d\psi_n \, \delta_D \left(\psi_n - \psi_{\text{sol},n}^K\right)\right] \exp\left[\sum_{\bar{n}=1}^{N} \epsilon J_{\bar{n}} \psi_{\bar{n}}\right]. \tag{B.15}$$

Assuming a unique solution, we can use the N-dimensional version of the Dirac-delta identity,

$$\prod_{n=1}^{N} \delta_{D} \left(\psi_{n} - \psi_{\text{sol},n}^{K} \right) = \left| \det \left(\mathcal{J} \right) \right| \prod_{n=1}^{N} \delta_{D} \left(\mathcal{E}_{n} \right) , \tag{B.16}$$

where

$$\mathcal{E}_n := \frac{\psi_n - \psi_{n-1}}{\epsilon} - (1 - a) \left(F_{n-1} - K_{n-1} \right) - a \left(F_n - K_n \right) - \frac{\eta_n}{\epsilon} \,, \tag{B.17}$$

corresponds to the discretized equation of motion and \mathcal{J} is the Jacobian arising from the above change of variables. It is defined by

$$\mathcal{J}_{nm} := \frac{\partial \mathcal{E}_n}{\partial \psi_m} = \frac{1}{\epsilon} \left(\delta_{nm} - \delta_{(n-1)m} \right) - (1 - a) F'_{n-1} \delta_{(n-1)m} - a F'_n \delta_{nm} , \qquad (B.18)$$

with $F' = \frac{\partial F}{\partial \psi}$. Importantly, we note that $\mathcal{J}_{nm} = 0$ if n < m. Thus, \mathcal{J} is an upper triangular matrix and its determinant is the product of its diagonal entries. We find

$$\det\left(\mathcal{J}\right) = \prod_{n=1}^{N} \mathcal{J}_{nn} = \prod_{n=1}^{N} \left[\frac{1}{\epsilon} - aF_n' \right] = \frac{1}{\epsilon^N} \prod_{n=1}^{N} \left[1 - a\epsilon F_n' \right]. \tag{B.19}$$

We can now see the advantage of the Itô prescription, as the above determinant becomes $\frac{1}{\epsilon^N}$ and is thus independent of ψ . If one wants to keep the discretization general, one could now proceed by introducing Grassmann valued fields, in order to exponentiate the above determinant, which is not constant in general. With this tick known from gauge theory, one can make the determinant dynamical such that the Grassmann fields cancel unphysical degrees of freedom. However, we are working in the Itô prescription, and therefore find

$$\prod_{n=1}^{N} \delta_{\mathcal{D}} \left(\psi_{n} - \psi_{\text{sol},n}^{K} \right) = \frac{1}{\epsilon^{N}} \prod_{n=1}^{N} \delta_{\mathcal{D}} \left(\mathcal{E}_{n} \right) . \tag{B.20}$$

We can exponentiate the Dirac-delta distribution that contains the discretized equations of motion by using its Fourier representation,

$$\frac{1}{\epsilon^N} \prod_{n=1}^N \delta_{\mathcal{D}}(\mathcal{E}_n) = \frac{1}{\epsilon^N} \int \frac{\mathrm{d}^N \hat{\psi}}{(2\pi)^N} e^{\mathrm{i} \sum_{n=1}^N \hat{\psi}_n \mathcal{E}_n}$$
(B.21)

$$= \int \frac{\mathrm{d}^N \hat{\psi}}{(2\pi)^N} \mathrm{e}^{\mathrm{i}\epsilon \sum_{n=1}^N \hat{\psi}_n \mathcal{E}_n} , \qquad (B.22)$$

where in the second line we absorbed the factor of $\frac{1}{\epsilon^N}$ into the exponent, to facilitate the continuum limit. We see, that nothing is left from the determinant anymore. Putting everything together, we arrive at

$$\mathcal{Z}[J,K] = \int d^N \eta_n \mathcal{P}[\{\eta_n\}] \int d^N \psi \int \frac{d^N \hat{\psi}}{(2\pi)^N} e^{i\epsilon \sum_{n=1}^N \hat{\psi}_n \mathcal{E}_n + \sum_{n=1}^N \epsilon J_n \psi_n}, \qquad (B.23)$$

which, under the continuum limit, yields the appropriate MSR/JD action stated in the main text (c.f. (3.68)).

Acknowledgements

Before concluding this thesis, I would like to thank several people who have supported me over the past years, be it professionally, personally or both.

First and foremost, I am deeply grateful to my supervisor *Matthias Bartelmann* who welcomed me into his group and gave me the opportunity to pursue own ideas, to which he was always open and encouraging. I have deeply profited from the positive ambiance in his group.

Next, I owe special thanks to *Thomas Gasenzer*, not only for agreeing to co-referee my thesis, but also for the many fruitful discussions and the collaboration that emerged from them.

Special thanks also go to *Björn Malte Schäfer*, whose office door was always open—for conversations about physics, memes as well as personal matters.

I also want to thank *Hans-Christian Schultz-Coulon* for agreeing to be part of my thesis committee.

I am extremely grateful to *Elena Kozlikin*, whose experience guided me through my first academic steps, from which I profited enormously. Our collaboration and the many intense discussions we shared have greatly enriched my work and my time as a PhD student. She has climbed every mountain with me, figuratively and literally.

I would like to sincerely thank *Robert Lilow* and *Saskia Lach* for their thoughtful proofreading and valuable contributions through discussion.

Many thanks go to my dear friends Fabian Hahner, Katrin Lehle, Iris Feldt, Christophe Pixius, Emre Adanali and Carlotta Spiegel, with whom I could speak about anything, from everyday thoughts to passionate political rants.

I would especially like to thank my bouldering crew. In particular, *Melanie Lilow*, *Jeremy Geiger*, *Joana Oster*, who challenged me (in the good way) in the bouldering gym ensuring that, alongside the intellectual demands of research, I also got the physical challenge I needed.

I am deeply grateful to my beloved *parents* and *sisters* for their invaluable emotional support throughout these past years, and for always being able to make me smile, even in difficult times.

Last, but not least I thank the "Studientstiftung des Deutschen Volkes" and the STRUCTURES Excellence Cluster for generously supporting my PhD.

Publications

This thesis contains results from the following publications which are either published or in preparation.

- Tristan Daus and Elena Kozlikin. Field Theory Approach to Classical N Particle Systems In and Out of Equilibrium. In: arXiv e-prints (June 2024). arXiv: 2406.03425 [cond-mat.stat-mech].
- Tristan Daus and Elena Kozlikin. Cosmic Large-Scale Structure Formation from Newtonian Particle Dynamics. In: arXiv e-prints (Jan. 2025). arXiv: 2501.11676 [astro-ph.CO].
- Tristan Daus and Elena Kozlikin. Klimontovich Field Theory for Classical Statistical Systems. (In preparation)
- Tristan Daus and Elena Kozlikin. Cosmic Large Scale Structure Formation with Full Phase-Space Information. (In preparation)

- [1] Euclid Collaboration. Euclid I. Overview of the Euclid mission. In: Astronomy & Astrophysics 697 (2025), A1. DOI: 10.1051/0004-6361/202450810. URL: https://doi.org/10.1051/0004-6361/202450810.
- [2] Zeljko Ivezić et al. LSST: From Science Drivers to Reference Design and Anticipated Data Products. In: Astrophysical Journal 873.2, 111 (Mar. 2019), p. 111. DOI: 10.3847/1538-4357/ab042c. arXiv: 0805.2366 [astro-ph].
- [3] Michael J. Chapman et al. The completed SDSS-IV extended Baryon Oscillation Spectroscopic Survey: measurement of the growth rate of structure from the small-scale clustering of the luminous red galaxy sample. In: MNRAS 516.1 (Oct. 2022), pp. 617–635. DOI: 10.1093/mnras/stac1923. arXiv: 2106.14961 [astro-ph.C0].
- [4] F. Bernardeau et al. Large scale structure of the universe and cosmological perturbation theory. In: Phys. Rept. 367 (2002), pp. 1–248. DOI: 10.1016/S0370-1573(02)00135-7. arXiv: astro-ph/0112551.
- [5] Martín Crocce and Román Scoccimarro. Renormalized cosmological perturbation theory. In: Phys. Rev. D 73 (6 Mar. 2006), p. 063519. DOI: 10.1103/PhysRevD.73.063519. URL: https://link.aps.org/doi/10.1103/PhysRevD.73.063519.
- [6] Sabino Matarrese and Massimo Pietroni. Resumming cosmic perturbations. In: Journal of Cosmology and Astroparticle Physics 2007.06 (June 2007), pp. 026–026. DOI: 10.1088/1475-7516/2007/06/026. URL: https://doi.org/10.1088%2F1475-7516%2F2007%2F06%2F026.
- [7] M. Pietroni et al. Coarse-grained cosmological perturbation theory. In: Journal of Cosmology and Astroparticle Physics 2012.1, 019 (Jan. 2012), p. 019. DOI: 10.1088/1475-7516/2012/01/019. arXiv: 1108.5203 [astro-ph.CO].
- [8] Daniel Baumann et al. Cosmological non-linearities as an effective fluid. In: Journal of Cosmology and Astroparticle Physics 2012.07 (July 2012), p. 051. DOI: 10.1088/1475-7516/2012/07/051. URL: https://dx.doi.org/10.1088/1475-7516/2012/07/051.
- [9] Mark P. Hertzberg. Effective field theory of dark matter and structure formation: Semianalytical results. In: Phys. Rev. D 89 (4 Feb. 2014), p. 043521. DOI: 10.1103/PhysRevD.89.043521. URL: https://link.aps.org/doi/10.1103/PhysRevD.89.043521.

[10] John Joseph M. Carrasco et al. *The Effective Field Theory of Large Scale Structures at two loops*. In: Journal of Cosmology and Astroparticle Physics 2014.07 (July 2014), pp. 057–057. DOI: 10.1088/1475-7516/2014/07/057. URL: https://doi.org/10.1088%2F1475-7516%2F2014%2F07%2F057.

- [11] Thomas Konstandin, Rafael A. Porto, and Henrique Rubira. The effective field theory of large scale structure at three loops. In: Journal of Cosmology and Astroparticle Physics 2019.11 (Nov. 2019), pp. 027–027. DOI: 10.1088/1475-7516/2019/11/027. URL: https://doi.org/10.1088%2F1475-7516%2F2019%2F11%2F027.
- [12] Diego Blas et al. Large scale structure from viscous dark matter. In: Journal of Cosmology and Astroparticle Physics 2015.11 (Nov. 2015), pp. 049–049. ISSN: 1475-7516. DOI: 10.1088/1475-7516/2015/11/049. URL: http://dx.doi.org/10.1088/1475-7516/2015/11/049.
- [13] Alaric Erschfeld and Stefan Floerchinger. Evolution of dark matter velocity dispersion. In: Journal of Cosmology and Astroparticle Physics 2019.06 (June 2019), pp. 039–039. ISSN: 1475-7516. DOI: 10.1088/1475-7516/2019/06/039. URL: http://dx.doi.org/10.1088/1475-7516/2019/06/039.
- [14] Mathias Garny, Dominik Laxhuber, and Román Scoccimarro. *Perturbation theory with dispersion and higher cumulants: Nonlinear regime*. In: Physical Review D 107.6 (Mar. 2023). ISSN: 2470-0029. DOI: 10.1103/physrevd.107.063540. URL: http://dx.doi.org/10.1103/PhysRevD.107.063540.
- [15] Alaric Erschfeld and Stefan Floerchinger. Dark matter vorticity and velocity dispersion from truncated Dyson-Schwinger equations. In: JCAP 02 (2024), p. 053. DOI: 10.1088/1475-7516/2024/02/053. arXiv: 2305.18517 [astro-ph.CO].
- [16] B. O. Koopman. Hamiltonian Systems and Transformations in Hilbert Space.
 In: Proceedings of the National Academy of Science 17.5 (May 1931), pp. 315–318.
 DOI: 10.1073/pnas.17.5.315.
- [17] J. v. Neumann. Zur Operatorenmethode In Der Klassischen Mechanik. In: Annals of Mathematics 33.3 (1932), pp. 587-642. ISSN: 0003486X. URL: http://www.jstor.org/stable/1968537.
- [18] P. C. Martin, E. D. Siggia, and H. A. Rose. Statistical Dynamics of Classical Systems. In: Phys. Rev. A 8 (1 July 1973), pp. 423-437. DOI: 10.1103/PhysRevA.8.423. URL: https://link.aps.org/doi/10.1103/PhysRevA.8.423.
- [19] Hans-Karl Janssen. On a Lagrangean for classical field dynamics and renormalization group calculations of dynamical critical properties. In: Zeitschrift für Physik B Condensed Matter and Quanta 23 (Jan. 1976), pp. 377–380. DOI: 10.1007/BF01316547.
- [20] C. De Dominicis and L. Peliti. Field Theory Renormalization and Critical Dynamics Above t(c): Helium, Antiferromagnets and Liquid Gas Systems. In: Phys. Rev. B 18 (1978), pp. 353–376. DOI: 10.1103/PhysRevB.18.353.

- [21] Roderick V. Jensen. Functional integral approach to classical statistical dynamics. In: Journal of Statistical Physics 25.2 (June 1981), pp. 183–210. DOI: 10.1007/BF01022182.
- [22] E. Gozzi. *Hidden BRS invariance in classical mechanics*. In: Physics Letters B 201.4 (1988), pp. 525-528. ISSN: 0370-2693. DOI: 10.1016/0370-2693(88) 90611-9. URL: https://www.sciencedirect.com/science/article/pii/0370269388906119.
- [23] E. Gozzi, M. Reuter, and W. D. Thacker. *Hidden BRS invariance in classical mechanics. II.* In: Phys. Rev. D 40 (10 Nov. 1989), pp. 3363-3377. DOI: 10.1103/PhysRevD.40.3363. URL: https://link.aps.org/doi/10.1103/PhysRevD.40.3363.
- [24] J. Zinn-Justin. Renormalization and stochastic quantization. In: Nuclear Physics B 275.1 (1986), pp. 135-159. ISSN: 0550-3213. DOI: https://doi.org/10.1016/0550-3213(86)90592-4. URL: https://www.sciencedirect.com/science/article/pii/0550321386905924.
- [25] Oldwig Von Roos. Formal Solution of Liouville's Equation. In: Journal of Mathematical Physics 1.2 (Mar. 1960), pp. 107–111. DOI: 10.1063/1.1703639.
- [26] R. Balescu. Equilibrium and nonequilibrium statistical mechanics. In: NASA STI/Recon Technical Report A 76 (May 1975), p. 32809.
- [27] Shankar P. Das and Gene F. Mazenko. Field Theoretic Formulation of Kinetic Theory: Basic Development. In: Journal of Statistical Physics 149.4 (Nov. 2012), pp. 643–675. ISSN: 1572-9613. DOI: 10.1007/s10955-012-0610-y. URL: https://doi.org/10.1007/s10955-012-0610-y.
- [28] Gene F. Mazenko. Smoluchowski dynamics and the ergodic-nonergodic transition. In: Phys. Rev. E 83 (4 Apr. 2011), p. 041125. DOI: 10.1103/PhysRevE.83.041125. URL: https://link.aps.org/doi/10.1103/PhysRevE.83.041125.
- [29] Matthias Bartelmann et al. A microscopic, non-equilibrium, statistical field theory for cosmic structure formation. In: New J. Phys. 18.4 (2016), p. 043020. DOI: 10.1088/1367-2630/18/4/043020.
- [30] Felix Fabis et al. Kinetic Field Theory: Exact free evolution of Gaussian phase-space correlations. In: J. Stat. Mech. 1804.4 (2018), p. 043214. DOI: 10.1088/1742-5468/aab850. arXiv: 1710.01611 [cond-mat.stat-mech].
- [31] Christophe Pixius, Safak Celik, and Matthias Bartelmann. *Kinetic field theory:* perturbation theory beyond first order. In: JCAP 12 (2022), p. 030. DOI: 10.1088/1475-7516/2022/12/030. arXiv: 2207.06852 [astro-ph.CO].
- [32] R. L. Stratonovich. On a Method of Calculating Quantum Distribution Functions. In: Soviet Physics Doklady 2 (July 1957), p. 416.
- [33] J. Hubbard. Calculation of Partition Functions. In: Phys. Rev. Lett. 3 (2 July 1959), pp. 77-78. DOI: 10.1103/PhysRevLett.3.77. URL: https://link.aps.org/doi/10.1103/PhysRevLett.3.77.

[34] Robert Lilow et al. Resummed Kinetic Field Theory: general formalism and linear structure growth from Newtonian particle dynamics. In: Journal of Cosmology and Astroparticle Physics 2019.04 (Apr. 2019), p. 001. DOI: 10. 1088/1475-7516/2019/04/001. URL: https://dx.doi.org/10.1088/1475-7516/2019/04/001.

- [35] Robert Lilow. Structure Formation in Dark and Baryonic Matter within Resummed Kinetic Field Theory. PhD thesis. U. Heidelberg (main), 2018. DOI: 10.11588/heidok.00024828.
- [36] Patrick Valageas. Large-N expansions applied to gravitational clustering. In: Astron. Astrophys. 465 (2007), p. 725. DOI: 10.1051/0004-6361:20066832. arXiv: astro-ph/0611849.
- [37] Jérôme Daligault. Renormalized Kinetic Theory of Classical Fluids in and out of Equilibrium. In: Journal of Statistical Physics 143.6 (May 2011), pp. 1189–1246. ISSN: 1572-9613. DOI: 10.1007/s10955-011-0228-5. URL: http://dx.doi.org/10.1007/s10955-011-0228-5.
- [38] Radu Balescu. Statistical Dynamics. Published by Imperial College Press and Distributed by World Scientific Publishing Co., 1997. DOI: 10.1142/p036. eprint: https://www.worldscientific.com/doi/pdf/10.1142/p036. URL: https://www.worldscientific.com/doi/abs/10.1142/p036.
- [39] Wilhelm Magnus. On the exponential solution of differential equations for a linear operator. In: Communications on Pure and Applied Mathematics 7.4 (1954), pp. 649-673. DOI: https://doi.org/10.1002/cpa.3160070404. eprint: https://onlinelibrary.wiley.com/doi/pdf/10.1002/cpa.3160070404. URL: https://onlinelibrary.wiley.com/doi/abs/10.1002/cpa.3160070404.
- [40] D.R. Nicholson. *Introduction to Plasma Theory*. Plasma Physics Series. Wiley, 1983. ISBN: 9780471090458. URL: https://books.google.de/books?id=fyRRAAAAMAAJ.
- [41] Y. L. Klimontovich. The Statistical Theory of Non-Equilibrium Processes in a Plasma. In: vol. 9. International Series in Natural Philosophy. Pergamon, 1967. DOI: https://doi.org/10.1016/B978-0-08-011966-3.50005-1.
- [42] John G. Kirkwood. The Statistical Mechanical Theory of Transport Processes I. General Theory. In: The Journal of Chemical Physics 14.3 (Mar. 1946), pp. 180–201. ISSN: 0021-9606. DOI: 10.1063/1.1724117. eprint: https://pubs.aip.org/aip/jcp/article-pdf/14/3/180/18793903/180_1_online.pdf. URL: https://doi.org/10.1063/1.1724117.
- [43] Max Born and H. S. Green. A general kinetic theory of liquids I. The molecular distribution functions. In: Proceedings of the Royal Society of London. Series A. Mathematical and Physical Sciences 188.1012 (1946), pp. 10–18. DOI: 10.1098/rspa.1946.0093. eprint: https://royalsocietypublishing.org/doi/pdf/10.1098/rspa.1946.0093. URL: https://royalsocietypublishing.org/doi/abs/10.1098/rspa.1946.0093.

- [44] John G. Kirkwood. The Statistical Mechanical Theory of Transport Processes II. Transport in Gases. In: The Journal of Chemical Physics 15.1 (Jan. 1947), pp. 72-76. ISSN: 0021-9606. DOI: 10.1063/1.1746292. eprint: https://pubs.aip.org/aip/jcp/article-pdf/15/1/72/18794263/72_1_online.pdf. URL: https://doi.org/10.1063/1.1746292.
- [45] A. A. Vlasov. Many-particle Theory and Its Application to Plasma. Russian Monographs. Gordon and Breach, 1961. ISBN: 9780677203300. URL: https://books.google.de/books?id=g04yAAAAMAAJ.
- [46] D. Mauro. On Koopman-von Neumann waves. In: Int. J. Mod. Phys. A 17 (2002), pp. 1301–1325. DOI: 10.1142/S0217751X02009680. arXiv: quant-ph/0105112.
- [47] E. Gozzi and R. Penco. Three Approaches to Classical Thermal Field Theory. In: Annals Phys. 326 (2011), pp. 876–910. DOI: 10.1016/j.aop.2010.11.018. arXiv: 1008.5135 [hep-th].
- [48] Denys I. Bondar et al. Operational Dynamic Modeling Transcending Quantum and Classical Mechanics. In: Phys. Rev. Lett. 109 (19 Nov. 2012), p. 190403. DOI: 10.1103/PhysRevLett.109.190403. URL: https://link.aps.org/doi/10.1103/PhysRevLett.109.190403.
- [49] M. H. Stone. On One-Parameter Unitary Groups in Hilbert Space. In: Annals of Mathematics 33.3 (1932), pp. 643-648. ISSN: 0003486X, 19398980. URL: http://www.jstor.org/stable/1968538 (visited on 05/08/2025).
- [50] P. Ehrenfest. Bemerkung über die angenäherte Gültigkeit der klassischen Mechanik innerhalb der Quantenmechanik. In: Zeitschrift für Physik 45.7 (July 1927), pp. 455–457. ISSN: 0044-3328. DOI: 10.1007/BF01329203. URL: https://doi.org/10.1007/BF01329203.
- [51] Fritz Bopp. La mécanique quantique est-elle une mécanique statistique classique particulière? fr. In: Annales de l'institut Henri Poincaré 15.2 (1956), pp. 81-112. URL: https://www.numdam.org/item/AIHP_1956__15_2_81_0/.
- [52] Leon Cohen. Can Quantum Mechanics be Formulated as a Classical Probability Theory? In: Philosophy of Science 33.4 (1966), pp. 317–322. DOI: 10.1086/288104.
- [53] Gerard McCaul and Denys. I. Bondar. How to win friends and influence functionals: deducing stochasticity from deterministic dynamics. In: The European Physical Journal Special Topics 230.4 (June 2021), pp. 733-754. ISSN: 1951-6401. DOI: 10.1140/epjs/s11734-021-00068-2. URL: https://doi.org/10.1140/epjs/s11734-021-00068-2.
- [54] M. Reed and B. Simon. Methods of Modern Mathematical Physics. 2. Fourier Analysis, Self-adjointness. 1975.
- [55] De Dominicis, C. Techniques de Renormalisation de la Théorie des Champs et Dynamique des Phénomènes Critiques. In: J. Phys. Colloques 37 (1976), pp. C1-247-C1-253. DOI: 10.1051/jphyscol:1976138. URL: https://doi.org/10.1051/jphyscol:1976138.

[56] B. Jouvet and R. Phythian. Quantum aspects of classical and statistical fields. In: Phys. Rev. A 19 (3 Mar. 1979), pp. 1350-1355. DOI: 10.1103/PhysRevA. 19.1350. URL: https://link.aps.org/doi/10.1103/PhysRevA.19.1350.

- [57] Tristan Daus and Elena Kozlikin. Field Theory Approach to Classical N-Particle Systems In and Out of Equilibrium. In: arXiv e-prints (June 2024). arXiv: 2406.03425 [cond-mat.stat-mech].
- [58] Tristan Daus and Elena Kozlikin. Cosmic Large-Scale Structure Formation from Newtonian Particle Dynamics. In: arXiv e-prints (Jan. 2025). arXiv: 2501.11676 [astro-ph.CO].
- [59] R. Phythian. The functional formalism of classical statistical dynamics. In: Journal of Physics A: Mathematical and General 10.5 (May 1977), p. 777. DOI: 10.1088/0305-4470/10/5/011. URL: https://dx.doi.org/10.1088/0305-4470/10/5/011.
- [60] Harvey A. Rose. Renormalized kinetic theory of nonequilibrium many-particle classical systems. In: Journal of Statistical Physics 20.4 (Apr. 1979), pp. 415– 447. ISSN: 1572-9613. DOI: 10.1007/BF01011780. URL: https://doi.org/ 10.1007/BF01011780.
- [61] Steven Weinberg. The quantum theory of fields. Vol. 2: Modern applications. Cambridge University Press, Aug. 2013. ISBN: 978-1-139-63247-8, 978-0-521-67054-8, 978-0-521-55002-4. DOI: 10.1017/CB09781139644174.
- [62] H. D. Ursell. The evaluation of Gibbs' phase-integral for imperfect gases. In: Mathematical Proceedings of the Cambridge Philosophical Society 23.6 (1927), pp. 685–697. DOI: 10.1017/S0305004100011191.
- [63] F. J. Dyson. The S Matrix in Quantum Electrodynamics. In: Physical Review 75.11 (June 1949), pp. 1736–1755. DOI: 10.1103/PhysRev.75.1736.
- [64] Julian Schwinger. On the Green's Functions of Quantized Fields. I. In: Proceedings of the National Academy of Science 37.7 (July 1951), pp. 452–455. DOI: 10.1073/pnas.37.7.452.
- [65] John A. Krommes and Robert G. Kleva. Aspects of a renormalized weak plasma turbulence theory. In: The Physics of Fluids 22.11 (Nov. 1979), pp. 2168-2177. ISSN: 0031-9171. DOI: 10.1063/1.862510. eprint: https://pubs.aip.org/aip/pfl/article-pdf/22/11/2168/12320260/2168_1_online.pdf. URL: https://doi.org/10.1063/1.862510.
- [66] Camille Aron. Classical and quantum out-of-equilibrium dynamics. Formalism and applications. Theses. Université Pierre et Marie Curie Paris VI, Sept. 2010. URL: https://theses.hal.science/tel-00538099.
- [67] D. Lynden-Bell and Roger Wood. The gravo-thermal catastrophe in isothermal spheres and the onset of red-giant structure for stellar systems. In: MNRAS 138 (Jan. 1968), p. 495. DOI: 10.1093/mnras/138.4.495.
- [68] D. Lynden-Bell. Negative Specific Heat in Astronomy, Physics and Chemistry. In: Physica A Statistical Mechanics and its Applications 263.1-4 (Feb. 1999), pp. 293-304. DOI: 10.1016/S0378-4371(98)00518-4. arXiv: cond-mat/9812172 [cond-mat.stat-mech].

- [69] H. J. de Vega, N. Sánchez, and F. Combes. Fractal dimensions and scaling laws in the interstellar medium: A new field theory approach. In: Phys. Rev. D 54 (10 Nov. 1996), pp. 6008–6020. DOI: 10.1103/PhysRevD.54.6008. URL: https://link.aps.org/doi/10.1103/PhysRevD.54.6008.
- [70] Freddy Bouchet and Julien Barré. Statistical mechanics of systems with long range interactions. In: Journal of Physics: Conference Series 31.1 (Mar. 2006), p. 18. DOI: 10.1088/1742-6596/31/1/003. URL: https://dx.doi.org/10.1088/1742-6596/31/1/003.
- [71] Hector J. de Vega and Norma G. Sanchez. Statistical mechanics of the self-gravitating gas: Thermodynamic limit, phase diagrams and fractal structures. In: International School of Astrophysics 'Daniel Chalonge' 8th Course: Opening the 3rd Millennium, Phase Transitions in the Early Universe: Theory and Observations. May 2005, pp. 303–372. arXiv: astro-ph/0505561.
- [72] B. Semelin, Norma G. Sanchez, and H. J. de Vega. Selfgravitating fluid dynamics, instabilities and solitons. In: Phys. Rev. D 63 (2001), p. 084005. DOI: 10.1103/PhysRevD.63.084005. arXiv: astro-ph/9908073.
- [73] H. J. de Vega and Norma G. Sanchez. The Statistical mechanics of the selfgravitating gas: Equation of state and fractal dimension. In: Phys. Lett. B 490 (2000), pp. 180–186. DOI: 10.1016/S0370-2693(00)00973-4. arXiv: hep-th/9903236.
- [74] Pierre-Henri Chavanis. Kinetic theory of collisionless relaxation for systems with long-range interactions. In: Physica A 606 (2022), p. 128089. DOI: 10. 1016/j.physa.2022.128089. arXiv: 2112.13664 [cond-mat.stat-mech].
- [75] Pierre-Henri Chavanis. Landau equation for self-gravitating classical and quantum particles: application to dark matter. In: Eur. Phys. J. Plus 136.6 (2021), p. 703. DOI: 10.1140/epjp/s13360-021-01617-3. arXiv: 2012.12858 [astro-ph.GA].
- [76] Pierre-Henri Chavanis. Statistical mechanics of self-gravitating systems in general relativity: II. The classical Boltzmann gas. In: Eur. Phys. J. Plus 135.3 (2020), p. 310. DOI: 10.1140/epjp/s13360-020-00291-1. arXiv: 1908.10817 [gr-qc].
- [77] P. H. Chavanis. Statistical mechanics of violent relaxation in stellar systems. In: (Dec. 2002). arXiv: astro-ph/0212205.
- [78] M. Kac. Foundations of Kinetic Theory. In: Volume 3 Proceedings of the Third Berkeley Symposium on Mathematical Statistics and Probability, Volume III. Ed. by Jerzy Neyman. Berkeley: University of California Press, 2023, pp. 173–200. ISBN: 9780520350694. DOI: doi:10.1525/9780520350694-012. URL: https://doi.org/10.1525/9780520350694-012.
- [79] D. R. Hartree. The Wave Mechanics of an Atom with a Non-Coulomb Central Field. Part II. Some Results and Discussion. In: Proceedings of the Cambridge Philosophical Society 24.1 (Jan. 1928), p. 111. DOI: 10.1017/S0305004100011920.

[80] D. R. Hartree and W. Hartree. Self-Consistent Field, with Exchange, for Beryllium. In: Proceedings of the Royal Society of London Series A 150.869 (May 1935), pp. 9–33. DOI: 10.1098/rspa.1935.0085.

- [81] V. Fock. Näherungsmethode zur Lösung des quantenmechanischen Mehrkörperproblems. In: Zeitschrift für Physik 61.1-2 (Jan. 1930), pp. 126–148. DOI: 10.1007/BF01340294.
- [82] Juergen Berges. Introduction to Nonequilibrium Quantum Field Theory. In: AIP Conference Proceedings. Vol. 739. AIP, 2004, pp. 3-62. DOI: 10.1063/1.1843591. URL: http://dx.doi.org/10.1063/1.1843591.
- [83] John M. Cornwall, R. Jackiw, and E. Tomboulis. Effective action for composite operators. In: Phys. Rev. D 10 (8 Oct. 1974), pp. 2428–2445. DOI: 10.1103/ PhysRevD.10.2428. URL: https://link.aps.org/doi/10.1103/PhysRevD. 10.2428.
- [84] P.J.E. Peebles. *Principles of Physical Cosmology*. Princeton Series in Physics. Princeton University Press, 1993. ISBN: 9780691019338. URL: https://books.google.de/books?id=AmlEt6TJ6jAC.
- [85] J.A. Peacock. Cosmological Physics. Cambridge Astrophysics. Cambridge University Press, 1999. ISBN: 9780521422703. URL: https://books.google.de/books?id=t80-yylU0j0C.
- [86] Steven Weinberg. Cosmology. 2008. ISBN: 978-0-19-852682-7.
- [87] Matthias Bartelmann. *General Relativity*. Lecture Notes. Heidelberg University Publishing, Oct. 2019. DOI: 10.17885/heiup.534. URL: https://heiup.uni-heidelberg.de/catalog/book/534.
- [88] Daniel N. Blaschke et al. The energy-momentum tensor(s) in classical gauge theories. In: Nuclear Physics B 912 (2016). Mathematical Foundations of Quantum Field Theory: A volume dedicated to the Memory of Raymond Stora, pp. 192-223. ISSN: 0550-3213. DOI: https://doi.org/10.1016/j.nuclphysb.2016.07.001. URL: https://www.sciencedirect.com/science/article/pii/S0550321316301845.
- [89] Barton Zwiebach. Curvature Squared Terms and String Theories. In: Phys. Lett. B 156 (1985), pp. 315–317. DOI: 10.1016/0370-2693(85)91616-8.
- [90] Planck 2018 results: VI. Cosmological parameters. In: Astron.; Astrophysics 641 (Sept. 2020), A6. ISSN: 1432-0746. DOI: 10.1051/0004-6361/201833910. URL: http://dx.doi.org/10.1051/0004-6361/201833910.
- [91] Dark Energy Survey and Kilo-Degree Survey Collaboration. *DES Y3 + KiDS-1000: Consistent cosmology combining cosmic shear surveys.* In: The Open Journal of Astrophysics 6, 36 (Oct. 2023), p. 36. DOI: 10.21105/astro.2305.17173. arXiv: 2305.17173 [astro-ph.CO].
- [92] Antony Lewis, Anthony Challinor, and Anthony Lasenby. Efficient Computation of Cosmic Microwave Background Anisotropies in Closed Friedmann-Robertson-Walker Models. In: Astrophysical Journal 538.2 (Aug. 2000), pp. 473–476. DOI: 10.1086/309179. arXiv: astro-ph/9911177 [astro-ph].

- [93] V. Silveira and I. Waga. Decaying Λ cosmologies and power spectrum. In: Phys. Rev. D 50 (8 Oct. 1994), pp. 4890–4894. DOI: 10.1103/PhysRevD.50.4890. URL: https://link.aps.org/doi/10.1103/PhysRevD.50.4890.
- [94] F. Bernardeau et al. Large-scale structure of the Universe and cosmological perturbation theory. In: Physics Reports 367.1–3 (Sept. 2002), pp. 1–248. ISSN: 0370-1573. DOI: 10.1016/s0370-1573(02)00135-7. URL: http://dx.doi.org/10.1016/S0370-1573(02)00135-7.
- [95] H. Martel and W. Freudling. Second-order perturbation theory in Omega is not equal to Friedmann models. In: Astrophysical Journal; (United States) 371 (Apr. 1991). ISSN: ISSN 0004-637X. DOI: 10.1086/169864. URL: https://www.osti.gov/biblio/5596351.
- [96] Diego Blas, Mathias Garny, and Thomas Konstandin. Cosmological perturbation theory at three-loop order. In: Journal of Cosmology and Astroparticle Physics 2014.01 (Jan. 2014), p. 010. DOI: 10.1088/1475-7516/2014/01/010. URL: https://dx.doi.org/10.1088/1475-7516/2014/01/010.
- [97] Thomas Buchert. Lagrangian Perturbation Approach to the Formation of Large-scale Structure. In: in: S. Bonometto, J.R. Primack, A. Provenzale (Eds.), Proceedings of the International School Enrico Fermi, Course CXXXII (Dark Matter in the Universe), Varenna, Italy (1996), pp. 543–564.
- [98] Gene F. Mazenko. Fundamental theory of statistical particle dynamics. In: Phys. Rev. E 81 (6 June 2010), p. 061102. DOI: 10.1103/PhysRevE.81.061102. URL: https://link.aps.org/doi/10.1103/PhysRevE.81.061102.
- [99] Enrico Cattaruzza, Ennio Gozzi, and Antonio Francisco Neto. *Diagrammar In Classical Scalar Field Theory*. In: Annals Phys. 326 (2011), pp. 2377–2430. DOI: 10.1016/j.aop.2011.05.009. arXiv: 1010.0818 [hep-th].
- [100] P. Hertel and W. Thirring. A soluble model for a system with negative specific heat. In: Annals of Physics 63.2 (1971), pp. 520-533. ISSN: 0003-4916. DOI: https://doi.org/10.1016/0003-4916(71)90025-X. URL: https://www.sciencedirect.com/science/article/pii/000349167190025X.
- [101] Earl Lawrence et al. The Coyote Universe. III. Simulation Suite and Precision Emulator for the Nonlinear Matter Power Spectrum. In: Astrophysical Journal 713.2 (Apr. 2010), pp. 1322–1331. DOI: 10.1088/0004-637X/713/2/1322. arXiv: 0912.4490 [astro-ph.CO].
- [102] Lavinia Heisenberg, Shayan Hemmatyar, and Stefan Zentarra. *Kinetic field theory: Higher-order perturbation theory*. In: Phys. Rev. D 106.6 (2022), p. 063513. DOI: 10.1103/PhysRevD.106.063513. arXiv: 2207.10504 [hep-th].
- [103] S. Floerchinger et al. Effective description of dark matter as a viscous fluid. In: EPJ Web Conf. 125 (2016). Ed. by V. A. Andrianov et al., p. 03018. DOI: 10.1051/epjconf/201612503018. arXiv: 1609.03466 [astro-ph.CO].

[104] John A. Hertz, Yasser Roudi, and Peter Sollich. Path integral methods for the dynamics of stochastic and disordered systems. In: Journal of Physics A: Mathematical and Theoretical 50.3 (Dec. 2016), p. 033001. ISSN: 1751-8121. DOI: 10.1088/1751-8121/50/3/033001. URL: http://dx.doi.org/10.1088/1751-8121/50/3/033001.

[105] Thibaut Arnoulx de Pirey et al. Discretized and covariant path integrals for stochastic processes. working paper or preprint. Nov. 2022. URL: https://cnrs.hal.science/hal-03865795.